bushfire CRC

FIRE DEVELOPMENT, TRANSITIONS AND SUPPRESSION

FINAL PROJECT REPORT

Andrew L. Sullivan, Miguel G. Cruz, Peter F. M. Ellis, Jim S. Gould, Matt P. Plucinski, Richard Hurley and Vijay Koul

CSIRO Ecosystem Science and CSIRO Climate Adaptation Flagship

CSIRO

Publisher: Bushfire Cooperative Research Centre, East Melbourne, Victoria.

Cover:
The CSIRO Pyrotron in Canberra allows fires to be studied under repeatable conditions in safety.
Photo by the Bushfire CRC.

ISBN: 978-0-9875218-9-7

Citation:
Sullivan AL, Cruz MG, Ellis PFM, Gould JS, Plucinski MP, Hurley R, Koul V, (2014) Fire Development, Transitions and Suppression Final Report. Bushfire CRC, Australia, ISBN: 978-0-9875218-9-7

Foreword

This report represents an extensive body of research that will support many aspects of operational fire management. In particular, this project provides a greater understanding of fire behaviour processes associated with fire initiation and development. The implications for firefighting agencies are significant.

The project has been funded through the Bushfire Cooperative Research Centre and has included end-user consultation throughout the project. Fire agencies provided input to the direction of the project as well as receiving ongoing updates on the progress of the research. This has been a successful implementation of the CRC model, partnering research with operational end users.

Fire behaviour models used in current fire management do not adequately consider the initial development phase of fires from their ignition. A greater understanding of the conditions for fire initiation and growth has the potential to substantially increase the accuracy of fire spread predictions. More accurate timing of early fire predictions will improve community warnings and advice and potentially save lives.

The results from this project will provide the evidence for fire agencies to refine management practices that rely on fire behaviour and fire load information. These improvements to operational procedures will increase fire fighter safety, assist with resource allocation specifically for first attack and potentially increase suppression effectiveness. For agencies with a volunteer based workforce, greater efficiency in resource allocation is increasingly important due to the ever increasing demands on the workforce.

I strongly support the ongoing development of fire occurrence and suppression resource allocation models based on this research. This work will play an important role in fire management in Australia in the future.

Simon Heemstra, Ph.D
Manager Community Planning
NSW Rural Fire Service

Contents

Acknowledgments

A project of this size and scope requires the input of many people from diverse sectors in addition to the authors to help achieve project objectives and outcomes. We would like to acknowledge the efforts of the following organisations and people in helping us along the way:

NSW Rural Fire Service: Laurence McCoy, Simon Heemstra, Mel O'Halloran.

CSIRO: Phil Polglase, Belinda Jonas, Trevor Booth, Craig James, Susan Duson, Xunguo Lin, Martyn Ellis

Bushfire Cooperative Research Centre: Lyndsey Wright, Richard Thornton, Noreen Krusel, Vaia Smirneos, Gary Morgan

WA Department of Fire and Emergency Services: Carole Dowd, Jared Ebrall, Gary Baxter

WA Department of Parks and Wildlife: Lachie McCaw, Neil Burrows, Craig Carpenter

ACT Parks and Conservation Service: Neil Cooper, Brian Levine

Vic Department of Primary Industries and Environment: Liam Fogarty

Queensland Rural Fire Service: Steve Rothwell

Canadian Forest Service: Mike Wotton

US Forest Service: Jeremy Fried

Ontario Ministry of Natural Resources: Robert McAlpine

EnviroPoint Systems: Ralph Dick

Executive Summary

Overview

STATE OF EXISTING KNOWLEDGE

All bushfires start small. Understanding how they progress from ignition to conflagration, from surface fire to high intensity crown fire, is critical to a range of needs, including planning appropriate suppression strategies, ensuring firefighter safety and issuing public warnings.

The period between the ignition of a fire and when that fire completes its development phase and attains its potential rate of spread for the prevailing conditions represents the only time when effective initial attack suppression can be undertaken.

All existing operational fire prediction systems assume a fire has completed its development phase and is spreading at its steady-state rate of spread and thus may over-predict the spread of fire and under-predict the potential affect fire suppression may have on fire behaviour.

No predictive capacity for determining fire occurrence, fire initiation probability, fire growth and fuel transitions, or suppression resource allocation is currently available for operational purposes in Australia. The aim of this work was to develop the fundamental understanding of these vital aspects of bushfire management.

PROGRESSION OF RESEARCH

This project ran over a period of three years, from January 2011 to December 2013 and utilised a range of research approaches, from case study analysis, laboratory-based experimentation, and statistical and physical modelling.

The project investigated factors important in influencing the occurrence of bushfires, the successful initiation of spot fires from firebrands, the rate of growth and development of new fires to steady state rate of spread, and the transitions of such fires through vertical fuel strata as it develops in intensity.

RESEARCH RESULTS

From the new knowledge gathered in this project, predictive models about the probability, number, size, and potential growth rate of fire ignitions were developed. These models can be used to determine the most effective allocation and deployment of suppression resources, on both a seasonal and incident basis, within a framework of suppression resource allocation also developed during this project.

Specifically, the results of this project include:

- A fire occurrence model derived for the case study area of south-west Western Australia that utilises readily available information on fire history, weather and fuel

conditions to determine the potential for fire to occur within a given region and the potential number of fires that may occur. (Chapter 2)

- A model for the initiation potential of fire starting from firebrands or similar forms of ignition, from both flaming combustion and glowing combustion. (Chapter 3)
- A model for the rate of growth of ignitions (in terms of rate of spread, perimeter increase and area increase) up to the steady state rate of spread. (Chapter 4)
- A model for the likely transition of fire through horizontally stratified fuel layers, incrementally increasing fireline intensity as it does. (Chapter 5)
- A framework for the incorporation of these predictive models into a tool for determining the likelihood of fire occurrence, the success rate of new ignitions to readily sustain combustion and the rate of development of new ignitions. (Chapter 6)

The results of this project will enable fire authorities to better determine the necessary level of suppression readiness required for given weather and fuel conditions, the potential for any fire outbreak to develop beyond initial attack resources before they arrive, and allow the prioritisation of suppression of fire outbreaks.

RESEARCH OUTPUTS

This research project generated 32 interim reports detailing progress of individual project components, five Fire Notes, six research posters presented at the annual Bushfire CRC conferences (held in conjunction with the Australasian Fire and Emergency Services (AFAC) national conference), and six draft research articles for submission to international peer-reviewed journals.

The project also organised and ran a three day Bushfire Science Symposium in Canberra where results were presented to an audience of fire behaviour practitioners. The symposium attracted over 140 participants and was well received.

Key outcomes and current state of knowledge

FIRE OCCURRENCE MODELLING (CHAPTER 2)

This chapter comprises of two sub-studies. The first study (Section 2.2) investigated the timing of vegetation fires from different causes (17 in total) in urban and peri-urban areas. The second study (section 2.3) developed models predicting the daily number of human caused fires within fire management regions.

The fire timing study used the urban and peri-urban areas around Perth as case study and utilised incident data from the Western Australian Department of Fire and Emergency Services. Fire timing was at a range of scales (hourly, daily, monthly and annually) and in terms of weather variables related to fire danger and fuel availability. The incidence of vegetation fires is strongly related to fire danger and fuel moisture conditions, with ignitions from all cause categories being more frequent during periods of elevated fire danger. The different cause categories had a range of sensitivities to fire danger and fuel moisture. Some causes that have small heat outputs, such as cigarettes, cutting and welding, were more restricted to periods with elevated fire danger conditions and low fuel moisture than other causes.

The timing of vegetation fires is also dependant on the presence of the ignition source. In terms of human caused fires this relates to human activity, which varies according to day type, as indicated by the increased rates of ignition on weekends, public holidays and non-school days.

Models predicting the number of daily human-caused bushfires were developed for 10 management regions in south-west Western Australia, using data from the Departments of Parks and Wildlife and Fire and Emergency Services. The models were developed using negative binomial regression with a dataset spanning three years. The most important variables in this analysis were:

- daily minimum fuel moisture content,
- the number of human-caused bushfires in the region over the preceding two weeks, and
- rainfall over the preceding 24 hours.

The models were tested against an independent year's data for each region. The models were found to perform reasonably well but analysis showed that they would only be of practical value in those regions that experience high numbers of fires as regions that do not experience high numbers of fires have insufficient day-to-day variability.

While model performance and reliability may be improved by utilising longer continuous data sets, analysis showed that duration of the training set made very little difference in model outcomes. Furthermore, using increasingly historical datasets may not reflect current fire activity.

The structure of the model is such that it could be applied to other regions of Australia provided sufficient data are available to determine critical model coefficients.

FIRE INITIATION FROM FIREBRANDS (CHAPTER 3)

The objective of this study was to quantify the probability of flaming ignition of a selected fuel bed type by firebrands. Spotfires ignited by firebrands lead to the breakdown of suppression efforts, enable bushfires to breach breaks in fuel and topography, and can result in situations which threaten the safety of firefighters and residents.

The firebrand samples had the combustion and aerodynamic characteristics of small firebrands from predominantly dry forests of southern Australia. Samples of bamboo 50-mm-long and about 2 mm in diameter were used to represent standard flaming firebrands. These had consistent flaming times of about nine seconds after ignition and terminal velocities of between 3 and 4 m s^{-1}. Samples of *Eucalyptus globulus* bark 50-mm-long were used as standard glowing firebrands. These were between 0.6 g and 0.9 g in mass, with terminal velocities of about 4 m s^{-1} and duration of glowing combustion of about 2.5 minutes in wind.

The fuel bed used was litter profile to soil depth of dry sclerophyll forest. This is a major vegetation type in south-eastern and south-western Australia where recurrent, large bushfires, in which spotting is a significant feature, cause devastation. The fuel bed samples were excised intact from Southern Tablelands dry sclerophyll forest and thus retained their structure. Each fuel bed sample was characterised for surface composition and roughness, and pre-conditioned for moisture content.

A purpose-built wind tunnel was used to supply airflow at speeds of 1 m s^{-1} and 2 m s^{-1} across the fuel bed sample. Such air velocities across the litter bed under dry sclerophyll are equivalent to wind speeds of about 15 km hr^{-1} and 30 km hr^{-1} respectively in the open. A

purpose-built firebrand generator was used to combust each glowing firebrand sample at its terminal velocity prior to deposition onto the fuel bed.

Logistic regression was used to derive models for the probability of ignition success. For flaming firebrands, fuel bed moisture content, the presence of wind, the interaction of moisture content and wind, and surface roughness were the key explanatory variables. In the absence of wind, a critical threshold fuel moisture content of 14% is necessary for ignition to occur. There is a 50% probability of successful ignition once fuel moisture content is below 9%. In the presence of wind, the critical threshold fuel moisture content is 21%. There is a 50% probability of successful ignition once fuel moisture content is below 13%. At moisture contents less than about 7%, ignition is guaranteed from any flaming firebrand equivalent to the standard sample.

A linear regression model for the time to establish ignition from flaming firebrands was also developed, using the key explanatory variables of fuel bed moisture content, the presence or absence of wind and their interaction.

For glowing firebrands, only fuel bed moisture content and wind speed were key explanatory variables. For a wind speed of 2 m s^{-1} at the fuel level, a critical threshold fuel moisture content of 10% is required for ignition from a standard glowing firebrand to occur. The results suggested that the nature of the air flow in regard to its turbulence intensity may play a large role in determining successful ignition from glowing firebrands.

FIRE GROWTH AND DEVELOPMENT (CHAPTER 4)

Once a fire successfully ignites, it will undergo a development phase in which the rate of spread of the fire increases steadily until it reaches the steady-state rate of spread for the prevailing conditions. This acceleration phases has long been recognised. It is of critical importance because often it is only during this period that direct attack by firefighters is successful. However, due to the complexity of the factors that influence a fire's acceleration, no operational model of rate of fire growth has been developed.

The objective of this study was to investigate in the controlled environment of a combustion wind tunnel the factors that influence the development of ignitions up to the steady-state. For this purpose the CSIRO Pyrotron was used to experimentally study fires lit from a range of ignition sizes (point ignition, 400 mm, and 800 mm ignition lines) in a continuous fuel bed of fine (< 6 mm diameter) dry sclerophyll litter. Two regimes of fine dead fuel moisture (7% and 5% oven dried weight) and two regimes of wind speed (1.25 and 2 m s^{-1}, equivalent to 13 and 22 km h^{-1} in the open) were studied. The fuel bed was fixed at a fuel load of 1.2 kg m^{-2} and characterised for composition, depth and moisture content.

A range of data on fire behaviour was collected, including thermocouple array data, visual and infra-red video imagery, still imagery and observational information of rate of spread, flame height, depth and angle. Rate of spread was calculated as interval (individual rate of spread for each 0.5 m increment) and cumulative (time averaged speed across cumulative distance since ignition). These were then used to define rate of spread during the acceleration phase and rate of spread during the steady-state phase.

Both interval and cumulative rate of spread were correlated with ignition size, with cumulative rate of spread more strongly correlated with all independent variables. There was no significant difference between interval rate of spread and ignition size under low wind speeds. Under high wind speeds there was no significant difference in the mean interval rate of spread between point and 400 mm line ignitions.

All line ignitions showed an immediate rapid increase in rate of spread over the first 1–1.5 m that then reduced in magnitude before steadily increasing again. This ignition line effect is similar to that witnessed in large field experiments.

A model for the time to reach steady-state rate of spread was developed using an accepted conceptual framework for fire growth. This model utilises only wind speed and fuel bed moisture content and suggests that under extreme fire weather conditions (fuel moisture content <5% and high wind speed), that a fire starting from a point in uniform dry sclerophyll litter will take 25 minutes to reach steady-state rate of spread for the prevailing conditions. Under milder conditions it may take a fire 60 minutes to reach steady state.

These results were contrasted with historical fire experiments conducted during the 1950s, '60s and '70s and sourced from CSIRO's archives and those of the Western Australian Department of Parks and Wildlife. A preliminary model constructed from these data for the rate of increase in fire area is also based on wind speed and fuel moisture content. This model provides a basis for predicting the area a fire starting from a point ignition will achieve after 60 minutes of growth. Due to the nature of the experimental fires used to develop the model, it is suitable only for low- to moderate-intensity fires burning under mild conditions similar to controlled burning operations, i.e. 10 m wind speeds in the open < 20 km h^{-1} and fuel moisture between 5% and 12%.

The results of these studies, being a result of laboratory scale fires or field experiments under mild conditions, are most applicable to prescribed fire used for hazard reduction. The models provide important insights into fire development in eucalypt litter and indicate the importance of time in fire control which increases with fire danger.

VERTICAL FIRE TRANSITION AND PROPAGATION (CHAPTER 5)

While fire growth in regard to the increase in fire area, perimeter length and rate of spread was the focus of the previous chapter, this study focussed on the development of fundamental understanding of the processes involved in the growth of fire through the vertically-separated, horizontally-stratified structure of dry sclerophyll forests predominant in Australia. The nature of our native forest fuels is such that fuel for each stratum is distinct (e.g. surface, near-surface, elevated, etc) and each stratum plays a different but significant role in determining the behaviour of a fire burning through each.

When a fire ignition occurs it is limited in size and heat output and thus spreads through the surface fuel layer only. As the fire builds in size and speed and intensity, it involves other strata until, if the conditions are conducive, it eventually involves the entire fuel complex–a so called crown fire.

In this study we developed a semi-physical model that describes behaviour of fire burning in the understorey of eucalypt forests. We did this by quantifying the vertical propagation transitions of fire between separate fuel layers, the steady-state forward rate of fire spread of the flame front through each fuel layer, and the energy released.

The model is based on an energy balance formulation that takes into account changes in temperature of unburned, thermally-thin fuel elements due to the impinging convective and radiative heat fluxes. The model is closed by using a number of sub-models. Radiative energy source is modelled as a solid flat surface with the radiometric temperature varying with height (for forward heat flux computations) and depth (for upward computations).

Fluid temperature and velocity fields necessary for convective heat transfer calculations are determined from a buoyant plume model and knowledge of a characteristic heating

distance. Limited sensitivity analysis and evaluation against experimental fire data shows acceptable agreement with expected trends and observed fire behaviour.

A better fundamental understanding of the thermodynamic environment preceding a flame front is necessary to fine tune the model. Such understanding will require instrumentation of field fires to measure radiative and convective heat transfer characteristics under a range of burning conditions.

FIRE SUPPRESSION RESOURCE ALLOCATION FRAMEWORK (CHAPTER 6)

Wildfire suppression resource allocation models estimate the optimal number and mix of wildfire suppression resources by simulating fire environments and management systems. They can be used to test a range of alternative resourcing and budget scenarios to assist long term strategic planning and can applied for research applications. They are regionally specific and few have been developed with only two in current operational use (California Fire Economics Simulator, California and LEOPARDS, Ontario Canada).

A framework for a bushfire suppression resource allocation model suitable for application in regions of Australia was developed. The framework uses inputs that describe the environment (weather, terrain, fuels and population), historical fire patterns and suppression (resources and dispatch protocols) to calculate fire load (number, extent and behaviour of fires in the landscape) and suppression capability available for each simulation scenario.

Fire load and suppression capability are then entered into a containment simulation to estimate the suppression effort (e.g. resource use and cost) and the fire outcome (e.g. area burnt, time to containment) for each simulated fire. The containment simulation will be based on fire initiation, fire growth and fire transition models developed in Chapter 3, 4 and 5 and combined with suppression productivity models. Simulations spanning multiple fire seasons will be used to predict the long term outcomes for each set of input scenarios.

Strategic resource allocation modelling systems require considerable time and resources to develop. The majority of work required to develop them for Australian regions would be in the development of input modules that represent the regional environment, fire history and suppression conditions. The development of a resource modelling system will require significant support from agencies responsible for fire management within the application region.

Implications and conclusions

This project is the first comprehensive investigation into the lifecycle of fire behaviour, from initiation, through development, to steady-state behaviour. Knowledge gained from this work will better enable fire authorities to understand the expected behaviour of fire outbreaks and how long they will have to successfully attack new fires before they become too big for direct attack and extended or indirect strategies are necessary.

The results of these studies are preliminary due to the restricted nature of the experimental conditions under which they were taken. They must be validated and extended into the range of conditions associated with wildfire. However, despite their limitations they provide insight into the dynamics of fire outbreaks and the transitions of fire ignitions into large high intensity fires.

The framework for fire suppression resource allocation also developed during this project provides a roadmap for linking the models developed for fire occurrence prediction, fire

initiation probability, fire growth and fire transitions into a coherent and cogent tool for improved use of existing fire suppression resources. In particular the results of such linking will provide tools to answer the critical questions asked by fire authorities, such how many resources are required for a given set of conditions, where should such resources be placed, and when one or more fires break out, how should the suppression actions be prioritised.

Ultimately a functioning fire suppression resource allocation tool, linked to necessary forecast environmental conditions (i.e. weather and fuels) will be able to provide guidance to fire authorities and land management agencies on the likely resource requirements on a daily, weekly, or seasonal basis. Such a tool will also enable the investigation of the effects of major drivers of environmental conditions such as climate change on resource requirements.

1 Introduction

1.1 Background

All wildfires start small, whether they are the result of a lightning strike, deliberately lit by an arsonist, accidently lit through negligence or an escaped burn-off.

In each case, the tiny spark or lick of flame initiates a fire that increases in size and intensity. If this fire continues to burn unrestricted in conditions that are conducive to development, it will spread faster and become more intense. If the fire is burning in a forest, then the fire may also begin to throw embers and firebrands ahead of the main fire. If these catch alight these new spotfires will also undergo the same development process until they too start throwing spots and the process repeats. Eventually the fire will become a conflagration that will be beyond all control efforts with the potential to cause great damage and loss of life.

Figure 1.1 illustrates this cycle of fire propagation in forest fuels. Understanding how a fire ignition progresses from initiation to conflagration, from surface fire to high intensity crown fire, from slowly spreading contiguous fire to one that is spotting heavily, is critical to planning the most appropriate and effective pre-suppression strategies and suppression actions. It is also essential for issuing timely and effective public warnings.

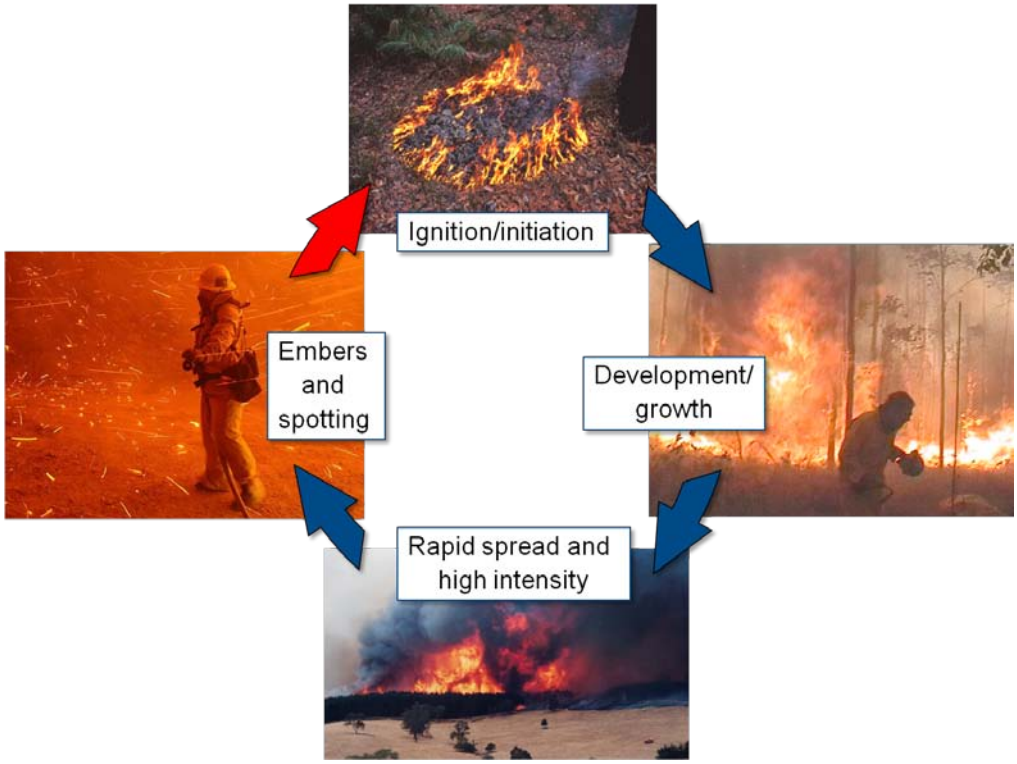

Figure 1.1. A schematic of the fire progression cycle, from ignition to steady-state, to spotting and new ignitions.

How long does it take a fire, once it starts, to accelerate up to a steady state rate of spread? How long does it take for a new ignition to develop to its full intensity? How long before it begins throwing spotfires? How long before these spotfires are throwing new spotfires themselves?

These are just some of the critical questions posed by firefighters because under most wildfire conditions, the only opportunity firefighters have to successfully suppress a wildfire is during the growth phase soon after ignition—called initial attack and is the most common form of direct suppression (Fig. 1.2). Once the fire is up and running and spreading at its potential maximum (steady-state) rate of spread, it will generally be beyond direct suppression and firefighters will have to fall back to indirect attack strategies in order to control it.

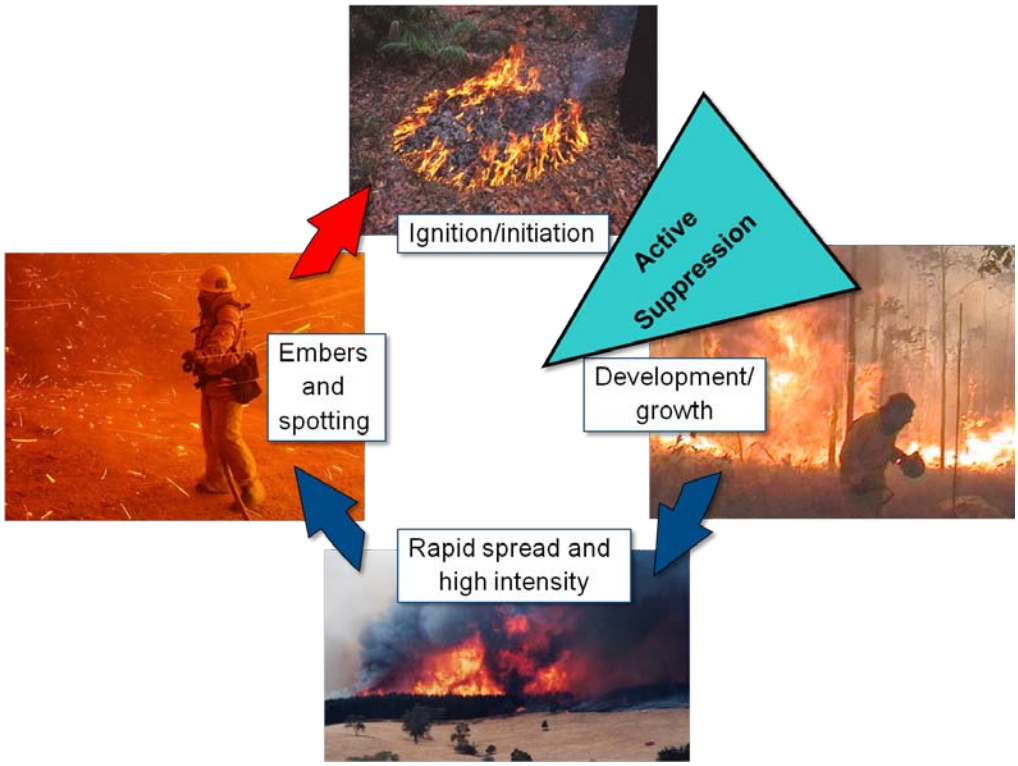

Figure 1.2. The best opportunity for direct suppression of wildfires is soon after ignition and before the fire has completed its development phase.

Information about the likely rate of growth of new ignitions will provide fire authorities with the ability to better plan for and respond to fire outbreaks and be more efficient in the deployment and use of suppression resources.

As part of the continuum of fire behaviour, this project aimed to investigate factors that influence the occurrence of fire outbreaks (i.e. fire occurrence) and the propagation and transitions of a fire's behaviour as it develops from ignition and involves different fuel layers. It also aimed to study the factors that determine the successful initiation of a fire resulting from flaming or glowing firebrands.

Understanding the rapidly changing demands for suppression and allocation of resources will provide fire managers with greater confidence in pre-season planning and incident management, particularly during multiple fire events. Determining the level of suppression resources required on any given day will depend on how soon the outbreak of a new fire, burning under given weather, fuel and topographic conditions, will be beyond successful first attack.

1.2 Objectives and aims

High intensity fire behaviour in Australia is generally associated with rapid development, high rates of spread, high heat flux, and extreme suppression difficulty, usually resulting in large fires. These fires are very dangerous to suppress, can kill people, destroy property and other assets, and threaten biodiversity and harm the environment. While the behaviour of low intensity fires burning under mild weather conditions is generally predictable in predominant fuel types, there is a poor understanding of the specific conditions under which a fire transitions to become high intensity and largely unpredictable.

In general terms, it is known from empirical evidence and limited theoretical understanding that the development and propagation of high intensity fires is dependent on a number of interacting conditions and processes, the most important of these being wide-spread drought and landscape dryness, a sufficient quantity and distribution of heavy dry fuel, hot, dry winds, sharply dissected terrain and unstable atmospheric conditions.

The classic approach to modelling bushfire behaviour is based upon the premise that under most conditions fire spread is a continuous, contiguous phenomenon that presents a distinct front burning through the landscape according to reasonably well understood functional relationships. Although firebrands and spotfires have long been identified as a primary source of new ignitions that allows a fire to overcome breaks in fuel and topography, it has been assumed that under uniform flat to undulating topography, most of these are quickly subsumed by the passage of the main front and do not increase rate of spread.

All current operational models of fire behaviour are built on this foundation (e.g. McArthur 1966, McArthur 1967, Sneeuwjagt and Peet 1985, Gould *et al.* 2007, Cheney *et al.* 2012) and for 'short distance' spotting under relatively mild burning conditions these models perform acceptably well. That is, our existing operational knowledge of fire behaviour and the tools developed for the prediction of fire spread assume that the fire has achieved a pseudo-steady-state rate of spread for the environmental conditions (Cheney and Gould 1995, 1997).

However, it has long been recognised (e.g. McArthur 1967, McAlpine and Wakimoto 1991, Cheney et al 1993) that a bushfire burning in continuous fuels in the open takes some time to reach its steady-state rate of spread. That is, a fire undergoes a development phase where the perimeter and area, the rate of forward spread and fireline intensity increases up to the steady-state behaviour for the prevailing conditions. Figure 1.3 shows the fire acceleration diagram presented by McArthur (1967) to illustrate the concept of the non-linear increase in

rate of spread (and thus intensity, fire perimeter length and area) that a forest fire starting from a point will undergo, if allowed to burn unrestricted.

In this model, McArthur has a fire burning in ground fuel increasing in rate of spread and asymptoting to a maximum (the steady-state). If the intensity of that fire is enough to involve the next fuel layer (i.e. shrubs), then the fire increases in speed and intensity again, following a repeated step-wise process until it involves all available fuel including the tree crowns or no longer increases in intensity. Thus, the speed of a fire depends on how long it has been burning and through what layers of forest fuel it is burning.

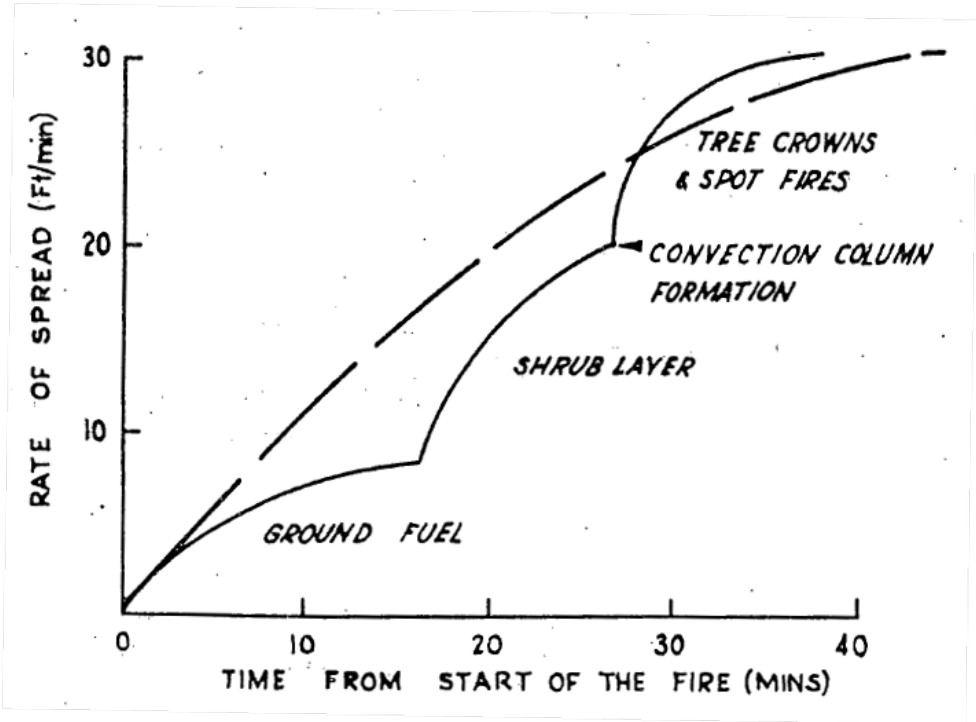

Figure 1.3. Conceptual model of the increase in rate of spread of a fire starting from a point (McArthur (1967).

Assuming that a fire ignition immediately spreads at the steady-state rate of spread for the conditions will grossly overpredict the likely propagation of the fire and provide no information about the likely success of initial attack. Similarly, assuming that spotfires spread at the steady-state rate of spread for the conditions will also overpredict their propagation and under estimate the potential for successful initial attack of these outbreaks.

Improved knowledge of the complex interactions that influence acceleration and transitions of these fires will extend existing understanding of fire spread, which is limited to continuous spread through surface fuels once a fire has reached a pseudo-steady state with the fire environment.

Therefore, one objective of this project was to contribute to a better understanding of the cyclic process of fire initiation, development, steady-state (surface) spread, and spotting under a broad range of conditions in dry eucalypt forests.

During the past decade there has been an increasing need to share resources between fire agencies during peak demand periods. It is therefore increasingly important to be able to anticipate short term fire danger, suppression, and resource demands in order to mobilise resources in time to be most effective. Fire propagation and development information can be used in conjunction with models of fire occurrence to develop models of the extent, behaviour and density of fire in the landscape (called 'fire load'). These models can be used as a tool to assist decision making about the necessary resource requirements for a given situation, allowing fire authorities to better determine the transition between successful initial attack and when extended attack resources are required, prioritise between fires, and generally improve planning for and combating of wildfires.

Fire occurrence models generally identify key independent variables such as weather and fuel information to provide a prediction of the likelihood of a fire occurring (breaking out) or the number of fires that might occur on a given day. Such models have been developed and used overseas to predict long term trends in fire load using climate change scenarios. There are no published fire occurrence models for either long or short term trends in Australia.

Another objective of this project was to develop a fire occurrence model for Australian conditions based on readily available historical and environmental information. The information provided by this model could then be used in conjunction with the new understanding of fire initiation and propagation to develop a framework for determining the optimal allocation of fire suppression resources on a daily, weekly, monthly or seasonal basis.

1.3 Project structure

As a result of the above objectives, this project consisted of three primary components, each of which is linked through the development of knowledge of fire propagation. These are:

A. Firebrand potential and spotfire initiation
B. Fire propagation and transitions
C. Fire load and suppression resourcing

Due to the three-year scope of the Bushfire CRC extension, these components (and the elements of which each is comprised) were not necessarily sequential or contiguous. In order to maximise return for effort, particularly in regard to suitable conditions for experimentation and bushfire observation, the execution of each component and element of each component was intended to be independent as far as possible such that progress could occur on multiple fronts simultaneously.

1.3.1 COMPONENT A: FIREBRAND POTENTIAL AND SPOTFIRE INITIATION

Principle investigator/s: Dr Peter Ellis (CSIRO)

Co-investigators: CSIRO research staff, Bureau of Meteorology, PhD scholar, University supervisor.

The nature and scale of the threat posed by spotting is the product of the availability (quantity) and characteristics of firebrand material, the local atmospheric boundary layer (ABL) meteorology that dictates the potential height to which a firebrand will be lofted and

the distance it will be carried downwind (and the interaction of the fire's convection column with the topography and the boundary layer), and the ignition probability of the firebrand (i.e. which affects the potential density of spot fires).

The aerodynamic and combustion characteristics for one particularly notorious bark species (messmate stringybark) have been described previously by Ellis (2000, 2011, 2012). The aim of this project component was to extend this knowledge to other notorious species and develop understanding of the transport and ignition potential of these firebrands under a range of fuel and weather conditions.

The hypotheses to be tested in this project are:

i. that bark is the agent of long distance (>10 km) spotting observed on high intensity fires; and
ii. that under extremely dry conditions (<5% fuel moisture content), even tiny glowing firebrands of less than 0.1 gram can ignite spot fires in forest litter fuels.

The proposed work plan of this component consisted of three elements:

1) Quantification of firebrand/ember potential for particular forest types/bark morphologies: Extension of the knowledge of bark firebrand flight and burning characteristics, particularly to include gum-bark types, by measuring and modelling aerodynamic and combustion behaviour in a vertical wind tunnel. To be completed as a post-graduate (PhD) study under the supervision of and in collaboration with CSIRO and an appointed university.
2) Development of high-resolution fire weather models to allow understanding of the interaction of the atmospheric boundary layer with complex topography and the fire convection column (including mechanical and shear induced turbulence and vortical structures) to quantify potential for lofting and transport of firebrands from fires with a range of fire sizes and intensities. To be undertaken by the Bureau of Meteorology.
3) Quantification and analysis of the effect of firebrand size and combustion state on ignition probability in a range of surface fuel beds under a range of conditions, primarily using the CSIRO Pyrotron combustion wind tunnel to replicate required fire weather conditions. To be completed by CSIRO research staff.

Element #2 was undertaken directly by the Bureau of Meteorology and the results will be reported separately by them.

Prerequisites: It was identified very early on that the success of this project component was conditional upon the timely commencement of a suitable PhD student to undertake element #1. Unfortunately not suitable candidate was found and this component was not commenced.

1.3.2 COMPONENT B: FIRE PROPAGATION AND TRANSITIONS

Principle investigators: Dr Miguel Cruz, Jim Gould (CSIRO).

Co-investigators: CSIRO research staff

The rate of development of point ignitions (new outbreaks and spotfires) is a limiting factor in achieving initial attack success in which a fire will either be suppressed or will escape initial attack and develop into an uncontrolled wildfire. That is, the acceleration phase of a bushfire, from ignition to quasi-steady spread, is often the only period in which direct

suppression efforts can be effective under extreme weather. Resources deployed to a fire are more likely to contain fires during this stage.

While there have been a number of efforts to study fire acceleration, developing an understanding of the fundamental processes involved in the combustion and dynamics of a bushfire as it is developing is essential in order to address this issue. This development occurs in two directions—horizontally in extent and vertically in fuel layers. A number of phase transitions in behaviour will occur as the fire develops in these directions: transition from ignition to surface fire propagation and rate of growth, transition from a surface fire to higher fuel strata culminating in crown fire, transitions involving convective interaction between the fire plume and the surrounding atmosphere, and ignitions of structures and other non-vegetative 'fuel' in the flame zone.

The critical hypothesis is that the rate of development of a fire ignition is dependent upon fuel moisture content, wind strength and the involvement of different fuel strata. More specifically this latter aspect may be extended to hypothesize that ladder fuels are a significant contributor to the ignition of the canopy strata in eucalypt forests and that crown fire propagation in eucalypt forests is dependent on the energy released by the combustion of sub-canopy fuels.

The proposed work plan of this component consisted of two primary elements:

1) Quantification and analysis of the effect of moisture content, wind speed, and fuel type and condition on rate of propagation of individual ignitions. This will analyse historical datasets of point and line ignition field experiments (e.g. CSIRO unpublished/archived data, Project Aquarius (requiring CSIRO and DEC approval for use)) as well as additional controlled experiments in the CSIRO Pyrotron and the field under a fixed range of fuel, weather and atmospheric conditions. From the analysis a model of fire ignition propagation to steady-state behaviour for dry eucalypt forests will be developed. To be completed by CSIRO research staff with in-kind contributions from DEC WA.
2) Determine the factors involved in the transition from moderate intensity flame in forest surface fuels to very high intensity fires that involve multiple layers of fuels including tree canopies (i.e. crown fire). To be completed by CSIRO research staff.

Prerequisites: It was identified early on that the success of this component was dependent upon successful execution of laboratory and possibly field experiments under an adequate range of fuel, weather and topographic conditions.

1.3.3 COMPONENT C: FIRE LOAD AND SUPPRESSION RESOURCING

Principle investigator: Dr Matt Plucinski

Co-investigators: Post-graduate scholar, supervising university, fire agencies.

Fire load is the number, extent and behaviour of active fires in a region of interest and it varies considerably with time and space. Suppression resourcing must be able to cope with a given fire load for most of the fire season, accepting that there will occasionally be peak times when the fire load will overwhelm resources. The optimal amount and type of suppression resources for a given region can be determined through the application of a

resource allocation tool. The critical hypothesis for this work is that fire load can be reliably predicted from forecast weather.

The proposed work plan for this component consisted of three elements:

1) Development of fire occurrence models for regions of Australia. This will require collection, collation and analysis of historical fire data from state land management and rural fire agencies in order to develop a predictive model of the number of new fire outbreaks in a defined region based on dynamic variables (including weather). To be completed by CSIRO research staff in conjunction with fire agencies.
2) Development of suppression productivity and response models. This will involve the collection of data and elicitation of expert knowledge from within agencies on the performance of specific resource types in rural and peri-urban study regions within each jurisdiction involved and under as broad a range of conditions as possible. To be completed by a suitable Postgraduate (Master of Science level) student supervised by appropriate University staff.
3) Development of a resource allocation framework. Combining suppression productivity and response models (C2) and fire load models (C1), a prototype framework for resource allocation models appropriate for Australian fire environments (physical and jurisdictional) will be developed. This framework will enable the future development of tools to examine the effects of fire management policies and budgets, and compare the overall effectiveness and efficiency of different suppression resources. To be completed by CSIRO research staff.

Prerequisites: It was identified at the outset that the successful completion of Component C2 was dependent upon the timely commencement of a suitable mature age and/or agency-based MSc student capable of undertaking this work with minimal supervision from CSIRO. This did not occur until 20 months into the project. This element was further delayed when the MSc student went on extended leave and so activity on this element has been significantly delayed and will not be reported in detail in this report.

1.3.4 OUTCOMES

The rate of development of a fire determines whether it can be suppressed by initial attack or will escape to potentially develop into an uncontrolled fire. Under most fire weather conditions it is only during the early developmental period of a fire (from ignition to quasi-steady spread) in which direct suppression efforts will be effective.

The outcome of this research project will be new fire behaviour knowledge that can be incorporated into existing fire behaviour modelling systems or used to improve planning for prescribed burning operations. This knowledge, directly linked to suppression resourcing requirements through a resource allocation model potentially based on a fire load predicted for any given day, month and season, will provide support for evolving fire management decision needs, including community warnings, planning, operations, monitoring and assessment.

1.4 Limitations and restrictions

As noted in section 1.3 above, each research element had a number of prerequisite requirements in order for the research to commence and results to be produced. As best as could be managed, the individual research elements were designed to be as separate from each other as possible so that there was a minimum of dependency between each element and each element could be run in parallel. Those research elements that were identified as being central to other research organisations (such as element A.2 and C.2) were removed from the project and ran by those organisations under a separate contract with no dependencies.

Key prerequisites were generally of the form of input data, either from the end user agencies or other organisations such as the Commonwealth Bureau of Meteorology. The details of the success of obtaining research prerequisites are present in the corresponding chapter.

The primary source of limitation in this project was the reliance upon experimental data to be generated during the project. The risks of conducting such experiments were mitigated somewhat by utilisation of the CSIRO Pyrotron laboratory facility (Sullivan *et al.* 2013). While such facilities are designed to minimise the impact of deleterious weather conditions on experimental success, such effects cannot not be totally removed. As a result, operation of the Pyrotron still remains somewhat exposed to ambient weather conditions.

The use of fuel conditioning methodologies using a large walk-in oven and formalised approval to conduct experimental burns in the Pyrotron on days of Total Fire Ban improves the probability of achieving experimental objectives.

This reliance upon predominantly laboratory-based experimentation means that any results and conclusions drawn there from must be treated with care until suitable field-based validation can be undertaken.

1.5 End user engagement

Dr Simon Heemstra, NSW Rural Fire Service, acted as the project's End-user Leader. In this role, Dr Heemstra provided input into the direction and detail of the project and provided feedback on developments and milestones throughout the life of the project.

Results of the project were presented to end users annually at the Bushfire CRC Research Advisory Forum.

Five Bushfire CRC FireNote publications detailing aspects of the project and progress were prepared during the life of the project. See Appendix 1.

Six research posters detailing aspects of the project and progress were prepared and presented at the annual AFAC/Bushfire CRC conference during the life of the project. See Appendix 2.

A Bushfire Science Symposium was organised and run during the closing stages of this project (October 2013) to celebrate 60 years of Commonwealth bushfire research in Australia and to present to fire behaviour practitioners and other end users the findings of this research project in the context of other bushfire behaviour science developments. See Appendix 3 for a copy of the symposium program.

At every opportunity throughout the life of this project researchers engaged with end users to promote the project, its objectives and results.

1.6 This report

The structure of this report follows that of the project. Each major element of the project provides a chapter in this report; each chapter is a standalone representation of the research conducted in that element and can be read as such or in conjunction with the other research elements.

The order of elements (and primary investigator and author) is:

1. Fire occurrence (M. Plucinski)
2. Fire initiation (P. Ellis)
3. Fire growth (J. Gould)
4. Fire transitions (M. Cruz)
5. Suppression allocation framework (M. Plucinski)

These are followed by a discussion and conclusions chapter in which the outcomes of the project are put into a general context and possible future work is outlined.

1.7 References

Cheney, NP, Gould JS (1995) Fire growth in grassland fuels. *International Journal of Wildland Fire* **5**, 237-247.

Cheney NP, Gould JS (1997) Fire growth and acceleration. *International Journal of Wildland Fire* **7**, 1-5.

Cheney NP, Gould JS, Catchpole WR (1993) The influence of fuel, weather and fire shape variables on fire-spread in grasslands. *International Journal of Wildland Fire* **3**, 31-44.

Ellis PFM (2000) The aerodynamic and combustion characteristics of eucalypt bark: A firebrand study. PhD Thesis, The Australian National University School of Forestry.

Ellis PFM (2010) The effect of the aerodynamic behaviour of flakes of jarrah and karri bark on their potential as firebrands. *Journal of the Royal Society of Western Australia* **93**, 21-27.

Ellis PFM (2011) Fuel bed ignition potential and bark morphology explain the notoriety of the eucalypt messmate `stringybark' for intense spotting. *International Journal of Wildland Fire* **20**, 897-907.

Ellis PFM (2013) Firebrand characteristics of the stringy bark of messmate (Eucalyptus obliqua) investigated using non-tethered samples. *International Journal of Wildland Fire* **22**, 642-651.

McAlpine R, Wakimoto R (1991) The acceleration of fire from point source to equilibrium spread. *Forest Science* **37**, 1314-1337.

McArthur AG (1966) *Weather and Grassland Fire Behaviour*. Forestry and Timber Bureau Leaflet 100, Commonwealth Department of National Development.

McArthur AG (1967). *Fire Behaviour in Eucalypt Forests*. Forestry and Timber Bureau Leaflet 107,Commonwealth Department of National Development.

Sullivan AL, Knight IK, Hurley R, Webber, C (2013) A contractionless, low-turbulence wind tunnel for the study of free-burning fires. *Experimental Thermal and Fluid Science* **44**, 264-274.

2 Fire occurrence

2.1 Introduction

The term fire occurrence is used to describe the spatial and temporal distribution of fires. Fire occurrence statistics account for all reported ignitions regardless of the area they burn or damage they cause. Historical fire data, incorporating timing, location and cause information for all incidents, is the basis of fire occurrence research (Finney 2005). Such data is typically sourced from fire and land management agency records and is combined with other environmental and geographical data such as weather, vegetation, terrain, and land use for analysis. Fire occurrence analyses and predictions provide important information for a variety of fire management functions including the planning of resource allocation and mitigation and risk reduction treatments.

2.1.1 FIRE OCCURRENCE RESEARCH

This section gives an overview of previous fire occurrence research. A more comprehensive review was written as a project milestone (see Plucinski 2011). Fire occurrence research has largely been undertaken to gain a better understanding of factors influencing wildfire ignitions, and to develop models that can be used to predict the probability of ignition in different areas. The availability of fire records has restricted fire occurrence research in the past. Recent trends for increased data capture within fire agencies in many countries and advances in computer programs designed for data analysis and modelling have enabled more research to be undertaken in this field, as demonstrated by the large number of papers published in the last few years. Most of these have focussed on spatial distributions.

Fire occurrence research has tended to focus on spatial and temporal issues separately, although some gridded temporal studies have also considered basic spatial variables. Spatially-based fire occurrence research is primarily concerned with the spatial distribution of ignitions in relation to geographic variables, such as terrain and human landscape features. This research relies on fire data with ignition point locations from multiple years and does not generally consider dynamic weather or time variables. Spatial fire occurrence analysis requires geographic data encompassing terrain, vegetation and human factors such as land tenure, population density and infrastructure. Predictor variables for these fields are either proximity measures, such as the distance between an ignition and the nearest road or town, or density measures.

Spatial fire occurrence research has been used to identify areas with high ignition risks (e.g.: Cardille and Ventura 2001; Díaz-Delgado *et al.* 2004; Syphard *et al.* 2008; Beverly *et al.* 2009; Catry *et al.* 2009; Liu *et al.* 2012). Findings from spatial fire occurrence analyses can be used to target fire management actions, such as the identification of the best locations for fuel treatments or dynamic allocation of suppression resources (Wotton 2004; Wotton and Martell 2005; Syphard *et al.* 2008; Dlamini 2010). Spatial fire occurrence analyses can also be used to judge the effectiveness of prevention programs (Donoghue and Main 1985; Donoghue *et al.* 1987).

Temporal fire occurrence research has also been undertaken to study the distribution of ignitions with time, and to predict the probability of a fire day and to estimate the number of fires that may occur on a given day. These studies are based on meteorological variables,

including weather indices and fuel moisture models, as well as variables classifying day type (e.g. weekend/weekday). These studies have tended to avoid spatial variables by dividing the landscape into units with similar spatial characteristics (e.g.: Cunningham and Martell 1973; Martell *et al.* 1987). Some studies have considered spatial variables by applying a grid across a landscape and considering the probability of fires in each cell at specified time steps (e.g.: Haines *et al.* 1983; Preisler *et al.* 2004; Reineking *et al.* 2010; Padilla and Vega-García 2011; Magnussen and Taylor 2012).

Predictions from temporal fire occurrence models can be used to estimate the potential load on suppression resources that a fire management agency will face, enabling them to plan levels of preparedness and manage resource locations (Haines *et al.* 1983; Tithecott 1992; Wotton 2004; Wotton and Martell 2005; Wotton *et al.* 2010). These actions help optimise suppression effectiveness by enabling planning that maximises resource availability and reduces response times, thereby increasing the probability of initial attack success (Todd and Kourtz 1991; Podur and Wotton 2010; Wotton *et al.* 2010).

Some fire occurrence research has been specifically undertaken to investigate the occurrence of large fires (e.g.: Dickson *et al.* 2006; Preisler and Westerling 2007; Preisler *et al.* 2008; Bermudez *et al.* 2009; Bradstock *et al.* 2009; Drever *et al.* 2009; Preisler *et al.* 2009; Hély *et al.* 2010; Mendes *et al.* 2010; Moreira *et al.* 2010). These studies aim to identify the conditions when fire management is unable to cope with the fire load. Occasionally, temporal fire occurrence and large fire occurrence studies have been undertaken to investigate the relationship between fire danger and fire occurrence as a means of determining the suitability of fire danger indices for a region (e.g.: Haines *et al.* 1983; Viegas *et al.* 1999; Andrews *et al.* 2003; Preisler *et al.* 2004; Preisler *et al.* 2009; Padilla and Vega-García 2011).

The factors that affect fire occurrence depend on ignition cause. Most fire occurrence studies have only considered bushfires attributed to a single cause type (e.g.: Wotton *et al.* 2003; Wotton and Martell 2005; Padilla and Vega-García 2011) or have considered bushfires from lightning and human causes separately (e.g.: Reineking *et al.* 2010; Vilar *et al.* 2010a; Wotton *et al.* 2010; Magnussen and Taylor 2012). This is because lightning and human caused ignitions are affected by distinctly different processes and have different temporal and spatial distributions

Fire occurrence research has always been applied to defined regions associated with management, environmental or political boundaries. This research has been undertaken in a variety of regions, with most papers originating from USA, Canada and Southern Europe. Fire occurrence related papers originating from Australia have considered causal factors for lightning-ignited fires (McRae 1992; Dowdy and Mills 2012b; Dowdy and Mills 2012a), the weather conditions on days of high fire activity in the Mallee region of Victoria (Krusel *et al.* 1993) and the spatial patterns of human and lightning caused fires in the Sydney region of NSW (Penman *et al.* 2013). No papers have specifically investigated the temporal patterns of Australian wildfires, which could be different to that in experienced in other countries because of the unique climate, vegetation and culture. The recent work of Penman *et al.* (2013) found that the distribution of human and lightning caused fires within the Sydney region to be consistent with that found in previous North American studies, with human ignitions most likely to be close to infrastructure such as roads and houses and lightning more frequent on ridges with no association with infrastructure.

2.1.2 FIRE OCCURRENCE WORK UNDERTAKEN IN THIS PROJECT

The remainder of this chapter provides an overview of the fire occurrence research that was undertaken within the Fire Development, Transitions and Suppression project. This work was focussed on temporal patterns of bushfire ignitions and used the south-west corner of Western Australia as a case study area, utilising fire incident records from the Department of Fire and Emergency Services (DFES[1]) and the Department of Parks and Wildlife (DPAW[2]). The main components of this work were an investigation of the timing of fires from different causes (Section 2.2) and the development of models predicting the number of daily fires within management regions (Section 2.3).

2.2 The timing of fires from different causes

2.2.1 INTRODUCTION

Unplanned bushfires originate from a range of ignition sources. Knowledge of the temporal patterns of vegetation fires that originate from different causes and the relationships that they have with weather conditions and fuel availability can lead to improvements in fire prevention and response by allowing fire agencies to proactively focus their efforts at times when fires are more likely to start (Asgary *et al.* 2010, Gonzalez-Olabarria *et al.* 2012). Fire agencies undertake a range of activities to prevent fires including implementing fire restrictions, such as total fire bans, and undertaking public education and awareness campaigns.

The ignitibility of bushfire fuel is determined by its moisture content (Anderson 1970, Nelson 2001), a link that has been well established in studies of ignition (e.g. Plucinski and Anderson 2008, Cruz *et al.* 2013). The occurrence of wildfire ignitions has been linked to the moisture content of dead surface fuels in many analyses of wildfire incident data (Viegas *et al.* 1992, Wotton *et al.* 2003, 2010, Reineking *et al.* 2010, Magnussen and Taylor 2012).

Little of the published research has focussed on the effect of timing and weather on the occurrence of outdoor fires from different causes in human landscapes. Some studies have investigated spatial and temporal distributions of a range of fire incident types in urban areas (e.g. Chhetri et al 2009, Asgary 2010, Corcoran et al 2011) but have not considered how these vary with cause. These studies have found variability in the timing of different types of fire, with structure fires occurring more frequently during winter periods and outdoor fires occurring more often in summer and during drier conditions (Chandler 1982, Holborn *et al.* 2003, Corcoran et al 2007, 2011). While some of these studies have considered outdoor fires, they have not broken them down into sub-categories, such as rubbish and vegetation fires or considered variation due to ignition cause or day to day weather.

The objective of this study is to investigate the timing of vegetation fires from different causes in urban and peri-urban areas using the city of Perth and its surrounds as a case study. Timing is considered at a range of scales (hourly, daily, monthly and annually) and in

[1] The Department of Fire and Emergency Services was known as the Fire and Emergency Services Authority (FESA) until 31 October 2012.
[2] The Department of Parks and Wildlife was known as the Department of Environment and Conservation (DEC) until 30 June 2013.

terms of weather variables related to wildfire danger and fuel availability. Ignition causes that have unusual time profiles are identified and discussed.

2.2.2 STUDY AREA AND DATA

The greater Perth area considered in this study (Figure 2.1) covers a variety of land uses, including residential, agricultural, forestry, industrial, conservation and recreational, and vegetation types including pasture grasses, dry eucalypt forest and woodlands, shrubland and suburban parks and gardens (Grose 2009). The region experiences a Mediterranean climate with a long dry period over the summer and autumn.

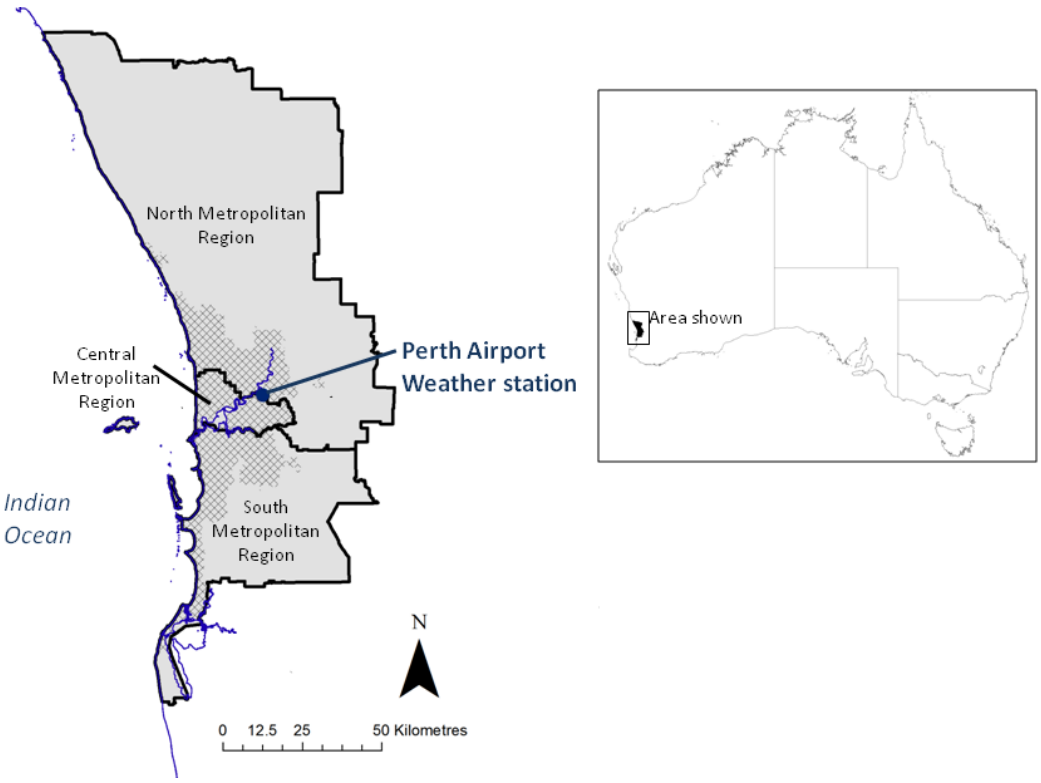

Figure 2.1. Location of the study area and the weather station used. The cross-hatching shows the extent of urbanised areas.

Vegetation fire incident records were obtained from DFES for the period 1 July 2004 to 30 June 2012. These records conform to the Australian Incident Reporting Standard (AIRS) (AFAC 2013), a national data standard that many fire agencies use for collecting, recording and reporting information about fire incidents that they attend (AFAC 2013). The data fields used for this analysis were “ignition heat form”, “ignition factor” and “report time”. The ignition heat form field lists the heat source that caused the ignition and may include items such as matches, cigarettes or hot sparks. The ignition factor field categorises the reasons for ignition heat sources combining with combustible material and starting a fire. Both of the ignition heat form and ignition factor fields require the ignition point to be located and investigated.

The report time field identifies the time that the agency was notified of the fire. In most cases detection and reporting are likely to come soon after ignition due to the relatively dense population in the study area; however some ignitions may lead to smouldering fires or may grow very slowly and go undetected for some time.

The DFES database contained 87 specific ignition heat form types and 85 specific ignition factor types. These fields were used to determine 17 ignition cause categories for this

analysis (Table 2.1), including two natural, three deliberate and ten accidental cause categories, and two categories for fires from undetermined causes. These categories were the smallest units that the data could be broken down into based on the AIRS fields. Records from DPAW were not used in this analysis because they had fewer categories for ignition cause and these did not readily translate to those available in the DFES database, particularly with the many types of accidental ignition cause. DPAW fires only comprised of 5.5% of the total vegetation fires that occurred in the study region and timeframe.

Table 2.1. Descriptions for the different ignition cause categories considered in this analysis.

CAUSE TYPE	CAUSE CATEGORY	DESCRIPTION
Natural	Lightning	Heat for ignition attributed to lightning strikes
	Spontaneous combustion	Spontaneous combustion of materials such as mulch or other organic debris
Deliberate	Incendiary	Arson, where a legal decision had been made or physical evidence could be used to prove that the fire was deliberately set
	Suspicious (known cause)	Circumstances indicated that fires were likely to be deliberately set (i.e. probably arson), with the ignition source identified
	Suspicious (unknown cause)	Circumstances indicated that fires were likely to be deliberately set (i.e. probably arson), however the ignition source was not or could not be identified
Accidental	Cigarettes and smoking material	Accidentally ignited by a cigarette or other smoking material
	Small open fires	Accidentally ignited by a small open fire, such as a camp fire, bonfire, or rubbish fire
	Inadequate control of burn offs	Escaped fires deliberately ignited for a management purpose, such as reducing fuels, removing stubble or pasture improvement
	Cutting or welding	Heat for ignition attributed to cutting or welding equipment
	Matches or lighter	Heat for ignition attributed to matches and other lighters such as cigarette lighters
	Fireworks and explosives	Heat for ignition attributed to fireworks or explosives
	Electrical failure	Ignition heat form attributed to malfunctioning electrical equipment, including powerlines and electrical devices
	Mechanical failure	Ignition heat form attributed to malfunctioning machinery causing ignition through the generation of sparks, arcs, or heat
	Vehicle	Ignition linked to heat or sparks from a vehicle
	Re-kindled from a previous fire	Re-ignition from a previously extinguished unplanned fire
Undetermined	Other	Other minor ignition causes not categorised elsewhere in the database
	Undetermined or not reported	Ignition cause was not able to be determined or was not reported

Hourly weather data were obtained from the Perth Airport Bureau of Meteorology weather station (-31.93 °S, 115.98 °E) and included observations of air temperature, relative humidity, wind speed and rainfall. Weather records from 1 January 2000 were used to allow time for drought indices to stabilise prior to the start of the study period (1 July 2004). Missing weather observations were supplemented with observations from the nearby Perth Metropolitan weather station (-31.92 °S, 115.87 °E).

Grassland Fire Danger Index (GFDI, McArthur 1966), Forest Fire Danger Index (FFDI, McArthur 1967) and surface fuel moisture content (SFMC) were calculated from weather observations. GFDI and FFDI were calculated using Noble *et al.*'s (1980) equations. FFDI was also used in this study because calculations for GFDI were based on an assumption that curing was constantly 100%. This assumption was required as there were no records of curing available to the study. It would have led to a significant over estimation of GFDI in the cooler and wetter times of the study period. All inputs for FFDI came from weather observations. The drought factor input was calculated using the Soil Dryness Index (Mount 1972), which is the preferred drought index for Western Australian fire agencies (Burrows 1987). SFMC was used to indicate the availability of the fine fuel for ignition and was determined using Matthews' (2006) model. Unlike the fire danger indices, SFMC is not sensitive to wind speed.

2.2.3 ANALYSIS METHODS

The timing of vegetation fires from each cause category were investigated at four scales: annual (8 years considered from July 1 to June 30); month of the year; day of the week; and hour of the day. The proportion of fires occurring in each element (year, month, day, hour) within these time scales were determined for all fires in the dataset and for fires from each cause category to establish time profiles for each individual cause class and for fires from all causes. Time profiles were also established for GFDI, FFDI and inverse SFMC, by determining the proportion of total sum for each of these that occurred within each time element. SFMC was inversed so that it would have a profile shape similar to the fire danger indices and ignitions. Each ignition cause profile was compared to the three weather profiles in order to determine the relationship between them. This was done using mean squared error (MSE) (Willmott 1982), which provided a suitable relative measure at each time scale.

Relationships between each of the cause categories and weather were further investigated by converting hourly GFDI, FFDI and SFMC values to deciles and determining the proportion of fires from each cause category occurring in each decile. This was done to produce profiles similar to those developed for the time scales. GFDI, FFDI and SFMC were considered as deciles because they have highly skewed distributions and this allowed the formation of groups with equal portions of time within the study period.

Cause categories that had unusual timing (i.e. different to the timing of fires from all cause categories) were identified using a method based on the MSE weighted by the number of observations in each group (see: Wickham in prep.). MSE comparisons that are not weighted by observation size would suggest that cause categories that have few observations are more likely to be unusual than those that have higher sample sizes. The MSEs between each cause profile and the profile for all causes were determined. These were then weighted by applying a linear model to the log of the number of fires and the log of the MSE for each cause category. The residuals from the linear model provided an estimate of the difference between the time profiles for fires from one cause category and that for fires from all cause categories. Cause categories with the highest residuals were those with the most unusual time profiles. In this study most of the residual plots for the different time scale and weather deciles had a break in residuals centred around 0.75 with only a few points greater than this. For this reason cause categories with residuals greater than 0.75 were considered to have timing profiles that were different to that of those for all causes in this study.

The effect of total fire bans was investigated by comparing the daily mean number of fires per day for all days to the number of fires experienced on days where the GFDI was exceeded 50. This is the cut off used for setting total fire bans in the study area and had to

be used in the absence of records of days that were declared total fire bans. Total fire ban declarations are made by DFES using forecast weather conditions across the study region using GFDI and may also consider other factors, such as resource availability and existing incidents. The majority of declared total fire ban days that occurred during the study period would have had GFDIs greater than 50, so would have been identified using this method.

2.2.4 RESULTS

There were 31,271 vegetation fires that occurred in the DFES Metropolitan fire management areas during the eight year period (2922 days) in the DFES database. The majority (55.24%) of these were attributed to one of the three deliberate cause categories, with suspicious fires from known causes being the most common individual cause category (Table 2.2). In contrast to this, there were very few fires (1.17 %) from natural causes. Fires attributed to accidental causes comprised 29.81% of the data, with cigarettes and smoking material being the most common of these. Fires with unknown causes comprised 13.92% of the dataset.

Table 2.2. The number, percent and mean number of vegetation fires per day on all days and total fire ban days for each cause category

CAUSE CATEGORIES	TOTAL NUMBER	% OF TOTAL
Lightning	171	0.55
Spontaneous combustion	150	0.48
Incendiary	3322	10.62
Suspicious (known cause)	11227	35.90
Suspicious (unknown cause)	2728	8.72
Cigarettes and smoking material	3955	12.65
Small open fires	252	0.81
Inadequate control of burn offs	786	2.51
Cutting or welding	165	0.53
Matches or lighter	1206	3.86
Fireworks and explosives	112	0.36
Electrical failure	496	1.59
Mechanical failure	699	2.24
Vehicle	57	0.18
Re-kindled from a previous fire	1593	5.09
Other	925	2.95
Undetermined or not reported	3427	10.96

The number of fires per year varied between 2803 and 4308 over the study period with a decreasing trend (Figure 2.2). The mean fire danger and fuel moisture conditions experienced during each fire season within this period were relatively uniform, other than slightly higher fire danger indices and lower fuel moisture contents during the 2010/11 season and lower fire danger indices during the 2005/06 season. Fires attributed to cigarettes and smoking materials and undetermined causes had profiles that were similar to that for GFDI, FFDI and inverse SFMC. Other causes exhibited year to year variation that was different to that of the weather variables.

The cause categories that had time profiles that were most different to that for all causes, once samples size had been considered, were lightning, cigarettes and smoking materials and suspicious fires of known causes (Figure 2.2). The suspicious fires of known cause appear to have a declining trend that is greater than that for fires from all causes over the eight fire seasons considered. The highly variable profile within the lightning plot reflects the fact that lightning fires occur on very few days, but these days usually have multiple lightning ignitions (Dowdy and Mills 2012a, McCaw and Read 2012). Highly variable profiles for fires from other cause categories (e.g. fireworks and vehicles) are likely to be influenced by the small observation sizes.

The monthly time profile for vegetation fires from all cause categories sees the majority of ignitions occurring during the summer months (Figure 2.3), which is when the fire danger is highest and fuels are at their driest. This profile is very similar to that of FFDI. Fires attributed to the deliberate and undetermined cause categories had profiles that were very similar to those for GFDI, FFDI and inverse SFMC.

There were five cause categories that had monthly profiles different to that for all causes (Figure 2.3). Four of these (lightning, cigarettes and smoking materials, fireworks and explosives and rekindled previous fires) had exaggerated seasonal profiles with higher proportions of fires in the summer months and fewer in the cooler months. Of these the most exaggerated was the fireworks and explosives cause category. The fires that originated from escaped burn offs occurred mostly in autumn and spring which are the times of the year that most burn offs are undertaken in this region. Burn offs are less likely to occur during winter because the fuels are usually too wet to sustain fire, where as in summer, the risk of escape is much higher and restrictions apply.

The daily profile for vegetation fires from all cause categories show that fires are more likely to occur on weekends than during the week (Figure 2.4). The profile for weather was relatively flat across the days of the week and only fires attributed to cigarettes and smoking material had a similar profile to it.

The cause categories that had daily profiles most different to that for all cause categories were lightning, suspicious fires of known cause, cigarettes and smoking material, cutting and welding and fireworks and explosives (Figure 2.4). Lightning-caused fires had a highly variable daily profile, which is likely to be related to the dataset containing a few days with multiple lightning-caused fires. Similarly, fires caused by cutting and welding activities had peaks on Mondays and Wednesdays, but were based on only 165 fires. Suspicious fires from known causes had slightly more ignitions on weekends and fewer on weekdays. Most ignitions attributed to fireworks and explosives occurred on Fridays, Saturdays and public holidays.

Fires from most cause categories have greater occurrence rates on weekends, public holidays, days when children are not attending school and days where the fire danger rating was very high or extreme (Table 2.3). There were 64 days within the study period where the GFDI exceeded 50 and total fire bans were likely to have occurred. Fires from all cause categories, except for vehicles, had higher rates of occurrence on these days. Fires attributed to electrical failures, fireworks and explosives, rekindled previous fires, cigarettes and smoking materials and lightning had daily occurrence rates on these days that were four or more times greater than for all days. Fires caused by cutting and welding, small open fires, incendiary arson, lightning and vehicles had higher rates of occurrence on days of very high fire danger than days of extreme fire danger when total fire bans are likely to have been declared.

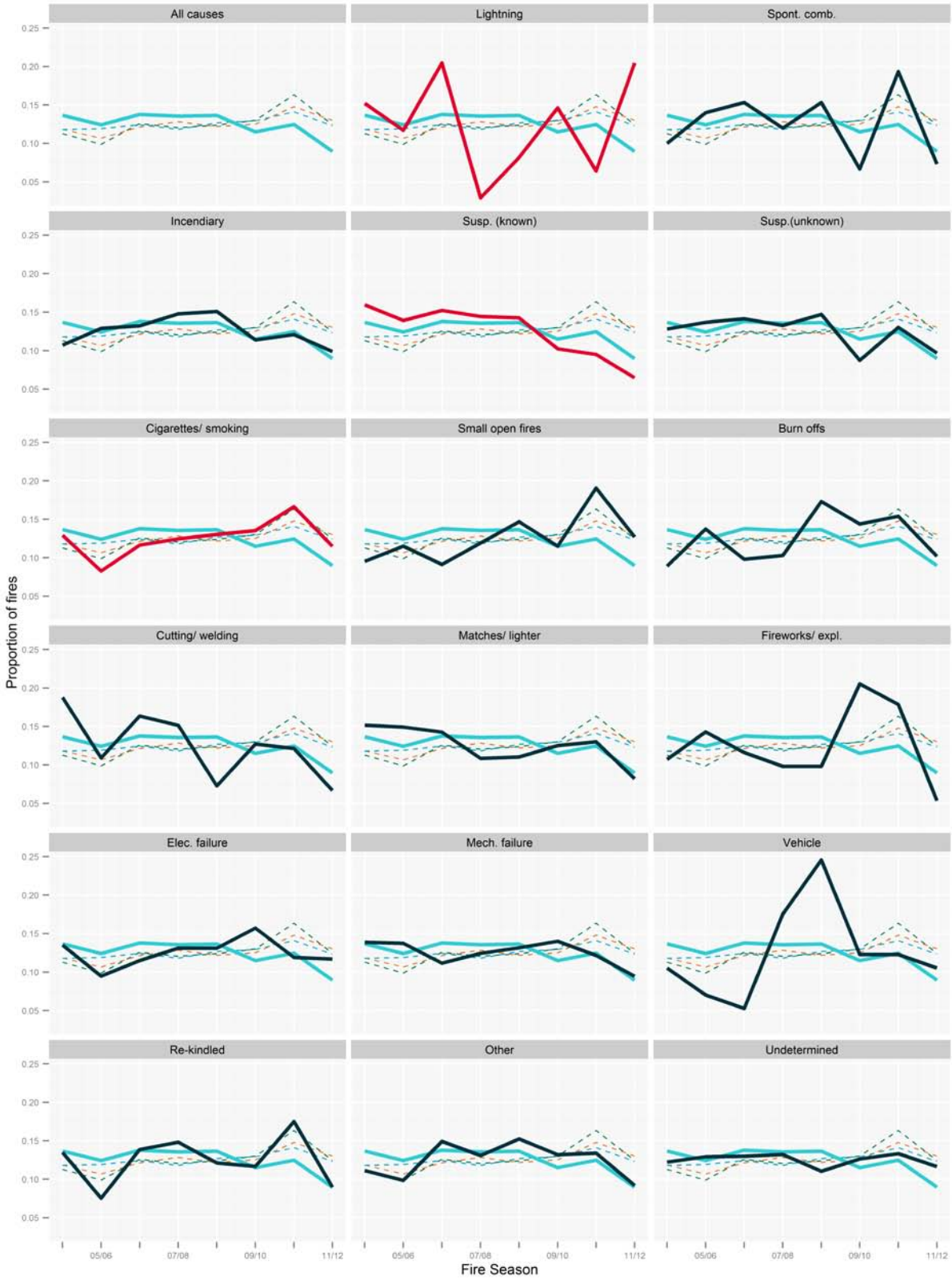

Figure 2.2. Yearly profiles for cause categories (black). The cause categories that had time profiles statistically different to those for all causes (top left panel) are shown in red and the inter-fire season time profile for all causes is shown in teal. Profiles for the GFDI, FFDI and inverse SFMC are shown by the thin dashed orange, green and blue lines respectively.

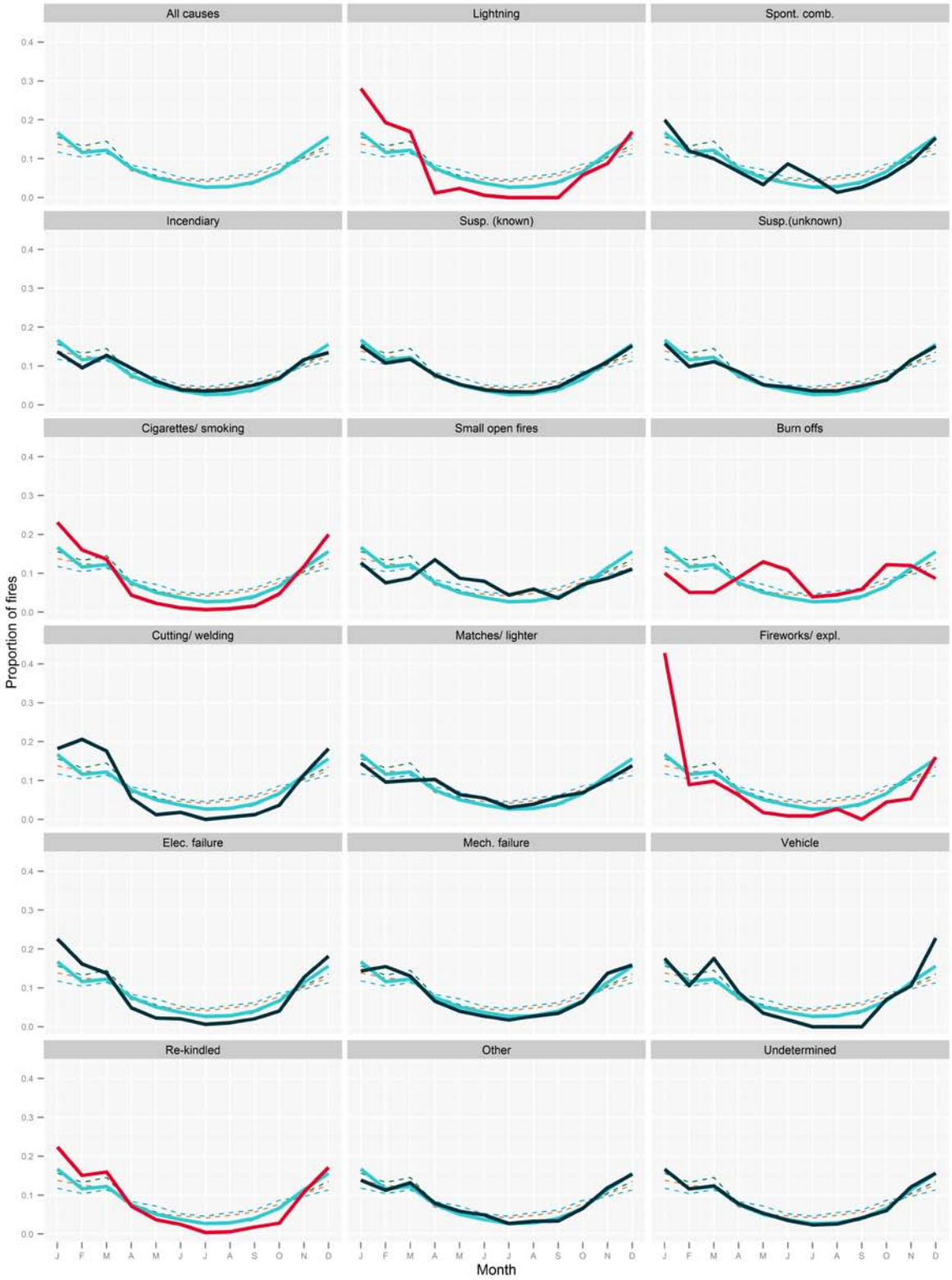

Figure 2.3. Monthly profiles for cause categories (black). The cause categories that had profiles statistically different to those for all causes (top left panel) are shown in red and the profile for all causes is shown in teal. Profiles for the GFDI, FFDI and inverse SFMC are shown by the thin dashed orange, green and blue lines respectively.

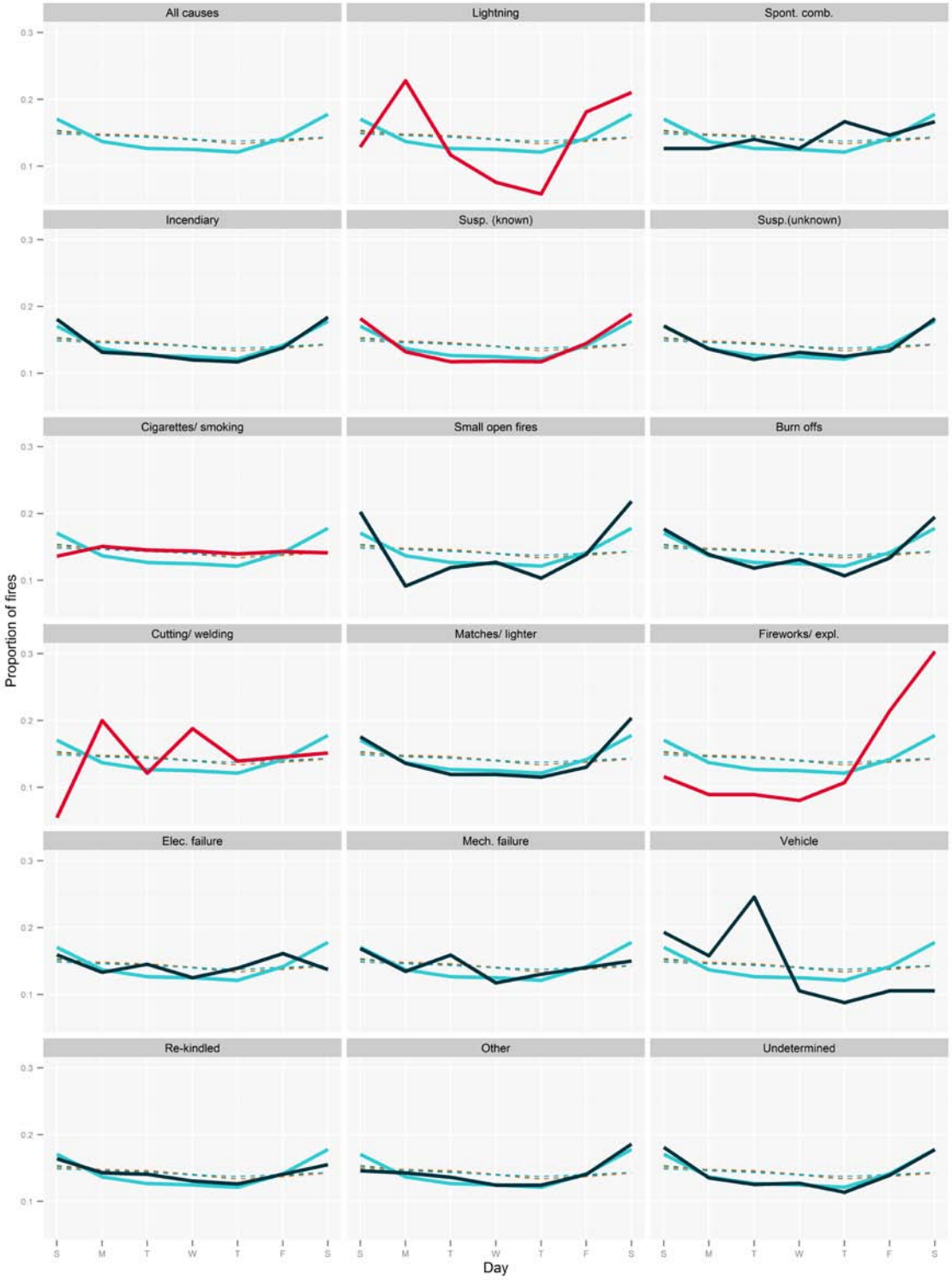

Figure 2.4. Daily profiles for cause categories (black). The cause categories that had daily profiles statistically different to those for all causes (top left panel) are shown in red and the profile for all causes is shown in teal. Profiles for the GFDI, FFDI and inverse SFMC are shown by the thin dashed orange, green and blue lines respectively.

The hourly profile for all vegetation fires is similar to the diurnal profile for inverse SFMC, which shows a 1-2 hour lag behind the fire danger indices (Figure 2.5). Fires attributed to electrical and mechanical failures, rekindled fires and undetermined causes had hourly profiles that were very similar to those for FFDI and GFDI.

Table 2.3. Mean number of fires per day type by cause category.

CAUSE CATEGORIES	ALL DAYS	WEEKENDS	PUBLIC HOLIDAYS	NON-SCHOOL DAYS	GFDI<32 (LOW, MOD, HIGH)	32<GFDI<50 (VERY HIGH)	GFDI>50 (EXTREME/ TOTAL FIRE BAN)
Lightning	0.06	0.07	0.06	0.07	0.03	0.28	0.23
Spontaneous combustion	0.05	0.05	0.03	0.06	0.05	0.09	0.14
Incendiary	1.14	1.45	1.73	1.40	1.03	2.11	1.91
Suspicious (known cause)	3.84	4.98	5.92	4.84	3.47	7.07	7.67
Suspicious (unknown cause)	0.93	1.15	1.61	1.15	0.83	1.79	2.17
Cigarettes and smoking material	1.35	1.31	1.81	1.57	1.02	3.92	5.83
Small open fires	0.09	0.13	0.18	0.11	0.08	0.07	0.09
Inadequate control of burn offs	0.27	0.35	0.55	0.32	0.26	0.35	0.29
Cutting or welding	0.06	0.04	0.06	0.05	0.05	0.16	0.09
Matches or lighter	0.41	0.55	0.57	0.52	0.39	0.64	0.74
Fireworks and explosives	0.04	0.06	0.16	0.06	0.03	0.07	0.19
Electrical failure	0.17	0.18	0.32	0.20	0.13	0.48	0.84
Mechanical failure	0.24	0.27	0.36	0.27	0.20	0.58	0.61
Vehicle	0.02	0.02	0.01	0.02	0.02	0.04	0
Re-kindled from a previous fire	0.55	0.61	1.12	0.66	0.41	1.61	2.39
Other	0.32	0.37	0.49	0.37	0.27	0.68	0.73
Undetermined or not reported	1.17	1.47	1.90	1.44	1.00	2.46	3.52
Number of days	2922 (100%)	835 (28.6%)	77 (2.6%)	1395 (47.7%)	2630 (90%)	228 (7.8%)	64 (2.2%)

The fire cause types that had hourly profiles that were most different to that for all causes were those caused by cigarettes and smoking material, cutting and welding, fireworks and explosives and re-kindled previous fires. The hourly profiles for fires caused by cigarettes and smoking material and cutting and welding exhibited exaggerated peaks, while re-kindled fires tended to occur earlier in the day than those from other causes. Fires caused by fireworks and explosives were more common at night, particularly in the hour following midnight. The profiles for fires attributed to deliberate causes showed higher representations during the night hours than for fires from all cause types. In contrast to this, fires attributed to rekindled previous fires, escaped burn offs and electrical and mechanical failures were less common at night than for fires from all cause types.

Fires from all cause categories had positive relationships with GFDI and FFDI deciles (Figures 2.6 and 2.7) and a negative relationship with SFMC (Figure 2.8). Fires caused by cigarettes and smoking material and cutting and welding had GFDI, FFDI and SFMC decile profiles that were different to those for all causes, while those resulting from re-kindled previous fires were sensitive to GFDI and FFDI. Ignitions attributed to these three cause classes are more sensitive to weather conditions than those from other causes, probably because they have a lower heat output.

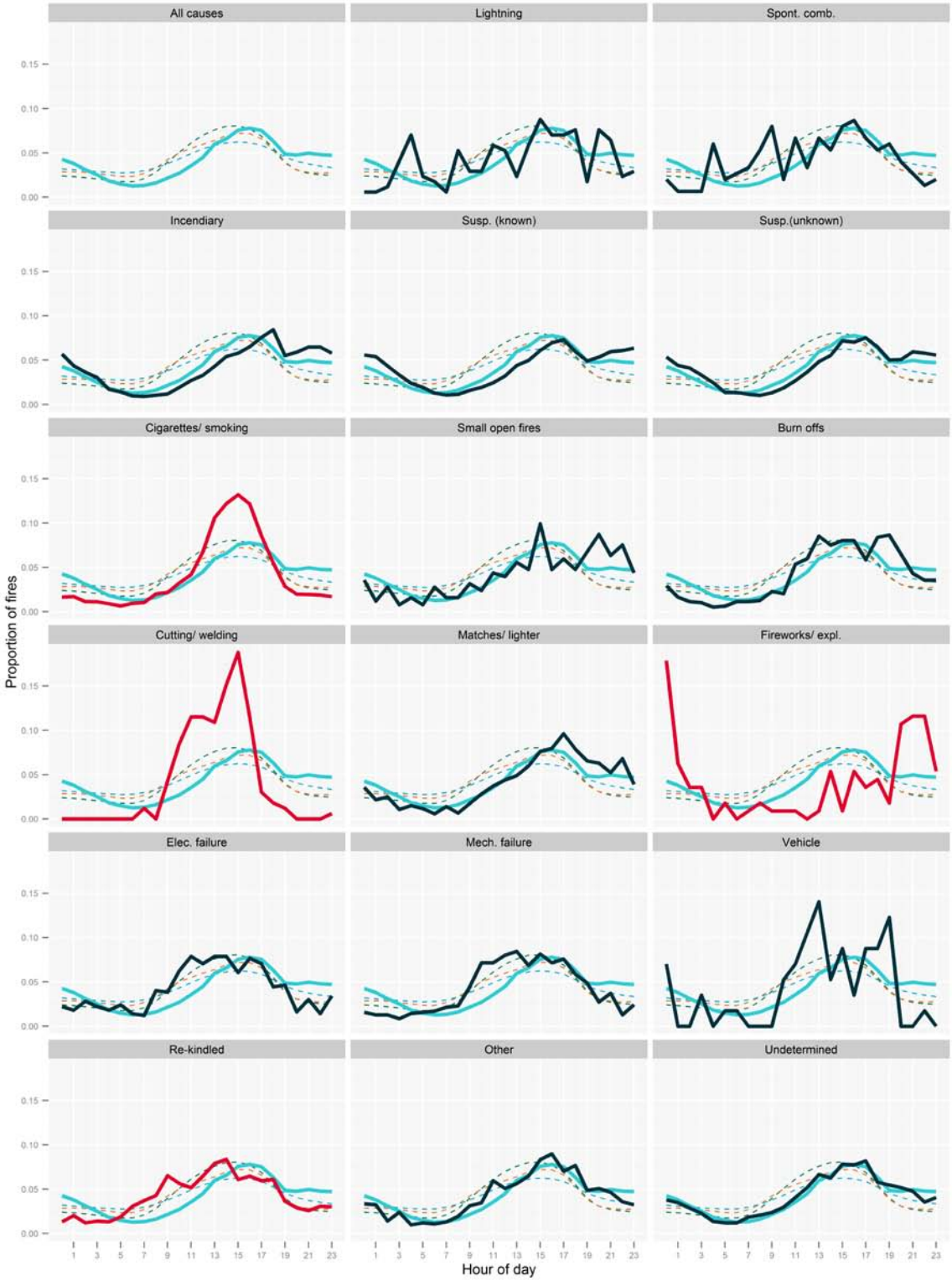

Figure 2.5. Hourly profiles for cause categories (black). The cause categories that had hourly profiles statistically different to those for all causes (top left panel) are shown in red and the hourly profile for all causes is shown in teal. Profiles for the GFDI, FFDI and inverse SFMC are shown by the thin dashed orange, green and blue lines respectively.

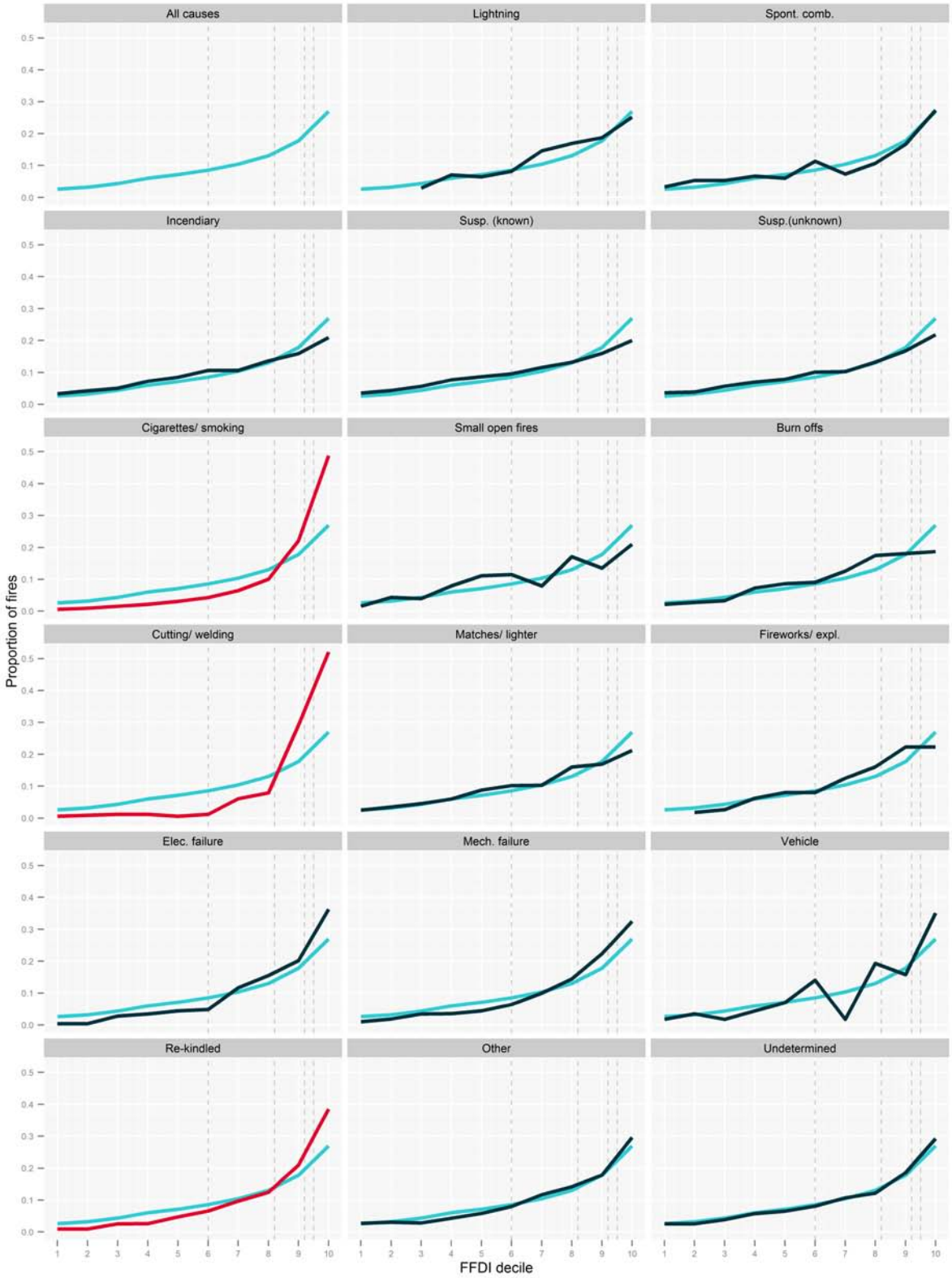

Figure 2.6. GFDI decile profiles for cause categories (black). The cause categories that had profiles statistically different to those for all causes (top left panel) are shown in red and the GFDI decile profile for all causes is shown in teal. The dashed vertical lines indicate the breaks for the different fire danger rating classes (low, moderate, high, very high, total fire ban).

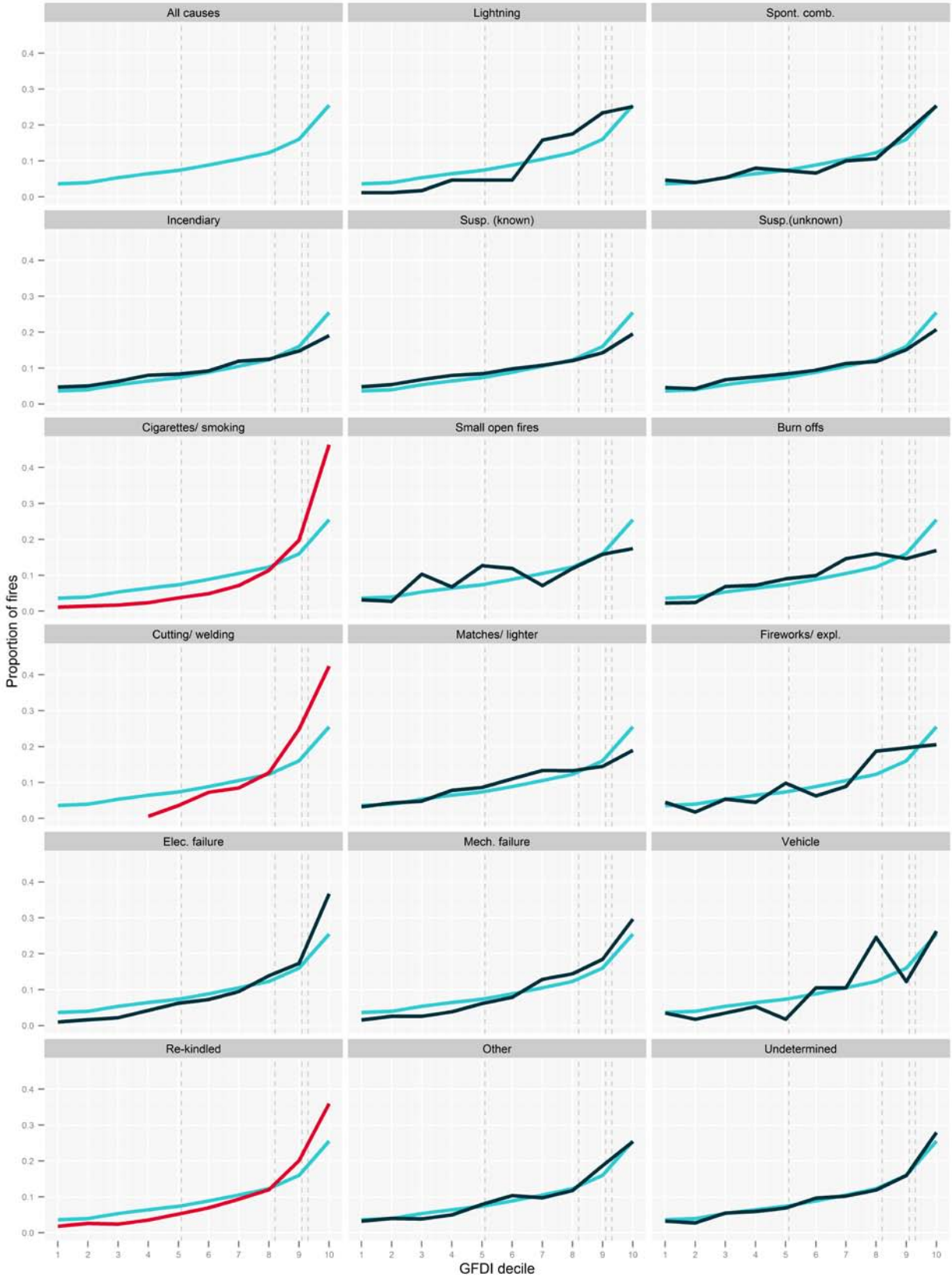

Figure 2.7. FFDI decile profiles for cause categories (black). The cause categories that had profiles statistically different to those for all causes (top left panel) are shown in red and the FFDI decile profile for all causes is shown in teal. The dashed vertical lines indicate the breaks for the different fire danger rating classes (low, moderate, high, very high, total fire ban).

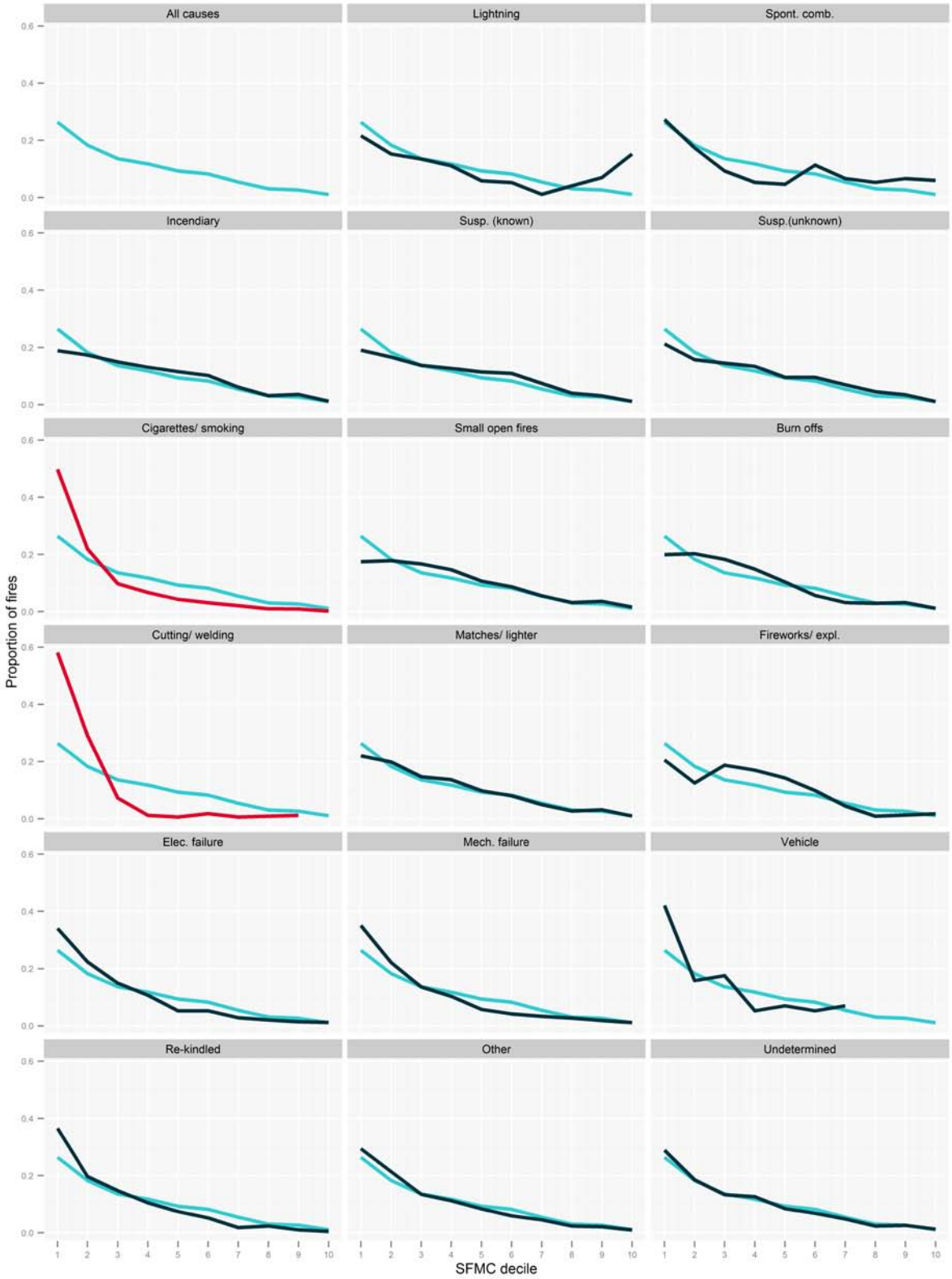

Figure 2.8. SFMC decile profiles for cause categories (black). The cause categories that had profiles statistically different to those for all causes (top left panel) are shown in red and the SFMC decile profile for all causes is shown in teal.

2.2.5 DISCUSSION

The incidence of vegetation fires within the Perth region is strongly related to fire danger and fuel moisture conditions, with ignitions from all cause categories being more frequent during periods of elevated fire danger. The different cause categories had a range of sensitivities to fire danger and fuel moisture. Some causes that have small heat outputs, such as cigarettes, cutting and welding, were more restricted to periods with elevated fire danger conditions and low fuel moisture than other causes.

The timing of vegetation fires is also dependant on the presence of the ignition source. In terms of human caused fires this relates to human activity, which varies according to day type, as indicated by the increased rates of ignition on weekends, public holidays and non-school days (Table 2.3). These relationships are consistent with the findings of previous studies that have investigated the timing of deliberate and accidental fires (e.g.: Chandler 1982, Holborn *et al.* 2003, Bryant 2008, Asgary 2010, Corcoran et al 2007, 2011).

The rate of ignitions on days that are likely to have been total fire bans is considerably higher for all cause categories except vehicles (Table 2.3). There are likely to be multiple reasons for this. Firstly, fuels are much more ignitable on total fire ban days. As a result, ignition sources that are unlikely to ignite fuels on any other day are more likely to result in successful ignitions on such days. These sources include those that have low heat outputs (e.g. cigarettes and sparks from cutting and welding equipment).

Secondly, there may be some undetected fires ignited on previous days that smoulder or burn slowly for extended periods. Increasing fire danger conditions on the mornings of total fire ban days can cause these hitherto quiescent fires to develop rapidly to detectable size. Finally, deliberate fires may be more common on these days as some arsonists may be alerted to the potentially devastating impacts of fires on such days due to the increased awareness of fire danger (Prestemon and Butry 2005, Bryant 2008, Corcoran *et al.* 2011, Prestemon *et al.* 2012).

Total fire ban restrictions limit the number of fires caused by cutting and welding and small open fires, which have considerably higher occurrence rates on days of very high fire danger compared to total fire bans (Table 2.3). Most of the other ignition cause categories had higher occurrence rates on total fire bans than days of very high fire danger. However, occurrence rates on very high fire danger days are still much higher than those for days with lower fire danger (Table 2.3). The high rate of ignitions on days of very high and extreme grassland fire danger is of concern given that the frequency of these days is predicted to increase under climate change (Pitman *et al.* 2007).

There was a general decline in the annual number of ignitions throughout the study period, which is mainly due to the reduction in deliberately caused fires (Figure 2.2). DFES, DPAW and the Western Australian Police have been implementing arson reduction activities in the study region since late 2001 (Smith 2004). These include a range of public education and fire awareness programs that are targeted at the whole community with an emphasis on children and their parents (Beale and Jones 2011). The Western Australian police also undertake patrols of areas with high arson rates on days of total fire ban. These are likely to curb deliberate ignition rates on these days. The education and awareness programs have developed over time and it is highly likely that the cumulative effect of these prevention efforts is influencing the decline in arson which is independent of annual variations in fire danger and fuel availability (Fig. 2.2).

High profile fire events also influence public fire awareness. In February 2011 a fire ignited by sparks from an angle grinder burnt through an area of urban bushland and destroyed 71 homes in the suburbs of Roleystone and Kelmscott within the study area (Keelty 2011). A

comparison of data from before and after this event shows a reduction in the number of fires per day for most cause categories (Table 2.4), with significant reductions in fires from the three deliberate causes as well as those attributed to matches and lighters, other causes and cutting and welding.

Table 2.4. Mean numbers of fires per day before (1 July 2004 – 6 Feb 2011) and after (7 Feb 2011 – 30 June 2012) the Roleystone-Kelmscott fire

	ALL DAYS		DAYS WITH GFDI>32	
CAUSE CATEGORY	BEFORE	AFTER	BEFORE	AFTER
Lightning	0.05	0.09	0.25	0.35
Spontaneous combustion	0.05	0.04	0.11	0.09
Incendiary	1.19	0.89***	2.23	1.46**
Suspicious (known cause)	4.21	2.10***	8.11	4.03***
Suspicious (unknown cause)	0.97	0.78**	1.90	1.78
Cigarettes and smoking material	1.37	1.25	4.36	4.28
Small open fires	0.08	0.09	0.15	0.17
Inadequate control of burn offs	0.28	0.23	0.38	0.18*
Cutting or welding	0.06	0.04*	0.18	0.03**
Matches or lighter	0.44	0.30***	0.73	0.45*
Fireworks and explosives	0.04	0.03	0.11	0.05
Electrical failure	0.18	0.14	0.62	0.35*
Mechanical failure	0.25	0.20	0.62	0.49
Vehicle	0.02	0.02	0.04	0.02
Re-kindled from a previous fire	0.56	0.49	1.91	1.34*
Other	0.33	0.24**	0.77	0.45**
Undetermined or not reported	1.19	1.10	2.76	2.46
Number of days	2412	510	227	65

*,**,***, signifies where groups are significantly different using the Wilcoxon two sample test at the p= 0.05, 0.01, and 0.001 levels respectively.

While the impact of increased public awareness due to arson reduction programs and high profile fire events are likely to have prevented fires originating from a range of potential causes, it may be possible to further reduce fires by focussing the maximum preventative efforts on very high and extreme fire danger days that coincide with weekends and public

holidays and by targeting specific causes. Targeted awareness campaigns would be most effective for fire causes with time profiles that have pronounced peaks, such as those that are more sensitive to fire danger and fuel moisture, than other causes. For example an awareness campaign aimed at reducing ignitions caused by discarded cigarettes could be specifically focussed on the peak hours of very high and extreme fire danger days. Such a campaign could use news media to state that police are specifically targeting enforcement of cigarette littering and encourage people to report others carelessly discarding cigarettes. Other actions that may further reduce unwanted vegetation fires could include the patrolling of recent fires during the morning of very high and extreme fire danger which is a time when re-ignitions are more likely to occur (Figure 2.5).

2.3 Predicting the number of human caused fires per day

2.3.1 INTRODUCTION

Every day fire management agencies undertake planning tasks to minimise the incidence and impact of bushfires. Extra resources are made available for tasks such as detection, public warnings, arson prevention and initial attack on days when the fire danger or expected fire load is high. Predictions of the daily number of bushfires and the potential fire behaviour allow suppression agencies to more accurately determine their resource needs (Haines *et al.* 1983; Tithecott 1992; Wotton and Martell 2005; Vilar *et al.* 2010a; Wotton *et al.* 2010) and thereby help to increase the probability of successful initial attack (Podur and Wotton 2010; Wotton *et al.* 2010).

This study developed and evaluated models predicting the number of daily human-caused bushfires in the study area of south-west Western Australia. These models could be used to inform daily fire management planning decisions within fire management areas. This study is concerned with bushfire ignitions in grass, shrubland and forest fuels that can potentially burn considerable areas. Urban areas have been omitted from each area used in this study as fires in these areas are typically small in extent as they are located in isolated patches of fuel such as gardens, vacant lots, urban parks and road verges. The model framework developed can be easily translated to other regions given sufficient suitable datasets.

2.3.2 METHODS

South-west Western Australia contains a range of fuel types including annual pasture grasses, dry eucalypt forest and woodland, and shrubland. The region experiences annual drought in summer and autumn, with the peak fire season extending from October to May in most years. The highest density of ignitions occurs in the bushland adjoining the Perth metropolitan area and the urbanised coastal strip south of Perth

Fire incident records from DPAW and DFES have been used to form datasets that contain the number of daily bushfire ignitions for ten management areas. The management areas include six DPAW districts (Swan Coastal, Perth Hills, Wellington, Blackwood, Donnelly and Frankland) and four DFES regions (North Metropolitan, South Metropolitan, South West and Lower South West) that overlap the DPAW districts (Figure 2.9).

The fire incident data were compiled with data related to weather, day type and recent bushfire activity. Weather data was obtained from a representative Bureau of Meteorology station in each region and used to calculate a range of fire danger indices, fuel moisture

models, and drought indices, that were tested as model variables (Table 2.5). Binary day type variables were used to categorise days into groups based on the occurrence of public holidays, weekends, work days (all days except public holidays and weekends), and school days (all days except public holidays, weekends and school holidays). The influence of recent bushfire activity was considered by constructing variables that summed the total number of bushfires occurring over the previous two to 14 days within each region. These recent bushfire activity variables were made for both the total number of bushfires (all causes) and those attributed to human causes.

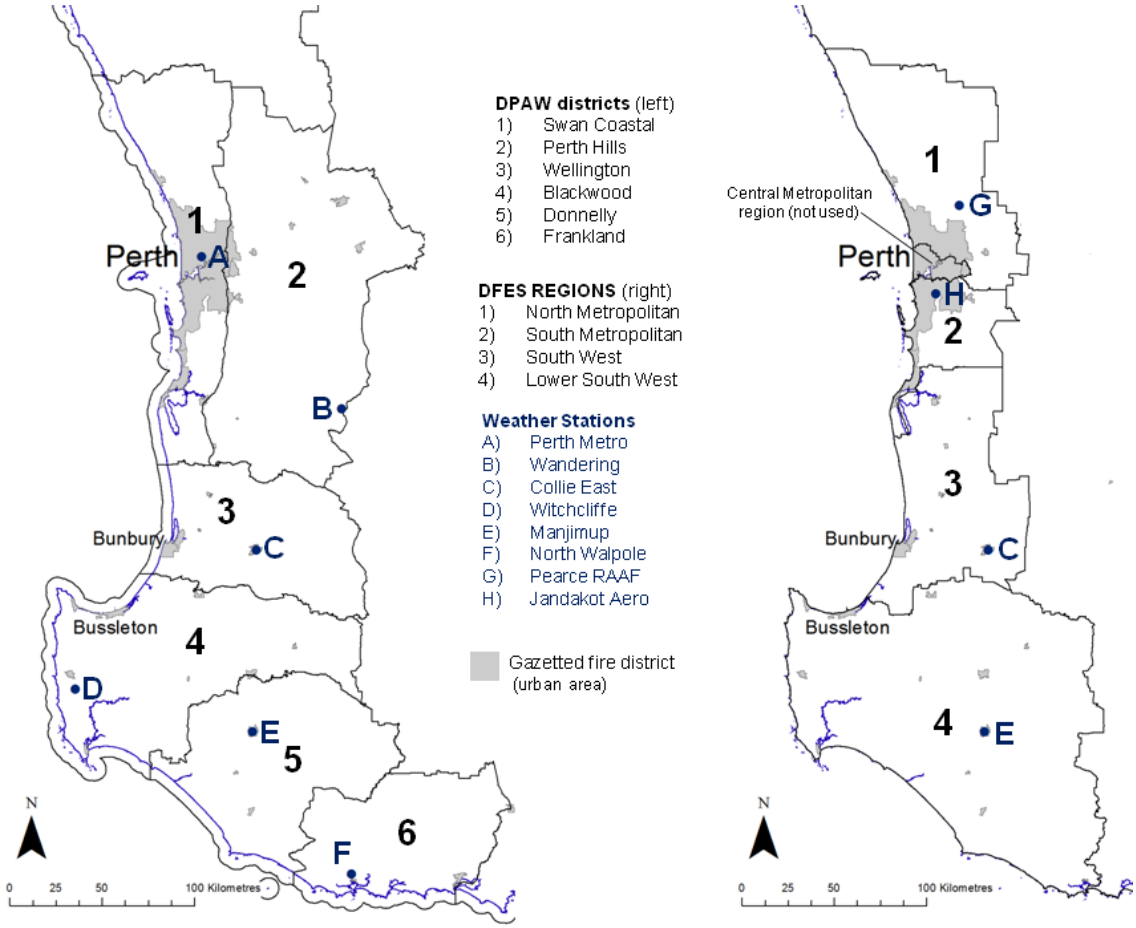

Figure 2.9. South-west Western Australian fire management areas considered in this study and weather stations used for each.

This study was restricted to a period where data was available from both state agencies. This limited our data to four fire seasons (2008/09 to 2011/2012), where a fire season covers a full year from 1 July to 30 June. The first three years of each dataset were used for model development while the data from the final year were reserved for model testing. A broad range of weather and day-type variables were considered during model development.

Models predicting the daily number of bushfires in each bushfire management area were developed using negative binomial regression, with a common model form (same variables) applied to all management areas. These models predict the number of human caused bushfires occurring in the region regardless of their specific cause (e.g. deliberate, accidental, unknown), land tenure or responding agency. A common model form is useful from an implementation perspective as it provides consistency in the input variables that

need to be calculated in each area and the ability to easily compare relative fire occurrence potential across regions. The 95% confidence interval for each model prediction was used to determine a prediction band, which was rounded to the nearest integer, hence providing a range of predicted daily bushfires. This provides the user with worst and best case estimates for each day, while the differences between them give a measure of the reliability of the prediction (Boyle *et al.* 2011).

Table 2.5. Weather variables considered for modelling

VARIABLE	SOURCE/ REFERENCE
Air temperature (°C), Relative humidity (%), Wind speed (km/h), Rainfall (mm), Days since last rainfall	Raw observations
Keetch-Byram Drought Index	Keetch and Byram (1968)
Soil Dryness Index	Mount (1972)
Drought factor	McArthur (1967)/ Noble *et al.* (1980)
Forest Fire Danger Index	McArthur (1967)/ Noble *et al.* (1980)
Grassland Fire Danger Index (assuming 100% curing)	McArthur (1966)/ Noble *et al.* (1980)
Forest Fire Behaviour Tables (Northern Jarrah & Karri)	Sneeuwjagt and Peet (1985)/ Beck (1995)
Canadian Fire Weather Index, Including: Build Up Index, Initial Spread Index, Fine Fuel Moisture Code, Duff Moisture Code, Drought Code	Van Wagner (1987)
Fosberg Fire Weather Index, including version modified to include drought effect	Fosberg (1978), Goodrick (2002)
Simple fire danger index and fuel moisture index	Sharples *et al.* (2009a; 2009b)
McArthur Grassland FMC (%)	McArthur (1966)/ Sullivan (2010)
McArthur Forest FMC (%)	McArthur (1967)/ Viney (1991)
Simard FMC (%)	Simard (1968)
Matthews Simple FMC (%)	Matthews *et al.* (2010)
Matthews process FMC (%) (surface and profile)	Matthews (2006)
Vesta FMC (%)	Gould *et al.* (2007)

Model performance was assessed using the evaluation dataset in two ways. Firstly, the proportion of daily human-caused bushfires within the predicted 95% confidence interval was determined (accuracy rate), as were the proportions that were under predicted and over predicted (under and over prediction rates). Secondly, distance measures were used to quantify the magnitude of the forecast error and to determine model bias. The distance measures used here were the Root Mean Square Error (RMSE) and the Mean Absolute Error (MAE), while bias was measured using the Mean Bias Error (MBE) (Willmott 1982).

In order to evaluate the sensitivity of predictions to the duration and age of the training dataset, common form negative binomial models predicting the daily number of human-caused bushfires attended by DPAW were developed for each of the 6 DPAW management areas using three independent training periods: the common period (2008/09-2010/11), an early period of the same duration (2003/04-2006/07) and the longest available period

(2003/04-2010/11). These models were evaluated on the human-caused bushfires in the DPAW data base for the 2011/12 season. Models developed using the common period and early period were compared to investigate the influence of age of the training dataset on fits. Models developed using the common period were compared to those developed using the longest available period in order to investigate the influence of the duration of the training period. Comparisons were based on distance measures, since models developed on longer duration datasets have narrow confidence intervals and therefore narrow prediction bands.

2.3.3 RESULTS

The most important variables found in the analysis were:

- fuel moisture content (daily minimum) (predicted using Viney's (1991) equation for McArthur's (1967) table)
- the number of human-caused bushfires within the region over the previous two weeks
- workday (a binary variable separating weekends and public holidays from other days)
- rainfall over the previous 24 hours.

These were combined in a predictive model to predict the number of fires per day (N_f) in each fire management area using the form:

$$N_f = exp(\beta_0 + \beta_1 V_1 + \beta_2 V_2 + \ldots + \beta_n V_n) \qquad [2.1]$$

where β_0, β_1 and β_n, are the coefficients listed in each management area columns in Table 2.6 and V_1, V_2 to V_n, are the associated variables. The coefficients and fits for this model form in each fire management area are given in Table 2.6 and graphical examples of the model predictions against observations from the evaluation season in each of the management areas are given in Figures 2.10-2.19.

The predicted number of daily human-caused bushfires is shown by the black line, while the daily range is indicated by the grey area. This example comes from the model being applied to independent data (2011–12) in DEC's Swan Coastal management region.

The models developed using the independent training periods (2003/04-2006/07, 2008/09-2010/2011, 2003/04-2010/11) in the DPAW data had very similar fits to each other (Table 2.7) indicating that there is very little difference in the models developed from these datasets. In most cases the training datasets contained seasons that had more and fewer fires than the evaluation season (2011/12). The relative fits of these models may have been different if this were not the case.

Table 2.6. Coefficients (standard errors) and fit statistics for Eqn 2.1 predicting the daily number of human caused fires (all cause types) applied to the ten bushfire management areas.

	SWAN COASTAL	PERTH HILLS	WELLINGTON	BLACKWOOD	DONNELLY	FRANKLAND	NORTH METRO	SOUTH METRO	SOUTH WEST	LOWER SOUTH WEST
Coefficients (Standard Error)										
Intercept	1.439[C] (0.195)	1.178[C] (0.171)	0.647[B] (0.232)	0.848[C] (0.256)	-0.604 (0.471)	-0.553 (0.460)	1.404[C] (0.182)	0.912[C] (0.242)	0.811[C] (0.208)	0.602[B] (0.211)
Minimum hourly equilibrium FMC (McArthur 1967) (%)	-0.279[C] (0.027)	-0.178[C] (0.019)	-0.238[C] (0.031)	-0.205[C] (0.028)	-0.310[C] (0.066)	-0.282[C] (0.064)	-0.237[C] (0.026)	-0.325[C] (0.068)	-0.216[C] (0.026)	-0.189[C] (0.021)
Number of human-caused bushfires in previous 14 days	0.026[C] (0.006)	0.018[C] (0.004)	0.047[C] (0.011)	0.046[C] (0.009)	0.151 (0.082)	0.162[A] (0.076)	0.020[C] (0.004)	0.039[C] (0.011)	0.036[C] (0.008)	0.046[C] (0.009)
Workday (binary 1=workday)	-0.504[C] (0.078)	-0.313[C] (0.082)	-0.351[B] (0.116)	-0.335[B] (0.113)	-0.067 (0.277)	-0.299 (0.279)	-0.530[C] (0.076)	-0.284[B] (0.107)	-0.312[B] (0.098)	-0.255[A] (0.116)
24 hour rainfall to 9 am (mm)	-0.045[A] (0.195)	-0.078[C] (0.022)	-0.184[B] (0.062)	-0.139[C] (0.034)	-0.098 (0.119)	-0.288 (0.216)	-0.122[C] (0.033)	-0.025 (0.021)	-0.168[C] (0.047)	-0.022 (0.023)
Fits (to 2011/2012 data)										
Accuracy rate	0.885	0.809	0.970	0.932	0.984	0.995	0.861	0.940	0.937	0.913
Under prediction rate	0.066	0.068	0.019	0.046	0.016	0.005	0.049	0.057	0.041	0.066
Over prediction rate	0.049	0.123	0.011	0.022	0	0	0.090	0.003	0.022	0.022
RMSE	0.972	0.974	0.551	0.878	0.427	0.257	1.073	0.761	0.801	0.886
MAE	0.670	0.681	0.390	0.577	0.159	0.107	0.730	0.489	0.537	0.559
MBE	0.078	0.145	0.095	0.096	-0.027	0.009	0.149	-0.012	0.069	0.035

The superscripts indicate the significance of the test statistic values, [A] <0.05, [B] <0.01, [C] <0.001. .

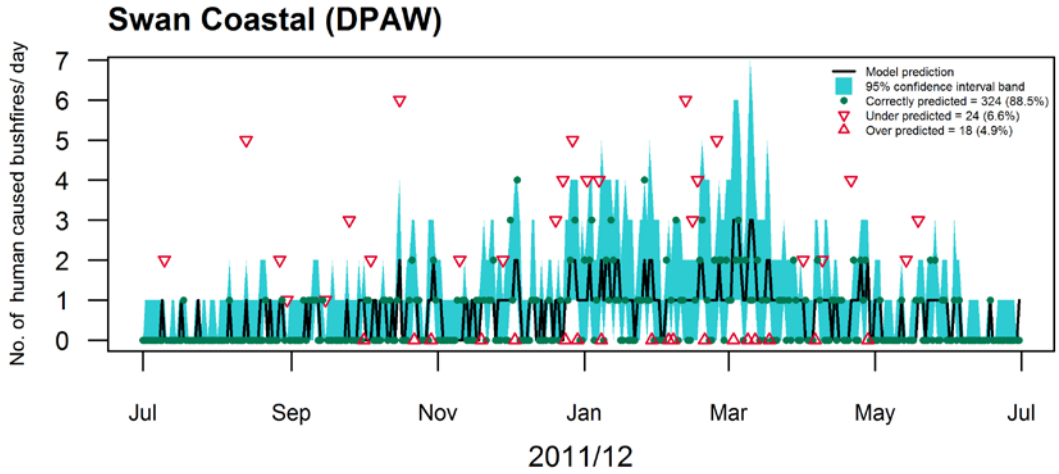

Figure 2.10. Eqn 2.1 with coefficients from Table 2.6 applied to the DPAW Swan Coastal district during the 2011/12 evaluation season.

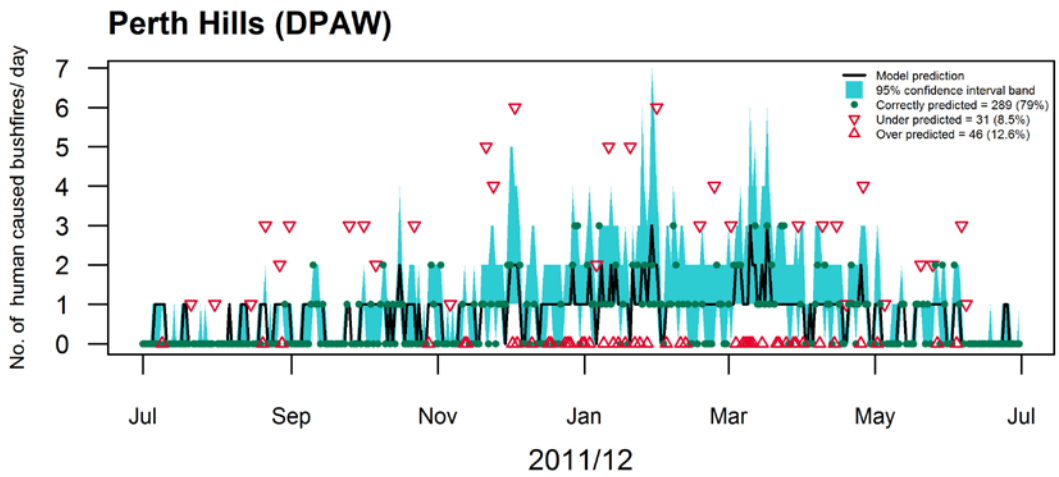

Figure 2.11. Eqn 2.1 with coefficients from Table 2.6 applied to the DPAW Perth Hills district during the 2011/12 evaluation season.

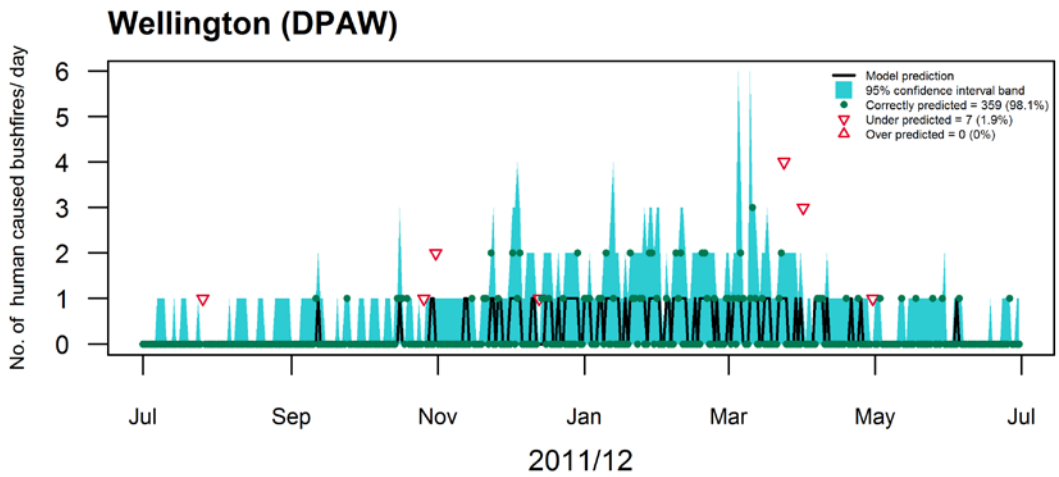

Figure 2.12. Eqn 2.1 with coefficients from Table 2.6 applied to the DPAW Wellington district during the 2011/12 evaluation season.

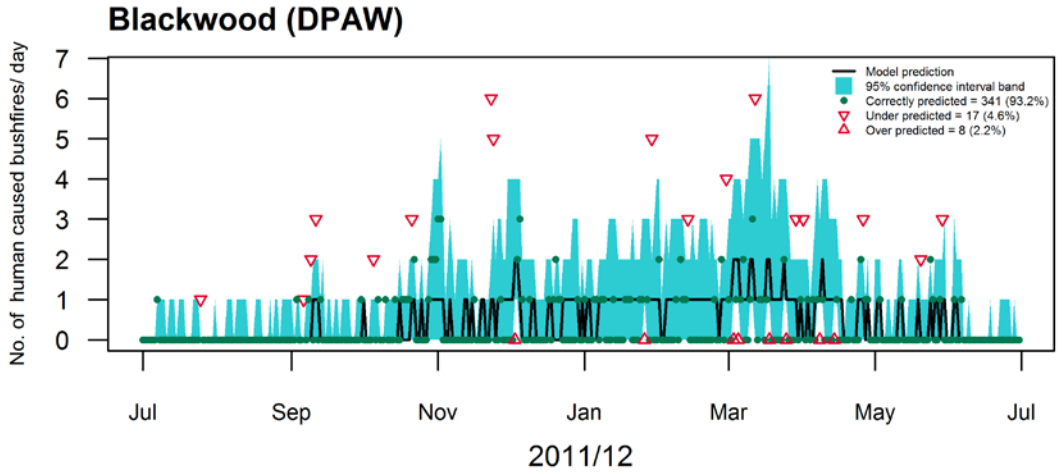

Figure 2.13. Eqn 2.1 with coefficients from Table 2.6 applied to the DPAW Blackwood district during the 2011/12 evaluation season.

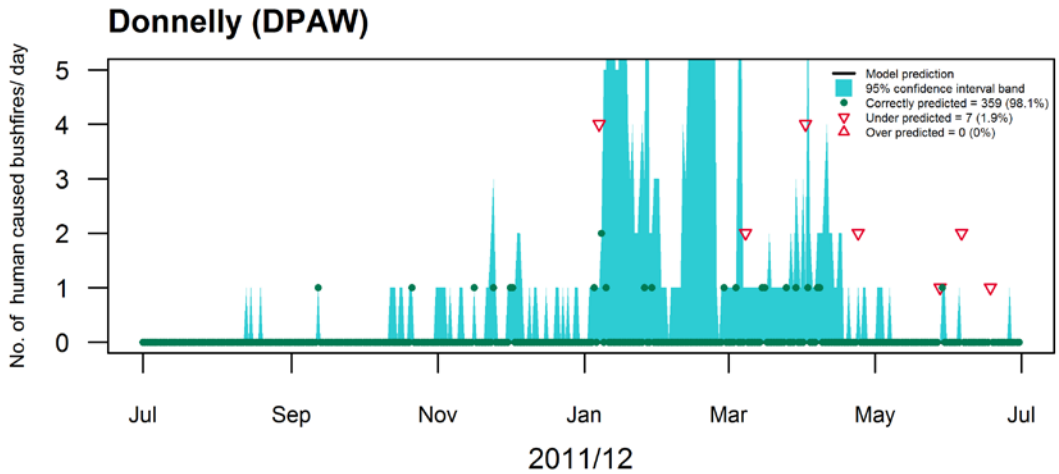

Figure 2.14. Eqn 2.1 with coefficients from Table 2.6 applied to the DPAW Donnelly district during the 2011/12 evaluation season.

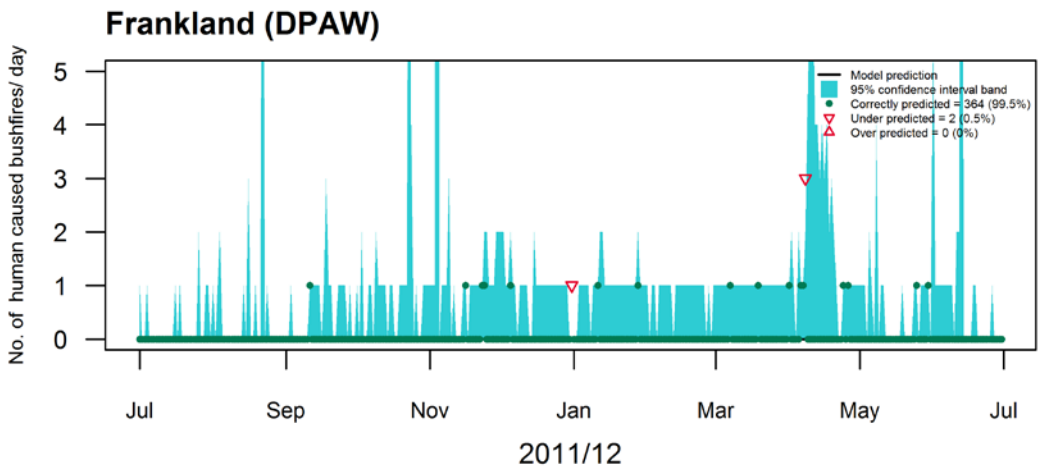

Figure 2.15. Eqn 2.1 with coefficients from Table 2.6 applied to the DPAW Frankland district during the 2011/12 evaluation season.

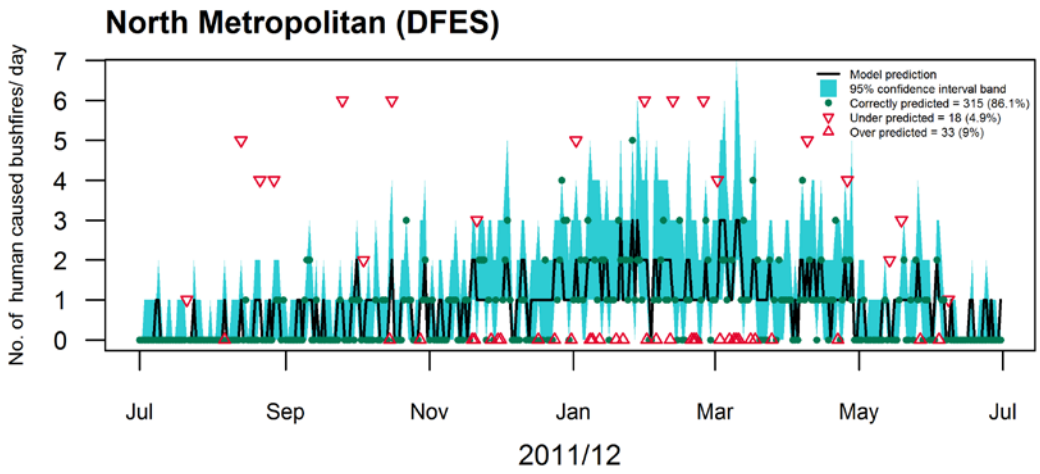

Figure 2.16. Eqn 2.1 with coefficients from Table 2.6 applied to the DFES North Metropolitan region during the 2011/12 evaluation season.

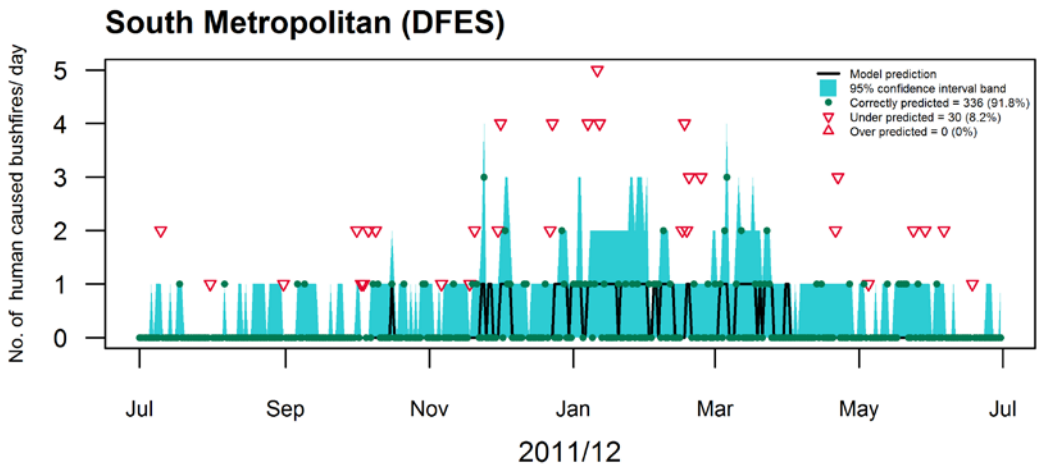

Figure 2.17. Eqn 2.1 with coefficients from Table 2.6 applied to the DFES South Metropolitan region during the 2011/12 evaluation season

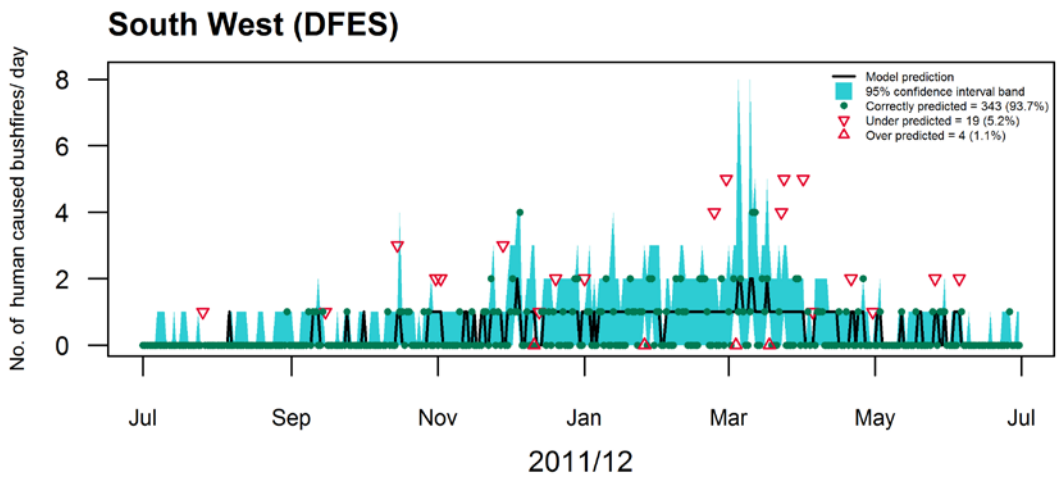

Figure 2.18. Eqn 2.1 with coefficients from Table 2.6 applied to the DFES South West region during the 2011/12 evaluation season.

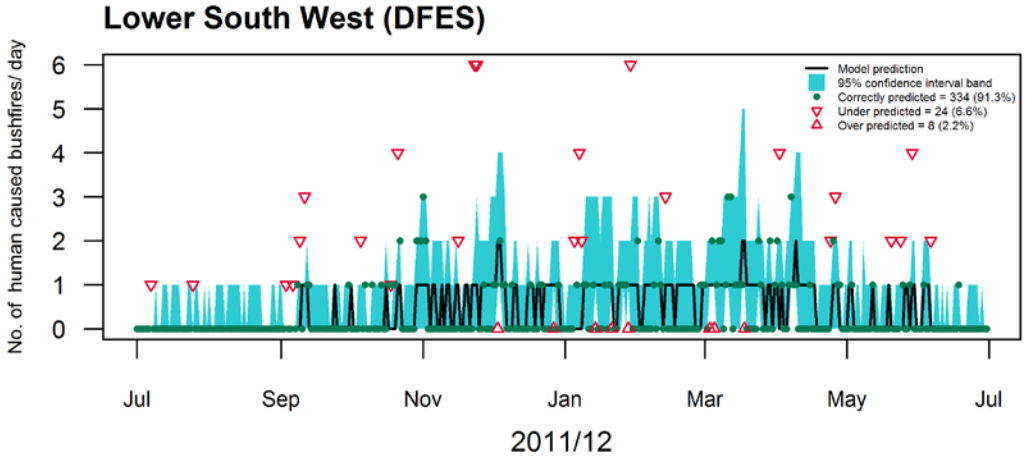

Figure 2.19. Eqn 2.1 with coefficients from Table 2.6 applied to the DFES Lower South West region during the 2011/12 evaluation season.

Table 2.7. Goodness of fit of the models developed using DPAW independent training datasets when applied to the evaluation dataset.

	SWAN COASTAL	PERTH HILLS	WELLINGTON	BLACKWOOD	DONNELLY	FRANKLAND
Early period (2003/04-2006/07)						
RMSE	0.656	0.516	0.365	0.413	0.386	0.248
MAE	0.373	0.302	0.211	0.227	0.172	0.078
MBE	0.003	-0.025	0.041	0.007	0.061	-0.014
Common period (2008/09-2010/11)						
RMSE	0.652	0.514	0.366	0.412	0.388	0.247
MAE	0.400	0.312	0.217	0.237	0.163	0.080
MBE	0.054	0.001	0.049	0.026	0.050	-0.012
Long period (2003/04-2010/11)						
RMSE	0.663	0.517	0.366	0.417	0.383	0.252
MAE	0.368	0.302	0.205	0.224	0.182	0.081
MBE	-0.007	-0.021	0.033	0.000	0.074	-0.012

2.3.4 DISCUSSION

This study demonstrated new models for predicting the daily number of human-caused bushfires at the scale of the management area used for administrative purposes by Western Australian fire agencies. The models had reasonable fit statistics (Table 2.6), however only models developed for areas that experience high numbers of fires showed enough day to day prediction variability to be of practical use. The models for these areas (Swan Coastal, Perth Hills, Wellington, Metropolitan North, Metropolitan South and South West) could be used by the agencies to help inform their daily operational resource planning.

The models included fuel moisture, day type, recent fire activity and rainfall as variables. In stepwise selection procedures, fuel moisture variables were consistently selected first. The moisture content of surface litter is strongly linked to the sustainability of ignition and the availability of fuels to support combustion (e.g. Anderson 1970; Nelson 2001), and is a key predictor in most existing daily fire occurrence models (e.g. Cunningham and Martell 1973; Wotton et al 2003; 2010; Wotton and Martell 2005).

The most common problem regarding the fit of the models related to the days with under predicted fire numbers, which were often the days with the highest number of fires. This is a major weakness in the application of this model as these are the days when more initial attack resources are required and when preparedness planning is crucial. Under prediction is a common feature of fire count modelling using relatively simple model forms such as Poisson or negative binomial because of the large number of days with low counts, and a variety of counts occurring on days with similar conditions. This is part of the compromise between trying to choose a region that is large enough to experience a reasonable number of fires, but small enough that the assumption that weather can be reasonably represented by a single point. This problem has previously been noted by Todd and Kourtz (1991) and Tithecott (1992), who also explained how fire managers are comfortable with predictions that provide a reliable indication of the severity of the day and do not expect models to provide exact numbers.

Previous models have also used variables related to day type and recent fire activity (e.g. Albertson 2009; Prestemon and Butry 2005; Prestemon *et al.* 2012). The day type variables in the models presented here indicates that fires are more likely to start during weekends, school holidays and public holidays, which is consistent with the findings of previous studies (Albertson 2009; Prestemon and Butry 2005; Prestemon *et al.* 2012). This was true for both deliberate and accidental ignitions. Daily rates of deliberate fires in Western Australia have been found to be strongly associated with day of the week in an investigation of bushfire arson trends (Bryant 2008). Recent fire activity variables have previously been used in arson studies, where it has been suggested that they could indicate a low chance of getting caught to copycat arsonists (Prestemon *et al.* 2012).

This study has considered weather variables at a coarse scale with only a single station used to represent each area, so is unlikely to represent local weather factors such as sea breezes and discrete rainfall events, or adequately reflect strong gradients in rainfall, temperature and humidity associated with distance from the ocean. However, the single measure of moisture for each area provides an index of the relative ease of ignition. This approach has been used in previous studies such as Wotton and Beverly (2007) who showed that the Fine Fuel Moisture Code tracked moisture across a range of forest types and could thus be used as a good relative indicator of day to day change in moisture content. Many studies have applied gridded approaches (e.g. Reineking *et al.* 2010; Padilla and Vega-García 2011; Magnussen and Taylor 2012) which have interpolated weather variables to predict the spatio-temporal probability of fire occurrence across broader areas, such as an entire state, province or country. These studies predict a daily probability of one or more fires in each grid cell and have estimated daily fire numbers by summing cell probabilities. These studies are not suited to the daily level of operational application sought by the present study.

The three year training dataset was much shorter than many of those used in previous studies based on fire incident records (e.g. Wotton *et al.* 2003;Wotton and Martell 2005; Albertson 2009; Reineking *et al.* 2010; Wotton *et al.* 2010; Magnussen and Taylor 2012), although some have relied on similar data durations (Viegas *et al.* 1999; Vilar et al 2010a; 2010b; Padilla and Vega-García 2011). The analysis into the effect of the duration of the training dataset found very little difference in the model outcomes (Table 2.7). This is an interesting finding that suggests that the factors driving human-caused ignition are relatively

constant and that fitting a model to more years of data may not necessarily improve predictions. This finding should be further investigated when data from all fires in a region is available. However, as dataset length increases and data from further in the past is used, the comparability of models to current fire activity may also be affected by changes in ignition factors, such as policies related to the setting of fire restrictions, laws related to arson, changes in population distribution and density resulting from urbanisation, and changes in land use.

The models demonstrated here can be used to estimate the likely range of human-caused fires for each day and the probability that a day will have one or more fires. These predictions can be used in conjunction with fire danger indices to more accurately determine the daily need for fire management resources and thereby increase the probability of initial attack success and help manage the cost of being over-prepared against the consequences of being under-prepared.

2.4 Conclusions

Fire occurrence analyses make good use of incident records by providing valuable information on real trends that are directly relevant to fire management agencies. There are many examples of studies that have developed useful models and undertaken informative analyses using agency fire incident data from across the world. Most of these have been undertaken in the last few years when incident records have been more available and computing technology has been available for detailed analyses of larger datasets. Very few of these studies have been undertaken in Australia.

The fire occurrence research undertaken in this project was focussed on temporal patterns of ignitions, specifically the timing of ignitions and predicting the number of human caused ignitions to occur on a given day. This high quality fire incident records from DFES and DPAW and the comprehensive weather records available from the Bureau of Meteorology were essential for this work.

The fire timing study presented in Section 2.2 has shown that the temporal distribution of vegetation fires is strongly influenced by weather conditions, with more ignitions occurring when fuels are dry and fire danger indices are high. Fires originating from sources that have low heat outputs, such as cigarettes and sparks from cutting and welding, are more sensitive to weather conditions than other causes, and mostly occur on dry days with very high fire danger. Fire timing is also influenced by the presence of ignition sources, which is related to human behaviour and varies with day type. Fire prevention measures should be targeted toward days with the highest fire danger, particularly when these coincide with weekends, public holidays and school holidays. Efforts should be made to heighten public awareness during the peak afternoon hours of days with very high and extreme fire danger.

The prediction of the daily number of human caused fires (Section 2.3) found this to be related to fuel moisture content, recent fire activity, day type and rainfall. Models developed in this study can be used to provide guidance for predicting the daily number of human-caused fires for the management areas with moderate to high ignition rates (Swan Coastal, Perth Hills, Wellington, North metropolitan, South metropolitan and South West), thereby improving daily fire preparedness planning. These models provide an estimate of the range of fires expected based on the input conditions.

Future work should see these methods applied to other parts of Australia as well as the extension of other work investigating lightning ignitions that have been developed in other

regions (Wotton and Martell. 2005, Dowdy and Mills 2012a). There is also a need to get a better understanding of the spatial aspects of bushfire occurrence in south west Western Australia, particularly in relation to socio economic situations, which have not been previously studied in Australia.

2.5 References

AFAC (2013) National Data, Australasian Fire and Emergency Service Authorities Council, (http://knowledgeweb.afac.com.au/data/national_data). Accessed 26/11/2013.

Albertson K, Aylen J, Cavan G, McMorrow J (2009) Forecasting the outbreak of moorland wildfires in the English Peak District. *Journal of Environmental Management* **90**, 2642-2651.

Anderson HE (1970) Forest fuels ignitability. *Fire Technology* **6**, 312-319.

Andrews, PL, Loftsgaarden, DO, Bradshaw, LS (2003) Evaluation of fire danger rating indexes using logistic regression and percentile analysis. *International Journal of Wildland Fire* **12**, 213-226.

Asgary A, Ghaffari A, Levy J (2010) Spatial and temporal analyses of structural fire incidents and their causes: A case of Toronto, Canada. *Fire Safety Journal* **45**, 44-57.

Beale J, Jones W (2011) Preventing and Reducing Bushfire Arson in Australia: A Review of What is Known. *Fire Technology* **47**, 507-518.

Beck JA (1995) Equations for the forest fire behaviour tables for Western Australia. *CALMScience* **1**, 325-348.

Bermudez, PD, Mendes, J, Pereira, JMC, Turkman, KF, Vasconcelos, MJP (2009) Spatial and temporal extremes of wildfire sizes in Portugal (1984-2004). *International Journal of Wildland Fire* **18**, 983-991.

Beverly, JL, Herd, EPK, Conner, JCR (2009) Modeling fire susceptibility in west central Alberta, Canada. *Forest Ecology and Management* **258**, 1465-1478.

Boyle J, Jessup M, Crilly J, Green D, Lind J, Wallis M, Miller P, Fitzgerald G (2011) Predicting emergency department admissions. *Emergency Medical Journal* **29**, 358-65.

Bradstock, RA, Cohn, JS, Gill, AM, Bedward, M, Lucas, C (2009) Prediction of the probability of large fires in the Sydney region of south-eastern Australia using fire weather. *International Journal of Wildland Fire* **18**, 932-943.

Bryant CJ (2008) 'Understanding bushfire: trends in deliberate vegetation fires in Australia.' Australian Institute of Criminology, Canberra.

Burrows N, McCaw L (2013) Prescribed burning in southwestern Australian forests. *Frontiers in Ecology and the Environment* **11**, e25-e34.

Burrows ND (1987) 'The soil dryness index for use in fire control in Western Australia.' Western Australian Deptartment of Conservation and Land Management.

Cardille, JA, Ventura, SJ (2001) Occurrence of wildfire in the northern Great Lakes Region: Effects of land cover and land ownership assessed at multiple scales. *International Journal of Wildland Fire* **10**, 145-154.

Catry FX, Rego FC, Bacao F, Moreira F (2009) Modeling and mapping wildfire ignition risk in Portugal. *International Journal of Wildland Fire* **18**, 921-931.

Chandler SE (1982) The effects of severe weather conditions on the incidence of fires in dwellings. *Fire Safety Journal* **5**, 21-27.

Cheney NP, Gould JS (1995) Separating fire spread prediction and fire danger rating. *CALMScience Supplement* 4, 3-8.

Chhetri P, Corcoran J, Stimson R (2009) Exploring the Spatio-Temporal Dynamics of Fire Incidence and the Influence of Socio-Economic Status: A Case Study from South East Queensland, Australia. *Journal of Spatial Science* **54**, 79-91.

Corcoran J, Higgs G, Brunsdon C, Ware A (2007) The use of comaps to explore the spatial and temporal dynamics of fire incidents: A case study in South Wales, United Kingdom. *Professional Geographer* **59**, 521-536.

Corcoran J, Higgs G, Rohde D, Chhetri P (2011) Investigating the association between weather conditions, calendar events and socio-economic patterns with trends in fire incidence: an Australian case study. *Journal of Geographical Systems* **13**, 193-226.

Cruz MG, McCaw WL, Anderson WR, Gould JS (2013) Fire behaviour modelling in semi-arid mallee-heath shrublands of southern Australia. *Environmental Modelling & Software* **40**, 21-34.

Cunningham AA, Martell DL (1973) A stochastic model for the occurrence of man-caused forest fires. *Canadian Journal of Forest Research* **3**, 282-287.

DFES 2013 Total fire bans factsheet, (http://www.dfes.wa.gov.au/safetyinformation/fire/bushfire/BushfireFactsheets/FESA_Bushfire_Factsheet-Total_Fire_Bans.pdf) Accessed 26/11/2013

Díaz-Delgado, R, Lloret, F, Pons, X (2004) Spatial patterns of fire occurrence in Catalonia, NE, Spain. *Landscape Ecology* **19**, 731-745.

Dickson, BG, Prather, JW, Xu, YG, Hampton, HM, Aumack, EN, Sisk, TD (2006) Mapping the probability of large fire occurrence in northern Arizona, USA. *Landscape Ecology* **21**, 747-761.

Dlamini, WM (2010) A Bayesian belief network analysis of factors influencing wildfire occurrence in Swaziland. *Environmental Modelling & Software* **25**, 199-208.

Donoghue, LR, Main, WA (1985) Some factors influencing wildfire occurrence and measurement of fire-prevention effectiveness. *Journal of Environmental Management* **20**, 87-96.

Donoghue, LR, Simard, AJ, Main, WA (1987) Determining the economic relationship between law-enforcement activities and arson wildfires - a feasibility study in Arkansas. *Journal of Environmental Management* **25**, 377-393.

Dowdy AJ, Mills GA (2012a) Atmospheric and Fuel Moisture Characteristics Associated with Lightning-Attributed Fires. *Journal of Applied Meteorology and Climatology* **51**, 2025-2037.

Dowdy, AJ, Mills, GA (2012b) Characteristics of lightning-attributed wildland fires in south-east Australia. *International Journal of Wildland Fire* **21**, 521–524.

Drever, CR, Bergeron, Y, Drever, MC, Flannigan, M, Logan, T, Messier, C (2009) Effects of climate on occurrence and size of large fires in a northern hardwood landscape: historical trends, forecasts, and implications for climate change in Témiscamingue, Québec. *Applied Vegetation Science* **12**, 261-272.

Finney, MA (2005) The challenge of quantitative risk analysis for wildland fire. *Forest Ecology and Management* **211**, 97-108.

Fosberg MA (1978) Weather in wildland fire management: the fire weather index. In 'Conference on Sierra Nevada Meteorology'. pp. 1-4. (Lake Tahoe, CA)

Gonzalez-Olabarria JR, Brotons L, Gritten D, Tudela A, Teres JA (2012) Identifying location and causality of fire ignition hotspots in a Mediterranean region. *International Journal of Wildland Fire* **21**, 905-914.

Goodrick SL (2002) Modification of the Fosberg fire weather index to include drought. *International Journal of Wildland Fire* **11**, 205-211.

Gould JS, McCaw WL, Cheney NP, Ellis PF, Matthews S (2007) 'Field guide- Fuel assessment and fire behaviour prediction in dry eucalypt forest.' (Ensis-CSIRO, Canberra ACT, and Department of Environment and Conservation, Perth WA)

Grose MJ (2009) Changing relationships in public open space and private open space in suburbs in south-western Australia. *Landscape and Urban Planning* **92**, 53-63.

Haines DA, Main WA, Frost JS, Simard AJ (1983) Fire-danger rating and wildfire occurrence in the northeastern United States. *Forest Science* **29**, 679-696.

Hély, C, Fortin, CM-J, Anderson, KR, Bergeron, Y (2010) Landscape composition influences local pattern of fire size in the eastern Canadian boreal forest: role of weather and landscape mosaic on fire size distribution in mixedwood boreal forest using the Prescribed Fire Analysis System. *International Journal of Wildland Fire* **19**, 1099-1109.

Holborn PG, Nolan PF, Golt J (2003) An analysis of fatal unintentional dwelling fires investigated by London Fire Brigade between 1996 and 2000. *Fire Safety Journal* **38**, 1-42.

Keelty M (2011) 'A shared responsibility: the report of the Perth Hills bushfire February 2011 review.' Government of Western Australia, Perth.

Keetch JJ, Byram GM (1968) 'A drought index for forest fire control.' USDA Forest Service, Southeastern Forest Experiment Station, SE-38, Asheville, North Carolina, USA.

Krusel, N, Packham, DR, Tapper, N (1993) Wildfire activity in mallee shrubland of Victoria, Australia. *International Journal of Wildland Fire* **3**, 277-288.

Liu, ZH, Yang, J, Chang, Y, Weisberg, PJ, He, HS (2012) Spatial patterns and drivers of fire occurrence and its future trend under climate change in a boreal forest of Northeast China. *Global Change Biology* **18**, 2041-2056.

Magnussen S, Taylor SW (2012) Prediction of daily lightning- and human-caused fires in British Columbia. *International Journal of Wildland Fire* **21**, 342-356.

Martell DL (1982) A review of operational research studies in forest fire management. *Canadian Journal of Forest Research* **12**, 119-140.

Martell DL, Boychuk D (1997) Levels of fire protection for sustainable forestry in Ontario: a discussion paper. In 'NODA/NFP Technical Report' pp. 34 pp. (Natural Resources Canada, Canadian Forest Service, Ontario Region: Sault Ste. Marie Canada)

Martell DL, Otukol S, Stocks BJ (1987) A logistic model for predicting daily people-caused forest fire occurrence in Ontario. *Canadian Journal of Forest Research* 17, 394-401.

Matthews S (2006) A process-based model of fine fuel moisture. *International Journal of Wildland Fire* **15**, 155-168.

Matthews S, Gould J, McCaw L (2010) Simple models for predicting dead fuel moisture in eucalyptus forests. *International Journal of Wildland Fire* **19**, 459-467.

McArthur AG (1966) 'Weather and grassland fire behaviour.' Department of Natural Development, Forestry and Timber Bureau Leaflet 100, Canberra, ACT.

McArthur AG (1967) 'Fire behaviour in eucalypt forests.' Commonwealth of Australia Forestry and Timber Bureau Leaflet 107, Canberra, ACT.

McCaw L, Read M (2012) Lightning fire ignitions in the Warren Region of south-west Western Australia, 1977-2012. In 'AFAC 12: Diverse country, common ground'. pp. 54. (Perth, 28-31 August 2012)

McRae, RHD (1992) Prediction of areas prone to lightning ignition. *International Journal of Wildland Fire* **2**, 123-130.

Mendes, JM, Bermudez, PCD, Pereira, J, Turkman, KF, Vasconcelos, MJP (2010) Spatial extremes of wildfire sizes: Bayesian hierarchical models for extremes. *Environmental and Ecological Statistics* **17**, 1-28.

Moreira, F, Catry, FX, Rego, F, Bacao, F (2010) Size-dependent pattern of wildfire ignitions in Portugal: when do ignitions turn into big fires? *Landscape Ecology* **25**, 1405-1417.

Mount AB (1972) The derivation and testing of a soil dryness index using runoff data. Tasmanian Forestry Commission Bulletin 4, 31pp. Hobart, Tas.

Nelson RM (2001) Water relations of forest fuels. In 'Forest fires: Behavior and ecological effects'. (Eds EA Johnson and K Miyanishi) pp. 79-150. (Academic Press: San Diego, USA)

Noble IR, Bary GAV, Gill AM (1980) McArthur's fire danger meters expressed as equations. *Australian Journal of Ecology* **5**, 201-203.

Padilla M, Vega-García C (2011) On the comparative importance of fire danger rating indices and their integration with spatial and temporal variables for predicting daily human-caused fire occurrences in Spain. *International Journal of Wildland Fire* **20**, 46-58.

Penman, TD, Bradstock, RA, Price, O (2013) Modelling the determinants of ignition in the Sydney Basin, Australia: implications for future management. *International Journal of Wildland Fire* **22**, 469-478.

Pitman AJ, Narisma GT, McAneney J (2007) The impact of climate change on the risk of forest and grassland fires in Australia. *Climatic Change* **84**, 383-401.

Plucinski MP, Anderson WR (2008) Laboratory determination of factors influencing successful point ignition in the litter layer of shrubland vegetation. *International Journal of Wildland Fire* **17**, 628-637.

Plucinski, MP (2011) A review of wildfire occurrence research.CSIRO Ecosystem Sciences and CSIRO Climate Adaptation Flagship Client Report EP112360, Canberra, ACT.

Podur J, Wotton M (2010) Will climate change overwhelm fire management capacity? *Ecological Modelling* **221**, 1301-1309.

Preisler, HK, Brillinger, DR, Burgan, RE, Benoit, JW (2004) Probability based models for estimation of wildfire risk. *International Journal of Wildland Fire* **13**, 133-142.

Preisler, HK, Burgan, RE, Eidenshink, JC, Klaver, JM, Klaver, RW (2009) Forecasting distributions of large federal-lands fires utilizing satellite and gridded weather information. *International Journal of Wildland Fire* **18**, 508-516.

Preisler, HK, Chen, SC, Fujioka, F, Benoit, JW, Westerling, AL (2008) Wildland fire probabilities estimated from weather model-deduced monthly mean fire danger indices. *International Journal of Wildland Fire* **17**, 305-316.

Preisler, HK, Westerling, AL (2007) Statistical model for forecasting monthly large wildfire events in western United States. *Journal of Applied Meteorology and Climatology* **46**, 1020-1030.

Prestemon JP, Butry DT (2005) Time to burn: Modeling wildland arson as an autoregressive crime function. *American Journal of Agricultural Economics* **87**, 756-770.

Prestemon JP, Butry DT, Abt KL, Sutphen R (2010) Net benefits of wildfire prevention education efforts. *Forest Science* **56**, 181-192.

Prestemon JP, Chas-Amil ML, Touza JM, Goodrick SL (2012) Forecasting intentional wildfires using temporal and spatiotemporal autocorrelations. *International Journal of Wildland Fire* **21**, 743-754.

Reineking, B, Weibel, P, Conedera, M, Bugmann, H (2010) Environmental determinants of lightning- v. human-induced forest fire ignitions differ in a temperate mountain region of Switzerland. *International Journal of Wildland Fire* **19**, 541-557.

Santos B, Clegg P, Courtney J, Burton A (In prep) Fire Weather Climatology of Western Australia, Part 1.

Sharples JJ, McRae RHD, Weber RO, Gill AM (2009a) A simple index for assessing fire danger rating. *Environmental Modelling and Software* **24**, 764-774.

Sharples JJ, McRae RHD, Weber RO, Gill AM (2009b) A simple index for assessing fuel moisture content. *Environmental Modelling and Software* **24**, 637-646.

Simard AJ (1968) 'Moisture content of forest fuels III: Moisture content variations below the fiber saturation point.' Forest Fire Research Institute, Department of Forestry and Rural Development, FF-X-16, Ottawa.

Smith R (2004) Community centred bush fire (arson) reduction. In '11th annual AFAC Conference and Inaugural Bushfire CRC Conference'. pp. 241-243. (Perth, Western Australia, 7-9th October 2004)

Sneeuwjagt RJ, Peet GB (1985) 'Forest fire behaviour tables for Western Australia.' (WA Department of Conservation and Land Management: Perth)

Sullivan AL (2010) Grassland fire management in future climate. *Advances in Agronomy* **106**, 173-208.

Syphard, AD, Radeloff, VC, Keuler, NS, Taylor, RS, Hawbaker, TJ, Stewart, SI, Clayton, MK (2008) Predicting spatial patterns of fire on a southern California landscape. *International Journal of Wildland Fire* **17**, 602-613.

Tithecott AG (1992) Application of fire occurrence prediction models in Ontario's fire management program. In 'Proceedings of the Eighth Central Region Fire Weather Committee Scientific and Technical Seminar'. Winnipeg Manitoba. (Ed. KR Anderson) pp. 57-72. (Forestry Canada, Northwest Region)

Todd B, Kourtz PH (1991) 'Predicting the daily occurrence of people-caused forest fires.' Forestry Canada, Petawawa Forest Experimental station, PI-X-103, Chalk River, Ontario.

Van Wagner CE (1987) 'Development and structure of the Canadian forest fire weather index system.' Canadian Forestry Service, 35, Ottawa.

Vasilakos C, Kalabokidis K, Hatzopoulos J, Matsinos I (2009) Identifying wildland fire ignition factors through sensitivity analysis of a neural network. *Natural Hazards* **50**, 125-143.

Vega-Garcia C, Woodard PM, Titus SJ, Adamowic V, Lee BS (1995) A logit model for predicting the daily occurrence of human caused forest fires. *International Journal of Wildland Fire* **5**, 101-111.

Viegas DX, Viegas MT, Ferreira AD (1992) Moisture content of fine forest fuels and fire occurrence in central Portugal. *International Journal of Wildland Fire* **2**, 69-86.

Viegas, DX, Bovio, G, Ferreira, A, Nosenzo, A, Sol, B (1999) Comparative study of various methods of fire danger evaluation in Southern Europe. *International Journal of Wildland Fire* **9**, 235-246.

Vilar L, Nieto H, Martin MP (2010b) Integration of lightning- and human-caused wildfire occurrence models. *Human and Ecological Risk Assessment* **16**, 340-364.

Vilar L, Woolford DG, Martell DL, Martin MP (2010a) A model for predicting human-caused wildfire occurrence in the region of Madrid, Spain. *International Journal of Wildland Fire* **19**, 325-337.

Vilar, L, Nieto, H, Martin, MP (2010a) Integration of lightning- and human-caused wildfire occurrence models. *Human and Ecological Risk Assessment* **16**, 340-364.

Vilar, L, Woolford, DG, Martell, DL, Martin, MP (2010b) A model for predicting human-caused wildfire occurrence in the region of Madrid, Spain. *International Journal of Wildland Fire* **19**, 325-337.

Viney NR (1991) A review of fine fuel moisture modelling. *International Journal of Wildland Fire* **1**, 215-234.

Wickham H (In Prep) Tidy data. http://vita.had.co.nz/papers/tidy-data.pdf. Accessed 26/11/2013.

Willmott CJ (1982) Some comments on the evaluation of model performance. *Bulletin of the American Meteorological Society* **63**, 1309-1369.

Wotton BM, Beverly JL (2007) Stand-specific litter moisture content calibrations for the Canadian Fine Fuel Moisture Code. *International Journal of Wildland Fire* **16**, 463-472.

Wotton BM, Martell DL (2005) A lightning fire occurrence model for Ontario. *Canadian Journal of Forest Research* **35**, 1389-1401.

Wotton BM, Martell DL, Logan KA (2003) Climate change and people-caused forest fire occurrence in Ontario. *Climatic Change* **60**, 275-295.

Wotton BM, Nock CA, Flannigan MD (2010) Forest fire occurrence and climate change in Canada. *International Journal of Wildland Fire* **19**, 253-271.

Wotton, BM (2004) Predicting Forest Fire Occurrence in Ontario. PhD thesis, University of Toronto.

3 Fire initiation

3.1 Introduction

The significance of firebrand transport and spotting in terms of direct and indirect costs and threat to human life has been frequently highlighted (McArthur 1969, Pagni 1993, McCarthy and Tolhurst (1998), Ellis 2000, Ellis and Sullivan 2003, Koo *et al*. 2010). The numbers of firebrands generated, their transport distances, the probability of the firebrands igniting the fuel and the rapidity of development of the subsequent spotfire, determine the nature, magnitude and effect of 'ember attack' and spotting. Spotting not only increases the demand on resources by starting new fires, but can increase the spread rate of the source fire (McArthur 1967, Tolhurst and MacAulay 2003, Porterie 2005). Entrapment of fire crews or civilians between developing spotfires and the source bushfire is potentially life threatening.

Mass ignition is possibly the most dangerous situation because very rapid coalescence of a dense distribution of spots over a relatively large area means that escape may be impossible. This phenomenon supposedly requires a certain density of spotfire ignitions (hence the importance of ignition probability), combined with conditions conducive to their rapid spread. McArthur (1967) supposed that concentrations of 100 ignition points per square mile (about 40 per square km) could produce fire storm (mass fire) effects, and McArthur (1969) described a 'critical level of fuel dryness…where the spotting process reaches maximum efficiency'.

The occurrence of spotting and the magnitude of its effect of multiplying fire occurrence and increasing fire growth depend on the probability that the embers or firebrands transported ahead of the main fire by wind or convection can ignite the forest fuel. In the great majority of cases, the fuel will be a fuel bed of litter or litter and grass fuels. In order to better predict and manage fire behaviour it is therefore essential that the conditions critical for spotfire ignitions are known and this requirement frames the key research questions:

- What are the critical variables that determine the probability that firebrands will ignite a given fuel bed, and what value do these variables have for the probabilities that are critical for fire managers?
- Can firebrands smaller than 0.1 g in mass ignite a given fuel bed?

Inherent in the research questions are additional questions fundamental to the investigation:

- What are the characteristics of the firebrands which should be used in the tests?
- Which fuel bed types should be investigated?
- What methodologies should be used in the tests?

3.2 Literature review

The research questions were initially addressed using a literature review of empirical studies of in-flight behaviour of firebrands and fuel bed ignition to inform the selection of methodologies for laboratory ignition tests of fuel beds. The following section includes those parts of the literature review most relevant to this study.

3.2.1 CONCEPT OF SPOTTING

In the context of bushfires or wildfires, a firebrand is burning vegetative material ranging from 'logs to lichens' (Cheney and Bary 1969) that is transported by wind alone, or wind and convection, ahead of the source fire. If it lands on unburnt fuel a firebrand has a probability of igniting a spotfire, thus 'spotting'. By definition an ember is a piece of burning material in its last stages of combustion. Hence all firebrands, including those that are flaming or glowing vigorously, are strictly not embers but the converse is true. The term 'ember' attack is commonly used to describe the deposition of firebrands at a given location, which may be house at the bush-urbaninterface, say.

A schematic of the concept of firebrand transport and spotting is shown in Figure 3.1.

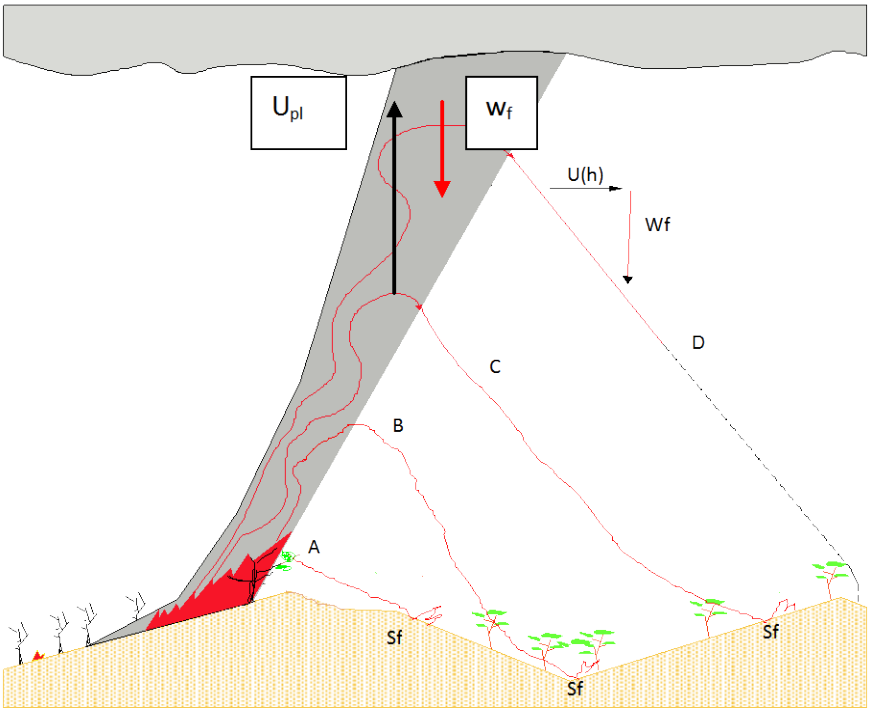

Figure 3.1. Schematic of the concept of firebrand transport and spotting

Trajectory A represents a firebrand that has been ignited and detached from an overstorey tree and transported by wind alone to start a new fire, a spotfire (S_f), ahead of the source fire. Trajectory B represents a firebrand that has an ultimate falling speed in still air (i.e., terminal velocity, W_f) that is less than the convective plume updraught velocity (U_{pl}) and hence is lofted in the convection column prior to exiting and descending while being transported in the ambient wind profile (U_h).

Albini (1979) supposed that for a given convection strength and wind profile there would be an optimum lofted height and maximum distance that a firebrand could be transported and yet retain sufficient energy to initiate a spotfire (Trajectory C). Trajectory D represents a firebrand that attains a greater distance than 'C' but which burns out during its descent and hence does not ignite a spotfire.

Although the vast majority of spotfire ignition in the field occurs in surface fuels (as depicted in Figure 3.1), Hodgson (1968) described tree-to-tree spotting by stringybark eucalypts. In

addition, in a process similar to 'saltation', strong winds and turbulence can 'bounce' firebrands along the ground for distances of tens of metres or more, as observed from burning mulch beds during the January 2003 Canberra fires.

3.2.2 CRITICAL FIREBRAND CHARACTERISTICS

In North America, Byram (1959) suggested that charcoal, decayed wood, bark and dry moss would be light enough to be lofted but capable of burning for several minutes and thus be potential firebrand material. Albini (1979) similarly supposed that stemwood sections, needles, bark flakes, seed cone scales, open seed cones and clumps of moss were all potential firebrands. He also proposed that a "two-stage" firebrand, for example a twig with foliage attached, might outdistance a simple wood cylinder such as a section of stemwood due to the enhancement of its lofting velocity while ascending and of its combustion endurance while descending. Animal dung is also potential firebrand material.

In Australia spotting occurs frequently, even during prescribed burning, and this has been largely attributed to the bark characteristics of about 150 eucalypt species, of a total exceeding 500. Typically, their trunks or branches have large quantities of suspended or easily-detached flakes, which may be aerodynamic. The supposed spotting behaviour of eucalypts, based on bark morphology, has been described (McArthur 1967, 1969, Cheney and Bary 1969). Fuel Hazard Guides in three States (NSW National Parks and Wildlife Service, 2003, SA Department of Environment and Heritage, 2006, Department of Sustainability and Environment 2010) have been developed from the original Victorian guide (McCarthy *et al.* 1998). The guides categorise Bark Hazard based on type, ease of detachment (i.e. tightly or loosely held) and availability. The last characteristic depends on whether the bark is persistent or is seasonally shed, and if the former, how much has been retained since the last fire.

There is little information on firebrand material other than eucalypt bark in Australian fires. McArthur *et al*. (1966) supposed that cones, cone bracts or bunches of needles caught in upper branches caused spotfires up to distances of about 2 km during the Wandilo fire in *Pinus radiata* plantation. Luke and McArthur (1978) presumed that thistle heads or grass seed heads allow grass fires to spot to distances of up to about 100 m. McCarthy[3] (*pers. comm*.) observed several spotfires up to a distance of about 200 m from a prescribed burn in heath-woodland, each ignited by the combusting woody axis of a *Banksia serrata* inflorescence. A banksia inflorescence could conceivably function as a 'two-stage' firebrand because the dead flowers on the axis would have a relatively low initial terminal velocity (until they burnt off), and the woody axis could potentially burn for minutes while being transported. However, it is likely that strong convection, as observed on this occasion, would be required in order to detach and loft the inflorescence.

Ease of ignition and detachment of a firebrand is critical to its transport and likelihood of spotfire ignition. A firebrand requiring an ignition time that exceeds the time during which effective convection occurs at its location may not be ignited in time to be detached and lofted. In the case of transport by wind alone an excessive ignition time may result in the firebrand landing on burnt ground well behind the front of the source fire. Fire vortices can loft firebrands from the ground but it assumed that the elevated locations on trunks and branches of trees are optimal for lofting by convection or wind generally.

[3] Greg McCarthy, Victorian Department of Environment and Primary Industry.

Firebrand shape has been shown to influence entrainment and thus lofting (Lee and Hellman 1969). It also influences terminal velocity, such that thin 'platelike' firebrands will have lower terminal velocities than thicker, 'block-like' ones of the same density. In addition, shape determines the property of 'fast spin', which has been shown to significantly affect terminal velocity of bark flakes (Ellis 2010). Because it affects terminal velocity, shape also potentially affects combustion behaviour.

The length of time in flight a firebrand flames (flameout time) is critical because a flaming firebrand has a significantly greater probability of igniting a fuel bed than one which is glowing (Ellis 2000, Ganteaume *et al*. 2010). For the same reason, momentary reflaming after removal from an air flow (Muraszew *et al*. 1976) or during the later stage of glowing combustion during flight (Ellis 2000, Ellis 2013) is also significant.

Total combustion time in flight (burnout time), which includes a typically short initial flaming phase followed by an extended glowing one, limits the maximum potential spotting distance of a firebrand for given convection strength and wind profile.

Terminal velocity, the maximum falling velocity attained in still air, usually decreases as the firebrand combusts. As shown in Fig. 3.1, terminal velocity and its rate of decay determine the height to which a firebrand will be lofted for a given convective velocity, and the distance the firebrand will be transported downwind for given lofted height and wind field. Terminal velocity is also critical in the study of firebrand aerodynamics and combustion and potentially to its success in igniting a fuel bed. Terminal velocity is attained when mass forces (firebrand mass × gravity) are balanced by drag forces (firebrand area × coefficient of drag × air density × fall velocity) and this condition is reflected in a standard equation for terminal velocity:

$$w = \left(\frac{2\,g\,m}{C_d\ A\,\rho_a} \right)^{0.5} \qquad [3.1]$$

where w is terminal velocity, m is mass (kg), A is the maximum projected area (m^2) which is the area normal to the air flow, ρ_a is the density of air (~1.27 kg m^{-3}) and C_d is the coefficient of drag. Eqn 3.1 shows that for a given drag coefficient, terminal velocity will be proportional to the square root of surface density (m/A).

Observations of non-combusting or combusting samples dropped from a tower (say) allows their free-fall behaviour to be described, and a single measurement of their terminal velocity obtained for each drop using Clements' (1977) equation:

$$w = \frac{gt - \sqrt{g^2 t^2 - 4gy\ln 2}}{2\ln 2} \qquad [3.2]$$

where g is acceleration due to gravity (9.8 m s^{-2}), t is the fall time (s) and y is the height (m) from which the sample is dropped.

Tarifa *et al*. (1965) proved that small, relatively light objects such as firebrands attain a relative air velocity equal to their terminal velocity within 2 to 3 s, which is a small fraction of total flight time. His assumption that firebrands can be assumed to always maintain this relative air velocity has been adopted by most subsequent researchers. However, Koo *et al*. (2010) have stated that while this assumption may be true for a simplified, steady state wind field, it will not be true for conditions during real fires where the wind field will constantly change on a smaller times scale. Potentially, the error will be greater for short trajectories than for long ones. Although it has potential shortcomings, this assumption allows the trajectories of firebrands of known terminal velocity to be estimated by approximating their lofting velocity as the difference between updraught velocity as determined by convection

strength and firebrand terminal velocity, and their descent rate in wind flow parallel to horizontal ground as equal to the terminal velocity.

Combustion behaviour at terminal velocity is also significant in fuel bed ignition tests using firebrand samples. In experiments testing the probability that a given firebrand material will ignite a given fuel bed, ideally the state and heat flux of the sample should reflect that of the same material after possibly extended aerial transport at a relative air velocity equivalent to its terminal velocity. To date, no fuel bed ignition studies have ensured this equivalence.

As discussed above, initial mass, and the rate of its decay, will affect terminal velocity. A flaming firebrand of any size is likely to ignite fine fuel during hot, dry conditions (Ellis 2000, Ganteaume *et al*. 2009). However, the mass of a glowing firebrand may significantly influence its fuel bed ignition probability Ellis (2000).

The critical characteristics of temperature and radiant heat flux (RHF) are influenced by firebrand state (flaming or glowing), material and possibly mass. The characteristics of a firebrand that lands on a fuel bed are significantly affected by its airborne transport during which it has been combusting in air flow approximately equal to its terminal velocity. In addition, combustion may be enhanced or retarded by the effect of natural gyration or movement on relative air flow.

Different firebrand materials combusting at their terminal velocity display different behaviour. Most timber firebrand samples have relatively high terminal velocities (Tarifa *et al*. 1967) and relatively short flameout times (Muraszew 1974, Muraszew *et al*. 1975, 1976). Ellis (2000) showed that samples of messmate stringybark (*Eucalyptus obliqua* L'Her) had relatively low terminal velocities, had long flameout times and occasionally reflamed during their glowing combustion stage.

The colour temperature of glowing firebrands at 500-600°C (dull red), 600-800°C (dark red) and 800-1000°C (bright red) correspond to theoretical ranges of RHF of 20 to 35, 35 to 75 and 75 to 150 kW m^{-2}. The number of fuel elements potentially contacted by a firebrand is affected by firebrand size. In cases of proximity rather than contact, the RHF incident on a given fuel element is the product of firebrand RHF flux and view factor. View factor is a function of size of the emitter (firebrand) and the proximity and size of the fuel element, and decreases quickly with distance.

For example, for a fuel element at a point orthogonal to a square emitting surface ($a \times a$), the view factors at distances $0.35a$ and a are 0.71 and 0.24, respectively (Drysdale 1985). Hence, a point fuel element at a distance of 5 mm from a firebrand with an emitting surface 5 mm × 5 mm would receive about a quarter of the theoretical maximum value of emitted radiative power. Huang *et al*. (2007) measured values of radiative power of between 9 and 13 kW m^{-2} for combusting 'plate' shaped pieces of charcoal with areas ranging from less than 1 cm^2 up to about 10 cm^2 but did not explain their methodology.

The period during which a firebrand maintains its heat flux, its endurance, is also important, and is likely to be affected by firebrand material and mass.

3.2.3 STUDIES OF IN-FLIGHT FIREBRAND BEHAVIOUR

The majority of empirical firebrand studies have determined:

- the terminal velocity of non-combusting samples
- the flameout time, burnout time and terminal velocity decay of samples burning at their terminal velocity, or,

- the above characteristics and loss of mass and density for a range of constant air flow speeds and then derived models for behaviour at terminal velocity.

Using a horizontal wind tunnel, Tarifa *et al*. (1965) found that in order to avoid subjectivity and the influence of differing ignition times on burnout time it was necessary to assign identical ignition times to identical firebrands. They found that, for their shielded, in-wind gas lighter, an artefact of the lower density of the ignition gases was that terminal velocity abruptly decreased after the cessation of the ignition flame. Tarifa *et al*. (1965) did not quantify ignition time.

Muraszew *et al*. (1975) emphasised the importance of a complete, short ignition time and used a shielded gas burner augmented with oxygen. They found that consistent ignition was essential to achieving consistent data and described 'complete flaming ignition of the whole surface', ideally representing less than 10% of sample burnout time. They quantified the optimum ignition time for dry, machined wood samples as:

$$t_i = 12\, D_0 \qquad [3.3]$$

where t_i is ignition time (s) and D_0 is sample thickness (cm). They also found an upper limit of D_0 for combustion in quiescent air of 8.45 cm.

Muraszew *et al*. (1976) reported a development of the ignition technique such that the sample was rotated during ignition and confirmed that the constant in Eqn 3.3 was between 12 and 14. However, they found that the mass loss during ignition of between 25 and 30% of initial mass exceeded that which would have been lost due to self-burning during the same period.

Ellis (2000) ignited prepared rectangular plates of the outer bark of messmate stringybark (*E. obliqua* l'Her) by placing them, weathered side down, on a wire bracket 35 mm above a 50 mm diameter propane burner. He found that the time required for full, uniform flaming of the entire surface, which he termed 'index ignition time' was a function of initial sample volume (V) to surface area (S) ratio:

$$t_{ii} = 228.3\frac{V_0}{S_0} - 26.8, \quad r^2 = 0.98 \qquad [3.4]$$

where t_{ii} is index ignition time (s), and V_0 and S_0 are initial sample volume (cm^3) and surface area (cm^2) respectively. Ellis (2000) quantified the effects of a range of ignition times for given sample sizes on flameout time (t_F), burnout time (t_B) and remaining mass at burnout (m_B). He found that mass loss and projected area loss (variable *A*, Eqn 3.1) were between 40 and 50% and between 10 and 20% of initial values respectively.

Woycheese (2000, 2001) used initial radiant heating at a temperature of 840 to 870°C, followed by ignition by a high-frequency spark after a 'set time' required in order to ensure complete ignition of wood disks with minimum mass loss. He did not quantify the latter variables.

Tarifa *et al*. (1965, 1967), measuring terminal velocity of potential firebrand materials, used 100 m and 200 m high drop tests from a balloon verified that the error introduced by fixing wood cylinders and plates in air flow, as opposed to allowing natural gyration, was of the order of 10%.

Clements (1977) made observations of combusting and non-combusting samples of North American firebrand material, including leaves, bark and cones, dropped from a 30 m tower, and calculated their terminal velocities using Eqn 3.2. He verified the accuracy of Eqn 3.2 using still images of burning firebrands at night. A light chopper in front of the lens meant that trajectories were represented on the images as dashed lines, with the length of the

'dashes' being proportional to velocity. He found that the terminal velocities of leaves, pine needles, pine cones ranged from 1.3 to 2.2 m s^{-1}, 2.8 to 4.1 m s^{-1} and 8.5 to 16.3 m s^{-1} respectively. However, he did not relate these velocities to measured sample variables. Clements (1977) also determined which types were more likely to flame in flight, although he did not give flameout times.

Ellis (2000, 2010) used Clements' (1977) equation (Eqn 3.2), and dropped non-combusting flakes of jarrah (*E. marginata* Don ex Smith) and karri (*E. diversicolor* F. Muell.) from a 23 m tower to determine their terminal velocities and free-fall behaviour. He found that their terminal velocities, as implied by Eqn 3.1 (which were a linear function of root surface density $(m/A)^{0.5}$ and category of *Spin*) ranged from 2.5 m s^{-1} to about 8 m s^{-1}. Ellis (2010) showed that the property of fast spin could decrease sample terminal velocity by up to about 20%, compared to a similar sample which did not spin.

Huang *et al*. (2007) measured characteristics of 140 non-combusting charcoal firebrands, originally generated from a burning house. The samples ranged in area (*A*) from less than 1 cm^2 up to about 10 cm^2 and had a mean density of 130 kg m^{-3}. They used high-speed digital imagery of sample fall in front of a marked background in order to measure their terminal velocities. They then calculated the equivalent Stokes diameter for each sample, and used these values to model firebrand generation from a burning building. They did not give values for the terminal velocities but if it is assumed that samples ranged in thickness between about 0.25 and 1.0 cm, their approximate terminal velocities (Eqn 3.1) would be between about 2.2 and 5.0 m s^{-1}. For plume velocities between 3.7 and 7.8 m s^{-1} and for 5 m s^{-1} wind, they modelled transport distances of up to 400 m. In addition, these authors measured a range in total emitted heat flux from similar sized samples of between 9 and 13 kW m^{-2} but did not explain their methodology.

Using a horizontal wind tunnel Tarifa *et al*. (1965) measured the decay of terminal velocity of machined spheres, cylinders and plates of oak, pine spruce, aspen, balsa and charcoal, (including some tests of samples at different moisture contents), using a downstream fan-design horizontal wind tunnel (i.e., 'sucking' design in which the fan is located downstream of the working section rather than a 'blower' type design in which the fan is upstream of the working section). In addition, they combusted pine cones, columns of pine cones, and pine cone bracts. They found that the coefficient of drag changed very little until the samples became very small. They also concluded that the change in sample mass and diameter that would occur in free-fall would not differ significantly from the changes that would occur if burned tethered at a velocity equal to its terminal velocity.

Tarifa *et al*. (1965) modelled the decay of terminal velocity, expressed as the ratio w_t/w_0, where w_0 and w_t are initial terminal velocity and terminal velocity at time *t* (s), respectively, as a function of parameter *Z*. Parameter *Z* is described by:

$$Z = \frac{w_O.t}{C_d}\left(\frac{w_0.D_0.\sigma_a}{\mu_a}\right)^{-0.4}.\left(\frac{\rho_a}{\rho_0}\right)^{1.3}.\left(\frac{L_0}{D_0}\right).K \qquad [3.5]$$

where *t* is time of flight (s), w_0 is initial terminal velocity (m s^{-1}), C_d is coefficient of drag, D_0 is initial firebrand diameter (cm), μ_a is air viscosity (poise), ρ_a and ρ_0 are air density and initial firebrand density respectively, L_0 is initial firebrand length (cm), and *K* is a shape factor.

This model was termed the 'Universal Burning Model'. They concluded that maximum lofting height and transport distance were positively correlated with wood density. They also concluded that charcoal firebrands would be far the most dangerous type due to their low density and very long burnout times. The conclusion concerning charcoal appears to contradict that concerning timber samples because the density of charcoal (~200 kg m^{-3}) is

less than that of most timbers (≥500 kg m^{-3}) except balsa. Tarifa *et al*. (1965) concluded that combustion characteristics of natural firebrands, such as sections of twigs, differed little from those of machined wood samples. In addition they concluded that different shapes would be more or less dangerous, depending on their type and the conditions, and that sample moisture content influences ignition time significantly but has a negligible effect on subsequent combustion. These authors did not measure or model flameout time.

Muraszew *et al*. (1975) concluded that the work of Tarifa *et al*. (1965), while describing terminal velocity decay such that trajectories could be calculated, was deficient because it did not describe combustion history. They stated that characteristics such as the decay of sample mass and density were essential in determining ignition probability for a given sample after a given flight time. Using a strain gauge balance they measured the mass of machined wood cylinders (birch, white pine and ponderosa pine) as well as natural fuels burning at a range of constant air velocities between zero and 12.5 m s^{-1}. Their wind tunnel was of 'sucking' design. They took pairs of photographic images to allow the calculation of sample volume and subsequently sample density.

Muraszew *et al*. (1975, 1976) modelled the decay of sample density of cylinders and square plates of timber in quiescent air and in air flow. They also concluded that firebrands shaped like flat plates would be superior firebrands because of their relatively low terminal velocities. Muraszew *et al*. (1975) found that the maximum flameout times of their (wood) samples in air flow was about 10 to 15 s and that at about 9 m s^{-1}, samples would not continue flaming after ignition. They also showed that their models for decay of terminal velocity approximated those of Tarifa *et al*. (1965). Muraszew *et al.* (1976) deduced probable flameout times at terminal velocity of timber cylinders and plates (Table 3.1).

Table 3.1. Probable flameout times deduced by Muraszew *et al.* (1976) from tests using a range of wood samples

SHAPE	THICKNESS OR DIAMETER (MM)	WOOD TYPE	DENSITY (KG M^{-3})	INITIAL TERMINAL VELOCITY (M S^{-1})	PROBABLE FLAMEOUT TIME (S)
cylinder	25.4	pine	400	10.2	0
	25.4	birch	660	13.2	0
	12.7	pine	400	7.3	<30
	12.7	birch	660	9.3	0
flat plate	6.4	cedar	320	5.2	<90
	6.4	pine	400	5.8	<60
	6.4	birch	660	7.4	<30

Muraszew *et al*. (1976) found that samples in the stage of glowing combustion in a wind, when removed from the wind tunnel after between 30 s and 210 s, would typically reflame for a period of between 1 and 5 s. They reasoned that this behaviour would have significant implications for the ignition probability of samples landing on the fuel bed after flight.

Woycheese (2000, 2001), using a horizontal wind tunnel, combusted 500 wood (balsa, Western Red Cedar, Douglas fir, Red Oak, Honduras Mahogany, Redwood and Walnut) disks of three sizes (25 mm dia. × 8.3 mm thick, 50 mm × 17 mm and 50 mm × 5.5 mm), in air flows of 1, 2, 3 and 4 m s^{-1}. A possible deficiency of the study is that these air speeds were typically only 50% or less of their modelled initial terminal velocity. The vast majority of the tests were of end-grain combustion, where the disks were cut so that grain, and subsequent air flow, was parallel to the disk axis. This grain orientation would not however reflect that of naturally occurring samples. The orientation was apparently selected to give consistent

results because the author stated that when air flow was perpendicular to grain direction, such as disks cut from shakes and shingles combusting on their flat surface, combustion was slow and 'spotty'. He concluded that disks partially ignited on their edges would propagate the farthest. He found that the low-density samples typically burnt completely while the high-density ones would typically have a large residual, unburnt mass. Woycheese (2001) concluded that sample size affected the mode of combustion, with lower density samples losing mass early in flight, while samples of greater density lost mass more slowly and consistently.

Tarifa *et al*. (1965, 1967) used a transparent vertical wind tunnel of 'blower' design and without contractor with a cylindrical section 1400 mm long × 560 mm wide, above a conical section 3000 mm long, to measure terminal velocities of samples such as pine cones. The conical section was marked to indicate air velocities. However, due to the amplitude of vertical movement it was necessary to use long-exposure photography in order to obtain mean position and hence mean terminal velocity. Clements (1977) used the methodology of Tarifa *et al*. (1965, 1967) and found that the vertical movement of pine cones about the mean position was about ±1 m. Tarifa *et al*. (1965, 1967) and Clements (1977) identified the problems of impact and of adhering in the boundary layer to the walls of tapered, vertical wind tunnels. Clements (1977) found the method unsuitable for studying leaves and moss for this reason.

Ellis (2000), using a vertical wind tunnel, performed preliminary studies of the combustion behaviour of four internally convoluted cylinders of bark of *E. globulus* subsp*. bicostata* (Maiden, Blakely and Simmonds) J.B. Kirkp. fixed with the axis perpendicular to air flow. Bark moisture contents were approximately 13%, which is considerably greater than would result on days of Very High to Extreme Fire Danger. One end of each sample was ignited and combusted in the working section of the vertical wind tunnel. Air velocities were 0, 1.7 6.3 and 12.3 m s^{-1} and thus included the values for terminal velocities of the cylinders estimated using Eqn 3.1, which were approximately 6 m s^{-1}.

It appeared that burnout time at bark cylinder terminal velocity increased as the degree of internal convolution increased. At their approximate terminal velocity samples exhibited glowing rather than flaming combustion and the maximum burnout time was 4 minutes. However, there was insufficient data to determine if such firebrands could burn for the 30 to 40 minutes required in order to produce spotfires at 30 km, for which candlebarks are notorious (Cheney and Bary 1969). Chandler *et al*. (1983) supposed that such long cylinders would be able to burn for long periods with fire inside the cylinder and hence protected from the ambient wind. Ellis (2000) concluded that the slow rate of loss of cylinder length due to combustion would mean that cylinder terminal velocity would remain constant during combusting flight. This finding of course implies that models appropriate for the behaviour of completely ignited wood samples will not be appropriate for bark cylinders burning from one end.

Ellis (2000) also measured the combustion and aerodynamic behaviour of prepared samples of the outer, weathered bark of messmate stringybark (*E. obliqua* L'Her). The bark is fragile and fibrous and has an oven-dry density of between 150 and 300 kg m^{-3} (mean 200 kg m^{-3}). Samples were cut with the fibres running parallel to their length. Samples had a length to width ratio of 10:3, lengths (l) of 35.4, 50 70.7 and 100 mm, and thicknesses (D_0) in proportion to length and typically ranging from 5 mm to 12 mm.

Ellis (2000) investigated the effects of ignition time and found that stringybark samples for which ignition time (t_i) was slightly less than index ignition time (t_{ii}), and hence partially ignited, had shorter flameout times but burnout times which could be up to three times those of fully ignited 'normally' combusting samples. He supposed that this 'extreme'

combustion pattern was very significant in terms of potential spotting distance by this bark type. Other behaviour not previously reported for wood samples included long flameout times, significant change to sample shape (and hence coefficient of drag), and the phenomenon of momentary reflaming during the latter stage of glowing combustion.

3.2.4 THE PROCESS OF IGNITION OF THE FUEL BED

Ignition probability is influenced by weather, firebrand and fuel bed variables (Cheney and Bary 1969), although the processes are generally poorly understood and quantified. Babrauskas (2003) summarised theories of heat transfer by small glowing and flaming particles to elements in a porous, organic fuel bed, and the results of laboratory and field ignition tests. Flaming ignition is defined as the exothermic combustion of gases obtained by (endothermic) pyrolysis of solid fuel, requiring adequate concentration and aeration as well as sufficient heat to ignite the gas mixture, or the presence of a pilot flame. Glowing combustion is the rapid oxidation of the surface of solid-phase char material.

The size of the elements of their fuel bed, their mineral and oil composition and their spatial arrangement, the last influencing aeration, are all potentially significant. Aeration is significant for the drying of the fuel bed as well its combustibility. In addition, fuel continuity and homogeneity may influence ignition probability on a broad scale. The moisture content of the profile of the surface fuel will influence rapidity of subsequent spotfire development and spread (McArthur 1967).

Conditions of Very High to Extreme Fire Danger (McArthur 1967) typically occur when the fuel bed and soil profiles are very dry, often due to drought, and ambient air temperatures are high, humidity low and winds strong. Such conditions enhance firebrand generation and spotfire ignition as well as subsequent spotfire growth. It is likely that the effect of solar radiation in heating surface fuel elements and affecting small-scale turbulence near the surface are also significant (Butler 2006). Topography will influence many of the above variables. In Australia, the presence of very dry 'cells' of air at altitude have been associated with subsequent extreme fire behaviour events (Mills 2008) which occur when cells are entrained to the surface by large-scale eddy mixing.

This mixing, which generally occurs as the surface heats due to solar radiation, also induces 'cascades' of turbulence to descend to the surface (Sullivan and Knight 2001) and, consequently, is potentially significant to ignition probability and subsequent spotfire spread. In addition, adiabatic lapse rate of the boundary layer to thousands of metres altitude has also been shown to influence fire development (Byram 1954). Keifer (2007) modelled the development of fire convection plumes under different conditions, and defined conditions during which intense plumes and firestorms could develop. It is not known what influence such atmospheric conditions have on early spotfire development.

Boonmee and Quintiere (2002) used a cone calorimeter to study flaming autoignition of wood and described two processes. At high heat fluxes of between 40 and 70 kW m^{-2} flaming ignition occurred with the initial flame appearing above the fuel surface in the gas phase and then propagating to the surface. Ignition is the commencement of some form of combustion. Glowing combustion, which is the solid phase oxidation of fuel (primarily char in this context), can occur at heat fluxes less than 40 kW m^{-2} once char has formed. Newly formed char is quite easy to oxidise and will react to oxygen able to reach the reactive surface. The competitive formation of char that leads to glowing combustion and volatile that leads to flaming combustion means that a fuel that has charred will not transition to flame, but the heat released in the solid phase oxidation is quite considerable (~30 MJ kg^{-1}) and this can quite easily initiate thermal degradation reactions of adjacent fuel substrate

that lead to pyrolysis and the formation of volatiles that oxidise in the gas phase as flames (Sullivan and Ball 2012)

Critical factors in ignition could be expected to include firebrand size, state, heat flux and remaining endurance after reaching the fuel bed, and the size, composition, including minerals, volatiles and moisture, and spatial arrangement of fuel elements, as well as exposure to wind.

Flaming firebrands generally have a significantly greater ignition probability than do glowing ones because they potentially generate greater heat flux and rate of heat transfer and because the presence of a flame provides small-scale turbulence for mixing which can also act to ignite the products of pyrolysis. Ignition probabilities of fine fuels by flaming firebrands during days of Very High to Extreme Fire Danger may be 100%.

For ignition by glowing firebrands, heat conduction may be the dominant mode of heat transfer (Babrauskas 2003). Countryman (1983) identified two fuel effects in ignition, one being the probability of achieving a minimum contact area between firebrand and fuel elements, and the other being presence of a sufficient density of fuel elements such that initial ignition points propagate. Hence, firebrand size (surface area) and fuel bed packing ratio or bulk density are potentially significant determinants of ignition probability.

Ignition cannot occur until most moisture is driven off and it therefore could be expected that for firebrands, which have a limited heat content, ignition success will be decreased by increasing fuel bed moisture content, as demonstrated by Dimitrakopoulos and Papaionnou (2001).

Air flow will affect the heat flux produced by firebrands and ignited fuel elements as well as the amount and mixing of concentrations of fuel and oxidizer in the gas stream, and depending on velocity and other conditions, could either aid or inhibit ignition. Air flow may be induced by wind, convection above the flaming or glowing firebrand, or by solar heating of the fuel bed (Butler 2006).

Firebrand moisture content can be expected to reduce its heat flux. However, in the case of a relatively small, glowing firebrand with low initial moisture content it is likely that all remaining moisture would have been driven off during its ignition and initial flaming combustion period.

3.2.5 METHODOLOGIES FOR TESTING FUEL BED IGNITION

Field investigations include those which test ignition using a standard 'firebrand' on a given fuel type (Blackmarr 1972), those which document spotfire occurrence from dedicated experimental fires (Gould *et al*. 2007), and those which collate spotfire occurrence during wildfires (SALTUS 2001). The data from Gould *et al*. (2007) quantify firebrand density and the number of spotfires and thus could be used to give an estimate of ignition probability. However, information concerning firebrand type and size is difficult to extract. The SALTUS study describes the combinations of fuel, fire behaviour and weather likely to cause spotting.

In order to investigate the influence of a limited number of specific, controlled variables and to investigate the process in detail, most ignition probability studies are performed in the laboratory. Typically, in order to obtain repeatable results from tests which may be limited in number for practical reasons, homogenous fuel beds of natural or artificial fuels are prepared and conditions such as moisture content and wind limited to a few values. In some investigations the ignition source is artificial and standardised. In others it may be natural 'firebrand' material, of uniform size or in a range of sizes. These are ignited to a consistent

standard prior to placement on the fuel bed. Such tests can be used to obtain threshold ignition criteria, such as the minimum temperature and radiant heat flux of the ignition source, or to investigate the effects of fuel bed moisture content or wind velocity, say, on ignition probability.

The process of ignition relevant to most ignition probability studies is the relatively rapid attainment of flaming ignition. Time to (flaming) ignition is another variable which will potentially influence the efficacy of firebrand transport, particularly at short distances. For example, a firebrand generated from a fire moving at 2 km hr^{-1} and landing 55 m ahead will be over-run before igniting a spotfire if its ignition time exceeds 100 s.

The definition of successful flaming ignition is important and may differ between researchers. For example, Ellis (2000) used small (50 mm × 50 mm) ignition sites in which firebrand samples were deposited and defined ignition as the merely occurrence flaming of fuel elements. Plucinski and Anderson (2008) defined an 'ignition threshold' as sustained combustion resulting in fire spread from the central test site to the edge of the fuel tray, a distance of 125 mm.

Problems with laboratory experiments include the potential effects on fuel bed ignitibility induced by artificial conditioning (Matthews 2010), the fact that the combustion characteristics of the firebrand samples may not be equivalent to those resulting from aerial transport, and that the turbulence of artificially-produced air flow may have unknown differences to wind in a forest (say). Hence the results of laboratory tests may not reflect ignition probability in the field. In addition, it may be very difficult to compare the results of experiments which employed different techniques.

3.2.6 FUEL BED IGNITION BY FLAMING SOURCES

Blackmarr (1972) tabled the ignition probabilities of slash pine litter at moisture contents up to about 30% by dropping single, flaming matches on to the fuel bed. He found ignition probabilities of 40% and 90% for moisture contents of 20% and 15%, respectively. However, the USDA National Fire-Danger Rating System (1974), which tables ignition probability applicable to all fine-fuel types for given ambient conditions, gives a maximum value of 5% ignition probability for a fuel moisture content of 20%. It is possible that this discrepancy is due to the difference in fuel bed uniformity between slash pine litter and that of other fuels.

Ellis (2000), Manzello *et al*. (2006, 2008), Plucinski and Anderson (2008) confirmed that the probability of ignition of fine fuels of less than about 10% moisture content by flaming samples is about 100%. Ellis (2000) used single samples of the outer bark of *E. obliqua* of initial mass between 0.8 and 1.8 g, ignited until well flaming and placed on the fuel bed when they were reduced to 60% of their initial mass. He used homogeneous intact fuel beds of *P radiata* needles excised from the litter bed under a mature stand and no-wind conditions.

Manzello *et al*. (2006) dropped single, flaming, machined disks of wood of *P. ponderosa*, 25 mm and 50 mm diameter, onto fuel beds of shredded hardwood mulch, pine straw mulch and cut grass, which had been conditioned to 0% and 11% moisture content. They tested wind conditions of 0.5 and 1.0 m s^{-1} and found that for 0% moisture content all fuel beds ignited, whereas at 11% moisture content only pine straw had 100% ignition probability.

Plucinski and Anderson (2008) tested the ignition probability of nine reconstructed shrubland litter types, conditioned to a range of moisture contents. They used methylated spirits applied to cotton balls or injected directly into the fuel bed, or aerial incendiaries as their standard ignition sources. They found that the thickness of the surface fuel elements,

their mineral and moisture content and state (live, dead, curing), their spatial arrangement in terms of bulk density (mass per unit volume) and packing ratio (volume of fuel per volume of fuel bed) and surface area of fuel per volume of fuel bed were all significant. Broadly, they found that all but two fuel bed types ignited at moisture contents less than about 20%. Those that did not had densely-packed fuel beds with bulk densities exceeding 115 kg m^{-3}.

Plucinski and Anderson (2008) also showed that the value for fuel bed moisture content at which 50% of tests resulted in ignition decreased from about 30% to 5% as bulk density increased from about 35 to 105 kg m^{-3}. They thus indirectly demonstrated that increasing bulk density between the values above effectively reduced ignition probability.

Ganteaume *et al*. (2009) tested flaming samples of twigs, barks, leaves, cones and cone scales commonly occurring in Europe, on fuel beds of needles of *P. pinea*, I. *pinaster* and *P. halepensis*, leaves of *E. globulus* as well as dried and cured grass with fuel moisture contents between 3.3% and 11.3%, in the absence of wind. Firebrand initial moisture contents ranged between 4% and 5%. The ignition probabilities (PI) and ignition times (TI) of combinations of firebrand and fuel bed most relevant to Australia are given in Table 3.2.

Table 3.2. Ignition probabilities (PI) in the absence of wind for combinations of flaming firebrand and fuel bed most relevant to Australia as from Ganteaume *et al.* (2009). Firebrand type and initial mass (m0), Fuel bed type and oven-dry moisture content (MC%)

FIREBRAND	M_0 (G)	FUEL BED	MC%	PI (%)
P. radiata bark	1.3 – 8.3	P. pinaster needles	3.98	45
P. radiata bark	1.3 – 8.3	E. globulus leaves	3.3	20
E. globulus bark	0.2 – 2.0	P. pinaster needles	3.98	97.5
E. globulus bark	0.2 – 2.0	E. globulus leaves	3.3	100
E. globulus leaf	0.2 – 1.4	P. pinaster needles	3.98	97.5
E. globulus leaf	0.2 – 1.4	E. globulus leaves	3.3	90

Ganteaume *et al*. (2009) did not find firebrand moisture content as a significant variable and modelled ignition probability for the fuel beds as a function of firebrand type, fuel bed bulk density and fuel bed moisture content.

3.2.7 FUEL BED IGNITION BY GLOWING SOURCES

Wright (1932), using heated iron discs, and Fairbanks and Bainer (1934), using simulated exhaust manifolds, found that surface temperatures of 725 and 760°C, respectively, were required to ignite pine needles. Harrison (1970) tested ignition of dry pine needles using a rod-shaped electric heating element. He found that for ignition times of 100, 50, 25 and 10 s, surface temperatures required were 375, 410, 460 and 575°C, respectively. Filippov (1974) found that pine needles from the forest floor autoignited in about 30 s when exposed to a radiant heat flux (RHF) of 45 kW m^{-2}. It is likely that, as for solid wood samples (Simms and Hird 1958), the flaming ignition of pine needles will occur for a continuum of combinations of RHF, exposure time and proximity of pilot flame.

Harrison (1970) found a wind speed of 0.9 m s^{-1} optimum for the ignition of pine needles by a heating element. A wind velocity that produces the maximum heat flux from a firebrand could be expected to decrease its burnout time (endurance). Ellis (2000), Manzello *et al*. (2006) and Ganteaume (2009) found that glowing firebrand samples could not ignite dry fuel beds in the absence of air flow ('wind'). It is likely that a wind velocity of about 1 m s^{-1} optimises the compromise between enhanced radiant heat flux and the transfer of oxygen to the reacting surface of the char.

McArthur (1969) described a 'critical level of fuel dryness…where the spotting process reaches maximum efficiency', but no studies to date have demonstrated such a phenomenon.

Ellis (2000) tested stringybark (*E. obliqua*) firebrand samples of initial mass 0.8 to 1.8 g ignited by match and allowed to combust until they had reached 20% of initial mass. The glowing samples were placed on excised sections of *Pinus radiata* litterbed exposed to a near-horizontal 'wind' produced by a domestic fan, of 1 m s^{-1}. He showed that ignition probability by single glowing firebrands of mass between about 0.1 and 0.4 g increased from about 10% to about 60% as fuel moisture content decreased from about 9% to about 3%. He found that glowing samples with a mass as small as 0.11 g could result in ignition.

Ganteaume *et al*. (2009) similarly tested the ignition probability by glowing samples, initially ignited using a small electric radiator and dropped on to fuel beds. 'Wind' across the fuel bed was produced by a domestic fan and varied in speed between 0.8 m s^{-1} and 4.5 m s^{-1}. They also tested the effect of horizontal and oblique (45°) orientation of air flow to fuel bed. The ignition probabilities (PI) and ignition times (TI) of combinations of firebrand and fuel bed most relevant to Australia are given in Table 3.3.

Table 3.3. Ignition probabilities (PI) and time to ignition (TI, mean bold, and range in brackets) for combinations of glowing firebrands and fuel beds most relevant to Australia, by Ganteaume *et al.* (2009). Firebrand type and initial mass (m_0), fuel bed type and oven-dry moisture content (MC%), orientation of 0.8 m s^{-1} air flow ('Wind') is oblique at 45° (O) or horizontal (H) to the fuel bed

FIREBRAND	M_0 (G)	FUEL BED	MC%	'WIND'	PI (%)	TI (S)
P. radiata bark	1.3 – 8.3	P. pinaster needles	3.98	O	2.5	**70** (NA)
P. radiata bark	1.3 – 8.3	P. pinaster needles	3.98	H	17.5	**55** (7-120)
P. radiata bark	1.3 – 8.3	E. globulus leaves	3.3	O	0	NA
P. radiata bark	1.3 – 8.3	E. globulus leaves	3.3	H	7.5	**63** (27-117)
E. globulus bark	0.2 – 2.0	P. pinaster needles	3.98	O	82.5	**15** (5-55)
E. globulus bark	0.2 – 2.0	P. pinaster needles	3.98	H	55	**10** (3-27)
E. globulus bark	0.2 – 2.0	E. globulus leaves	3.3	O	20	**9** (3-25)
E. globulus bark	0.2 – 2.0	E. globulus leaves	3.3	H	22.5	**15** (12-21)
E. globulus leaf	0.2 – 1.4	P. pinaster needles	3.98	O	2.5	**14** (NA)
E. globulus leaf	0.2 – 1.4	P. pinaster needles	3.98	H	0	NA
E. globulus leaf	0.2 – 1.4	E. globulus leaves	3.3	O	0	NA
E. globulus leaf	0.2 – 1.4	E. globulus leaves	3.3	H	0	NA

For the former three combinations, Ganteaume *et al*. (2009) found that in addition to 'wind' orientation and firebrand type, firebrand sample initial mass, surface area and moisture content were significant. For the latter three, they found that sample surface area was significant. The results show that 'wind' orientation can potentially affect ignition probability but the authors did not explain it. It is likely that different orientation of air flow results in different patterns of turbulence at the surface of the fuel bed, thus influencing ignition.

3.2.8 INITIAL RATE OF SPOTFIRE GROWTH

Ganteaume *et al*. (2009) also tested ignition frequency, the time to ignition, subsequent rate of spread, rate of fuel consumption, mean flame height and fuel consumption ratio, of fire within prepared trays (0.70 m square, or 0.70 m dia.) of five common European litter types. Their standard 'firebrand' was a 2 × 2 × 1 cm block of *Pinus sylvestris* wood ignited using an electric radiator (Standard NF P 92-509-1985) and tests were carried out in the absence of wind. They modelled the six parameters of ignition and growth as linear functions of fuel moisture content and fuel bed bulk density.

The pine needle fuel beds of *P. halepensis* and *P. pinaster* in these experiments potentially have similarities with those of *P. radiata*, and hence data from those tests may be relevant to Australia but this will require verification. The *E. globulus* litter fuel beds had mean values for fuel load, moisture content and bulk density of 1.01 kg m^{-2}, 7.89% and 35.72 kg m^{-3} respectively. The ignition probability and mean values for time to ignition and rate of spread for 64 tests of *E. globulus* litter were 94%, 9.1 s and 0.17 cm s^{-1}.

Butler (2006) investigated the effect of surface fuel heating by solar radiation by comparing the rate of combustion of 2.4 m long non-irradiated and halogen irradiated fuel beds in a horizontal wind tunnel. He postulated that the faster rate of spread observed in fuels irradiated at between 0.8 and 1.0 kW m^{-2} could be attributed to increased turbulence at velocity scales less than 0.1 m s^{-1}, decreased fuel moisture and increased preheating of the fuel bed. He envisaged that the turbulence created by irradiation would act to increase the mixing of oxygen adjacent to the surface.

3.2.9 IMPLICATIONS OF PREVIOUS WORK FOR THIS PROJECT

Ignition probability is a critical variable in determining the number of spotfires resulting from a given number of firebrands transported to a fuel bed and hence subsequent potential impact on firefighters and communities. In Australia, eucalypt barks are supposed to be the principal firebrand material (McArthur 1966, Cheney and Bary 1969). There have been few published studies of ignition of Australian litter types or of ignition by eucalypt barks. Plucinski and Anderson (2008) compared the ignition probabilities by a standard flaming 'firebrand', of prepared trays of Australian shrubland litters and determined the significant fuel bed variables. These authors confirmed the influence of fuel moisture content and bulk density on ignition probability.

Ellis (2000), Plucinski and Anderson (2008) and Ganteaume *et al*. (2009) confirmed that flaming sources typically had 100% ignition probability of fine fuels at low moisture contents. Ellis (2000) and Ganteaume *et al*. (2009) showed that glowing samples of eucalypt bark had high ignition probabilities of such fuels. The latter authors showed that 'wind' orientation to the fuel bed, fuel bed type and moisture content, firebrand sample state, and to some extent its size and mass, were all important. These authors also measured the initial spread rate following ignition trays of this litter type.

However, it is arguable that the firebrand samples used in either study did not reflect the condition of similar samples following airborne flight. In addition, because fuel bed ignition methodologies are not standardised, it is very difficult to make comparisons between studies. Thus, there is a need to validate and extend the ignition probability work by Ellis (2000) and Ganteaume *et al*. (2009) to other firebrand types and fuel beds implicated in major spotting events. As well there appears to be no information concerning the phase of early spotfire growth in 'wind' conditions, apart from unpublished data by McArthur on fire

growth from point ignitions. Table 3.4 lists details of methodologies which should be considered before designing experiments to investigate ignition and early spotfire growth.

Table 3.4. Details of methodologies which should be considered in the design of experiments to investigate fuel bed ignition and initial spotfire growth

VARIABLE	CONSIDERATION	POSSIBLE SOLUTION
Natural wind over fuel bed surface in the field	How will laboratory 'wind' compare with natural wind?	Characterise surface wind in the open and under open forest
Laboratory 'wind'	How to transfer lab results to field and comparison of results between experiments?	Design an air flow system, then describe the resulting air flow across the fuel bed trays
Natural solar radiation, which is particularly relevant in open eucalypt forest	How will laboratory 'solar radiation' compare with natural radiation?	Set a laboratory standard of 1 kW m^{-2}, say, and measure its effect on fuel temperature and turbulence at the surface of the fuel beds.
Variations in heat flux for samples of natural material	How to compare ignitibility of different fuel beds?	For some tests use 'standard' firebrands to produce a consistent flaming or glowing ignition source.
Differences between the characteristics of a firebrand sample burning in the laboratory and one which has been transported by air in the field	How to relate ignition probability for a particular firebrand material measured in the laboratory with that in the field?	Characterise the difference between laboratory sample and sample which has been burning at its terminal velocity.
Differences between the characteristics of a fuel bed which has been dried artificially in the laboratory and one which has dried naturally in the field	How to relate ignition probability for a particular fuel bed type measured in the laboratory with that in the field?	Difficult.
Variation in ignitibility between different fuel beds of given moisture content	How to compare ignition success by different firebrands?	For some tests use a 'standard' fuel bed to allow comparison.

In summary, it was concluded from the literature review that where practical:

- Ignition tests would be performed in a horizontal wind tunnel for which air flow velocity and turbulence would be accurately measured to enable comparison with natural wind under forest;
- The fuel bed selected should be a type which is significant in major fires and sections of the litter profile of this type to be tested should be excised in such a way that they represent natural fuel bed as closely as possible;
- Characteristics of the fuel bed for each sample, including the proportion of different surface components such as leaves and twigs, be measured;
- Where possible, firebrand material used in tests should be a natural, common firebrand material, preferably a eucalypt bark;
- Firebrand samples should represent firebrands that would theoretically be generated commonly and have relatively low initial terminal velocities of between 3 ms^{-1} and 5 m s^{-1};
- Ideally, firebrand samples should be combusted in such a manner that their characteristics would be similar to a firebrand transported with a relative air velocity equal to its terminal velocity;
- Firebrand samples would be standardised in order to measure the effect of fuel bed characteristics on ignition probability.

3.3 Experimental determination of probability of ignition of dry-eucalypt forest litter by firebrands

The number and density of ignitions by firebrands and the rapidity of their subsequent spread, determine the nature and magnitude of the effect of spotting (Byram 1959; McArthur 1967; 1969b; Cheney and Bary 1969; Luke and McArthur 1978; Pagni 1993; McCarthy and Tolhurst 1998). Hence, ignition probability influences the likelihood that natural or artificial firebreaks will be breached, the multiplication effect of additional remote ignitions, the likelihood of enhanced fire spread, and the onset of unpredictable behaviour such as results from mass ignition.

Dry sclerophyll forest is a major vegetation type in the south-east and south-west of Australia, where large devastating bushfires (Cruz *et al*. 2012) are recurrent phenomena (McArthur 1969a). In addition it is likely that the litter of wet eucalypt forest during extended drought will have many of the characteristics of dry forest. However, there are few studies or models of ignition probability of this fuel type by firebrands which have application in the field.

Investigations using flaming matches on natural fuels (Keetch 1941, Fons and Stromberg 1941, Parrot and Donald 1970, Lawson *et al*. 1993) and artificially arranged natural fuels (Blackmarr 1972) found fine fuel moisture content (FMC) and the size of the flaming source to be the most significant variable. Fons and Stromberg (1941) found that winds speeds greater than about 2 m s^{-1} tended to extinguish matches. Tests using cigarettes as a glowing source (Keetch 1941, Fons and Stromberg 1941) found wind important for achieving flaming ignition. Countryman (1983) found that the coarseness of his chopped grass fuel and FMC determined success of glowing ignition for a wind speed of 1.5 m s^{-1}. He had earlier concluded (Countryman 1980) cigarettes would be marginal as firebrands because their heat content was lower than for woody fuels, their slow, glowing combustion and their propensity to form ash on their surface.

Bunting and Wright (1974) found that air temperature, relative humidity, FMC and average wind speed affected the ignition of cow dung and decayed wood by glowing samples of juniper wood but that the dominant variables were 10-hour timelag fuel (fuels between 6 mm and 25 mm in diameter) moisture content and maximum wind speed. Manzello *et al*. (2006) found that four 50 mm glowing wood samples were required to initiate flaming ignition of pine straw with a 'wind' of 1 m s^{-1}.

Plucinski *et al*. (2008) found for samples of leaves of *Eucalyptus. dives* Schauer that the interval of oven-dried FMC of about 19% to 30% encompassed the range of zero to 100% ignition for a standard flaming ignition source of methylated spirits. However, this ignition source shares few characteristics with flaming firebrands. Ganteaume *et al*. (2009) measured the probability that flaming and glowing samples of the bark of *E. globulus* would ignite artificially arranged fuel beds of leaves of this species. However, they did not show FMC to have a significant variable, although expert knowledge (Albini 1979) and authors such as Blackmarr (1972) have demonstrated otherwise.

Ellis (2011) showed that 'wind' was essential to ensure that small, glowing bark samples of *E. obliqua* L'Her would ignite needle litter of *Pinus radiata*, but did not demonstrate a steep response to FMC. He also indicated the potential difficulty in comparing the results of ignition tests due to the absence of common procedures and standards, particularly with respect to air flow characteristics. The finding that orientation of air flow with respect to the surface of fuel samples may significantly affect ignition (Ganteaume *et al*. 2009) suggests that turbulence as well as air speed may be critical.

In addition, few researchers have used litter profiles collected with minimal disturbance as performed by Lin (2005), Ganteaume *et al.* (2011a) and Ellis (2011), although variables such as bulk density are significant (Plucinski *et al*. 2008). Furthermore, few researchers compared the characteristics of their standard ignition sources to those of firebrands (Bunting and Wright 1974, Countryman 1980).

Indirect measurement in North America (Manzello *et al*. 2007, 2008, Foote *et al*. 2011, Rissel and Ridenour 2013), and unpublished data from Project Vesta (Gould *et al.* 2007) in Western Australia of firebrand size indicates that the vast majority of firebrands are less than 0.3 g in mass or 1 cm^2 in projected area on landing. The initial size of firebrand samples used in ignition tests generally reflects this (Ganteaume *et al*. 2009, Ellis 2011, Ganteaume *et al*. 2011b). Unpublished measurements (Tolhurst[4] *pers. comm*.) of burnt-out firebrands generated by a prescribed burn in *E. obliqua* forest gave a mean value for projected area of 4 cm^2. It is recognised that the samples used in these experiments would probably be above average in size compared to firebrands in the field.

The aim of the current work was to measure ignition probability by small firebrand-like samples of a fuel bed significant in high-intensity bushfires. Characterisation of the velocity and turbulence of the air flow was expected to potentially allow comparisons with air flow in the field and with findings from other investigations.

3.3.1 FUEL BED SAMPLES

Samples of well-developed litter profile under Southern Tablelands Dry Sclerophyll Forest (STDSF, Keith 2004) were collected from two adjacent sites at two locations (Table 3.5) in long-unburnt forest. Samples from the two locations were collected during early autumn (April) in consecutive years. STDSF is typically open eucalypt forest or woodland 15-20 m tall with *E. macrorhyncha* F. Muell. ex Benth., *E. rossii* R.T. Baker & H.G. Sm and *E. mannifera* Mudie the dominant over-storey species.

Table 3.5. Description of fuel bed sample collection sites. Site, Location, Number of samples (n), Altitude above mean sea level (Alt), Aspect and Slope, Over-storey cover (OSC) and height (OSHt), Over-storey diameter at breast height over-bark (OSD), Under-storey cover (USC) and height (USHt). Mean annual rainfall at both locations is about 620 mm

SITE	LOCATION	N	ALT (M)	ASPECT SLOPE (°)	OSC (%) OSHT (M)	OSD (CM)	USC (%) USHT (M)
Kowen1	S35° 18.822'	8	750	W	35	20-42	< 1
	E149° 15.422'			15	15-18		~ 1
Kowen2	S35° 18.769'	8	750	NW	30	20-37	< 1
	E149° 15.504'			15	15		~ 1.5
Googong1	S35° 25.597'	16	860	NNE	25	25-40	10
	E149° 17.455'			5	15-20		6
Googong2	S35° 25.591'	16	860	NNE	25	25-40	< 10
	E149° 17.408'			5	15-20		5

[4] Dr K G Tolhurst, University of Melbourne, Victoria.

Fuel bed samples 400 mm by 400 mm were collected using a custom fork (Fig 3.2) with 41 tines of 5 mm diameter carbon fibre tube 435 mm long and 5 mm apart. Litter to soil was cleared along an edge of the intended sample and the tines inserted along the fuel-soil interface. After trimming the edges, the sample was placed in a sheet-steel tray 400 mm square and 25 mm deep (Fig 3.2). During transport tray lids were supported to avoid compressing the profile.

Figure 3.2. Fuel bed sample 400 mm × 400 mm after lifting from the litter profile using the custom 41-tine fork.

One corner of each tray was marked as a reference for its orientation during experiments and the percent cover of surface components and surface roughness measured. The latter variable can potentially affect ignition due to its effect on wind velocity and turbulence.

3.3.2 SURFACE COMPONENTS AND ROUGHNESS

Each tray was placed in a reference frame with two opposite sides marked at 10 mm intervals in order to locate sampling transects (Fig 3.3). The order in which trays were measured, the orientation of the tray in the frame, and the location of each transect, were selected randomly. The outer 25 mm width of fuel in each tray was excluded because of potential disturbance. The rod for point-transect sampling was 500 mm in length with ten 35-mm-long pins at 37 mm centres.

The category of fuel component (Table 3.6) touched by, or perpendicularly below, the point of each sampling pin was recorded for 10 transects for each tray. 'New' leaves were any distinct colour other than dull brown, although the distinction was somewhat subjective. The mean and standard deviation of percent cover for each fuel component and for each site is given in Table 3.6.

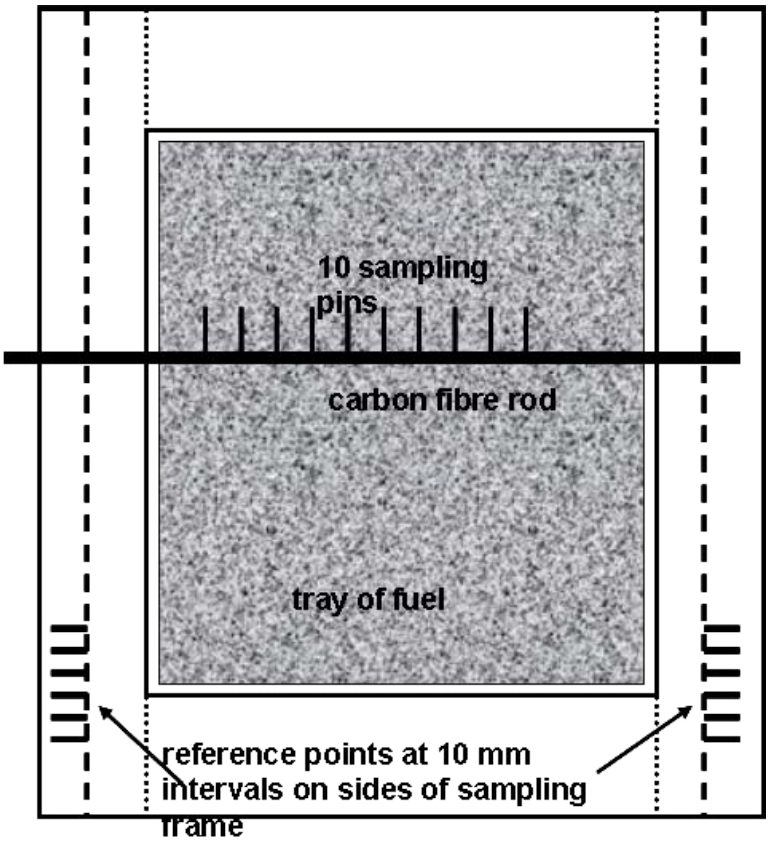

Figure 3.3. The reference frame in which trays of fuel were placed for measuring percent cover of litter surface components and surface roughness. The rod for point sampling cover of surface fuel components is shown.

Table 3.6. Surface components and surface roughness for each fuel collection site means and standard deviations. Percent cover for each surface component. Roughness measurements are fuel profile depth (*D*), root mean square of deviations from *D* (R_{yi}) and root mean square of difference between adjacent measurements ($R_{\Delta h}$)

SURFACE COMPONENT	KOWEN1	KOWEN2	GOOGONG1	GOOGONG2
1. Older Leaf	40.88 (12.53)	42.57 (8.54)	27.00 (10.49)	20.25 (8.44)
2. Bark (< 3 mm thick)	30.5 (20.32)	25.10 (7.50)	19.19 (6.82)	26.25 (7.22)
3. Thin Twig (< 3 mm dia.)	12.5 (3.77)	14.63 (5.42)	15.13 (5.28)	15.13 (3.98)
4. New Leaf	3.75 (6.78)	2.07 (2.12)	24.75 (6.86)	23.00 (10.35)
5. Thick Twig (> 3 mm dia.)	4.63 (4.66)	5.33 (2.10)	9.38 (5.49)	10.81 (5.10)
6. Thick bark (> 3 mm thick)	0.25 (0.46)	0.13 (0.36)	1.38 (2.36)	1.69 (2.77)
7. Fruit/Other (not scat)	0.25 (0.71)	0.14 (0.39)	0.56 ().89)	0.88 (1.20)
8. Decayed Leaf, Bark, Twig	7.00 (2.93)	9.92 (4.26)	2.50 (2.28)	1.63 (1.75)
9. Scat	-	-	0.13 (0.50)	-
10. Dead Grass	0.13 (0.36)	-	-	-
SURFACE ROUGHNESS				
D (mm)	27.34 (4.19)	26.26 (2.82)	35.03 (3.81)	34.40 (4.14)
R_{yi} (mm)	8.43 (1.29)	8.37 (0.76)	7.86 (1.88)	8.67 (2.39)
$R_{\Delta h}$ (mm cm^{-1})	8.76 (2.05)	8.75 (1.14)	8.67 (2.39)	9.40 (1.65)

The device for measuring surface roughness was a 450 mm × 100 mm rectangle of 6-mm-thick Perspex mounted on 60-mm-tall sheetmetal legs with a 30 mm × 30 mm × 2 mm aluminium stiffener running its length. A line of 2.5 mm diameter holes at 10 mm centres extended from side to side (Fig 3.4). The position of the first of a sequence of 10 consecutive holes and the direction (left or right) of the transect, was selected randomly. A 2 mm diameter bamboo probe 100 mm long was placed vertically in each hole and rested on the surface of the fuel (Fig. 3.4).

Figure 3.4. Device for measuring surface roughness. The 2 mm diameter probe is inserted vertically through a hole so that it rests on the surface of the fuel bed and the height projecting above the top surface of the Perspex is the raw measurement.

The raw reading was the length, to the nearest millimetre, of probe projecting above the Perspex surface. Ten transects were made for each tray. The raw reading was converted to profile depth (d_i), and the deviation (y_i) from the mean profile depth for the tray (d_T) calculated for each position. The root mean square (RMS) of y_i (R_{yi}) was calculated for each tray using:

$$R_{yi} = \sqrt{1/n \sum y_i^2} \qquad [3.6]$$

where y_i is the deviation of each measurement from mean profile depth of the tray (d_T) and n is the number of measurements (100). The RMS of the slope of the profile between adjacent measurements ($R_{\Delta h}$) was derived similarly using the square of the difference between adjacent measurements (Δi) along each transect:

$$R_{\Delta h} = \sqrt{1/N \sum \Delta_i^2} \qquad [3.7]$$

where N is the number of values of Δi (90). The mean and standard deviation of profile depth (D), R_{yi} and $R_{\Delta h}$ for each site are given in Table 3.6.

3.3.3 STANDARD FIREBRAND SAMPLES

To facilitate preparation and provide consistency it was intended to use samples of a manufactured material, or machined natural material, with similar combustion and aerodynamic properties to eucalypt bark (Ellis 2000, Ellis 2010, 2011, 2013). For 'flaming' samples, three hundred sections 50 mm long were cut from bamboo sticks and a sub-sample of 34 sections had a mean diameterof 2.37 mm (s.d. 0.080). The modelled terminal velocities of the samples (Ellis 2010) were between 3 m s^{-1} and 4 m s^{-1} and they flamed for about 9 s in zero wind after 3 s ignition using a Bernzomatic propane gas torch. These characteristics are commensurate with those of small samples of the bark of *E. obliqua* L'Her. after a few tens of seconds of flight (Ellis 2000).

For 'glowing' samples all substitute materials trialled were inferior to the bark of *E. globulus* in terms of endurance in the glowing state and ability to ignite fine fuels. Samples of the outer fibrous bark of *E. obliqua* (Ellis 2000, 2011, 2012) are efficient firebrands but their combustion behaviour is variable due to weathering. The 'ribbon' or 'candlebark' bark morphology of *E. globulus* results in a High to Very High hazard rating for short distance and long distance spotting (> 2 km) when bark thickness is about 2 mm or less and the bark on the boles is such that flames can easily ascend the trunks (Hines *et al*. 2010). Its potential as a firebrand material has been confirmed in the laboratory (Ganteaume *et al*. 2009). Samples can be easily prepared from shed flakes about 2 mm in thickness and have modelled initial terminal velocities of about 4 m s^{-1}, and hence could easily be lofted in the convection of bushfires of moderate intensity (Ellis 2010).

Five hundred samples 50 mm long, 15 mm wide and between about 1.3 mm and about 2.0 mm in thickness were cut from the shed flakes of a number of trees of *E.globulus* subsp. bicostata (Maiden, Blakely & J.Simm.) in amenity plantings around Canberra. About 80% of samples achieved the target mass of between 0.6 and 0.9 g and the thickness of the remainder was reduced using a blade in order to achieve uniformity. A 3 mm diameter hole was drilled in the centre of each sample and the samples randomised and stored.

In order that the state and heat flux of the standard glowing samples resembled that of glowing firebrands, samples were combusted at their terminal velocities for 12 s to 15 s prior to deposition. A purpose-built glowing firebrand generator (Fig 3.5) was designed and constructed to allow combustion at sample terminal velocity and easy deposition of the glowing sample onto the fuel bed.

The combustion chamber was in the shape of a truncated cone, with 55 mm and 110 mm diameter apertures at either end. It was constructed of transparent 'makrolon' polycarbonate sheet 0.5 mm in thickness. The ratio of air velocity at the top and bottom of the chamber was 1:4. This chamber was attached to short sections of 110 mm diameter PVC pipe which incorporated a straightening section, a turning section, a choke and an adapter for the pipe of an 850 W vacuum cleaner. The choke was adjusted such that samples would remain supported by air flow while free to rotate and move vertically on a 1.5 mm diameter steel guide coaxial to the combustion chamber.

3.3.4 THE WIND TUNNEL

A horizontal wind tunnel 3250 mm long, comprising a 2D curvilinear diffuser section 940 mm long and a straight section 200 mm tall, 500 mm wide and 2310 mm long, was constructed of 0.6 mm galvanised sheet steel (Fig. 3.6). A plywood adapter 120 mm wide and 200 mm high was attached to the exit of a 270 W Elektrobau Mulfingen GmbH & Co. centrifugal fan. The 2D diffuser increased the width of flow from 120 mm to 500 mm over its length with an

inflexion point 367.5 mm from the inner face of the adaptor. The curves of the diffuser are described by co-ordinates X and Y (Table 3.7). Fan speed was adjusted using a Yamabishi Type S260-2M voltage regulator (not shown).

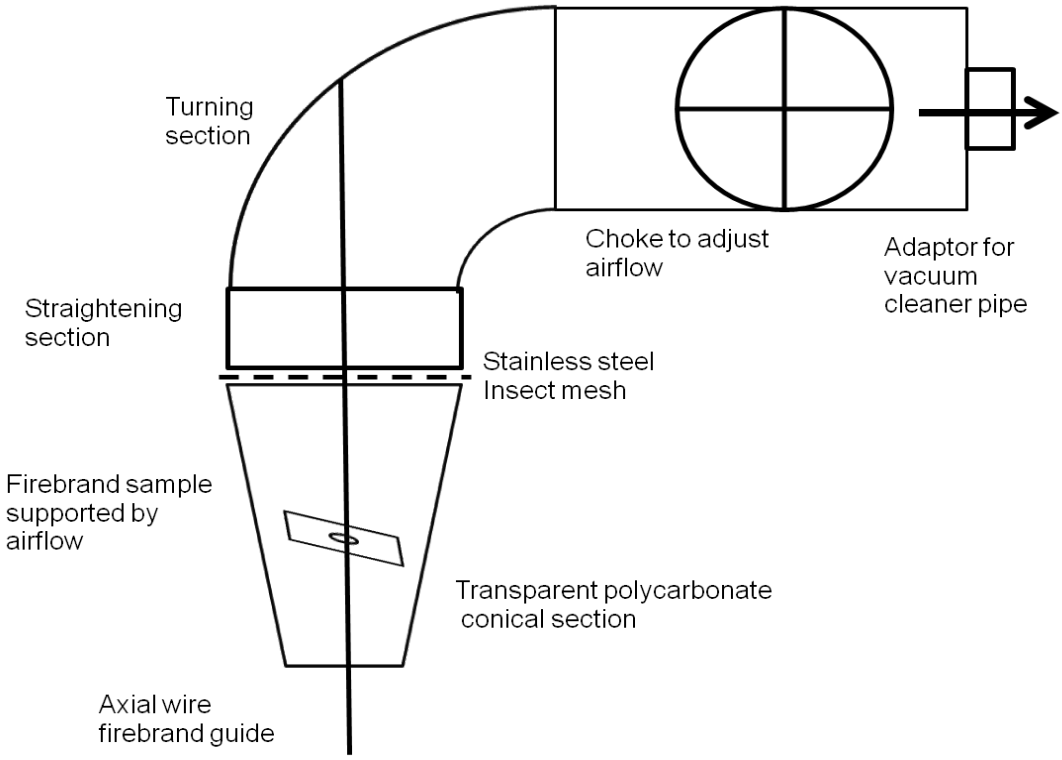

Figure 3.5. Side view of generator to produce glowing firebrands. It was constructed using 110 mm diameter PVC pipe with a conical combustion chamber of polycarbonate sheet 1 mm in thickness. Sections of plastic drinking straws 3 mm diameter and 35 mm long fill the straightening section.

Figure 3.6. Plan view of horizontal wind tunnel and ignition stage, 200 mm tall for its entire length and constructed using 0.6 mm galvanised steel sheet. The 270 W centrifugal fan is connected via an adaptor to the 2D curvilinear diffuser. The straightener is constructed from strips of hollow polycarbonate sheeting 10 mm in thickness and 100 mm wide. The plan shows the screen arrangement (SA) which produced non-laminar air flow. The 60° staggered, perforated metal screen, has 4.55 mm dia. holes at 6.35 mm centres giving an Open Area Ratio of about 46%, and is located 500 mm from the exit.

Two different screen configurations were used (SA and SB), which produced non-laminar (turbulent) and quasi-laminar air flow, respectively. SA, which is depicted in Fig. 3.6, used a straightener with an open area ratio (OAR) of approximately 88% and a 60° staggered, perforated metal screen with an OAR of about 46% located 500 mm upstream of the ignition

stage. The straightener was constructed from 100 mm wide strips of hollow polycarbonate sheeting (Sunlite 'Palram') 10 mm in thickness with square pores approximately 9 mm × 9 mm, and the metal screen had 4.55 mm dia. holes at 6.35 mm centres.

Table 3.7. Co-ordinates describing the 2D curvilinear section the horizontal wind tunnel (Fig. 3.6). Co-ordinate *x* is the axial distance from the inside face of the adaptor on the fan, and *y* and y_1 are half-widths of the diffuser, measured either side of the central axis

X (MM)	*Y*, Y^1 (MM)
0	60
100	62
200	70.5
300	94
367.5	111
400	122
500	160
600	196
700	225
800	242.5
900	249.5
940	250

An alternative screen arrangement (SB), which produced a near-laminar air flow, retained the straightener but replaced the perforated metal screen in SA with a wire mesh screen with 6 mm apertures and 0.6 mm diameter wire of OAR approximately 76.5%. In addition, three screens of the same mesh were placed in the curved diffuser section at distances 400 mm, 600 mm and 940 mm from the face of the fan adaptor. The ignition stage, in which fuel trays were placed, was 600 mm long with side walls 200 mm tall and was open at the top.

A digital stills camera was mounted directly above the ignition stage.

3.3.5 AMBIENT AND WIND TUNNEL AIR FLOW

A 3D RM Young 81000 ultra-sonic anemometer with a resolution of 0.02 m s^{-1} and an accuracy of ±1% in speed and ± 2% in direction was used to quantify air flow velocity and turbulence.. The anemometer was supported inverted on a sheet of steel level with the floor of the exit section (Fig. 3.7) and thus sampled air flow 115 mm above the nominal centre of the fuel surface in the tray.

Several minutes of data, sampled at 10 Hz, were obtained for screen arrangements SA and SB at constant fan speeds delivering approximately 1 m s^{-1} and 2 m s^{-1}. For a randomly selected interval of 60 s of data, mean air speed, *s*, (scalar, m s^{-1}) was calculated using:

$$s, = \sqrt{u_{,}^2 + v_{,}^2 + w_{,}^2} \qquad [3.8]$$

where u_1, v_1 and w_1 are the mean velocities for the U, V and W vectors.

Turbulent kinetic energy, *K* (m s^{-2}), was calculated using:

$$K = \frac{1}{2}[(u')^2 + (v')^2 + (w')^2] \qquad [3.9]$$

where u', v' and $w'$are the fluctuations of orthogonal velocity vectors *u*, *v* and *w*, for 1 s of data.. The mean and standard deviations of mean *s,* and *K* for the four combinations of screen arrangement and velocity were then calculated (Table 3.8).

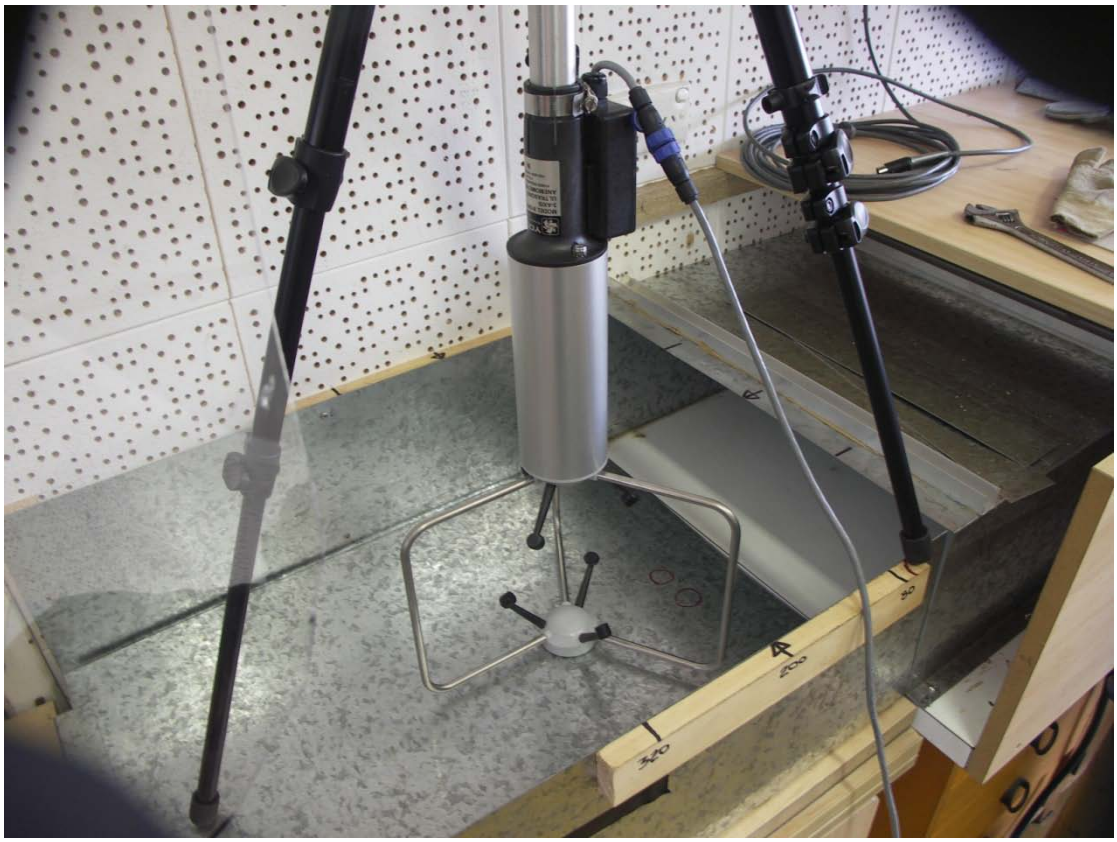

Figure 3.7. The 3D RM Young 81000 ultra-sonic anemometer mounted inverted in the ignition stage at the exit of the horizontal wind tunnel. It is located on a steel sheet such that it samples air flow 115 mm directly above the centre of a fuel tray.

Table 3.8. Air flow characteristics measured 115 mm above the nominal surface of a tray of litter in the wind tunnel (WT) ignition stage (Fig. 3.7). Mean and (standard deviation) of *s*, and *K* were obtained from 1 minute of data, for two alternative arrangements of screens SA (non-laminar) and SB (quasi-laminar)

	WT SA (NON-LAM)	WT SA (NON-LAM)	WT SB (LAMINAR)	WT SB (LAMINAR)
s, (m s^{-1})	1.005	1.958	1.044	1.91
	(0.0199)	(0.024)	(0.004)	(0.019)
K (m s^{-2})	0.0042	0.0155	0.00011	0.0011
	(0.00133)	(0.0055)	(0.00011)	(0.00032)

3.3.6 EXPERIMENTAL PROCEDURE

Firebrand samples were dried to a moisture content of between about 3% and 5% oven-dried weight. Fuel trays were conditioned using ambient conditions, a drying oven, a humidity chamber, or water spray and storage in a sealed bag. The aim was to complete a set of eight ignition tests on a single tray expediently so that changes in ambient conditions and FMC would be minimised. Wet and dry bulb temperature was measured before and after each experiment using an Assman psychrometer. The fan voltage regulator was set to give a nominal mean air speed of 1 m s^{-1} or 2 m s^{-1} which varied in practice by ± 5%.

Trays were subdivided into 3 × 3 ignition cells 120 mm × 120 mm. Tray orientation and test order of the cells was randomly selected. The tray was placed in the ignition stage of the wind tunnel such that the surface of the fuel was level with the floor of the wind tunnel exit. Air flows used were 'No-wind', 1 m s^{-1} or 2 m s^{-1} for flaming samples (FL), and 1 m s^{-1} or 2 m s^{-1} for glowing samples (GL).

Previous work (Ellis 2000, 2011) had shown that small glowing firebrands could not ignite fine fuels in the absence of air flow. FL samples were ignited for 3 s using a propane torch, and deposited on the appropriate cell. GL samples were ignited on a gas stove for 12 s and placed on the axial wire of the generator (Fig. 3.5) using tongs. After 12 s the vacuum cleaner was turned off and the GL deposited on the selected fuel ignition cell. One function of the firebrand generator was to ensure that the firebrand sample was past the stage of possible reflaming at deposition.

Ignition success was defined as sustained flaming of the fuel which could be ascertained for FL in 60 s or less. Success showed as growth of the area flaming, while failure showed as a diminishing area flaming and extinguishment of flame in 30 s or less. For GL, success required the transition of glowing combustion of fuel elements to flaming. It appeared that if transition to a flame of any size occurred, FMC was such that flaming ignition would be sustained. Success could occur up to 2 or 3 minutes after deposition, which corresponded to GL burn out time. In one case, transition to flaming occurred at 10 minutes as a result of substantial glowing combustion within the fuel profile.

Time to ignition was recorded for about half the FL tests. Ignition success scored 1 and failure zero. Four samples of surface fuel not affected by tests were oven dried to determine mean tray FMC.

3.3.7 ANALYSIS

Data for flaming (FL) and glowing (GL) firebrand tests were analysed separately using two-way analysis of variance (AOV) and logistic regression to model the effects of ambient conditions, air flow and fuel parameters on ignition probability . Two-way AOV and linear regression were similarly used to model 'time to ignition'. The criterion for statistical significance was $P \leq 0.05$, and all analysis was performed using 'R' (R Core Development Team 2012). The logistic regression model for the probability of flaming ignition by flaming (FL) or glowing (GL) firebrand samples ($P_{IG(FL)}$, $P_{IG(GL)}$) is expressed as:

$$P_{IG(FL)}, P_{IG(GL)} = 1/(1+e^{-z}) \qquad [3.10]$$

where z is of the form

$$z = a + \sum b_i x_i \qquad [3.11]$$

and a is constant and b_i the estimated coefficients for relevant variables x_i determined experimentally.

The goodness-of-fit for logistic models was measured using Nagelkerke's pseudo r^2 statistic (Nagelkerke 1991). Also, the area under the Receiver Operating Characteristic Curve (ROC) was used to determine the discriminative ability of the model over a range of cut-off points (Hosmer and Lemeshow 2000).

3.4 Results

Table 3.9 gives the details of the experiments. A total of 50 were conducted, 23 using fuel collected at Kowen and 27 with fuel collected at Googong. The obvious difference in cover of Older and New Leaf components between Kowen and Googong fuels (Table 3.5) was significant ($P < 0.05$) and apparently due to seasonal differences in rainfall.

Table 3.9. Ignition experiments details. Experiment number (Expt), collection site of fuel tray (Kowen1(A1), Kowen2 (A2), Googong1 (B1), Googong2 (B2), tray number (Tray), standard firebrand used (flaming FL, glowing GL), firebrand moisture content (MC), standard deviation of MC (MCstd), fuel moisture content of surface fuel of tray (FMC), standard deviation of FMC (FMCstd), the screen arrangement of the wind tunnel (Scrns, SA non-laminar flow, SB quasi- laminar flow), mean air speed (s, 1 m s^{-1} or 2 m s^{-1}), wet and dry bulb (WB, DB) temperatures and relative humidity (RH) obtained from these values. Each experiment typically comprised 8 ignition tests, occasionally 4.

EXPT	SITE	TRAY (#)	FB	MC (%)	MC STD (%)	FMC (%)	FMC STD (%)	SCRNS	*S* (M/S)	WB (°C)	DB (° C)	RH (%)
1	A2	12	GL	4.6	0.56	5.5	0.64	SA	1	16.65	28.85	27
2	A2	11	FL	NA	NA	8.6	0.3	NA	0	16.65	28.85	27
3	A1	5	GL	5.5	0.44	5.6	0.26	SA	1	18.1	29.5	32
4	A1	8	FL	3.1	0.31	8.0	0.12	SA	0	15.5	25.5	34
5	A2	10	GL	3.7	0.4	4.0	0.50	SA	1	14.5	20.5	52
6	A2	10	GL	3.7	0.4	4.0	0.50	SA	2	15.5	25.5	59
7	A1	7	FL	2.2	0.26	7.7	0.38	NA	0	18.4	31.4	27
8	A1, A2	15,4	GL	3.8	0.59	7.2	0.17	SA	1	18.5	32.5	24
9	A1, A2	15,4	GL	3.8	0.59	7.2	0.17	SA	2	18.5	32.5	24
10	A2	14	GL	4.3	0.01	4.4	0.25	SA	2	18.1	29.8	31
11	A1	3	FL	3.1	NA	14.2	1.23	SA	2	18.1	29.8	31
12	A1	2	GL	3.0	0.13	4.6	0.22	SA	1	19.5	32.5	29
13	A2	16	FL	2.2	0.39	13.1	0.43	SA	1	21	33.75	31
14	A1	1	FL	3.7	0.00	4.0	0.22	NA	0	18.5	28.5	38
15	A2	15	FL	NA	NA	14.5	0.47	NA	0	19.1	31	32
16	A2	15	FL	NA	NA	12.2	0.83	NA	0	19.4	31.6	31
17	A2	9	FL	NA	NA	10.8	0.94	NA	0	19	32	28
18	A1	3, 6	GL	4.3	0.65	5.2	0.52	SB	1	19.2	27.15	47
19	A1	3, 6	GL	4.3	0.65	5.2	0.52	SB	1.9	19.2	27.15	47
20	A1	3, 6	GL	4.4	1.6	4.7	0.13	SB	1	19.2	27.15	47
21	A1	3,6	GL	4.4	1.6	4.7	0.13	SB	1.9	19.2	27.15	47
22	A2	12	FL	6.8	NA	10.0	0.55	SB	1	22	29.5	52
23	B2	18	FL	5.5	NA	10.3	0.13	SB	1	22	29	54
24	A2	13	GL	4.2	0.74	9.7	0.44	SB	1.9	22	29	54
25	B2	25	FL	2.3	NA	10.4	0.49	SB	1	21.75	26.18	68
26	B2	34	FL	2.4	NA	13.4	0.73	SB	1	21.75	26.18	68
27	B2	45	FL	2.4	NA	9.7	0.44	SB	1	21.75	26.18	68
28	B1	37	FL	2.1	NA	11.0	0.35	SB	1	19.5	26.3	53
29	B1	20	GL	2.2	NA	3.7	0.41	SB	1	19.3	26.6	50
30	B1	23	GL	3.4	NA	3.6	0.22	SB	1.9	19.3	26.6	50
31	B1	6	GL	3.3	1.10	2.7	0.23	SB	1.9	20.7	29.5	45
32	B2	48	GL	2.8	NA	4.5	0.32	SB	1.9	20.5	29.35	45

33	B1	4	FL	3.8	NA	5.7	0.42	SB	1	18.75	28.5	39
34	B1	40	FL	3.3	NA	5.1	0.38	SB	1.9	18.7	29.5	35
35	B2	27	FL	5.4	NA	6.0	0.41	SB	1	19.5	27.8	46
36	B1	29	FL	1.6	0.56	12.0	0.63	SB	1.9	20.5	31	38
37	B2	21	GL	2.2	0.06	5.5	0.11	SB	1.9	19.5	30.5	35
38	B2	43	GL	3.1	NA	4.4	0.17	SB	1.9	20.1	30.85	37
39	B2	26	FL	2.6	NA	9.5	0.73	NA	0	19.15	26.55	50
40	B1	42	FL	3.0	NA	11.3	0.62	SA	1	18.8	26.7	47
41	B1	19	FL	2.6	NA	10.3	1.50	SA	1.9	19.35	27.45	47
42	B1	39	GL	4.3	NA	7.1	0.52	SA	1.9	18.8	28	41
43	B2	41	GL	5.3	NA	7.1	0.52	SA	1.9	18.8	28	41
44	B1	32	GL	4.3	NA	3.8	0.21	SA	1	20.6	31.8	36
45	B2	28	FL	2.4	NA	12.1	0.65	NA	0	20.5	31.5	36
46	B2	31	GL	5.7	NA	4.4	0.36	SA	2	20.65	30.2	42
47	B2	44	GL	3.8	0.21	4.6	0.33	SA	1	20	32	32
48	B2	45	GL	3.8	0.21	4.6	0.33	SA	2	20	32	32
49	B2	38	FL	8.2	NA	20.7	1.05	SA	2	21	30	44
50	B1	47	FL	2.5	NA	20.3	3.09	SA	1	21	30	44

3.4.1 IGNITION BY FLAMING FIREBRAND SAMPLES

Two-way AOV found that FMC (P < 0.000), air speed (P < 0.000), RH (P = 0.004), the interaction FMC:air speed (P = 0.01), fuel surface roughness R_{yi} (P=0.04) and the interaction surface roughness R_{yi} :FMC (P=0.03) were explanatory variables for ignition. Wind tunnel screen arrangement, ignition cell position on the tray, and surface fuel components were not found to be significant.

There was no significant difference in ignition success between air speeds of 1 m s^{-1} and 2 m s^{-1}, and hence wind was categorised as 'no-wind' (*Wind* = 0) and 'wind' (*Wind* = 1), respectively. Logistic regression showed that RH and the interaction surface roughness R_{yi} were not significant and produced Eqn 3.12:

$$z = 8.832 - 1.208FMC - 5.59Wind - 0.721FMC{:}Wind + 0.311R_{yi} \qquad [3.12]$$

$$(s.e. = 2.931)(s.e. = 0.319)\ (s.e. = 3.133)\quad (s.e. = 0.335)\qquad (s.e. = 0.152)$$

$$(P < 0.003)\ \ (P < 0.000)\qquad (P = 0.07)\qquad (P < 0.03)\qquad (P = 0.04)$$

where *z* is used in Eqn 3.10, *FMC* is oven-dried fuel moisture content (%), *Wind* is absence or presence of air flow (0, 1) and R_{yi} is surface roughness (Table 3.6). The values for pseudo R^2 and ROC are 0.56 and 0.88, respectively. Figure 3.8 shows the probabilistic models of Eqn 3.10 using Eqn 3.12 for R_{yi} = 8.0 mm, and plots the difference in modelled ignition probability due to Wind to illustrate the effect of the interaction FMC:Wind.

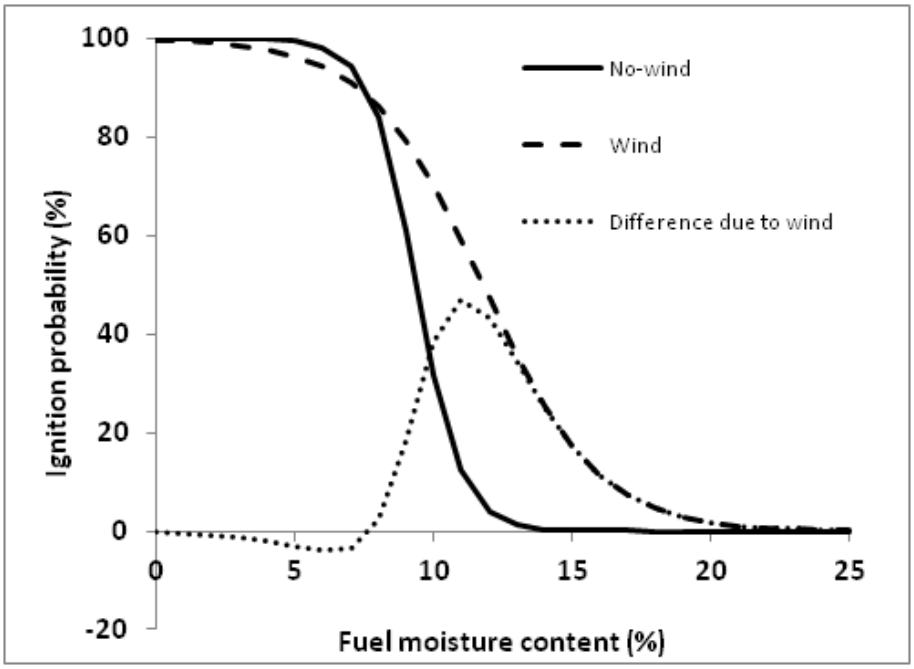

Figure 3.8. Probabilistic model of ignition success by flaming firebrand samples, given by Eqn 3.10 and Eqn 3.12, for absence and presence of wind (air flow of 1 m s^{-1} or 2 m s^{-1}), for a value for surface roughness R_{yi} of 8.0 mm. The difference in ignition probability between No-wind and Wind illustrates the effect of the interaction between FMC and Wind.

Linear regression was used to derive a model for the time to establish ignition (t_I):

$$t_I = -42.78 - 12.24FMC + 12.39Wind - 5.62FMC{:}Wind \qquad [3.13]$$

$$(s.e. = 15.51)\ (s.e. = 2.04) \quad (s.e. = 18.05) \quad (s.e. = 2.25)$$

$$(P = 0.007)\ (P < 0.000) \quad (P{=}0.49) \quad (P < 0.014)$$

where *FMC* is oven-dried fuel moisture content (%), *Wind* is presence (1) or absence (0) of (n = 96, R^2 = 0.48).

3.4.2 IGNITION BY GLOWING FIREBRAND SAMPLES

The influence of screen arrangement and fuel was confounded and hence only the data for screen arrangement, SA, (n=89) were analysed. Two-way AOV was used to test the same variables as for $P_{IG(FL)}$ and found that significant variables in ignition success were FMC (P = 0.03) and Wind (P=0.0001). Logistic regression analysis produced:

$$z = -3.23 - 0.008FMC + 3.136s \qquad [3.14]$$

$$(s.e. = 2.613)\ (s.e. = 0.351)\ (s.e. = 1.135)$$

$$(P = 0.22) \quad (P < 0.02) \quad (P{=}0..006)$$

where *z* is used in Eqn 3.10 ($P_{IG(GL)}$) to describe the probability of ignition by glowing samples, *FMC* is fuel moisture content (%) and *s* is mean air speed (m s^{-1}). Eqn 3.14 has values for R^2 and ROC of 0.36 and 0.85, respectively. Figure 3.9 shows the probabilistic form of function Eqn 3.10 using Eqn 3.14 for wind speed of 2 m s^{-1} and plots ignition success measured for individual trays of fuel.

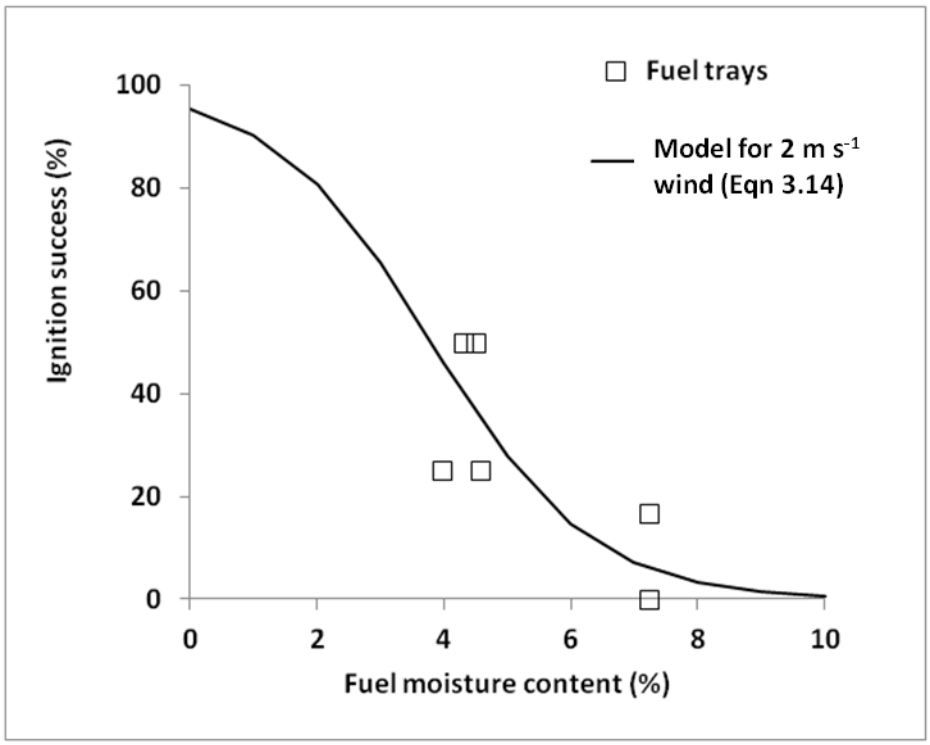

Figure 3.9. Ignition success for each fuel tray (%), for glowing firebrand samples, for a wind speed of 2 m s^{-1}, and logistic model derived from data of individual tests (Eqns 3.10 and 3.14)

3.5 Discussion

No measurements were made of the bulk density of the fuels in the trays. Values of 37±3 kg m^{-3} and 35.72 kg m^{-3} (*s.d.* 11.49) for loosely packed leaves of *E. globulus* were obtained by Matthews (2005) and Ganteaume *et al*. (2009), respectively. Plucinski and Anderson (2008) obtained a value of 35.61±0.42 for leaves of *E. dives*. It is likely that the values for the top of the profile in the trays would be in this range. However, it is arguable whether a meaningful value for the bulk density at the surface of the fuel, where most firebrand samples were observed to land, can be obtained.

3.5.1 IGNITION BY FLAMING FIREBRAND SAMPLES

Equations 3.10 and 3.12 shows that at an FMC of 10.83%, an increase in R_{yi} 1 mm from the mean value tested (8.0 mm) increases ignition probability ($P_{IG(FL)}$) from 14.6% to 19.0% for No-wind and from 61.2% to 68.3% for Wind. This indicates that increasing turbulence increases ignition likelihood. Butler (2006) showed that turbulence due to radiant heating of surface fuel increased fire rate of spread. At higher FMC (Fig 3.8), the effect of Wind is to significantly increase the ignition threshold from about 14% FMC to about 23%. At an FMC of 11%, Wind exhibits its maximum effect by increasing $P_{IG(FL)}$ by about 47%, while at FMC of less than 8% and greater than 23% the effect is minimised. The negative effect at FMC<8% may be an artefact.

Cheney *et al*. (1998) proposed two different functions for fuel moisture coefficients for rate of fire spread in grassland for FMC below 12%, for wind velocities greater than or less than 10 km hr^{-1} in the open. Their conclusion may also reflect a FMC:wind interaction. The model (Eqns 3.10 and 3.12, Fig 3.8) shows that ignition likelihood increases steeply as fuel moisture content falls below a critical level as shown by authors such as Blackmarr (1972).

Comparisons with Plucinski and Anderson (2008) for eucalypt litter, the National Fire-Danger Rating System (NFDRS, 1974) for all North American fuel types, and Blackmarr (1972) for slash pine needles were made by estimating the values for threshold FMC at which ignition can occur ($FMC_{THRESHOLD}$) and when ignition likelihoods are 10%, 50% and 100% (FMC_{10}, FMC_{50} and FMC_{100}), Table 3.10.

Table 3.10. Values for the threshold FMC for ignition (Threshold) and FMC at which modelled or measured ignition likelihood by flaming firebrand samples is 10%, 50% and 100% (FMC_{10}, FMC_{50} and FMC_{100}) for No-wind and Wind (wind of 1 m s^{-1} or 2 m s^{-1}, Eqn 3.12), *E. dives* litter in no wind, using 1 mL of methylated spirits in a cotton ball (Plucinski and Anderson 2008), the National Fire-Danger Rating System (1974) for North American fine-fuel types, and as measured and modelled by Blackmarr (1972) for Pinus litter.

MODEL	THRESHOLD (%)	FMC_{10} (%)	FMC_{50} (%)	FMC_{100} (%)
No-wind (Eqn 3.12) Eucalypt litter	14.5	11	9	5
Wind (Eqn 3.12) Eucalypt litter	21	16	12.5	6.5
Plucinski and Anderson (2008) Eucalypt leaves	34	28	22.7	12-18
NFDRS (1974) Range of fuels	23	17	6.5	2
Blackmarr (1972) Slash pine needles	35	27.5	22	10

The threshold and FMC_{10} values for Wind (Eqns 3.10 and 3.12) are very similar to those for the NFDRS, although the FMC_{50} and FMC_{100} for the latter model seem conservative. The values for the Plucinski and Anderson (2008) model are significantly greater than for the other models and this is probably due to differences in the standard ignition sources. Those authors used methylated spirits in a cotton ball or injected into the fuel. The value of 5% for FMC_{100} (No-wind) is in close agreement with the ignition probability of about 98% for ignition of *E. globulus* leaves (FMC=3.9%) by flaming bark samples of the same species (Ganteaume *et al*. 2009). However, for a fuel bulk density of about 36 kg m^{-3} the model produced by these authors generates a value for $FMC_{THRESHOLD}$ of greater than 40%, which is possibly too great a value. This result is probably due to the limited range of FMC tested. It was expected that wind of 1 m s^{-1} or 2 m s^{-1} would increase ignition likelihood, as shown by Eqns 3.10 and 3.12 and Fig 3.8. However, it is possible that further increases in wind speed could reduce ignition likelihood by increasing the rate of heat loss.

It appeared that the relatively high heat flux of FL resulted in an initial flaming ignition of fuel elements and that successful establishment was determined by FMC. Differences in critical values for FMC between different fuels (Table 3.10) are probably due to differences in the chemistry, coarseness, and arrangement of fuel elements.

3.5.2 IGNITION BY GLOWING FIREBRAND SAMPLES

Bark or timber samples which are glowing prior to deposition may momentarily flame in flight (Ellis 2000, Ellis 2013) upon removal from air flow (Muraszew *et al*. 1976), or potentially, upon fracture. However, such behaviour was not observed. Only one ignition resulted for SA at a wind speed of ~1 m s^{-1} and this suggests that the combination of firebrand sample characteristics, ambient conditions (including fuel surface temperature), turbulent kinetic energy and air speed is a threshold for this ignition source and fuel. Hence, it is possible that under field conditions, where ambient conditions including turbulence (Table 3.9) are more favourable, the probability of ignition by these glowing samples could be greater.

Equation 3.10 and 3.14 (Fig. 3.9) indicates a likely threshold FMC of between 8% and 10%, which compares well with a table based on expert opinion and field observation and reproduced by Albini (1979). Ganteaume *et al*. (2009) found that glowing samples of *E. globulus* bark of mean initial mass of 0.66 g ignited leaves of the same species at 3.3% FMC in horizontal wind of 0.8 m s^{-1} in 22.5% of tests. This value is in contrast to the predicted ignition probability of 3.4% determined for these conditions using Eqn 3.14. This difference may reflect differences in firebrand sample characteristics, fuel type and arrangement, and possibly, air flow turbulence.

A model by Ellis (2011) for ignition of *P. radiata* needles at FMC 10% by glowing samples of the bark of *E. obliqua* for 'wind' of 1 m s^{-1} gives an ignition probability of 15% for samples with a 0.2 g mass at deposition. This probability is much greater than for STDSF eucalypt litter (Fig. 3.9) and is probably due to differences in the coarseness of the fuel elements.

Eqn 3.14 shows that an increase in moisture content increases the time taken for the establishment of a successful ignition. Mean t_I for the ignition of a fuel bed of FMC 3.8% was 3 s, which is less than the means of between 9 s and 15 s the ignition of a leaf bed of *E. globulus* leaves at 3.3% FMC in wind (Ganteaume *et al*. 2009). This difference may reflect differences in the definition of 'established' ignition or because these authors used disturbed litter samples (Ganteaume[5], *pers. comm*.) rather than different ignition processes.

It appeared that ignition likelihood was increased if, by chance, the GL sample was positioned such that air flow velocity and turbulence was optimised by fuel micro-topography thus maximising its heat transfer flux. The edges of some samples attained a colour in between bright red and yellow, indicating possible temperatures of up to 1000°C and a radiant heat flux (RHF) exceeding 100 kW m^{-2}. If transition requires a RHF of between 40 and 70 kW m^{-2} incident on the fuel, as shown by Boonmee and Quintiere (2000), a small firebrand would require RHF significantly in excess of this due to the moderating effect of view factor (Drysdale 1985). Digital images of two transitions from glowing to flaming ignition suggested that very thin elements that were glowing were instrumental in the ignition of volatiles (Figs 3.10 and 3.11).

[5] Prof. Anne Ganteaume, Cemagref Aix-en-Provence, France

Figure 3.10. Transition from glowing to flaming ignition. The leading edge of the firebrand sample of bark of *E. globulus* is about 45 mm long and less than 2 mm in thickness with a mass of approximately 0.2 g and is glowing pale yellow. The yellow flame appears to have resulted from heat transferred from glowing combustion of fine twigs and the blue flame apparently from combustion of mixed products of pyrolysis above and below the illuminated leaf in the foreground.

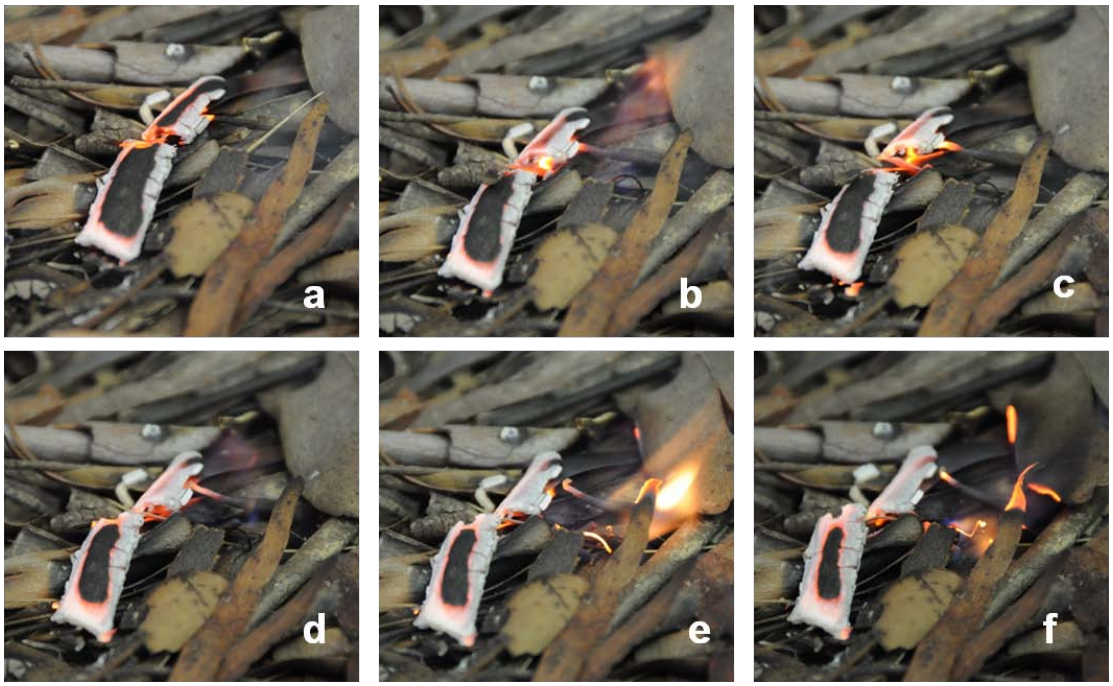

Figure 3.11. Sequence of six images 0.1 s apart, illustrating high-frequency rapid on-off flaming, as well as the apparent significance of bright red glow of the firebrand sample, glowing of thin fuel elements, and blue flame.

Pitts (2007) indicated that transition to flaming combustions requires both high-temperature glowing areas and an optimum mixture of air and volatile products of pyrolysis. The flame in Figs 3.10 and 3.11 represents the combustion of the products of pyrolysis emanating from fuel adjacent to glowing surfaces heated to the point that thermal degradation reactions have initiated (>550K) (Sullivan and Ball 2012). Pitts (2007) used a heated metal surface and 262 cm^3 of fuel and hence his tests differ radically from the firebrand tests here. However, in every case of flame transition captured on video he reported an initial occurrence of blue flame. Blue flame indicates that little to no residual carbon particles exist in the flame to radiate as yellow in the flame.

In contrast to ignition by FL, it appeared that at an FMC low enough for a GL sample to induce transition, it is very likely that flaming combustion will become established. The fact that such a small amount of heat flux is available in a small, glowing sample suggests that very small changes in any variable may significantly influence ignition probability. The variables not tested in these experiments include fuel temperature and its influence on fine-scale turbulence (Butler 2006), ambient air temperature at the fuel surface, which is likely to be influenced by fuel temperature, and relative humidity. Most authors have concluded that relative humidity only acts indirectly on ignition by influencing FMC. However, Bussman and Baukal (2009) concluded that water vapour in furnace combustion air can absorb heat from the flame, and Peterson (1995) found that the probability of ignition of methane by spark was reduced by increases in relative humidity. These findings indicate the potential for relative humidity to affect ignition by small, glowing sources.

These experiments failed to show that differences in air flow turbulence affect ignition probability by glowing firebrand samples. However, in informal tests, a household fan and a hair dryer readily induced ignition, when ignition at the same FMC occurred rarely during experiments. This indicates the need for further investigation of the combined effects of turbulence and wind speed.

3.6 End-user summary

3.6.1 POTENTIAL APPLICATION OF MEASUREMENTS AND MODELS OF IGNITION BY SMALL, FIREBRAND-LIKE SAMPLES

This study was constrained by resources and investigated the ignition probability of litter of one type of dry sclerophyll forest by one standard firebrand type for each combustion phase (flaming and glowing) for a limited range of ambient conditions of wind, turbulence, air temperature and relative humidity, and did not include investigation of the effects of solar radiation. Nonetheless, although further research is required, the results appear to be at least partly verified by previous work. The models should not be extended to or applied beyond the range of air velocities used in the experiments; zero wind and wind of 1 m s^{-1} or 2 m s^{-1} for flaming firebrands, and 1 m s^{-1} or 2 m s^{-1} for glowing ones.

Fine-scale turbulence of the air flow, or wind, over the fuel is the variable that has been least measured and it appears to exert a large influence on ignition by glowing firebrands. The unknown differences between the turbulence and orientation of air flow across the fuel in different laboratory experiments, as well as the difference between these air flows and air flow in the field, makes it difficult to compare the results of different experiments and to relate them to the field.

One approach might be to use air flow in the laboratory that has maximum turbulence and oriented obliquely to the fuel. Such an air flow could be provided by a domestic fan that naturally generates highly turbulent flows and without housing or screens to reduce the turbulence. A potential drawback might be that laboratory-measured thresholds of FMC for ignition by glowing firebrands will significantly exceed those possible in the field. This potentially could lead to the implementation of management decisions that are not justified in reality and hence waste resources.

3.6.2 THE MODELS

The model for logistic regression, where the probability of flaming ignition by flaming (FL) or glowing (GL) firebrand samples ($P_{IG(FL)}$, $P_{IG(GL)}$) is expressed as:

$$P_{IG(FL)}, P_{IG(GL)} = 1/(1+e^{-z}) \qquad [3.10]$$

where z is of the form:

$$z = a + \sum b_i x_i \qquad [3.11]$$

and a is constant, and b_i the estimated coefficients for relevant variables x_i determined experimentally.

A model is presented for each firebrand type (flaming and glowing):

1. Ignition by flaming firebrands

Equation 3.12 is a logistic model of ignition probability by small flaming firebrands;

$$z = 8.832 - 1.208FMC - 5.59Wind - 0.721FMC{:}Wind + 0.311R_{yi} \qquad [3.12]$$

$(s.e. = 2.931)(s.e. = 0.319)\ (s.e. = 3.133)\ \ (s.e. = 0.335)\ \ (s.e. = 0.152)$

$(P < 0.003)\ \ (P < 0.000)\ \ (P = 0.07)\ \ (P < 0.03)\ \ (P = 0.04)$

where z is used in Eqn 3.10, *FMC* is oven-dried fuel moisture content (%), *Wind* is the absence or presence of air flow (0, 1) and R_{yi} is surface roughness (Table 3.6). Increasing surface roughness, decreasing FMC and having wind all significantly increase ignition probability. For application in the field, the model is also presented in probabilistic form (Figure 3.12)

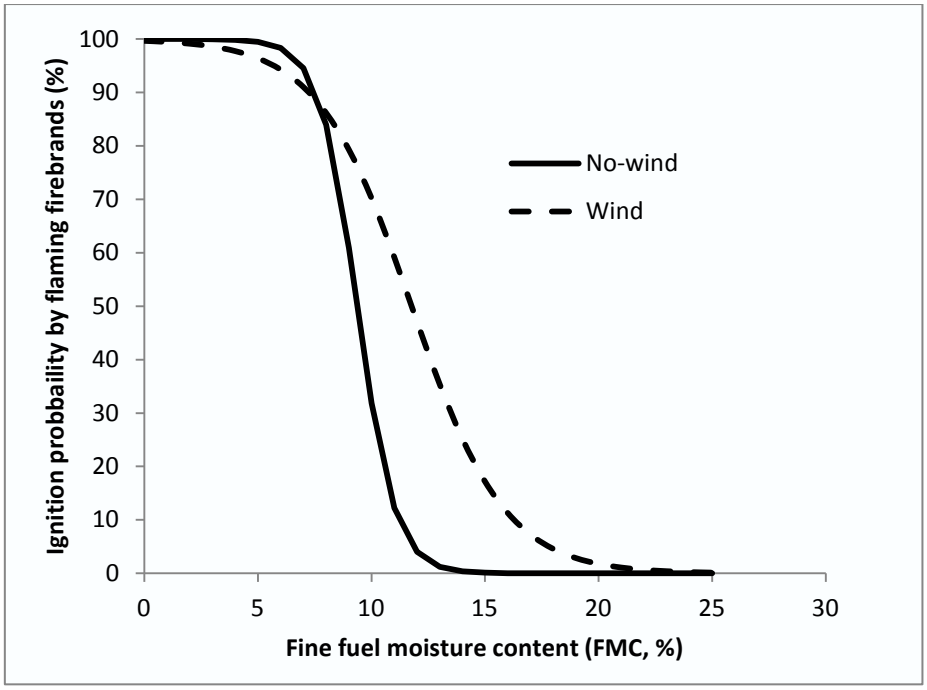

Figure 3.12. Probabilistic model of ignition success by flaming firebrand samples, given by Eqn 3.10 and 3.12, for No-wind (zero air flow) and Wind (air flow of 1 m s^{-1} or 2 m s^{-1}), for a value for an average surface roughness (R_{yl}) for the samples of dry sclerophyll forest (Southern Tablelands Dry Sclerophyll Forest) litter of 8.0 mm.

2. Ignition by small glowing firebrands

The logistic regression model for the ignition probability by small flaming firebrands has the exponent:

$$z = -3.23 - 0.008FMC + 3.136s \qquad [3.14]$$

$$(s.e. = 2.613)\ (s.e. = 0.351)\ (s.e. = 1.135)$$

$$(P = 0.22) \quad (P < 0.02) \quad (P = 0..006)$$

where z is used in Eqn 3.10 and describes the probability of ignition by glowing samples ($P_{IG(GL)}$), *FMC* is fuel moisture content (%) and s is mean air speed (m s^{-1}). Eqn 3.14 has values for R^2 and ROC of 0.36 and 0.85, respectively. Equation 3.14 shows that increases in wind speed and decreases in fuel moisture content will result in significantly greater probability of ignition by small glowing firebrands. The probabilistic form of Equation 3.14 is given in Figure 3.13.

Figure 3.13 shows that for a wind flow across the litter fuel of 2 m s^{-1}, the ignition threshold for small glowing firebrand samples is about 10% FMC and that below this value ignition probability increases rapidly.

3.6.3 APPLICATION OF MODELS

If the occurrence of wind in the field can be assumed, selection of the values for fine fuel moisture content (FMC) to underpin fire management decisions depends on the choice of a critical probability of ignition by firebrands: a critical amount of spotting. Given the large numbers of firebrands that can be generated by medium to high-intensity fires in this forest type (Gould *et al*. 2007, McCaw et *al*. 2012), a low ignition probability may be appropriate.

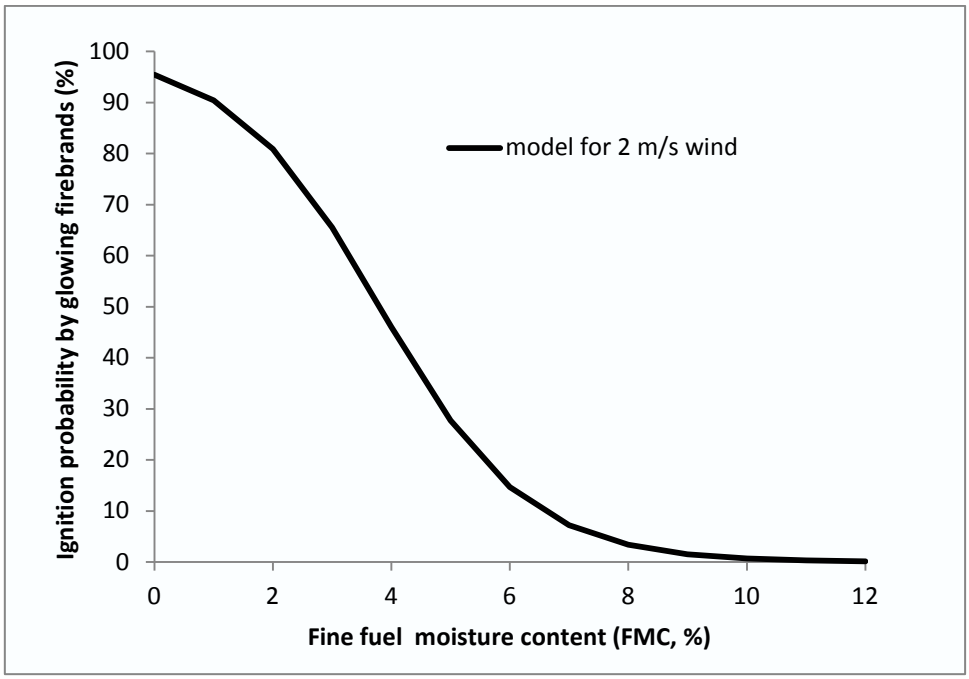

Figure 3.13. Probabilistic model of ignition success by glowing firebrand samples, given by Eqns 3.10 and 3.14, Wind of 2 m s^{-1}, for the samples of dry sclerophyll forest (Southern Tablelands Dry Sclerophyll Forest) litter.

A management decision made on the basis of a 'trigger' value for FMC can potentially be costly if it requires aircraft surveillance or extended fire suppression and hence the context of the decision in terms of estimation of FMC in the field and the FFDI is important.

Fuel moisture content (FMC)

Field FMC can be obtained by sampling fine fuel or by modelling. Error is possible even with systematically collected samples that are oven dried and more so for samples measured using commercially available field instruments. Because of the difficulty of sampling, it may be increasingly likely that management decisions will be based on thresholds for FMC determined using landscape moisture modelling. There are spatial considerations. Depending upon management objectives, gullies with high fuel loads may be more significant in terms of potential ignitions by firebrands than the relatively small, exposed ridges which may be relatively drier but have less fuels.

Forest Fire Danger Index (FFDI)

Spotting is intimately linked to weather and hence FFDI and management decisions based on ignition probability should be considered in relation to other facets of fire behaviour at a given FFDI. For example, a given threshold for flaming firebrands in wind could be 15% ignition probability, which occurs at an FMC of about 16% (Fig. 3.12). This FMC corresponds to a relative humidity of about 65% on a fuel desorption curve and to a rate of spread (adjusted for FMC) of roughly one quarter of the rate of spread at 7% FMC and roughly one tenth of the rate of spread at 3% FMC (Gould *et al*. 2007). Rate of spread is also dependent on Fuel Hazard Score (FHS). At 15% FMC, there is a very low chance of ignition by glowing firebrands. Flaming firebrands are likely to be a relatively small proportion of total firebrand numbers. Spotfire occurrence is intimately linked with fire behaviour and firebrand numbers

and spotting distance are significantly affected by FHS (Gould *et al*. 2011). Depending on the FHS of the given fuel, spotting may not be a significant issue in terms of numbers or spotting distance when the FMC is 16% or greater. Thus, although an FMC of 16% may be a rational threshold to 'trigger' a decision regarding management, it should not be used in isolation from other variables such as Fuel Hazard Score and Rate of Spread.

Hence, there may be a need for the construction of a framework on which to base management decisions which are a consequence of ignition probability by firebrands rather than base decisions on FMC alone.

3.7 Conclusions

This chapter presented the findings of a laboratory investigation into the ignition probability of a typical dry eucalypt fuel bed by standard flaming and glowing firebrands utilising a small scale wind tunnel. This investigation provided models of ignition probability as functions of wind across the fuel bed and moisture content of the litter.

Samples of complete and intact litter profile were collected from local forest sites with minimum disturbance to ensure representativeness of field conditions. Flaming and glowing firebrand samples with the aerodynamic and combustion properties of firebrands but with consistent structure and combustion behaviour were selected as standard firebrands for the study. The air flow in the wind tunnel was accurately quantified for mean air speed and turbulent kinetic energy and was compared to air flow measured in the field on the surface under forest canopy.

The models for flaming firebrands in the absence of wind (no-wind case) and for the presence of wind (1 m s^{-1} and 2 m s^{-1} wind speeds) were verified to a limited extent by comparison with other studies which tested eucalypt litter (Plucinski and Anderson 2008, Ganteaume *et al*. 2009).

Comprehensive investigation of ignition by glowing firebrands may only be possible by conditioning fuel samples and conducting ignition tests under controlled conditions of very low RH. Proof of the influence of turbulence and hence the significance of the relatively high levels of turbulence in the field also requires additional work.

3.8 References

Albini FA (1979) Spotfire distance from burning trees, a predictive model. USDA Forest Service, Intermountain Forest and Range Experiment Station, General Technical Report INT-56. Ogden, UT.

Blackmarr (1972) Moisture content influences ignitibility of slash pine litter. USDA Forest Service Research Note SE-173. Southeastern Forest Experimental Station, Asheville, NC.

Boonmee N, Quintiere JG (2000) Glowing and flaming autoignition of wood. *Proceedings of the Combustion Institute* **29**, 289-296.

Bunting SC, Wright HA (1974) Ignition capabilities of non-flaming firebrands. *Journal of Forestry* **72**, 646-649.

Bussman WR, Baukal CE (2009) Ambient conditions impact CO and NO_x emissions: part 2. *Petroleum Technology Quarterly* **Q3**, 37-41.

Butler BW (2006) The effect of solar irradiation on the spread rate of fires burning over a horizontal fuel array. In 'Proceedings of 5th International Conference on Forest Fire Research'. (Ed. DX Viegas)

Byram GM (1959) Combustion of Forest Fuels. In Davis KP, Byram GM and Krumm WR (eds.) *Forest Fire: Control and Use*. (McGraw-Hill Book Company)

Cheney NP, Gould JS, Catchpole WR (1998) Prediction of fire spread in grasslands. *International Journal of Wildland Fire* **8**, 1-13.

Cheney NP, Bary GAV (1969) The Propagation of Mass Conflagrations in a Standing Eucalypt Forest by the Spotting Process. In 'Mass Fire Symposium', Canberra, February 1969, Commonwealth of Australia.

Countryman CM (1980) Some physical characteristics of cigarettes as firebrands. Forest Service Contract 43-9AD6-0-755, Pacific Southwest Forest and Range Experimental Station, Riverside CA.

Countryman CM (1983) Ignition of grass fuels by cigarettes. *Fire Management Notes* **44**, 3-7.

Cruz MG, Sullivan AL, Gould JS, Sims NC, Bannister AJ, Hollis JJ, Hurley RJ (2012) The anatomy of a catastrophic wildfire: the Black Saturday Kilmore East fire in Victoria, Australia. *Forest Ecology and Management* 284, 269–285.

Drysdale D. (1985). *An Introduction to Fire Dynamics*. John Wiley and Sons.

Ellis PF (2000) The aerodynamic and combustion characteristics of eucalypt bark – a firebrand study. A Thesis submitted to the Australian National University for the Degree of Doctor of Philosophy.

Ellis PFM (2010) The effect of aerodynamic behaviour of flakes of jarrah and karri bark on their potential behaviour as firebrands. *Journal of the Royal Society of Western Australia* **93**, 21-27.

Ellis PFM (2011) Fuel bed ignition potential and bark morphology explain the notoriety of the eucalypt messmate 'stringybark' for intense spotting. *International Journal of Wildland Fire* **20,** 897-907.

Ellis PFM (2013) Firebrand characteristics of the stringy bark of messmate (*Eucalyptus obliqua*) investigated using non-tethered samples. *International Journal of Wildland Fire* **22**, 642-651.

Foote EID, Liu J, Manzello SL (2011) Characterizing firebrand exposure during wildland–urban interface (WUI) fires. In 'Proceedings of Fire and Materials 2011 Conference', 31 January–2 February 2011, San Francisco, CA. pp. 479–491. Interscience Communications: San Francisco, CA.

Fons WL, Stromberg RW (1941) Fire ignition progress report 1. U.S. Forest Service, California Forest and Range Experimental Station. 23p.

Ganteaume A, Lampin-Maillet C, Guijarro M, Hernando C, Jappiot M, Fonturbel T, Pérez-Gorostiaga P, Vega JA (2009) Spot fires: fuel bed flammability and capability of firebrands to ignite fuel beds. *International Journal of Wildland Fire* **18**, 951-969.

Ganteaume A, Jappiot M, Lampin-Maillet C, Curt T, Borgniet L. (2011a) Effects of vegetation type and fire regime on flammability of undisturbed litters in Southeastern France. *Forest Ecology and Management* **261**, 2223-2231.

Ganteaume A, Guijarro M, Jappiot M, Hernando C, Lampin-Maillet C, Perez-Gorostiaga P, Vega JA (2011b) Laboratory characterization of firebrands involved in spot fires. *Annals of Forest Science* **68**, 531-541.

Gould J S, McCaw WL, Cheney NP,.Ellis PF, Knight IK, Sullivan AL (2007) *Project Vesta--Fire in Dry Eucalypt Forest: fuel structure, dynamics and fire behaviour*. Ensis-CSIRO, Canberra ACT, and Department of Environment and Conservation, Perth WA. 228 pp.

Gould JS, McCaw WL, Cheney NP (2011) Quantifying fine fuel dynamics and structure in dry eucalypt forest (Eucalyptus marginata) in Western Australia for fire management. *Forest Ecology and Management* **262**, 531-546.

Hines F Tolhurst KG Wilson AG McCarthy GJ 2010 Overall fuel hazard assessment guide,4th edition. Fire and adaptive management, report no. 82. Victorian Government Department of Sustainability and Environment, Melbourne.

Hosmer DW and Lemeshow S (2000) *Applied Logistic Regression* (2nd edition). Wylie Interscience: New York

Huang HW, Zhang Y (2008) Flame colour characterisation on the visible and infrared spectrum using a digital camera and image processing. *Measurement Science and Technology* 19, 085406, 9 pp.

Keetch JJ (1941) Smoker fires and fire brands. Technical Note No. 49, USDA Forest Service, Appalachian Forest Experimental Station, Asheville, NC, 4 p.

Keith DA (2004) Ocean Shores to Desert Dunes. The Native Vegetation of New South Wales and the ACT. Department of Environment and Conservation NSW: Hurstville.

Koo E, Pagni PJ, Weise DR, Woycheese JP. (2010) Firebrands and spotting ignition in large-scale fires. *International Journal of Wildland Fire* **19**, 818-843.

Lawson BD, Armitage OB, Dalrymple GN. (1993) Ignition probabilities for simulated people-caused fires in British Columbia's lodgepole pine and white spruce-subalpine fir forests. In: Proceedings of the 12th Conference on Fire and Forest Meteorology, October 26-28, 1993, Clarion Resort Buccaneer, Jekyll Island, Georgia. Society of American Foresters. Bethesda, MD. 1994.

Lin CC (2005) Influences of temperature, relative humidity and heat sources on ignition: a laboratory test. *Taiwan Journal of Forest Science* **20**, 89-93.

Luke RH, McArthur AG (1978) *Bushfires in Australia*. Australian Government Publishing Service, Canberra.

MacAulay AJ, Tolhurst KG (2001) Using computer simulation to determine the effects of short distance spotting on head fire rate of spread. Australian Bushfire Conference, 3-6 July 2001, Christchurch N.Z. pp 334-338.

Manzello SL, Cleary TG, Shields JR, Yang JC (2006) Ignition of mulch and grasses in wildland-urban interface fires. *International Journal of Wildland Fire* **15**, 427-431.

Manzello SL, Maranghides A, Mell WE (2007) Firebrand generation from burning vegetation. *International Journal of Wildland Fire* **16**, 458-462.

Manzello SL, Thomas GC, Shields JR, Maranghides A, Mell W, Yang JC (2008) Experimental investigation of firebrands: Generation and ignition of fuel beds. *Fire Safety Journal* **43**, 226-233.

Matthews S (2005) The water vapour conductance of Eucalyptus litter layers. *Agricultural and Forest Meteorology* **135**, 73-81.

McArthur AG (1967) Fire behaviour in eucalypt forests. Forestry and Timber Bureau Leaflet No. 107. Commonwealth of Australia, 36 pp.

McArthur A.G., (1969a) The fire control problem and fire research in Australia. In Proceedings of the 1966 Sixth world forestry congress, Volume 2, 1986-1102 1991. Spanish Minister of Agriculture, Madrid.

McArthur AG (1969b) The Tasmanian bushfires of 7th February, 1967, and associated fire behaviour characteristics. In 'Mass Fire Symposium', Canberra, February 1969, Commonwealth of Australia, p 7.

McCarthy GJ, Tolhurst KG (1998) Effectiveness of firefighting first attack operations 1991/92 – 1994/95. Research Report No. 45, Fire Research, CFTT., Department of Natural Resources and Environment. (Victoria)

Muraszew A, Fedele JB, Kuby WC (1976) Investigation of firewhirls and firebrands. Aerospace Report ATR-76(7509)-1. The Aerospace Corporation, El Segundo, California.

Nagelkerke NJD (1991) A note on a general definition of the coefficient of determination. *Biometrika* **78**, pp 691-692.

National Fire Danger Rating System (rev) (1974) Research Paper RM-84, USDA Forest Service, Rocky Mountain Forest and Range Experiment Station, Fort Collins, Colorado.

Pagni P (1993) Causes of the 20th October 1991 Oakland Hills conflagration. *Fire Safety Journal* **21**, 331-340.

Parrot RT, Donald CM (1970) Growth and ignitability of annual pastures in a Mediterranean environment. 2. Ignitability of swards of various annual species. *Australian Journal of Experimental Agriculture and Animal Husbandry* **10,** 76-83.

Perryman HA, Dugaw CJ, Varner JM, Johnson DL (2013) A cellular automata model to link surface fires to firebrand lift-off and dispersal. *International Journal of Wildland Fire* **22**, 428-439.

Peterson JS (1995) Influence of environmental factors on spark ignition probability. Report of Investigations 9566, United States Department of the Interior, Bureau of Mines, 12 p.

Pitts WM (2007) Ignition of cellulosic fuels by heated and radiative surfaces. National Institute of Standards and Technology, Technical Note 1481, U.S. Department of Commerce (106 pp). CODEN:NSPUE2.

Plucinski MP, Anderson WR (2008) Laboratory determination of factors influencing successful point ignition in the litter layer of shrubland vegetation. *International Journal of Wildland Fire* **17**, 628-637.

R Core Development Team (2010) 'The R Project for Statistical Computing'. Internet site www.r-project.org. Last accessed 2010.

Rissel S, Ridenour K (2013) Ember production during the Bastrop Complex fire. *Fire Management Today* **72**, 7-13.

Sakuma H, Munakata S, Sugawara S (1981) Volatile products of cellulose pyrolysis. *Agricultural and Biological Chemistry* **45**, 443-451.

Sullivan A, Ball R (2012) Thermal decomposition and combustion chemistry of cellulosic biomass. *Atmospheric Environment* **47**, 133-141.

4 Fire growth and development

One variable which has received very little mention in fire control literature is the effect of time on many aspects of fire behaviour, especially such factors as rate of spread, area increase and spotting potential (A. G. McArthur 1958)

4.1 Introduction

An active bushfire front is said to have three basic characteristics: (i) it spreads, (ii) consumes fuel, and (iii) it produces heat energy in the form of a visible flaming combustion reaction (Van Wagner 1970). The progressive development of the fire to its potential rate of spread and associated increase in fire size and intensity for the prevailing conditions is properly described as fire growth (Pyne 1984, Cheney and Gould 1997).

Fire behaviour modelling in Australia has been empirical in nature, concerned mostly with the equilibrium rate of spread of an established line fire for a particular type of fuel (McArthur 1962, 1966, 1967 and 1973, Peet 1965, Sneeuwjagt and Peet 1998, Marsden-Smedley and Catchpole 1995, Cheney *et al.* 1998, Gould *et al.* 2007 a & b, Cruz *et al.* 2010, 2012, Cheney *et al*. 2012). These experiments, with the addition of data from well-documented wildfires, form the basis of existing quantitative fire behaviour prediction systems.

Limited experimental results on point source ignition fires (i.e. those that start from a single point rather than a line or already going fire) exist. Cheney and Gould (1995, 1997) reported experiments investigating point source growth in grasslands but were unable to develop a relationship to predict rate of spread of an initiating fire using time since ignition and wind speed; no attempt was made to develop either an acceleration or a growth function. Cheney and Gould (1997) concluded that the required head fire width in grassfires to achieve the potential quasi-steady rate of forward spread for the prevailing conditions increased with increasing wind speed. They noted the time taken to reach the potential quasi-steady rate of spread at any wind speed was highly variable and the time was strongly influenced by the frequency of changes in wind direction and the rate of development of a wide head fire.

Conceptual theories exist on predicted fire acceleration rate. McAlpine and Wakimoto (1991) provided several examples of acceleration curves from other authors (McArthur 1966, 1967, Cheney and Bary 1969, Van Wagner 1985). Luke and McArthur (1978) provided a series of possible principle factors contributing to fire acceleration:

- moisture content of fine fuels (<6mm)
- moisture content of live vegetation and heavy dead material (coarse woody debris >25mm)

- understorey fuels (surface, near-surface and elevated) horizontal and vertical distribution
- combustion rate and burn-out time of fuels
- surface wind speeds
- atmospheric instability
- slope, and
- spotting process.

McArthur (1967) proposed a stepwise progression for acceleration in a eucalypt fuel type containing a well-developed elevated fuel layer. The acceleration process may not be a smooth progression but may proceed in a series of steps or jumps as successive elevated layers of fuel in the forest ignite (See Figure 1.3). Thus, fuel dryness, fuel quantity and fuel distribution (structure) are three major variables controlling the acceleration effect on eucalypt fire. So as the heat output of a fire front increases, thresholds of a further fuel involvement are achieved, thus beginning further acceleration.

Studies of point source fire growth have been few. McAlpine and Wakimoto (1991) carried out a number of point source experiments using ponderosa pine (*Pinus ponderosa* Laws.) needles and excelsior (wood wool) fuel beds in a wind tunnel to develop predictive equations to describe the fire growth phase. Cheney and Gould (1995) carried out point source ignition fires in grassland and woodland and found that width of the head fire is determined by frequency of changes in wind direction was important. Cheney and Bary (1969) suggest the following growth relationship when fuel moisture and weather conditions are stable in a standing forest by equation:

$$R(t) = R_{ss}\, e^{-a/t} \qquad [4.1]$$

where R represents the head fire rate of spread at time (t) since ignition, R_{ss} represents the forward steady-state rate of spread of the head fire and a is a constant determining growth rate. A similar equation was given by Van Wagner (1985) in the form of:

$$R(t) = R_{ss}\, (1 - e^{-bt}) \qquad [4.2]$$

where b is a constant determining growth rate.

These different equations for the theoretical fire growth for forest fires are shown in Figure 4.1. Both functions produce steeply rising curves attaining more than 50 percent of equilibrium spread rate within 10 minutes of ignition.

Chandler *et al.* (1983), Cheney (1981), and McAlpine and Wakimoto (1991) suggested that the two models are not mutually exclusive; the asymptotic curves represent uniform fuel, weather and topographic conditions, whereas the stepwise progression is characteristic of a heterogeneous fire environment.

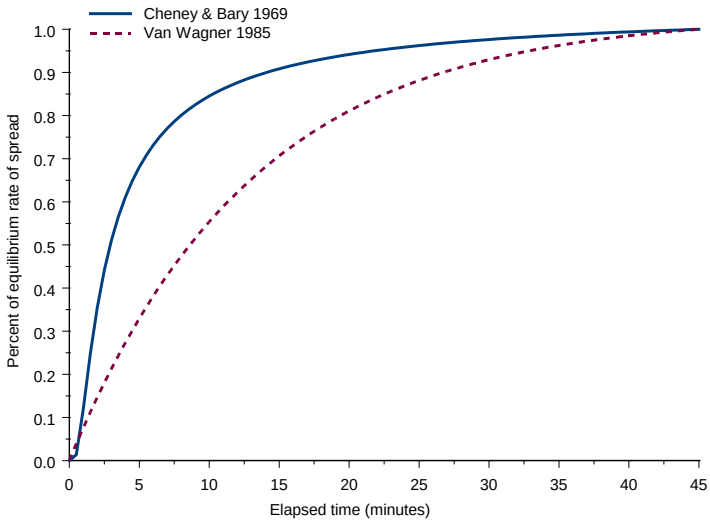

Figure 4.1. Comparison of two theoretical asymptotic fire growth equations for forest fires.

Weber (1989) also used a natural growth function in his model for a point source fire and concluded that "accelerating behaviour is related to curvature of the fire front; the higher the curvature, the greater the acceleration". Cheney and Gould (1995), however, could not verify this relationship.

The time for a point source fire to reach steady-state varies widely depending on a range of factors. Cheney (1981) and Gould *et al.* (2003) considered that fire growth patterns were extremely variable and fires reached a steady state after a few minutes under mild conditions, and the more severe the burning conditions the longer it is likely the growth phase will take. Others reported that the time for a point-source fire to reach equilibrium ranged from 5 to 10 minutes in grassy fuels to more than 60 minutes in heavy logging slash (Chandler *et al.* 1983) and could remain well below the potential rate of spread for several hours in eucalypt forest (Gould *et al.* 2003).

Fires burning under severe burning conditions will always have the potential to suddenly and dramatically increase the fire spread rate and intensity as a result of small changes in conditions (Cheney *et al.* 2001). Thus the role of fire growth and acceleration in fire behaviour is a critical factor that has to be taken into consideration when undertaking prescribed burning or fire suppression.

The study objective was to investigate the growth of fire from point and line source ignitions in eucalypt litter fuel. In this chapter we summarise a series of experimental fires conducted in the CSIRO Pyrotron (Sullivan *et al.* 2013) investigating fire growth of point and line source ignition fires under very dry fuel moisture conditions. Also, we examine the relationship between forward rate of spread, area and perimeter growth with fuel, weather and topography variables from a series of historical point ignition experimental fires in eucalypt forest. The aim of this work was to determine the growth rate of free burning fires with the goal to give fire managers guidelines on how quickly a fire may reach steady-state spread in eucalypt litter fuel.

4.2 Fire growth and acceleration in eucalypt litter: Laboratory experiments

4.2.1 OBJECTIVES

The original eucalypt forest fire behaviour models were developed from small, low intensity (<750 kW m^{-1}) experimental fires conducted under mild weather conditions (McArthur 1962, 1967; Peet 1972). The recent studies by Gould *et al.* (2007a) and Cheney *et al*. (2012) developed fire behaviour models predicting behaviour of moderate to high intensity fires (< 7500 kW m^{-1}) burning under warm dry summer conditions. These models assume steady-state spread rates but do not predict the time required to reach steady-state spread. The pioneering work of McArthur (1962), Peet (1972), Gould *et al*. (2007a) and Cheney *et al*. (2012) provided little detailed experimental and statistical examination on fire growth for eucalypt litter fuel especially under very dry fuel conditions (i.e., fuel moisture <5%).

Laboratory studies are a useful, safe and inexpensive adjunct to field studies to further the understanding of fire behaviour. While scale is an important factor between fire behaviour and fuel and weather variables in regard to equilibrium being reached (steady-state spread rate) (Cheney and Gould 1995), these relationships can be examined in a controlled laboratory environment with a series of well-designed and replicated experiments of uniform wind speed and fuel continuity with controlled fuel moisture conditions and different ignition sources (point versus different ignition line widths).

The primary objective of the laboratory study was to develop a function to quantitatively predict the time taken to reach steady-state spread rate under dry fuel moisture conditions. The model developed here is solely based on the evidence collected from the series of laboratory experiments. The effect of different ignition sizes on the initial rate of spread to steady-state is presented. The results of these laboratory experiments are fitted to theoretical fire growth models and compared to some field studies.

4.2.2 METHODS

1) *Combustion wind tunnel*:- the CSIRO Pyrotron is a 25-m-long fireproof wind tunnel with a 1.5 m x 4.8 m fuel bed working section (Sullivan *et al.* 2013). This facility will be used to investigate the effects of fire line width on fire propagation, fire growth, and acceleration. Even though laboratory scale studies have limiting factors to study fire behaviour, the Pyrotron provides an opportunity to design small scale fire behaviour studies that are relatively safe and employ inexpensive methods to assess existing relationships between the different variables involved in fire growth and acceleration.

2) *Fuel preparation*:- the fine litter fuel (< 6mm) used to conduct the fire growth experiments was collected from eucalypt woodland vegetation (*Eucalyptus rossii, E. macrorhyncha*) within the Kowen Forest east of Canberra, ACT (ACT Parks, Conservation and Lands). At each collection site 10 random fuel samples were taken. At each sample point the litter depth was recorded and all the vegetation < 6 mm was harvested, labelled and bagged from a circular 0.05 m^2 quadrat. Samples were taken back to a laboratory and oven dried at 104°C and weighed. Fuel load was expressed as the mass per unit area (kg m^{-2}) and gives an indication of the natural fuel condition where the fuel was collected for the Pyrotron experiments. At the collection site the fuel was carefully raked to separate the top surface layer

from the decomposing fuel and the larger woody material. The litter was collected in bags and transported to the laboratory for additional sorting and pre-drying before the experiments. The fuel was sorted and sieved to remove broken fuel fragments, rocks and other inorganic debris, and coarse woody material (> 6 mm diameter) to obtain a uniform litter fuel structure.

The moisture content of sorted fuel was taken using a Wiltronic T-H Fine Fuel Moisture Meter[6] in addition to five grab samples of 20-30 grams of fuel which were weighed, oven-dried at 104°C for 24 hours and reweighed to determine the oven-dried fuel moisture content.

The fuel was weighed and boxed to equivalent oven-dried weights for the 7% or the 5% moisture content regimes to represent 1.2 kg m^{-2} fuel loading for each 0.75 m x 1.0 m (8 head fire) sections and 0.75 m x 0.8 m (2 backing fire) sections of the Pyrotron burning bed. The boxes were placed in a large dehydrating oven with the temperature set between 30 and 35°C for 24–36 hours to obtain 7% moisture content (±2%) or at 40°C for 24–36 hours to obtain 5% moisture content (±2%).

The pre-dried fuel was transported to the Pyrotron 30 minutes prior to ignition and spread evenly across the fuel bed (1.5 m x 4.8 m). The fuel depth was measured at five random points across the fuel bed using a rule and guide. Fuel component presence was measured using a 20-pin (25 mm separation) point sample transect 500 mm in length. Sampling pin contact counts of leaf, twig and bark material were recorded from four random transect lines across the fuel bed to record the different components of the fuel. Prior to ignition five samples of 20–30 grams of fuel were taken, weighed, oven-dried at 104°C for 24 hours and reweighed to determine fuel moisture content, expressed as a percentage of oven-dried weight, at ignition.

3) *Ignition procedures*:- three different ignition line widths were evaluated: point ignition, 400 mm, and 800 mm line ignitions. The fires were lit using 90% ethanol (~5 mL for point ignition, 30 mL, and 60 mL for the 400 mm and 800 mm ignition lines respectively).

4) *Thermocouple instrumentation*:- an array of K-type thermocouples located at -0.5, 0, 0.5, 1.0, 1.5, 2.0, 2.5 and 3.0 metres from ignition line (0= ignition line) with one thermocouple located at the centre of the fuel bed and two thermocouples to the left and right of the centre line at 300 mm apart. At the 3.0, 3.5 and 4.0 meter lines from the ignition, there were nine thermocouples spaced 150 mm apart across the fuel bed.

   Figure 4.2 illustrates the location of the 62 thermocouples across the Pyrotron burning bed. The thermocouples were approximately 25 mm above the burning bed floor and logged the temperature at 100 Hz (100 readings per second). The data was recorded on a customised LabVIEW[7] program for the experiments. This program allows the researcher to view the data acquisition in real time and check that all instrumentation is recording correctly and automatic archiving of files for future data reduction and analysis. Temperature, relative humidity and air speed were also recorded during the experiments at two Hz (two readings per second).

[6] Chatto K., Tolhurst KG. (1997) Development and testing the Wiltronic T-H Fine Fuel Moisture Meter. Department of Natural Resources and Environment, Creswick Research Station, Fire Management Branch Research Report No. 46. Melbourne, Victoria.
[7] LabVIEW Software- data acquisition software by National Instruments

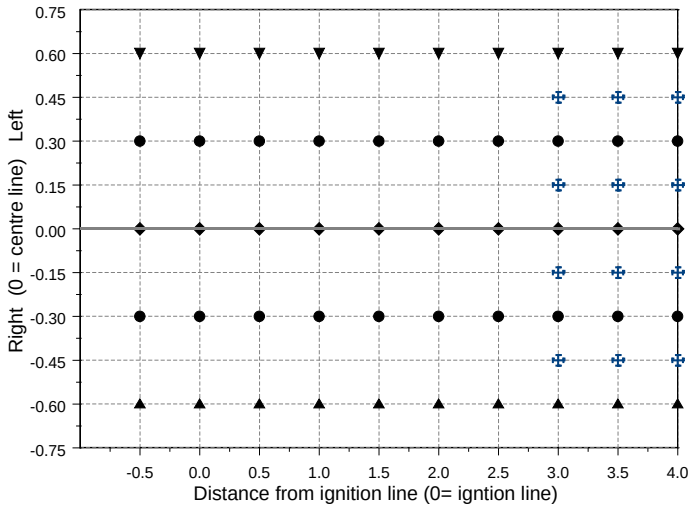

Figure 4.2. Schematic diagram showing 62 thermocouples array for the fire growth experiments (zero is location of the ignition line).

5) *Thermal imagery*:- an infra-red camera was mounted on top of the Pyrotron at 2.0 metres from the ignition line with a view looking vertically down to record planar thermal images of the fire progression. The field of view of the camera was the width of the fuel bed and between 1.3 and 2.8 m from the ignition line as illustrated in Figure 4.3.

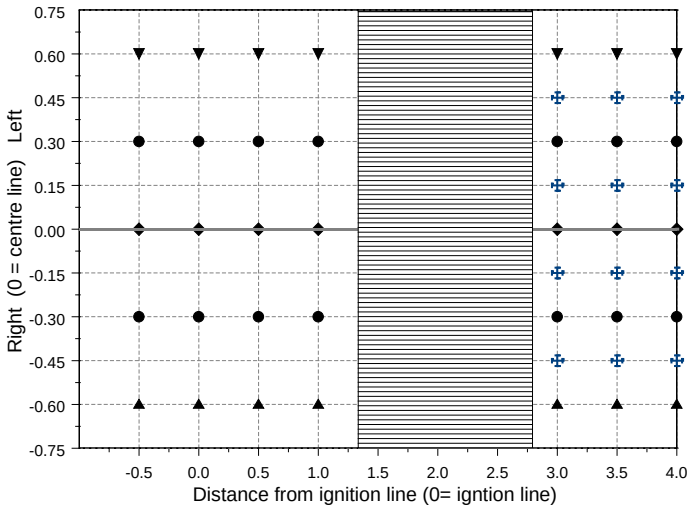

Figure 4.3. Illustration of the infrared camera field of view (shaded area) over the thermocouple fuel bed array.

6) *Video imagery*:- progression of the fire was recorded using an RGB video camera (GoPro) located in a view opening in the Pyrotron ceiling located at 1.5 m line. The camera was set at wide angle setting in 1080-30p mode to get a complete view of the fuel bed (see Fig. 4.4). This wide angle setting gives high image distortion (fisheye view) that requires rectification before acquisition of fire behaviour data.

Two addition RGB video cameras were located at the left and right flank fire to record the flank progression of the fire between 2.5 m and 4.0 m spread.

Figure 4.4. Frame grab photo from the GoPro RGB video image showing the complete fuel bed. The wide angle produced a very-distorted image that requires rectification before acquisition of fire behaviour data.

7) *Fire behaviour observation*:- observers described fire behaviour and recorded the time of the fire reaching the 0.5 m line intervals across the fuel bed. The fire behaviour at the headfire was recorded at the 0.5 m intervals using the following descriptors:
    - time
    - ocular estimates of flame depth, height, angle
    - shape, direction or skewness of the headfire progression

8) *Data acquisition*:- the experimental fires were conducted under dry conditions with the fuels pre-dried to the predetermined fuel moisture content of 7% (±2%) and 5% (±2%). In each experiment there was up to 10 gigabytes of data collected and backed-up for detailed analysis. Also, fire behaviour observation field sheets on the visual observation of the data and fuel descriptions for each fire were collated into a data file.

4.2.3 ANALYSIS

Fire behaviour data included continuous data (rate of spread, fuel moisture content, fuel depth, bulk density, temperature and relative humidity) and observational data grouped by experimental code (E_c) based on two different wind speeds and three different ignition sizes (I_s). As a result, a variety of statistical methods were used to compare the behaviour of fire spread under different wind speeds, ignition, fuel moisture content and the development phases of the fire. Symbols and subscripts used to represent fuel, Pyrotron burning conditions, and fire behaviour variables are listed in Table 4.1. Results were analysed in S-Plus (S-PLUS, 2006) and "R" (R core Development Team 2011) using correlation, scatter plots, box-and-whisker plots, linear and nonlinear regression analysis. A multi comparison of all pairwise differences in rate of fire spread means based on wind speed, ignition size length and fuel moisture groupings was performed using the multi comparison function in S-PLUS (Kramer 1956, Bechhofer *et al.* 1995, Hsu 1996, SPLUS 2006).

Table 4.1. Symbols for variable used in analysis.

SYMBOL	VARIABLE
R_f	Forward rate of spread (m min^{-1})
R_c	Cumulative rate of spread (m min^{-1})
R_{ac}	Rate of spread (m min^{-1}) during the acceleration phase
R_{ss}	Rate of spread (m min^{-1}) during the steady-state phase
R_{ssf}	Fraction of steady-state spread rate
t	Time required to reach steady-state spread
M_f	Fine dead fuel moisture content (%)
F_h	Flame height (m)
F_d	Flame depth (m)
F_a	Flame angle (degrees)
Rh	Relative humidity (%)
T	Temperature (^oC)
D_s	Depth of litter fuel bed (mm)
BD_s	Bulk density (kg m^{-3})
I_s	Size of ignition line (mm)
E_c	Experimental code: L= low wind speed experiments (1.25 m s^{-1}), H= high wind speed experiments (2.00 m s^{-1}), Ignition size: 000 (point ignition), 400 (400 mm ignition line length, 800 (800 mm ignition line length)

4.2.4 RESULTS

Fifty-eight experimental laboratory fires were carried out in the CSIRO Pyrotron (Sullivan *et al.* 2013) at two different wind speeds and three different sizes of ignition line. The range of the observed fire spread, fuel and burning conditions are given in Table 4.2.

The experimental design sought to determine the growth rate of fire from different wind speeds and ignition sources. Thus, the analysis of fire progression (i.e., distance travelled over time) from the observed values were used for this study. The additional data from the thermocouple array (i.e., time-temperature data), infra-red thermal and RGB video imagery will be used for future investigation into the effects of head fire shape on fire spread and the perimeter and growth rates of fires burning under dry fuel conditions. Examples of the thermocouple data and imaginary data acquisition from these experiments are presented in Appendix 4.1.

Correlation matrices, scatter, and box-and-whisker plots were used to explore relationships between rate of spread and experimental variables, including size of ignition line, time since ignition, two wind speed groups and fuel moisture content. The variation in rates of spread of fires in the two different winds speed classes and three different sizes of ignition are illustrated in Figure 4.5 for:

1. Forward rate of spread (R_f), the rate of fire spread of each 0.5 m increment divided by the time (minutes) the fire took to travel the 0.5 m increment.
2. Cumulative rate of spread (R_c), the cumulative distance (m) divided by cumulative time since ignition (minutes).

Table 4.2. Range of fire spread, fuel, and burning conditions (minimum, mean (bold), maximum) from the fire growth experiments conducted in the CSIRO Pyrotron by wind speed and size of the ignition line

	L000	L400	L800	H000	H400	H800
	0.09	0.17	0.15	0.09	0.29	0.31
R_f	**0.44**	**0.43**	**0.66**	**0.81**	**0.90**	**1.22**
	1.58	1.30	3.00	5.00	2.50	4.28
	0.09	0.21	0.27	0.18	0.41	0.49
R_c	**0.23**	**0.36**	**0.55**	**0.44**	**0.67**	**1.05**
	0.39	0.50	0.88	0.89	1.41	1.78
	5.26	5.76	6.30	3.97	3.97	4.09
M_f	**7.22**	**6.54**	**7.24**	**5.08**	**5.44**	**5.72**
	9.80	7.91	8.75	7.05	7.76	9.20
	0.10	0.10	0.10	0.02	0.10	0.1
F_h	**0.17**	**0.17**	**0.20**	**0.23**	**0.24**	**0.29**
	0.30	0.30	0.25	0.24	0.60	0.45
	0.10	0.10	0.10	0.10	0.10	0.10
F_d	**0.15**	**0.15**	**0.16**	**0.26**	**0.28**	**0.41**
	0.30	0.30	0.35	1.0	0.75	1.00
	45	45	45	45	45	20
F_a	**58**	**59**	**58**	**60**	**60**	**52**
	90	60	60	60	60	60
	19	21	17	17	13	12
Rh	**33**	**28**	**35**	**26**	**23**	**29**
	47	40	71	43	36	71
	22	21	21	19	18	23
T	**25**	**27**	**25**	**28**	**29**	**29**
	32	30	30	37	39	36
	14.2	14.0	12.2	14.0	16.0	15.6
D_s	**15.4**	**15.2**	**16.3**	**18.3**	**18.8**	**19.0**
	17.6	16.8	18.8	21.0	21.0	21.2
	68.18	71.43	63.82	57.14	57.14	56.60
BD_s	**78.27**	**79.37**	**75.18**	**66.53**	**64.18**	**63.48**
	84.51	85.71	98.36	85.71	75.00	76.92
No. of experiments	6	6	6	16	12	12

Both forms of rate of spread (R_c and R_f) were significantly correlated with size of ignition line (I_s), with the cumulative rate of spread (R_c) correlation significantly higher than the forward rate of spread (R_f), r=0.63 and r=0.24 respectively. The correlation between the rates of spread (R_c and R_f) and most of the measured variables were significant (Table 4.3). There was a stronger correlation of the measured values with (R_c) compared to (R_f).

The rates of spread increased with ignition line size (I_s), with a significant difference between the mean R_c and I_s for both wind speed experiments (Fig. 4.5). However, there was no significant difference between the mean R_f and I_s under wind conditions of 1.25 m s^{-1}. With wind speeds at 2.00 m s^{-1} there was no significant difference in the mean R_f between the

point ignition and 400 mm line ignition. The mean R_c was significantly different for fuel moisture content <7.5% for the two wind speed groups and three different ignition size classes. Under wind conditions of 1.25 m s^{-1} and moisture content >7.5% there was no significant difference in the mean R_c between point ignition and 400 mm ignition line (Fig. 4.6).

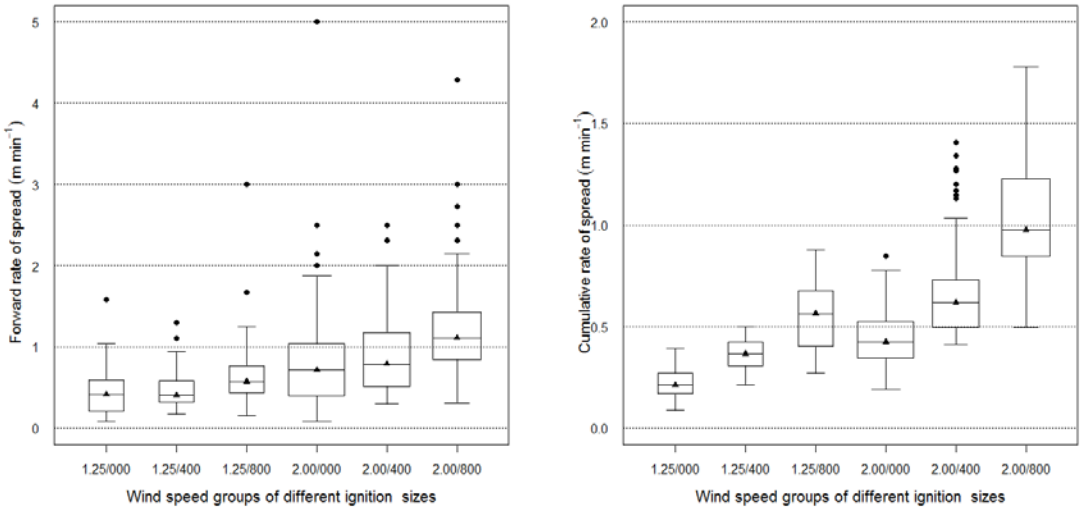

Figure 4.5. Variation in the forward rate of spread (R_f) (left) and the cumulative rate of spread (R_c) (right) with associated wind speeds (1.25 and 2.00 m s^{-1}) and different ignition sizes (000 = point ignition, 400 = 400 mm ignition line length, and 800 = 800 mm ignition line length). Box-and-whisker plot shows the median value (²), 25th and 75th quartiles (i.e., 50% of cases have values within the box) and dots (•) represents outliers more than 1 box-length from the 25th and 75th percentiles. The width of the box is proportional to the square root of the number of observation in each group.

The mean R_f for the drier fuels (M_f ≤5%) and high wind speed (2.00 m s^{-1}) and long ignition line (800 mm) was significantly different to that of the point and 400 mm ignition sizes under similar burning conditions. When M_f >5% there was no significant difference in the mean R_f for the different wind speeds and ignition sizes (Figure 4.7).

Table 4.3. Correlation between fire spread, fuel, and ignition line length from 58 laboratory experimental fires with a constant fuel load of 1.2 kg m^{-2} and two different wind speeds.

VARIABLE	R_F	R_C	BD_S	D_S	M_F	RH	T	I_L
R_f	1.00							
R_c	0.67**	1.00						
BD_s	-0.31**	-0.48**	1.00					
D_s	0.34**	0.51**	0.99**	1.00				
M_f	-0.31**	-0.35**	0.50**	-0.55**	1.00			
Rh	0.25**	-0.28**	0.20**	-0.24**	0.54**	1.00		
T	0.30**	0.40**	-0.40**	0.44**	-.47**	-0.48**	1.00	
I_l	0.24**	0.63**	0.10*	0.11*	0.15	0.08	0.03	1.00

** Correlation indicated as significant (2-tailed) at p=<0.05
* Correlation indicated as significant (2-tailed) at p=<0.01

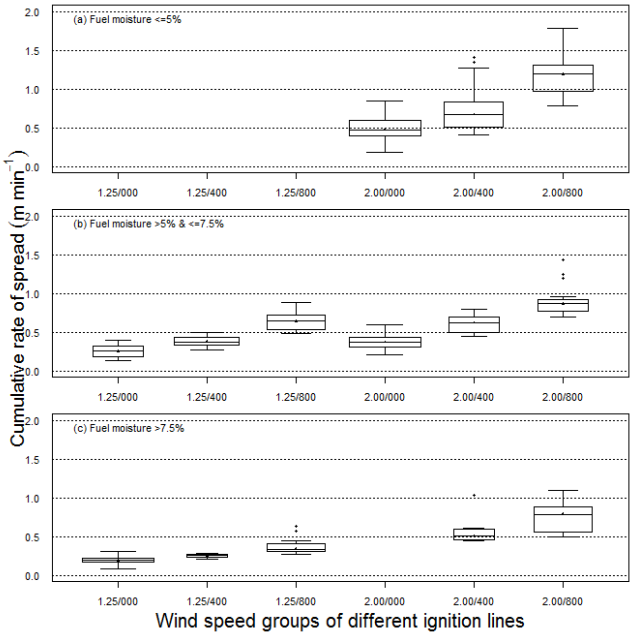

Figure 4.6. Variation in the cumulative rate of spread in relation of wind speeds (1.25 and 2.00 m s^{-1}) and different ignition sizes (000 = point, 400 mm length, 800 mm length) for three fuel moisture groups (a) fuel moisture ≤ 5%, (b) fuel moisture 5% - ≤ 7.5% and (c) fuel moisture >7.5%. Box-and-whisker plot shows the median value (²), 25th and 75th quartiles and dots (•) represents outliers more than 1 box-length from the 25th and 75th percentiles. The width of the box is proportional to the square root of the number of observation in each group.

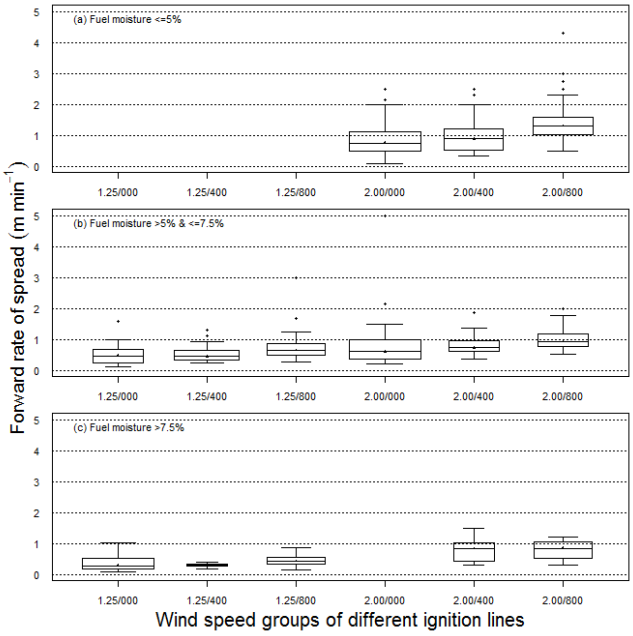

Figure 4.7. Variation in the forward rate of spread in relation of wind speeds (1.25 and 2.00 m s^{-1}) and different ignition sizes (000 = point, 400 mm length, 800 mm length) for three fuel moisture groups (a) fuel moisture ≤ 5%, (b) fuel moisture 5% - ≤ 7.5% and (c) fuel moisture >7.5%. Box-and-whisker plot shows the median value (²), 25th and 75th quartiles and dots (•) represents outliers more than 1 box-length from the 25th and 75th percentiles. The width of the box is proportional to the square root of the number of observation in each group.

4.2.5 EFFECTS OF IGNITION SIZE (LENGTH)

The initial spread rate of the experimental fires varied with ignition size (I_s). The rate of spread of point ignition fires gradually increased as the fire progressed from ignition to the 4.0 m distance mark. Tukey's HSD analysis indicated that there was no significant difference in the mean rates of spread up to 2.0 m and 2.5 m from ignition for R_f and R_c respectively.

There was no significant difference in R_c after the fire passed the 2.0 m mark (Table 4.4 and Figure 4.8). For fires ignited from 400 mm and 800 mm lines, there was no significant difference in R_c as the fire burned through the 4 m fuel bed.

Table 4.4. Asterisk (*) identified the pairwise mean rates of spread (R_c and R_f) that are significantly different at 95 percent confidence by Tukey's HSD method by 0.5 m fire spread increment for each ignition size (I_s)

DISTANCE FROM IGNITION (M)	CUMULATIVE RATE OF SPREAD (R_C) IGNITION SIZE (I_S)			FORWARD RATE OF SPREAD (R_F) IGNITION SIZE (I_S)		
	POINT	400 MM	800 MM	POINT	400 MM	800 MM
0.5-1.0						
0.5-1.5						
0.5-2.0						
0.5-2.5	*			*		
0.5-3.0	*			*		
0.5-3.5	*			*	*	
0.5-4.0	*			*	*	*
1.0-1.5						
1.0-2.0						
1.0-2.5						
1.0-3.0	*			*		
1.0-3.5	*			*	*	
1.0-4.0	*			*	*	*
1.5-2.0						
1.5-2.5						
1.5-3.0						
1.5-3.5	*			*	*	
1.5-4.0	*			*	*	*
2.0-2.5						
2.0-3.0						
2.0-3.5				*	*	
2.0-4.0	*			*	*	*
2.5-3.0						
2.5-3.5						
2.5-4.0				*	*	*
3.0-3.5						
3.0-4.0				*		*
3.5-4.0						

[1]The sample sizes were unequal, thus the Tukey method used was equivalent to what is commonly known as Tukey-Kramer (Kramer, 1956) multiple comparison method (SPLUS, 2006).

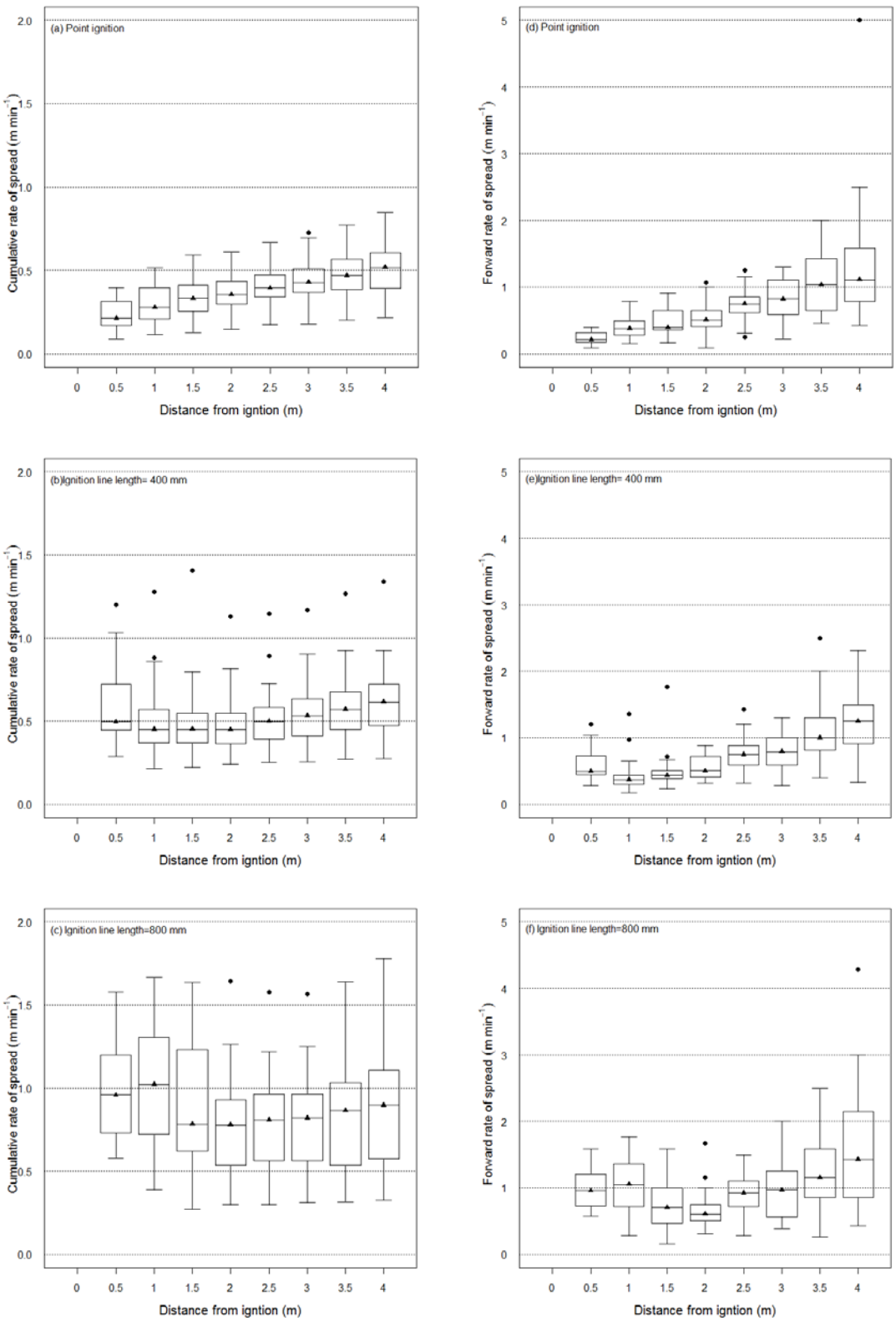

Figure 4.8. Cumulative rate of spread (left) and forward rate of spread (right) in relation to the distance from ignition line for the three different ignition sizes (000 = point, 400 mm length, 800 mm length). Box-and-whisker plot shows the median value (²), 25th and 75th quartiles and dots (•) represents outliers more than 1 box-length from the 25th and 75th percentiles. Width of the box is proportional to the square root of the number of observation in each group.

Even though the initial rates of spread for the 400 mm and 800 mm ignition lines were high at the 0.5 and 1.0 m mark, presumably as a response to the effects of the line ignition, both R_f and R_c reduced in magnitude at the 1.5 m and 2.0 m mark for the 400 mm and 800 mm ignition lines respectively (Fig. 4.8). This rapid initial spread effect of line ignitions fires was also observed by Gould *et al.* (2007a) from field experimental fires ignited from 120 m lines, where the first 25 m of spread was initially higher compared to the spread rates beyond 25 m from the ignition line.

The original data were manipulated to produce R_f values for each 0.5 m spread increment. These data are plotted on R_f versus time since ignition graph (Figure 4.9). This approach proved to be awkward as slight errors in measurement of time values and small fluctuations in fuel bed characteristics caused uneven spread. To rectify this problem those data were analysed as if they had been measured as cumulative rate of spread (R_c) i.e., cumulative distance over cumulative time.

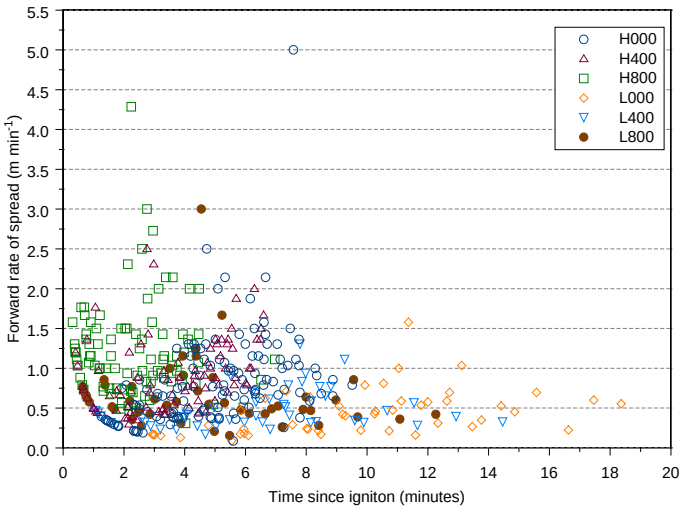

Figure 4.9. Forward rate of spread (R_f) versus time since ignition for eucalypt fuel bed with a fuel load of 1.2 kg m^{-2} with the symbols representing the different experimental wind speeds and ignition sizes (L= low wind speeds 1.25 m s^{-1}, H = high wind speed 2.00 m s^{-1}, 000 = point ignition, 400 = 400 mm ignition line, and 800 = 800 mm ignition line).

Figure 4.10 illustrates the fire progression from time since ignition for the two wind speed groups and the three different ignition sizes for fuel moisture contents ≤5% and >5%. The distance of travel of the head fire for each individual fire spread interval from the point of origin shown in Figure 4.10 illustrates the variation in spread (rate of spread for any given time period is given by the slope of the line). The slope of the line generally varied with time, with flatter slopes in the early stages of fire development compared to steeper slopes after the 2.0 m mark. There were higher spread rates at the 0.5 and 1.0 m mark for the 400 mm and 800 mm ignition lines then a dip in the spread rate around the 2.0 m mark.

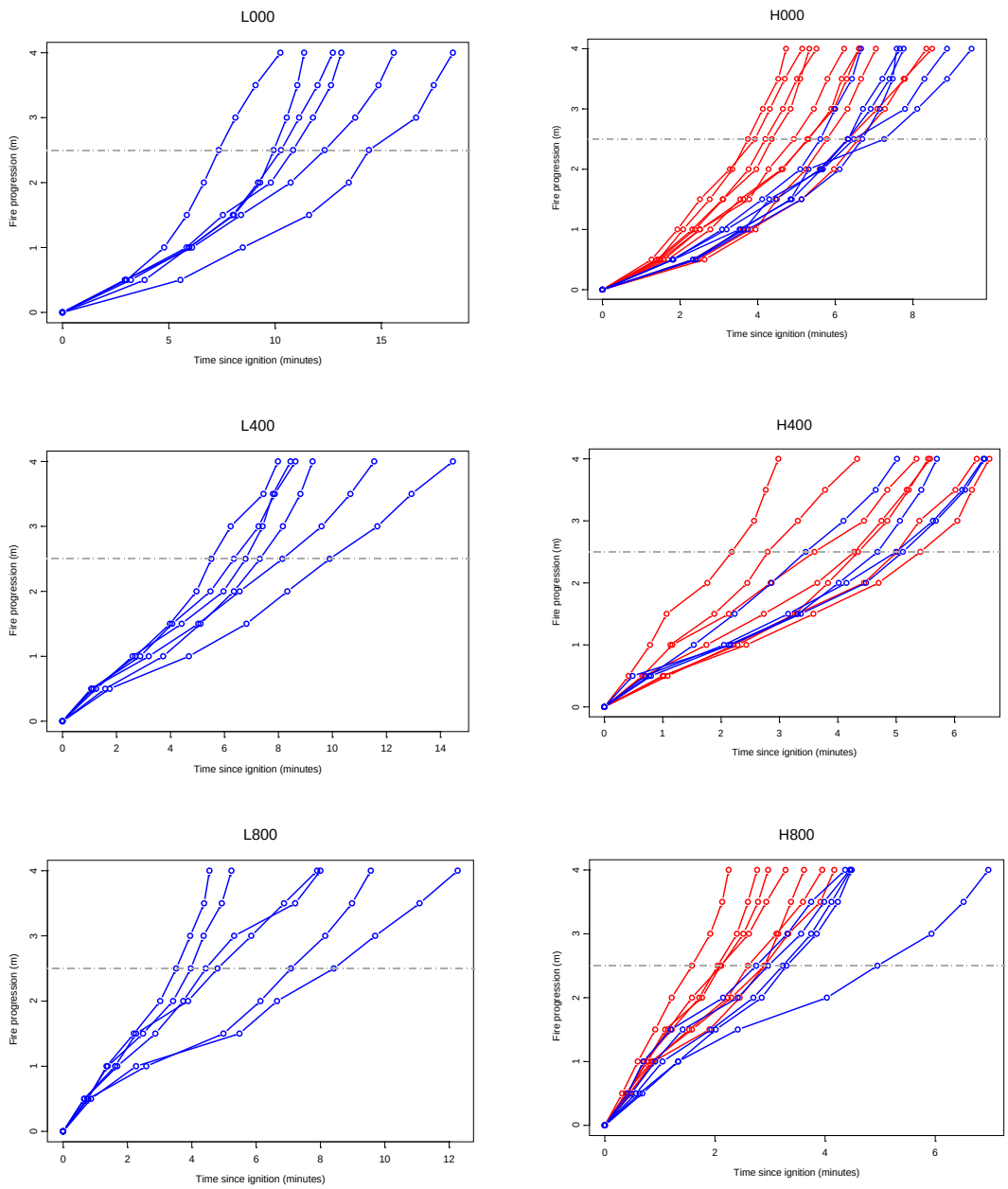

Figure 4.10. Fire progression (cumulative distance (m)) from time since ignition for the two wind groups and three different ignition sizes (L = low wind speeds 1.25 m s^{-1}, H = high wind speed 2.00 m s^{-1}, 000 = point ignition, 400 = 400 mm ignition line and 800 = 800 mm ignition line). Red lines represent fuel moisture ≤5% and blue lines fuel moisture > 5%. Dashed horizontal line at 2.5 m indicates R_{ac} below the line and R_{ss} above the line. The slope of the line indicates the rate of spread.

The results given in Figure 4.10 suggest a change in fire spread around the 2.0 m mark. On this basis the fire spread data was divided into two phases, the acceleration phase (R_{ac}) (initial spread up to the 2.0 m mark) and the steady-state phase (R_{ss}) (fire progression after 2.0 m mark). For each individual fire the rate of spread for the two phases were determined by a simple linear regression where the constant (i.e., the *y-axis* intercept) was ignored:

$$Y = ax \qquad [4.3]$$

where Y is the progression of the fire from the beginning of the acceleration phase (it begins at 0.0 m or the steady-state phase starting at 2.5 m mark and is adjusted to an origin), x is the time of the fire progress from the beginning of its phase, and a is the regression constant

(i.e. slope of the line). The regression results of the individual slopes of line (Eqn 4.3) for the acceleration and steady-state phases gave r^2 >0.96 and p values <0.001 for the value a for all 58 fires. Figure 4.11 gives sample slope of lines for the two phases by two winds and different ignition lines. Summary R_{ac} and R_{ss} with the observations are displayed in Table 4.5.

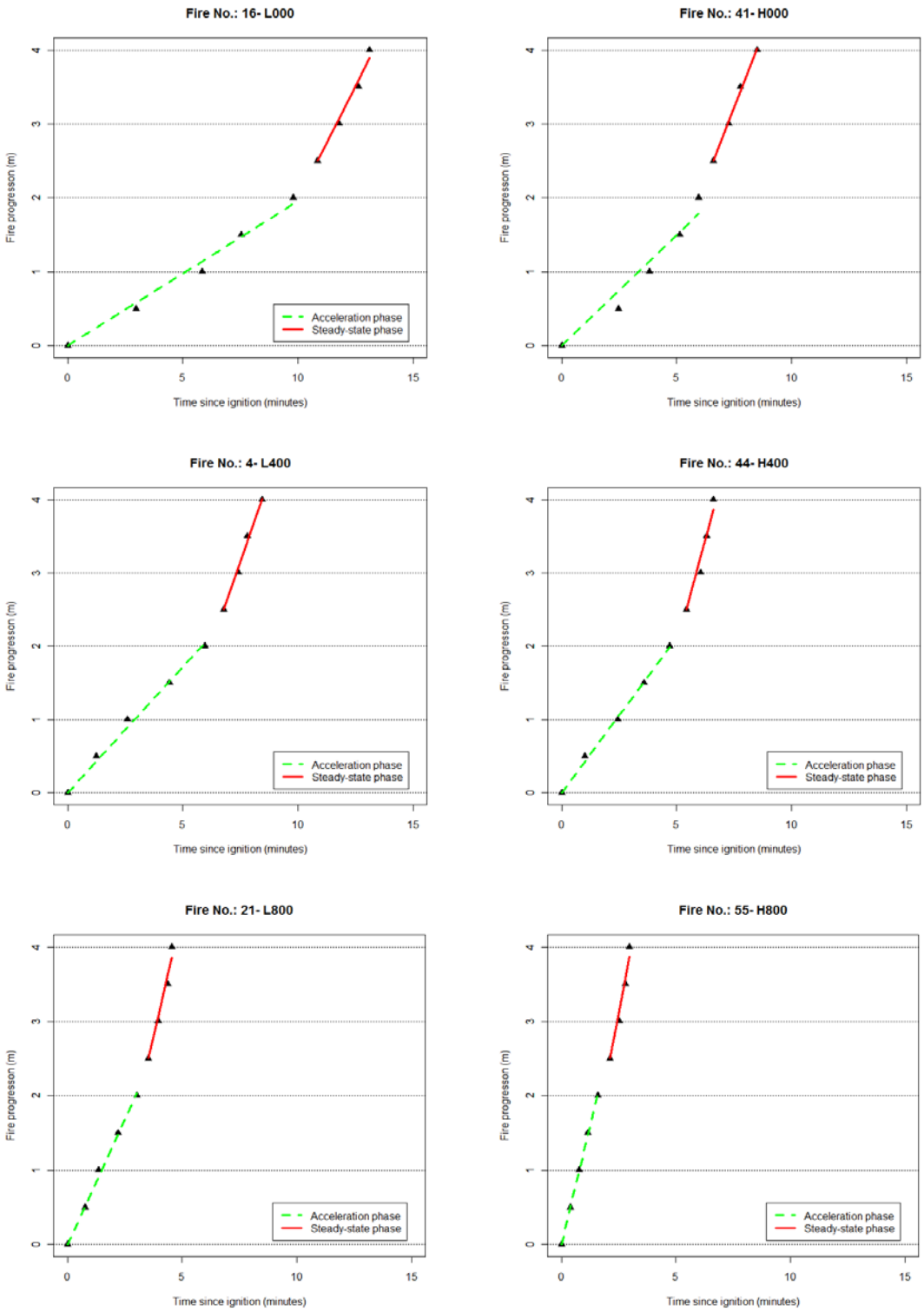

Figure 4.11. Example of results of the regression fits for *Y=ax* (Eqn 4.3) for the acceleration and steady-state phases of dry eucalypt fuels burning in CSIRO Pyrotron combustion wind tunnel. (L = low wind speeds 1.25 m s^{-1}, H = high wind speed 2.00 m s^{-1}, 000 = point ignition, 400 = 400 mm ignition line and 800 = 800 mm ignition line).

Table 4.5. Mean and standard deviation *(brackets, italics)* rates of spread (m min^{-1}) of laboratory fires burning in eucalypt fuels during the acceleration phase (R_{ac}- initial spread up to 2.0 m mark) and the steady-state phase (R_{ss}- fire spread after the 2.0 m mark).

WIND SPEED (M S^{-1})	IGNITION SIZE (MM)	NUMBER OF FIRES	M_F GROUP	M_F (%)	ACCELERATION PHASE R_C (M MIN^{-1})	ACCELERATION PHASE R_F (M MIN^{-1})	ACCELERATION PHASE R_{SS} (M MIN^{-1})	STEADY-STATE PHASE R_C (M MIN^{-1})	STEADY-STATE PHASE R_F (M MIN^{-1})	STEADY-STATE PHASE R_{SS} (M MIN^{-1})
1.25	0	0	<5%	-	-	-	-	-	-	-
		4	5-7.5%	6.19	0.22	0.31	0.23	0.35	1.07	0.89
				(0.77)	*(0.05)*	*(0.07)*	*(0.05)*	*(0.08)*	*(0.73)*	*(0.43)*
		3	>7.5%	8.51	0.16	0.19	0.17	0.23	0.53	0.46
				(1.17)	*(0.03)*	*(0.02)*	*(0.03)*	*(0.04)*	*(0.11)*	*(0.14)*
	400	0	<5%	-	-	-	-	-	-	-
		5	5-7.5%	6.26	0.36	0.36	0.34	0.41	0.69	0.65
				(0.42)	*(0.04)*	*(0.04)*	*(0.03)*	*(0.06)*	*(0.17)*	*(0.18)*
		1	>7.5	7.91	0.23	0.26	0.23	0.26	0.33	0.32
				(na)	*(na)*	*(na)*	*(na)*	*(na)*	*(na)*	*(na)*
	800	0	<5%	-	-	-	-	-	-	-
		4	5-7.5%	6.62	0.64	0.61	0.60	0.63	0.95	0.83
				(0.29)	*(0.03)*	*(0.05)*	*(0.06)*	*(0.13)*	*(0.52)*	*(0.46)*
		2	>7.5	8.48	0.41	0.38	0.31	0.35	0.49	0.47
				(0.39)	*(0.01)*	*(0.01)*	*(0.02)*	*(0.05)*	*(0.18)*	*(0.12)*
2.00	0	9	<5%	4.43	0.39	0.50	0.43	0.58	1.16	1.18
				(0.29)	*(0.09)*	*(0.14)*	*(0.10)*	*(0.12)*	*(0.29)*	*(0.24)*
		5	5-7.5%	5.97	0.43	0.43	0.33	0.44	0.94	0.93
				(0.89)	*(0.02)*	*(0.06)*	*(0.02)*	*(0.05)*	*(0.32)*	*(0.33)*
		0	-	-	-	-	-	-	-	-
	400	8	<5%	4.38	0.65	0.65	0.64	0.73	1.19	1.15
				(0.35)	*(0.29)*	(0.26)	*(0.27)*	*(0.23)*	*(0.28)*	*(0.27)*
		3	5-7.5%	7.2	0.57	0.58	0.55	0.64	1.08	1.08
				(0.20)	*(0.08)*	*(0.10)*	*(0.11)*	*(0.10)*	*(0.21)*	*(0.29)*
		1	>7.5%	7.76	0.60	0.55	0.45	0.55	1.04	1.01
				(na)	*(na)*	*(na)*	*(na)*	*(na)*	*(na)*	*(na)*
	800	7	<5%	4.45	1.21	1.17	1.15	1.18	1.69	1.57
				(0.29)	*(0.22)*	*(0.26)*	*(0.28)*	*(0.25)*	*(0.45)*	*(0.44)*
		3	5-7.5%	6.65	0.93	0.87	0.85	0.85	1.14	1.09
				(0.11)	*(0.24)*	*(0.22)*	*(0.17)*	*(0.05)*	*(0.21)*	*(0.13)*
		2	>7.5%	8.79	0.83	0.74	0.73	0.70	0.88	0.83
				(0.58)	*(0.25)*	*(0.25)*	*(0.26)*	*(0.23)*	*(0.17)*	*(0.22)*

4.2.6 FIRE GROWTH FROM POINT SOURCE IGNITION

Bushfires generally start in the surface fuels and, depending on the surface fuel properties and environmental conditions, grow in size and intensity, with the potential to develop into large destructive wildfires. The data from the laboratory studies suggest that the time required for a fire burning in eucalypt litter fuel to reach steady-state spread rate depends on ignition line size, wind speed and fuel moisture content. Here we present analysis of the first stages of fire development to estimate the time to reach steady-state spread for point ignition fires for different wind speeds (1.25 and 2.00 m s^{-1}) and fuel moisture classes (i.e., <5%, 5-7.5% and >7.5%).

The fraction of the steady-state spread rate (R_{fss}) was determined by dividing the R_f by R_{ss} values from the slope fitted regression for each individual fire spread observation. If R_{fss} equals one, we assume the fire has reached steady-state. The R_{fss} depends on the time to reach steady-state (t) for a given fuel moisture class and wind speed are shown in Figure 4.12.

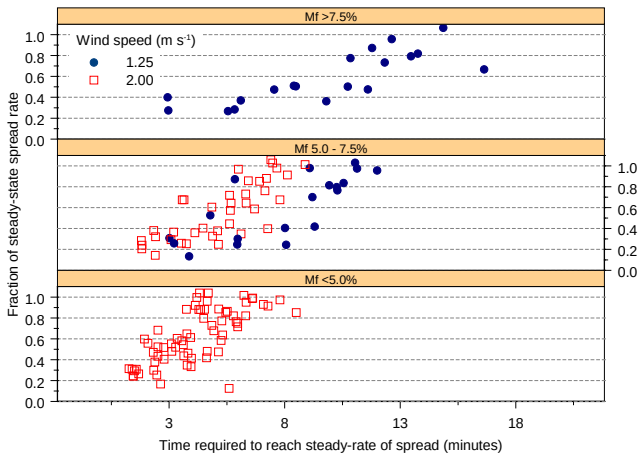

Figure 4.12. Trellis plot of point ignition fires fraction of steady-state spread rate against time required to reach steady-state for two wind speeds and three fuel moisture classes.

The results in Figure 4.12 show that R_{fss} rapidly increases with time and asymptotes towards one but varies with wind speed and fuel moisture. These results permit one to determine which, if any, of several growth curves might fit the data. Current hypothetical fire growth models by Cheney and Bary (1969) and Van Wagner (1985) were previously described in Equations 4.1 and 4.2 respectively. Our data in Figure 4.12 indicates a similar asymptotic relation between R_{fss} and t so we fitted:

$$R_{fss} = b_0 e^{-b_1/t} \qquad [4.4]$$

$$R_{fss} = b_0(1 - e^{-b_1 t}) \qquad [4.5]$$

where:

b_0 = 1 (assumption that R_{fss} will asymptote when R_{fss}=1); and

b_1 (Eqn 4.5) ≠ b_1 (Eqn 4.6);

and solve for b_1 by nonlinear regression techniques using S-Plus (SPLUS, 2006) and R (R Core Development Team, 2011) for each wind and fuel moisture class.

The results of fitting our data to these equations are shown in Table 4.6. The correlation coefficient (r^2) from the nonlinear regression analysis represents the proportion of the total variation of the dependent variable (R_{fss}) around the mean that is explained by the fitted equations (SPLUS, 2006). The r^2 values suggest that Equation 4.4 fits the observed values better Equation 4.5. However, Equation 4.4 did not asymptote to one and the coefficients do not reflect the effects of fuel moisture and wind speed compared to Equation 4.5. The coefficients for Equation 4.5 are given in Figure 4.13, showing a good relationship of b_1 coefficient with wind speed and fuel moisture. We fitted a logarithmic linear model to estimate b_1 coefficient for Equation 4.5 by a logarithmic transformation on wind speed and fuel moisture. The result of this model is given in equation 4.6 and Figure 4.13 with a correlation coefficient of r^2= 0.98:

$$b_1 = 0.6658 \times U^{0.7087} \times M_f^{-1.0288} \qquad [4.6]$$

where:

b_1= coefficient for equation 4.5

U= wind speed above the surface fuel layer in the wind tunnel (m s^{-1}),

M_f= dead fuel moisture content (%)

Table 4.6. Fraction of steady-state spread rate (R_{fss}) coefficients (b_1) and correlation coefficients (r^2) for the two fire growth equations relating fraction of steady-state to time required to reach steady-state (t) for different wind speeds and fuel moisture classes.

WIND SPEED (M S^{-1})	FUEL MOISTURE GROUP	$R_{fss} = b_0 e^{-b_1/t}$ [EQN 4.4]		$R_{fss} = b_0(1 - e^{-b_1 t})$ [EQN 4.5]	
		B_1	R^2	B_1	R^2
1.25	5 – 7.5%	3.888	0.43	0.120	0.35
	>7.5%	5.002	0.53	0.091	0.21
2.00	<5%	1.803	0.48	0.249	0.51
	5 – 7.5%	2.924	0.48	0.159	0.51

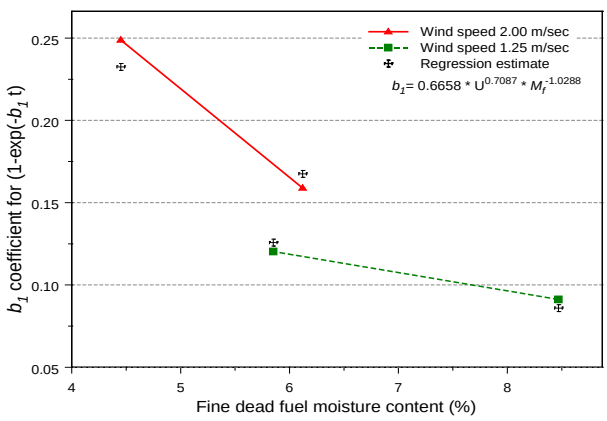

Figure 4.13. The effect of fuel moisture and wind speed on coefficient b_1 for Equation 4.4 and regression estimates for b_1 from Equation 4.6.

The time required to reach steady-state rate of spread is difficult to determine directly from the observed data. An estimate of this time for different wind speeds and fuel moisture content can be determined by substituting equation 4.6 for b_1 in a rearranged form of equation 4.5:

$$R_{fss} = 1 - e^{-B_1 t} \qquad [4.7]$$

where:

$B_1 = 0.6658 \times U^{0.7087} \times M_f^{-1.0288}$

t = time required to reach steady-state rate of spread.

The results of Equation 4.7 are given in Figure 4.14 showing the t value on the vertical axis with R_{fss} on the horizontal axis. The time to reach steady-state spread rates are approximately 38 and 50 minutes for 2.00 and 1.25 m s^{1} wind speed respectively for fine fuel moisture content at 7.5%. In the dry fuels (M_f = 5%) at 2.00 m s^{-1} wind speed, the time to reach steady-state was approximately 25 minutes in uniform eucalypt fuel litter load of 1.2 kg m^{-2}.

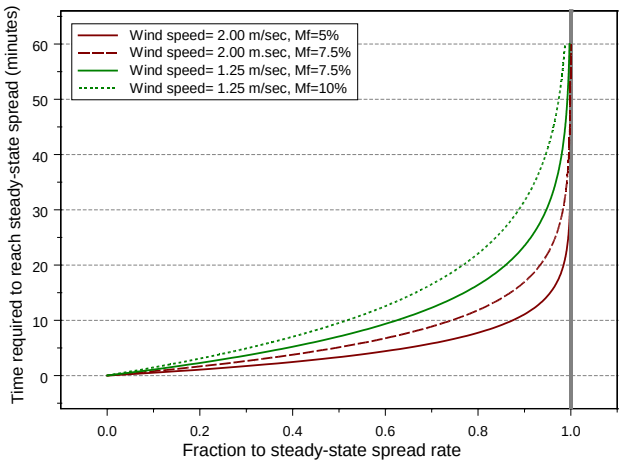

Figure 4.14. Comparison of time required to reach steady-state spread rates for different wind speeds and fuel moisture contents (Equation 4.7).

4.2.7 DISCUSSION

The process of fire growth depends, in part, on the development of flame into the fuel bed, the development of convection and development of headfire width (Cheney and Gould, 1995). This process may occur within a few minutes in a fine homogenous fuel bed. The process can take longer, in some cases over one hour or more, in deep heterogeneous fuel beds that vary greatly in structure and the level of moisture in the fuel. Atmospheric stability and wind direction variability near the flaming zone also effects fire growth.

In this Chapter we presented empirical evidence of fire growth in a heterogeneous reconstructed eucalypt litter fuel burning in a controlled wind tunnel environment. This

allowed us to investigate the effects of fire growth under repeatable burning conditions which are almost impossible to replicate in a field environment. Even under these laboratory conditions it was difficult to achieve constant values for fuel moisture, ambient air temperature and relative humidity and fuel bed uniformity (i.e., bulk density). The results from this study also exhibited a high degree of variability in the observed rate of spread (see Table 4.2 and Figure 4.9).

It is evident that more than one growth curve can fit the given data set. We presented two hypothetical fire growth curves proposed by Cheney and Bary (1969) and Van Wagner (1985) (Equations 4.1 and 4.2). These growth curves were used in other studies (McAlpine and Wakimoto, 1991; Cheney and Gould, 1995) to describe fire acceleration and growth. The McAlpine and Wakimoto (1991) study applied these proposed growth curves to support their experimental data from laboratories fires in pine needles (*Pinus ponderosa*) and excelsior fuel to determine the acceleration of point source fires to equilibrium spread.

Cheney and Gould (1995) applied these equations to field experimental grass fires to investigate the head fire width required to achieve potential quasi-steady rate of forward spread. The study presented here represents the most complete empirical analysis of fire acceleration in eucalypt litter fuel type which is more heterogeneous compared to the laboratory studies by McAlpine and Wakimoto (1991).

In the absence of a sound theoretical explanation of the physical process of fire acceleration we applied these hypothetical fire growth models to the ratio (R_{fss}) of observed rate of spread (R_f) to steady-state rate of spread (R_{ss}). We assumed this ratio (R_{fss}) asymptotes to unity at the time the fires reach the steady-state rate of spread for different wind and fuel moisture conditions. Here we define steady-state rate of spread as that determined by the mean values of the environmental and fuel variables. While these experiments demonstrated that fires accelerate from ignition (faster acceleration from line ignition compared to point ignition), the condition required to reach steady-state has been difficult to define.

The time required to reach steady-state spread rates from these experiments appear to be at odds with field observations with faster spreading fires taking longer to reach steady-state (Curry and Fons 1938, 1940; McArthur 1968 (see Figure 4.15); Cheney and Gould 1995; Gould *et al*. 1996). However the models presented here are in agreement with the hypothetical models by Cheney and Bary (1969), Van Wagner (1985) and McAlpine and Wakimoto (1991). McRae (1999) demonstrated the relative growth of point source ignition fires in pine slash fuels was independent of fire weather. The coefficient values in equation 4.7 were highly correlated with wind speed and fuel moisture content (r^2= 0.98). This disparity between field and laboratory observations may be explained by the atmospheric stability and wind turbulence under forest canopy (Sullivan and Knight 2001) as opposed to the highly laminar wind flow in the wind tunnel. In addition, the absence of multilayered fuel strata in the laboratory experiments does not reflect the fuel characteristics of eucalypt forest (Gould *et al*. 2011).

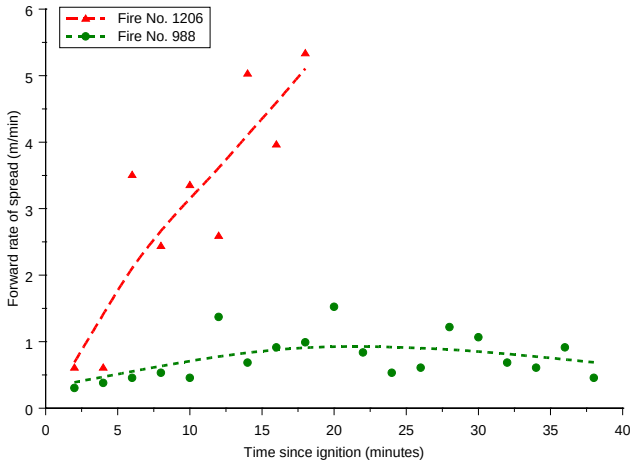

Figure 4.15. Fire acceleration during the initial stages of a fire starting from a point source ignition:
[2] Fire No. 1206: Black Mountain ACT (20/02/1968), Slope = 16%, *T* = 30°C, *RH* = 31%, Open 10 m wind speed = 26 km h^{-1}, Fuel quantity = 20 t ha^{-1}, M_f = 5%, Forest Fire Danger Index (FFDI) = 34 (Very high).
• Fire No. 988: Black Mountain ACT (13/02/1968), Slope = 9%, *T* = 27°C, *RH* = 21%, Open 10 m wind speed = 9 km h^{-1}, Fuel quantity = 15 t ha^{-1}, M_f = 5%, FFDI = 17 (High) (Source: McArthur 1968).

The air flow in CSIRO Pyrotron is highly laminar, with a turbulence intensity of <0.6% (Sullivan *et al*. 2013). Extrapolation of wind tunnel air flow into operational guidelines for field estimates for fire growth is problematic and a potential source of significant errors in predicting fire growth in the field. One of the major sources of error in the application of this fire growth model based on air flow within a wind tunnel is the selection of an appropriate wind ratio for the wind under forest canopy at 2 m or in the open or above canopy to wind.

Preliminary studies were conducted in open dry eucalypt forest measuring wind speed at 2.0 and 0.15 m above the ground under the forest canopy. Figure 4.16 shows a typical trace of wind speed under the forest canopy at 2.0 m and just above the forest litter floor (0.15 m above ground). Cheney *et al*. (2012) applied a wind ratio for 10 m open wind speed to 2.0 m under canopy wind speed of 2.55:1 which is representative of an open forest, and would be applicable to many dry eucalypt forests across southern Australia. The adjustment of this wind ratio to account for wind flow above the litter fuel layer can be expressed as 4.25:1. Applying this ratio to the 1.25 m s^{-1} and 2.00 m s^{-1} air flow in the wind tunnel represents an open 10 m wind speed of 20 km h^{1} and 30 km h^{-1} respectively. We would expect this adjustment of wind tunnel air speed to open 10 m wind speed or at 2 m under forest canopy wind will still give uncertainty in the prediction of fire growth because these values do not account for under forest canopy turbulence and atmospheric stability.

Fires burning in dry eucalypt forest are subject to successive changes in wind speed and direction (Sullivan and Knight 2001) and fuel characteristics (Gould *et al.* 2011, McCaw *et al*. 2012) which will affect the acceleration phase of the fire. The magnitude and rate of these changes will most likely be random or haphazard. Thus, it can be expected that the relationship between rate of spread and time since ignition will have poor predictive qualities (Lawson 1972).

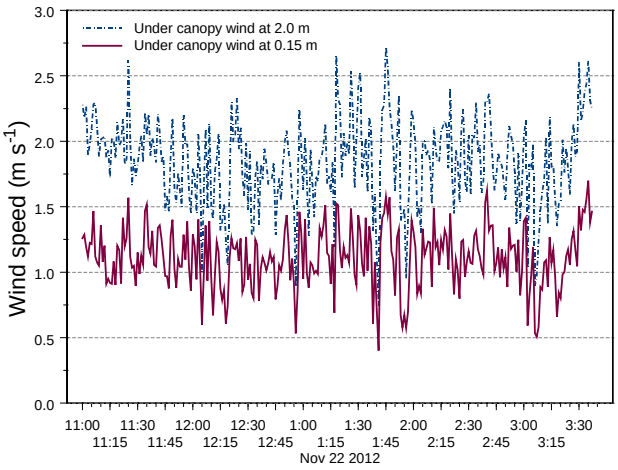

Figure 4.16. Typical under-canopy 1-minute average wind speed from anemometers at 2.0 and 0.15 meters above ground under forest canopy.

While the hypothetical fire growth curve such as Cheney and Bary (1969), Van Wagner (1985) and the growth curves presented here may be useful to describe fire acceleration to steady-state of laboratory fires, it cannot be expected to provide a general acceleration model for field observations. Therefore, the acceleration curves for point ignition fires derived from laboratory experiments could be misleading and should be used with care in planning initial attack and to manipulate fire behaviour during prescribed burning (i.e., ignition spacing and techniques).

While this study is not a definitive analysis of fire growth in eucalypt fuel, it is, however, a first step. Further investigation is needed to extend the results presented here to determine the disparities between field observations and laboratory studies of time to reach steady-state spread rates. This would provide more accurate models for current fire behaviour predictions and better simulation of fire growth between the time of ignition and steady-state spread.

Further rectification and analysis of the vertical video images of each experimental fire is needed to investigate length-to-breath ratios and perimeters to verify the extrapolation of operational models outside their range of empirical developmental data. This additional research on fire development from point and line source ignition fires will provide better knowledge to improve initial response to fires and planning ignition patterns for prescribed burning operations.

4.2.8 CONCLUSIONS

Wind speed and fuel moisture content were found to have an effect on fire acceleration for ignition sources of point, 400 mm and 800 mm in length in wind tunnel experimental fires burning through a 1.5 m wide and 4.0 m long fuel bed of dry eucalypt litter fuel. There was a distinct change in the rate of spread between the 2.0 and 2.5 m mark along the fuel bed and the spread rate was divided into an acceleration phase (first 2.0 m of fire spread) and a steady-state phase (fire spread after the 2.0 m mark).

The line ignition fires burned faster than the point ignition fires and exhibited the same behaviour observed in field experiments (Gould *et al.* 2007a) with a rapid increase in spread at ignition followed by a dip in spread rate around the 2 m mark. Published hypothetical fire growth curves by Cheney and Bary (1969) and Van Wagner (1985) were used to estimate the time required to reach steady-state spread rates. While these curves represent the acceleration of laboratory fires the results differ to field observations. The disparity between laboratory experiments and field observation could be due to the highly laminar wind flow in the wind tunnel compared to the turbulent wind conditions found in the forest environment. Therefore care should be taken when attempting to apply these fire growth curves to operational practices in the field. Further investigation of fire development from point and line source ignitions is needed to provide better knowledge for improved initial response to fires and planning ignition patterns for prescribe burning operations.

4.3 Fire growth and acceleration in eucalypt litter: Historical field experiments

4.3.1 INTRODUCTION

Forest fire behaviour research in Australia has evolved over several decades (McArthur 1962, 1967, Peet 1965, 1972, Peet and Sneeuwjagt 1979, 1985, Burrows 1994, 1999, Gould *et al*. 2007a, Cheney *et al*. 2012). The pioneering fire behaviour research by McArthur (1962, 1967) and Peet (1965, 1972) were the bases for the McArthur Forest Fire Danger Rating System (McArthur 1973) and the Forest Fire Behaviour Tables for Western Australia (Sneeuwjagt and Peet 1979, 1985).

McArthur's and Peet's original experiments were primarily aimed at improving the techniques for fire suppression and controlled burning. Their work was conducted on small-scale field experiments of point source ignition under relatively mild burning conditions in which the fire's development was restricted. The limitations of these studies have been discussed by Burrows (1994), Gould *et al*. (2007a) and McCaw *et al*. (2008). They concluded that the original fire behaviour models that resulted from this work under-estimated fire spread under dry summer conditions (McCaw *et al*. 2008).

One of the possible causes of this under-estimation is that the fires from which the data were compiled were still developing in size and speed (i.e. accelerating), thus were not spreading at their full potential rate of spread, i.e., steady-state. Additionally, it appears that McArthur's experimental data was not fully analysed possibly because of the dual purpose of the experimental fires.

Many of the fires McArthur carried out in the Australian Capital Territory (ACT) were conducted as part of a two-week summer field exercise for students of the Australian Forestry School as part of their fire control subject. Furthermore, a limited number of his experimental fires were conducted in different forest types in Victoria and New South Wales to instruct State fire researchers in experimental techniques so that they could conduct further experimental studies to develop fire behaviour guides for specific fuel types (P Cheney pers. comm.). This resulted in a large experimental dataset with limited data analysis. Today this data provides an excellent source for investigating fire growth and development of point ignition fires in dry eucalypt forest.

This section of the Chapter presents a summary of the original experimental data predominantly collected under the supervision of McArthur between 1953 and 1975 and which were digitised and collated into electronic data files for more robust analysis utilising modern statistical methods. We present a proposed fire growth model for area and perimeter based on tables produced by McArthur (1958) and compare these results with other independent experimental data. The results from this analysis highlight the complexity of modelling fire growth, area and perimeter with time since ignition for a range of fuel, weather and topographic conditions.

4.3.2 DATA REDUCTION

The data for this study were obtained from a number experimental records on fire behaviour, fuel, and weather conditions dating from the early 1950s to the present which were held at CSIRO Ecosystem Sciences Bushfire Dynamics and Application Group, ACT, and the Department of Parks and Wildlife, Western Australia. Specifically, the experimental fires are those conducted by:

1. Alan G. McArthur during the 1950s, 1960s and 1970s. These experiments were carried out in open dry eucalypt forest located in ACT (Black Mountain, Kowen Forest, and Bull's Head), Victoria (Traralgon and Daylesford experiments), and Western Australia (jarrah fire experiments).
2. George Peet during the 1960s in jarrah forest in Western Australia. The transfer of Peet's experimental records to electronic data files is incomplete, thus not included in this study.

The first phase of the data reduction was the collation of all the experimental fires conducted in dry eucalypt forest (primarily sourced from Alan McArthur's experimental fires). These fires were predominantly lit from a point and allowed to burn for around 30 to 50 minutes, depending on the weather conditions and if the head or flank fire spread was constrained by a track or firebreak. In the majority of these fires the perimeters were marked at two-minute intervals with metal or other markers. At these two minute intervals in-forest wind speed at 1.5 m height was recorded and experienced fire behaviour observers made ocular estimates of fuel continuity, flame height, flame depth, flame length and flame angle of the head fires. Additional notes were made on changes of wind speed and direction, up-draughts, down-draughts, smoke characteristics, spotting and fire behaviour.

After the fire had been extinguished, the positions of the fire perimeter markers were surveyed. The positions of the markers were plotted and fire perimeter isochrones were drawn freehand between the plotted perimeter markers for each time interval. The fire perimeter, fire area, cumulative forward rate and maximum rate of spread were then calculated from these fire perimeter isochrones maps. Figure 4.17 is an illustrative example of fire isochrones representing the fire perimeter at two-minute intervals. More detailed description of the methods used during McArthur's experimental fires between 1962 and 1975 are given in Appendix 4.2.

4.3.3 RESULTS

Information for each two-minute interval fire observation from the field fire behaviour field sheets and other recorded information for each fire were transferred to electronic data files. The individual fire perimeter isochrones maps were digitally photographed to be included in

the metadata for each fire. Some fire records such as the fire area, perimeter and rates of spread were missing and were obtained by analysing digitised fire isochrones maps for this data. In the end, there were over 450 experimental fires collated into five different datasets representing the size of the experiment and the location of the experimental site. Table 4.7 lists the range of key weather, fuel and fire behaviour experiments conducted in the ACT and Victoria.

Figure 4.17. Experimental fire 929 in dry eucalypt forest at Black Mountain, ACT (left) and the fire isochrones represents the fire perimeter at 2-minute intervals (right).

The first experimental fires conducted by McArthur in the 1950s were small scale point ignition fires with a burning duration between 1 and 8 minutes spreading up to 13 m from ignition. In the 1960s and 1970s fire experiments were larger in size burning between 4 and 74 minutes depending on the burning conditions and spreading up to 71 m from ignition line (See Table 4.7).

The duration of the experimental fires conducted near Daylesford, Victoria were similar to the medium-scale fires at Kowen and Black Mountain, ACT. Median values of the fine fuel moisture content of the Daylesford fires were 3% wetter compared to the ACT experiments and the wind conditions were lighter, resulting in a narrower range of spread rates between 0.4 and 4.9 m min^{-1} compared to ACT fires which were between 0.1 and 16.9 m min^{-1}.

Figure 4.18 illustrates the comparison of the range of the maximum rate of spread by 1.5 m wind speeds of the Daylesford experimental fires with the ACT Black Mountain experiments. There was very little information on the specific location and types of forest where the Daylesford fires were conducted and additional work is required to obtain this information on the location and description of 'Pinchgut' and 'Buckstead' blocks at the time of the Victoria Forestry Commission in the early 1960s.

Exploratory analyses using graphical representations carried out used to help examine some of the preliminary concepts of the fire growth. We examined how the response variables (e.g. Area) depend on time since ignition (Ignition) for given intervals of in-forest wind speed (Wind) and fuel moisture (Moisture).

Figure 4.19 is a coplot of the medium scale fires. The dependence panels are 6 × 6 array of graphs with the given panels of fuel moisture and in-forest wind speeds. In each dependent panel Area is plotted against Ignition for those observations whose value of Moisture and Wind lie within a given interval; thus seeing how fire area depends on time since ignition, fuel moisture and wind speed under forest canopy. The intervals are shown on the given panel.

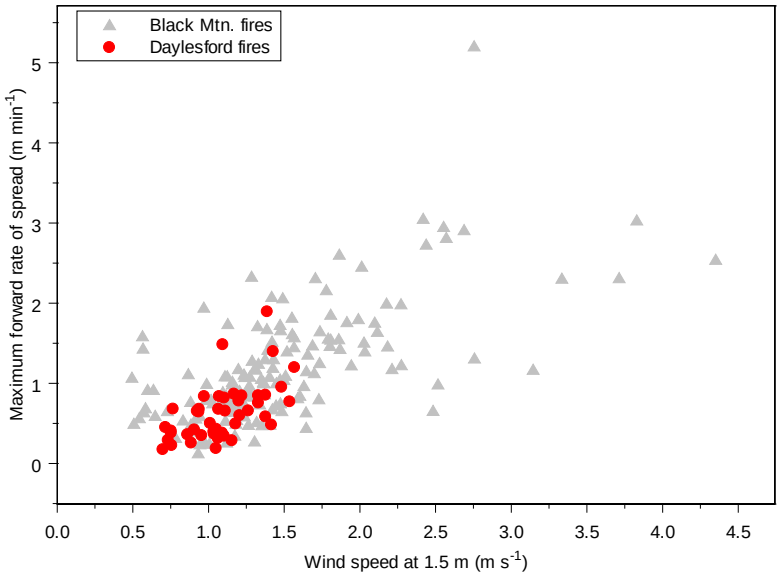

Figure 4.18. Comparison of the in-forest wind speed at 1.5 m and maximum forward rates of spread from McArthur's experimental fires in dry eucalypt forest at Daylesford, Victoria and Black Mountain, ACT.

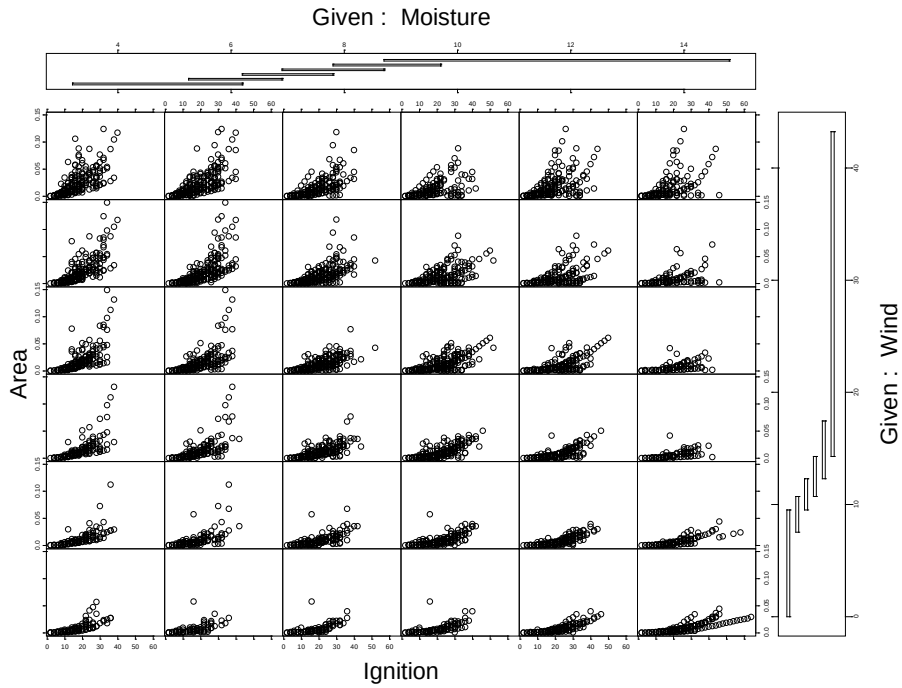

Figure 4.19. Coplot of Black Mountain, ACT experimental fires (Table 4.7) illustrating the relationship between fire area (Area, hectares) and time since ignition (Ignition, minutes) for given fuel moisture (Moisture, %) and open wind speed 10 m (Wind, km h^{-1}) grouping. The Moisture and Wind bar (left to right, or bottom to top) are associated with the dependence panels moving left to right and bottom to top with a 25% overlap between panels.

The far left column in Figure 4.19 shows an increasing exponential relationship between area and time since ignition with increasing wind speed which becomes less pronounced as fuel moisture increases (moving right). For wetter fuels with fuel moisture >12%, the relationship between area and in time since ignition is almost linear except for the higher winds (top row in Fig. 4.19). The fire area was significantly correlated with time since ignition, wind speed and fuel moisture *r*= 0.68, 0.22, 0.10 respectively. Fuel load was not significant with fire areas *r*= 0.07. There was a similar correlation with fire perimeter to these

variables, with fuel load slighter stronger with r= 0.11. There was a poor correlation between slope and fire area and perimeter with r values <-0.10.

4.3.4 PRELIMINARY FIRE GROWTH MODEL

The initial stage of development the behaviour of the fire is dominated by the environmental conditions and suppression is relatively easy provided suppression resources arrive early. This initial stage may last a few minutes to hour or more, depending on such factors as quantity, condition and arrangement of fuel, and the influence of weather and topography. A preliminary model based on McArthur's Black Mountain experimental fires is presented here. From the results above and illustrated in Figure 4.19, a practical model to predict fire area from point source ignition for the first hour of spread can be written:

$$A(t) = Ø_1\,(t)\,Ø_2\,(M_f, U_{10}) \qquad [4.8]$$

where A is area of the fire (hectares) at time (t) since ignition (minutes), M_f is the dead fuel moisture content (%), and U_{10} is the open wind speed at 10 m (km h^{-1}). We fitted the relationship between the area of the fire with time since ignition as a power function, and then tested for the effect of fuel moisture and wind speed. The logarithm of A was regressed on t and various forms of M_f and U_{10} were used to obtain the best fitting model. After incorporating all the above analysis, our proposed model for predicting A is:

$$A = b_o\,(t)^{b1}\,\exp(b_2\,Mf + b_3\,U_{10}) \qquad [4.9]$$

The fitted model had a R^2 value of 0.79. Plotted residuals from the model were examined for normality and homogeneity of variance and found to be satisfactory. The results of the regression model was:

$$A = 0.00001624\,(t)^{2.2026} \bullet \exp(-0.2070\,Mf + 0.0846\,U_{10}). \qquad [4.10]$$

The prediction from equation 4.12 using the mean fuel moisture and wind speed in Table 4.7 is compared to the observed area of the fire from commencement of ignition in Figure 4.20. These fires were small scale experiments of point source ignition which restricted full development and burned under relatively mild burning conditions.

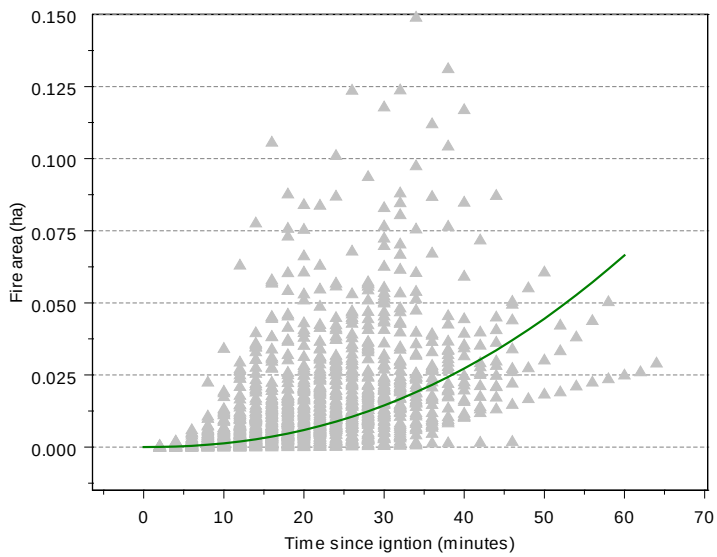

Figure 4.20. Comparison of predicted area (solid line) using the mean values of fuel moisture and wind speed of the Black Mountain experimental data with observed area (^{2} symbol).

Table 4.7. Weather and fire behaviour data from McArthur's experiments in the ACT and Victoria. Median and range (minimum – maximum)

FIRE BEHAVIOUR PARAMETER	SMALL SCALE EXPERIMENTS KOWEN, ACT 1955 - 1956	MEDIUM SCALE EXPERIMENTS KOWEN, ACT 1957 - 1961	MEDIUM SCALE EXPERIMENTS BLACK MTN., ACT 1960 - 1971	MEDIUM SCALE EXPERIMENTS DAYLESFORD, VIC 1964 - 1966	MEDIUM SCALE EXPERIMENTS TRARALGON, VIC 1962 - 1964
Number of fires	46	191	136	52	29
Number of fire spread observations	284	2280	1951	751	334
Duration (min)	**3.5** (1-8)	**31** (4 – 74)	**30** (10 – 64)	**34** (14 – 60)	**28** (6 – 40)
Ignition length (m) (0=point ignition)	0	0	0	0	0
Mid-flame height wind speed (m s^{-1})	**2.52** (0.31 – 6.3)	**1.8** (0.04 – 6.4)	**1.2** (0 – 4.8)	**1.05** (0.02 – 2.69)	**1.06** (0.22 – 2.29)
Temperature (^{o}C)	**23** (18 – 29)	**22** (10 37)	**22** (10 – 32)	**18** (13 – 24)	**23** (17 – 32)
Relative humidity (%)	**44** (25 – 72)	**40** (9 – 91)	**42** (19 – 68)	**47** (23 – 80)	**50** (29 – 60)
Fuel moisture content (%)	**6.9** (4.5 – 17.6)	**6.9** (3.2 – 22.0)	**7.8** (4.3 – 14.8)	**10.0** (6.2 – 16.0)	**11.3** (8.6 – 18.5)
Fine fuel load (kg m^{-2})	na	na[1]	**1.17** (0.45 – 2.11)	**1.01** (0.6 – 2.67)	**1.25** (0.65 – 1.54)
Maximum distance travelled (m)	**3.1** (0.6– 13)	**22** (1.8 – 63)	**22** (1.2 – 71)	**10.2** (2.9 – 33.1)	**14.5** (4.9 – 32.9)
Slope (^{o})	0	**10** (-7.5 – 17.0)	**7.5** (2.3 – 21.0)	**5** (-7.0 – 10)	**7.5** (-2 – 9)
Rate of spread (m min^{-1})	**0.8** (0.1 – 16.9)	**0.9** (0.4 – 7.8)	**0.71** (0.01 – 7.2)	**0.61** (0.4 – 4.9)	**0.67** (0.1 – 5.7)
Flame length (m)	Na	**0.6** (0.5 – 5.5)	**0.6** (0.3 – 18.3)	0.45 (0.02 – 6.7)	**1.1** (0.15 – 7.2)

[1] Fuel load was ranked into three major fuel quantity classes: Sparse (S: 0.45 – 0.99 km m^{-2}), Moderate (M: 1.0 – 1.8 kg m^{-2}) and Heavy (H: >1.8 kg m^{-2})

Results from extrapolation of the model to a larger range of fuel moistures and wind speeds in the open are given in Figure 4.21. This model provides the basis for predicting the growth of a fire for the first hour (60 minutes) from a point source ignition for predominantly low to moderate intensity fires burning under mild conditions, similar to controlled burning operations, with application bounds for M_f between 5% and 12.5% and U_{10} <20 km h^{-1}.

Due to the limited data for high wind speeds and low fuel moisture content, the model may under-estimate fire growth during severe to extreme fire weather conditions, thus the model is not suitable for these conditions. Equation 4.12 can be used to predict fire growth via computer models and can be presented as tables and nomograms that are easy to use in the field and are useful for illustrating the relative importance of each variable for prescribed burning operations.

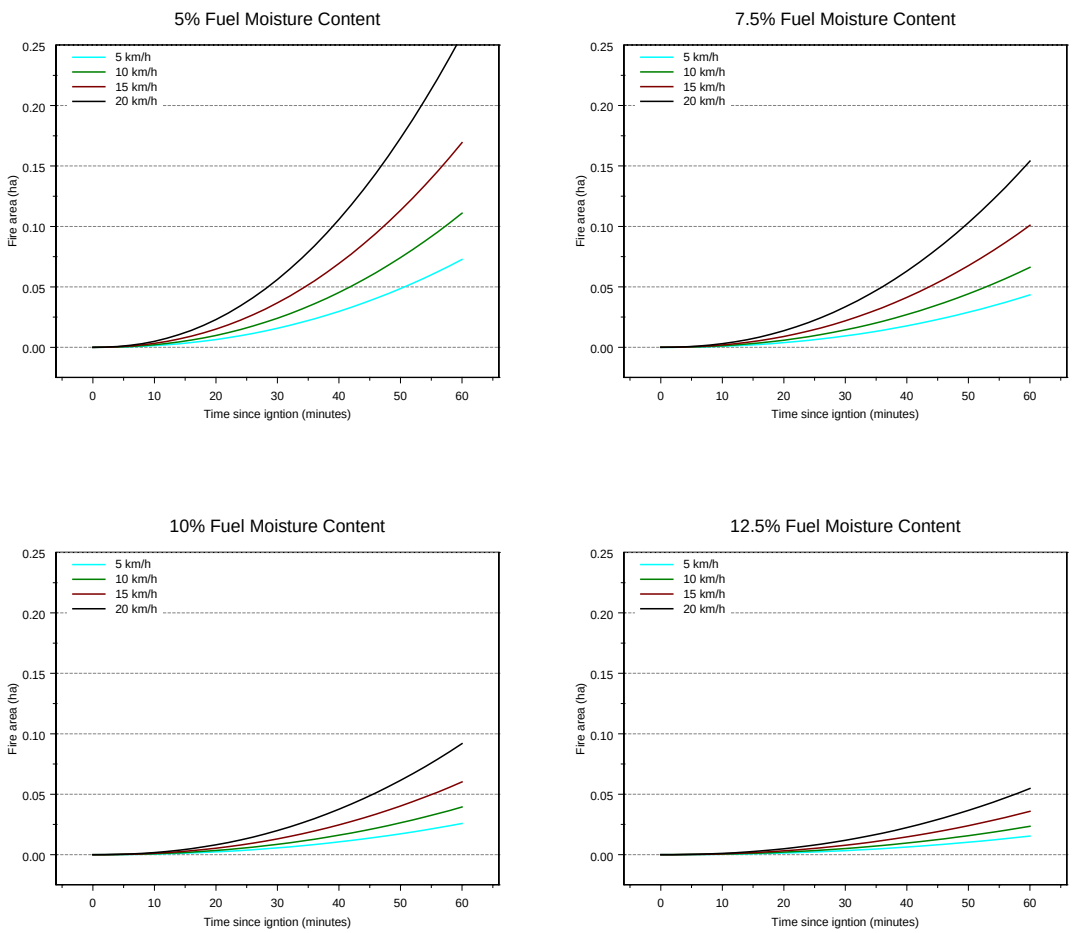

Figure 4.21. Predictive curves for fire area from commencement of point ignition fires for different wind speeds and fine dead fuel moisture content (Equation 4.12) with application bounds of fuel moisture 5% to 12.5% and 10 m open wind speed <20 km h^{-1}.

4.4 Practical Applications

4.4.1 PRESCRIBED BURNING

Most prescribed burning guides (e.g. McArthur 1962) for fuel or hazard reduction have been compiled from experimental fires that have burnt at a steady-state rate of spread that is well below the potential rate of spread under any but the mildest of conditions. When the aim of the burn is to achieve fuel reduction with low intensity fire, individual fires are lit at a spacing so that they maintain this reduced rate of spread until the burning conditions become milder or the fires run into each other and go out. When carried out correctly prescribed fires can burn at steady-state spread rates over much of the intended area at one third or less of the intensity of the potential rate of spread during the peak of the day. When they do join together (i.e. fire coalescence) the burning conditions and the intermediate steady-state spread is reduced so that the increase in spread resulting from the development of a wide headfire or from the junction zone effect is also reduced and the behaviour mostly remains within the prescription.

Prescribed fires that are lit too close together will join during the peak of the diurnal burning conditions and the coalesced fire is likely to burn at the potential rate of spread which will be well above the intensity prescribed to minimise damage to the overstorey vegetation. The potential rate of spread of a single fire can be exceeded when multiple fires join together and the convective interaction induces higher wind speeds in the forest. Thus, under moderate burning conditions, bushfires starting from a point may develop different steady-state spread rates that are well below the potential rate of spread. Conversely, if lit too far apart each individual fire can develop and reach its potential rate of spread, again exceeding prescription. The example, illustrated in Figure 4.22, of 17 fires lit simultaneously at a point and measured periodically by infrared line scan shows all fires remained well below the potential rate of spread. Only two fires developed to the stage where, after 120 minutes, they exhibited rates of spread that were close to the potential rate of spread (from Gould *et al.* 1996).

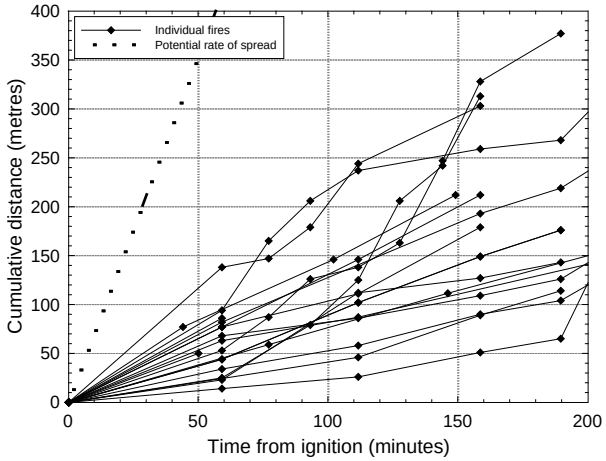

Figure 4.22. Cumulative distance of forward spread of 17 point source ignition fires lit simultaneously, Block 17 McCorkhill WA 10/01/1983. The slope of the line indicates the rate of spread and the dashed line indicates the potential rate of spread (from Gould *et al.* 1996).

4.4.2 FIRE SUPPRESSION

Wildfires often start at a point but generally maintain a steady-state spread rate that is well below the potential rate of spread for the prevailing conditions for several hours. Firefighters may assume that all fires initiating in dry summer conditions will spread below their potential rate of spread. However, while it is imperative to take advantage of this reduced fire behaviour for initial attack they must always adopt a safe work practice that ensures egress to a safe area should the fire develop a wide head and suddenly increase in intensity to the potential rate of spread.

A major shift in wind direction is the most common reason for fires increasing the head fire width and accelerating but there are other ways that are more subtle and can occur without a major change in the weather. These include the onset of spotting and the coalescence of spot fires or, more importantly, when spot fires are drawn into the head of the main fire by local in-draught winds at right angles to the prevailing wind. A change in fuel type or topography that allows the fire to be more responsive to local fluctuations in wind direction may also increase the width of the headfire.

The Mount Muirhead fire in South Australia on Ash Wednesday (16 February 1983) started from arcing powerlines in grassy fuel along the roadside verge running through the pine plantation (Cheney pers. comm. 2003). This grassfire spread rapidly along the narrow verge between the road and the plantation perimeter firebreak at right angles to the prevailing wind because the fire in the fine fuel could respond to gusts in the wind. The fire eventually spread from the verge into the plantation, forming a wide front that burnt at its potential rate of spread of 12 km h^{-1} almost immediately.

Lighting lines of fire during burning-out operations is another common way of fires rapidly reaching their potential rate of spread and increasing their intensity unnecessarily. This can create obvious problems if the fire burns up to the fireline that is being secured. The problems may be less obvious when the fire burns away from the fireline. However, lighting lines of fire, while rapidly securing the upwind edge of the fire, has often caused problems downwind by threatening firefighters on other sections of line, increasing the overall width of the fire and dramatically increasing spotting from the fire, sometimes across control lines established several kilometres down wind.

4.5 Conclusions

One element that has received little mention in fire control literature and operating procedures is the effect of time on many aspects of fire behaviour, especially such factors as rate of spread, area increase and spotting (McArthur 1968). In this chapter we tried to address some of these concerns. The processes involved in fire propagation during the period between the time ignition occurs until suppression action commences form some of the most critical and significant studies of fire behaviour. During the first 60 minutes or so of a fire's life, suppression forces have their greatest chance of success purely because the fire is still accelerating and has not reached its maximum rate of spread and thus fireline intensity and flame height.

The thorough planning of an initial attack system must be based on knowledge that all fires accelerate from the time flame first appears through variable periods until a steady-state is reached. The models developed here provide some insight into the different rates of acceleration for fires in eucalypt litter fuel. The laboratory studies conducted in the CSIRO Pyrotron are in agreement with the theoretical models by Cheney and Bary (1969) and Van Wagner (1985) but appear to be at odds with field observations with faster fires taking longer to reach steady-state (see Figure 4.15). This disparity between field and laboratory observations may be explained by other factors not present in the laboratory studies such as atmospheric stability, wind turbulence under forest canopy and the absence of multilayered fuel strata. Therefore, care should be taken when attempting to apply these fire growth models to operational practices.

The historical empirical observations of small scale (< 1 ha) experimental fires are those in which fire development was restricted. These were largely conducted under mild burning conditions. The analysis of these data resulted in a fire growth model for area increase since ignition with time (t), fuel moisture (M_f) and wind speed (U_{10}) as good predictor variables, producing a R^2 value of 0.79. This model has application bounds on the predictor variables that are in the range of operational prescribed burning conditions.

Both models presented here provide some important insights into fire development in eucalypt litter fuel. They indicate the importance of the time factor in fire control which increases with increasing fire danger. However, further work in the analysis on both laboratory and field datasets is required to develop a better understanding of fire growth for a wide range of fire behaviour conditions. Continuing investigation of fire development from point and line source ignitions is needed to provide better knowledge to improve initial response to fires and planning ignition patterns for prescribe burning operations.

4.6 References

Bechhofer RE, Santner TJ, Goldsman DM (1995) *Design and Analysis of Experiments for Statistical Selection, Screening, and Multiple Comparisons*. John Wiley & Sons, Inc., New York.

Burrows ND (1994) Experimental development of a fire management model for jarrah (*Eucalyptus marginata* Donn ex Sm.) forest. PhD Thesis, Australian National University, Canberra, ACT.

Burrows ND (1999) Fire behaviour in jarrah forest fuels: 2. Field experiments. *CALMScience* **3,** 57-84.

Chandler C, Cheney P, Thomas P, Trabaud L, Williams D (1983) *Fire in Forestry, Volume I: Forest fire behaviour and effects.* John Wiley & Sons Inc: New York.

Cheney NP (1981) Fire Behaviour. In*: Fire and the Australian Biota* (ed. A.M. Gill, R.H. Groves, and I.R. Noble). Australian Academy of Science, Canberra, pp 101-127.

Cheney NP and Bary GAV (1969) The Propagation of Mass Conflagrations in a Standing Eucalypt Forest by the Spotting Process. Paper A6, Mass Fire Symposium, Canberra, February 1969, Commonwealth of Australia.

Cheney NP and Gould JS (1995) Fire growth in grassland fuels. *International Journal of Wildland Fire* **5**, 237-247.

Cheney NP and Gould JS (1997) Fire growth and acceleration. Letter to the Editor: *International Journal of Wildland Fire* **7**, 1-5.

Cheney NP, Gould JS and Catchpole WR (1998) Prediction of fire-spread in grasslands. *International Journal of Wildland Fire* **8**, 1-13.

Cheney NP, Gould J and McCaw L (2001) The dead-man zone – a neglected area of firefighter safety. *Australian Forestry* **64**,45 – 50.

Cheney NP, Gould JS, McCaw LW, Anderson WR (2012) Prediction fire behaviour in dry eucalypt forest in southern Australia. *Forest Ecology and Management* **280**, 120-131.

Cruz MG, Matthews S, Gould J, Ellis P, Henderson H, Knight I, Watters J (2010) Fire dynamics in Mallee-heath- fuel, weather and fire behaviour prediction in south Australian semi-arid shrubland. Bushfire CRC Report No. A.10.01, Melbourne, Victoria.

Cruz MG, McCaw WL, Anderson WR, Gould JS (2012) Fire behaviour modelling in semi-arid mallee-heath shrublands of southern Australia. *Environmental Modelling & Software* **40**, 21-34.

Gould JS, Cheney NP, Hutchings PT, Cheney S (1996) Prediction of bushfire spread. IDNDR Project 4/95. CSIRO Forest and Forest Products, Unpublished Report.

Gould JS, Cheney NP, McCaw l, Cheney S (2003) Effects of head fire shape and size on forest fire rate of spread. 3rd International Wildland Fire Conference, Sydney NSW, October 3-6 2003.

Gould JS, McCaw WL, Cheney NP, Ellis PE, Knight IK, Sullivan AL (2007a) Project Vesta- Fire in Dry Eucalypt Forest: Fuel structure, fuel dynamics, and fire behaviour, Ensis-CSIRO, Canberra, ACT and Department of Environment and Conservation, Perth, WA.

Gould JS, McCaw WL, Cheney NP, Ellis PE, Matthews S (2007b) Field Guide- Fuel assessment and fire behaviour prediction in dry eucalypt forest, Ensis-CSIRO, Canberra, ACT and Department of Environment and Conservation, Perth, WA.

Gould JS, McCaw WL, Cheney NP (2011) Quantifying fine fuel Dynamics and structure in dry eucalypt forest (Eucalyptus marginata) in Western Australia for fire management. *Forest Ecology and Management* **262**, 531-546.

Hsu JC (1996) *Multiple Comparisons: Theory and Methods.* Chapman and Hall, London.

Kramer CY (1956) Extension of multiple range tests to group means with unequal numbers of replications. *Biometrics* **12**, 309-310.

Lawson BD (1972) Fire spread in lodgepole pine stands. Environment Canada, Canadian Forest Service, Pacific Forest Research Centre, Victoria B.C. Internal Report BC-36. 63 pp

Luke RH, McArthur AG (1978) *Bushfires in Australia*. Australian Government Publishing Service, Canberra. 359 pp.

Mardsen-Smedley JB, Catchpole WR (1995) Fire modelling in Tasmanian buttongrass moorlands II. Fire behaviour. *International Journal of Wildland Fire* **10**, 241-253.

McAlpine RS, Wakimoto RH (1991) The acceleration of fire from point source to equilibrium. *Forest Science* **37**, 1314-1337.

McArthur AG (1959) Report on fire behaviour studies in jarrah fuel types, Dwellingup, Western Australia. Forestry and Timber Bureau, Canberra, ACT.

McArthur AG (1962) Control burning in eucalypt forests. Forest and Timber Bureau Leaflet 80, Commonwealth of Australia, Canberra, ACT.

McArthur AG (1966) Weather and grassland fire behaviour. Forest and Timber Bureau Leaflet 100, Commonwealth of Australia, Canberra, ACT.

McArthur AG (1968) The effect of time on fire behaviour and fire suppression problems. EFS Manual, S.A. Emergency Fire Services, Keswick, South Australia. pp 3-6, 8, 10-13.

McArthur AG (1967) Fire behaviour in eucalypt forests. Forest and Timber Bureau Leaflet 107, Commonwealth of Australia, Canberra, ACT.

McArthur AG (1973) Forest Fire Danger Meter MkV. CSIRO Canberra, ACT.

McCaw WL, Gould JS, Cheney NP (2008) Existing fire behaviour models under-predict the rate of spread of summer fires in open jarrah (*Eucalyptus marginata*) forest. *Australian Forestry* **71**, 16-26.

McCaw WL, Gould JS, Cheney NP (2012) Changes in behaviour of fire in dry eucalypt forest as fuel increases with age. *Forest Ecology and Management* **271**, 170-181.

Peet GB (1965) 'A Fire Danger Rating and Controlled Burning Guide for the Northern Jarrah (*E. marginata*) Forest, of Western Australia. Forests Department Western Australia, Bulletin No. 74.

Peet GB (1972) Fire studies in jarrah (*Eucalyptus marginata* Sm.) forest. M.Sc. Thesis, University of Melbourne, Melbourne.

Pyne SJ (1984) *Introduction to Wildland Fire*. John Wiley and Sons, New York, 455 pp.

Sneeuwjagt RJ and Peet GB (1979) Forest Fire Behaviour Tables for Western Australia (2nd edn). Forest Department of Western Australia.

Sneeuwjagt RJ and Peet GB (1985) Forest Fire Behaviour Tables for Western Australia (3rd edn). Department of Conservation and Land Management.

S-PLUS (2006) *S-PLUS 6 for Windows Guide to Statistics, Volume 1*. Insightful Corporation, Seattle, WA.

Sullivan AL, Knight IK (2001) Estimating error in wind speed measurements for experimental fires. *Canadian Journal of Forest Research* **31**, 401-409.

Sullivan AL, Knight IK, Hurley RJ, Webber C (2013) A contractionless, low-turbulence wind tunnel for the study of free-burning fires. *Experimental Thermal and Fluid Science*. **44**, 264-274.

Weber RO (1989) Analytical models for fire spread due to radiation. *Combustion and flame* **78**, 398-408.

Van Wagner CE (1970) On the value of temperature data in forest fire research. Canadian Forest Service Internal Report PS-20, Ontario, Canada.

Van Wagner CE (1985) Fire spread from a point source. Govt. Can., Canadian Forest Service, Petawawa National Forest Institute, Chalk River, Ont. Memo PI-4-20 dated January 14, 1985 to PH Kourtz (unpublished)

Appendix 4.1 Samples of experimental data from the laboratory

APPENDIX 4.1.1.

TIME TEMPERATURE PLOTS

Experiment Fire #1, Wind speed= 1.25 m s^{-1}, Fuel moisture content= 9.8%. Example of thermocouple output

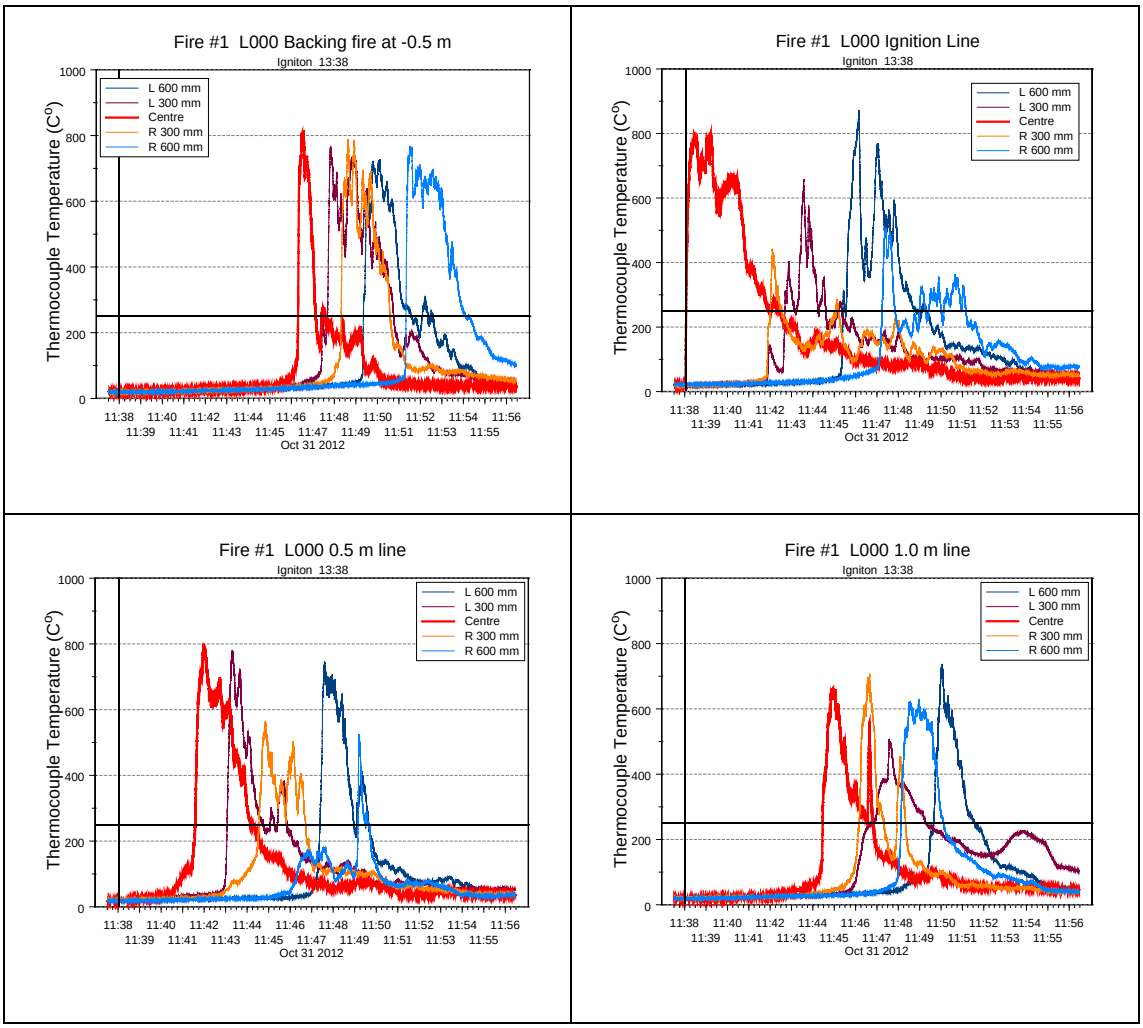

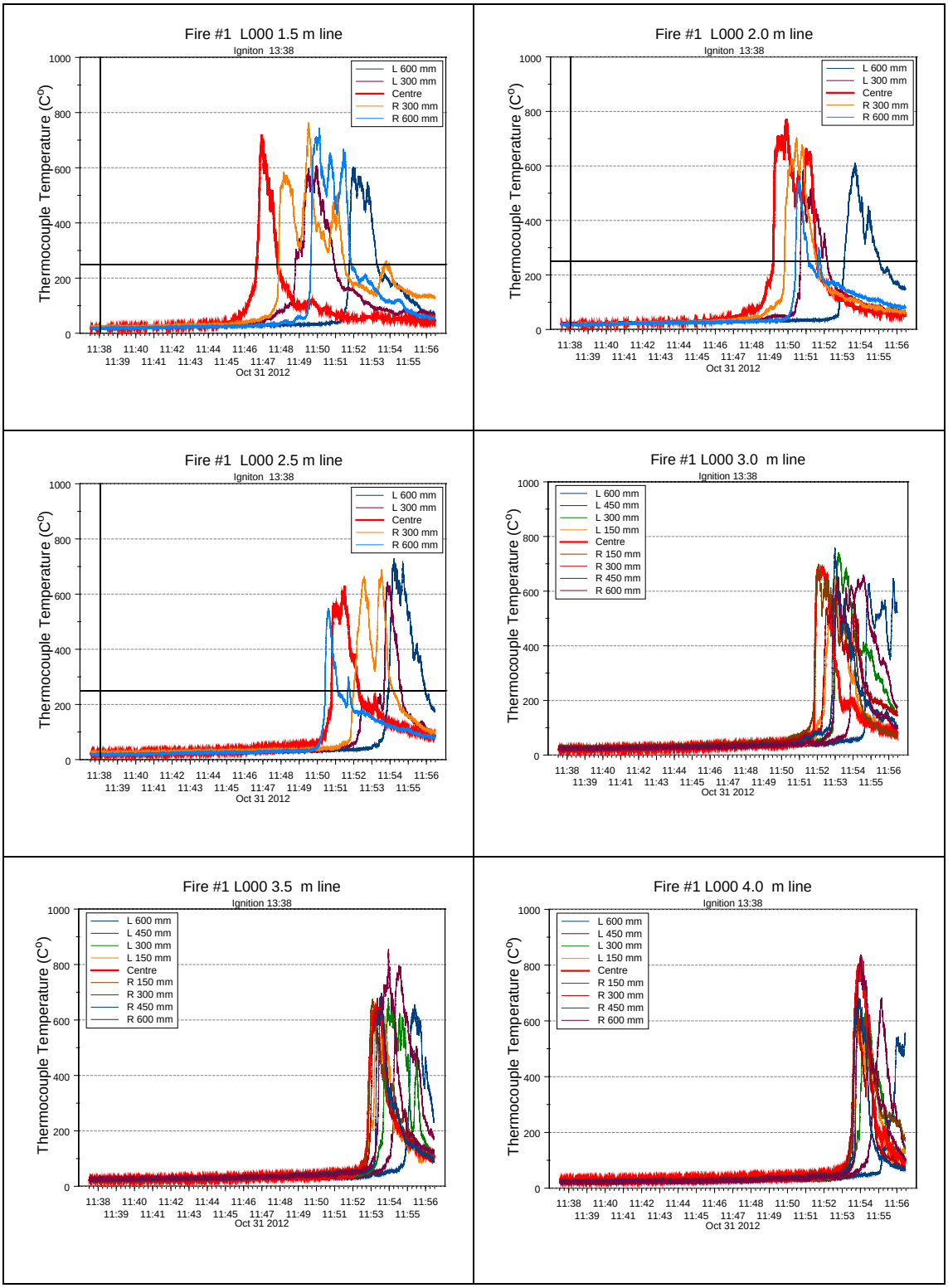
Fire #1 L000 1.5 m line
Igniton 13:38
Fire #1 L000 2.0 m line
Igniton 13:38
Fire #1 L000 2.5 m line
Igniton 13:38
Fire #1 L000 3.0 m line
Ignition 13:38
Fire #1 L000 3.5 m line
Ignition 13:38
Fire #1 L000 4.0 m line
Ignition 13:38
Thermocouple Temperature (C°)
0
200
400
600
800
1000
L 600 mm
L 450 mm
L 300 mm
L 150 mm
Centre
R 150 mm
R 300 mm
R 450 mm
R 600 mm
11:38 11:40 11:42 11:44 11:46 11:48 11:50 11:52 11:54 11:56
11:39 11:41 11:43 11:45 11:47 11:49 11:51 11:53 11:55
Oct 31 2012

APPENDIX 4.1.2.

EXAMPLE OF INFRARED CAMERA IMAGES FROM A POINT IGNITION AND 800 M LINE IGNITION FIRES

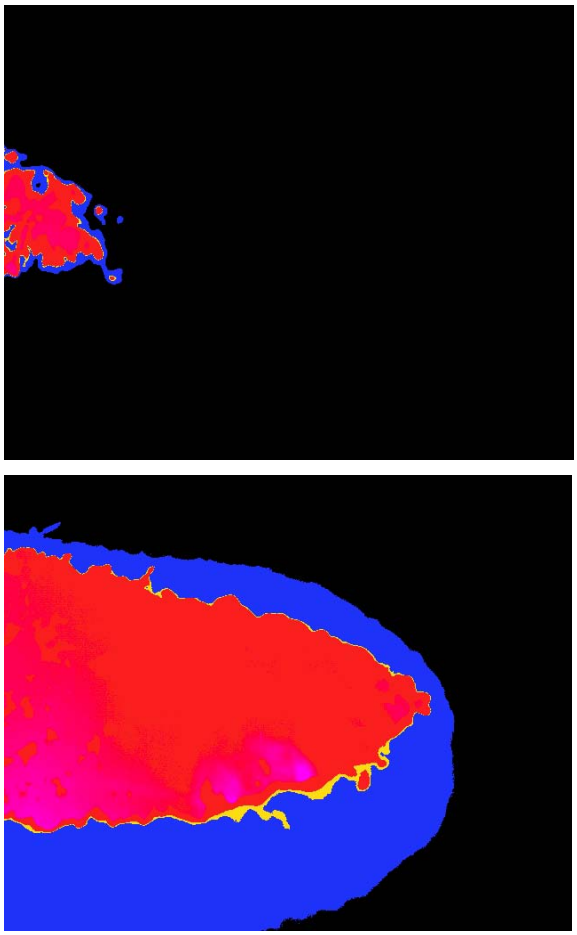

Infrared images from point ignition fire 35-L000, Top- 5 minutes since ignition, approximately at 1.5 m mark and Bottom- 7 minutes since ignition, approximately at 2.5 m mark. Temperature colour legend: Black < 250°C, Blue = 250 – 310°C, Yellow = 311 – 320°C, and Red- > 321°C.

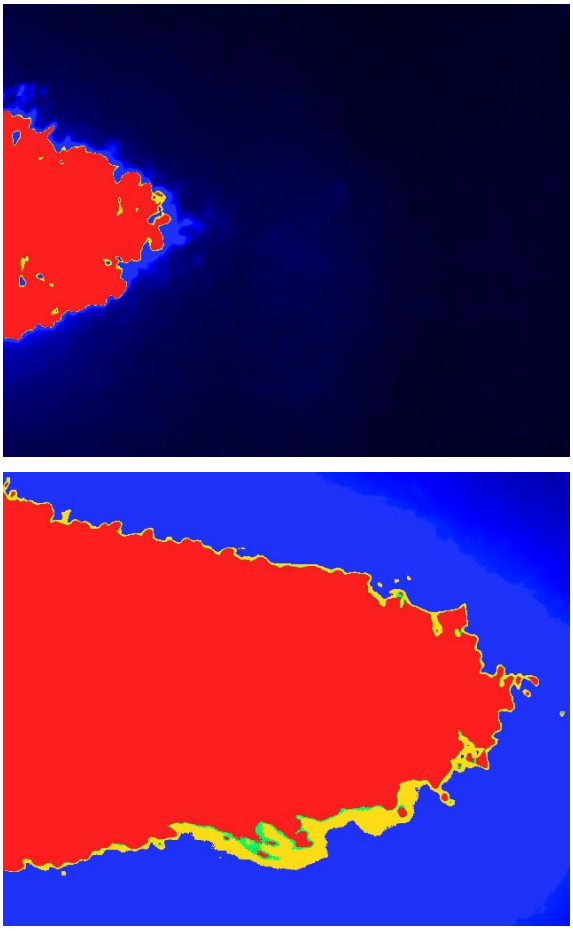

Infrared images from 800 mm line ignition fire 36-L800, Top- 2 minutes since ignition, approximately at 1.5 m mark,and Bottom- 3 minutes since ignition, approximately at 2.5 m mark. Temperature colour legend: Black < 250°C, Blue = 250 – 310°C, Yellow = 311 – 320°C, and Red > 321°C.

APPENDIX 4.1.3.

EXAMPLES OF RGB VIDEO IMAGES FROM A POINT IGNITION FIRE

Frame grab photo from the RGB video image showing the complete fuel bed in the CSIRO Pyrotron working section. The wide angle produced a much distorted image, which requires rectification before acquisition of fire behaviour data.

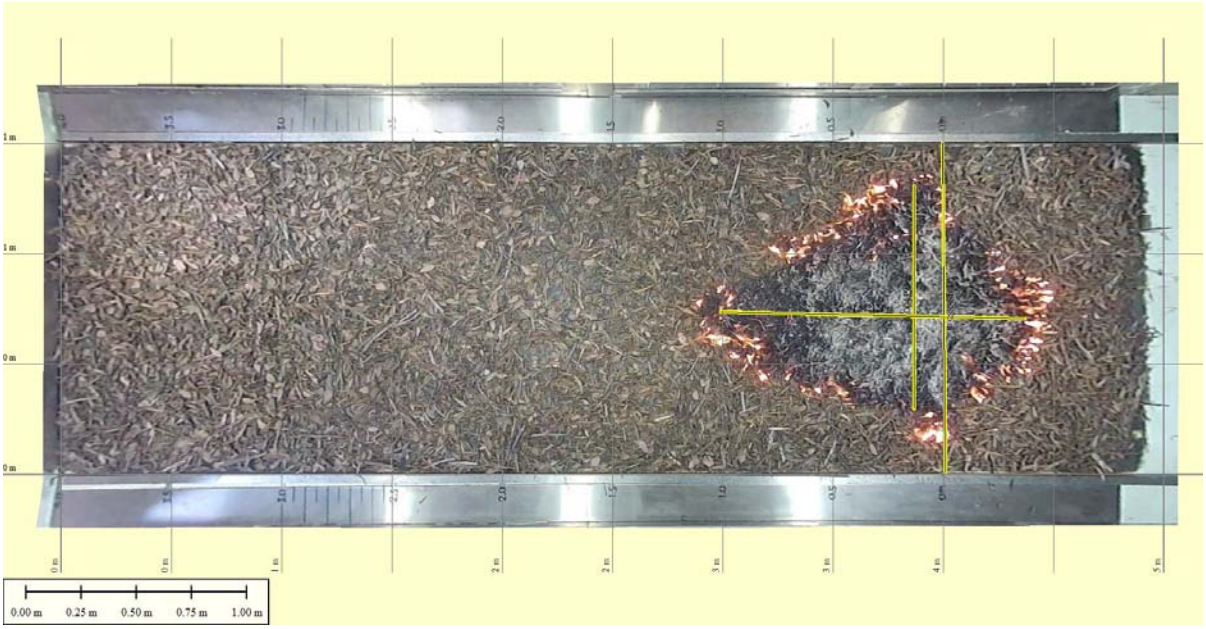

Rectification of RGB video image of a fire with length-breath measurements (1.38m and 1.00 m respectively) and ignition reference line.

Appendix 4.2 Methods Used During Experimental Fires 1962 - 1975[8]

Location and fuel type

Experiments were conducted in a wide range of fuel types:-

- Dry sclerophyll forest on Black Mountain, ACT;
- Messmate forest at Mirboo North and Daylesford, Vic;
- Alpine forest at Bulls Head, ACT;
- Plantations of Flooded gum (*E. grandis*) and Blackbutt (*E. pilularis*) at Coffs Harbour, NSW
- *P. radiata* plantations, ACT;
- *P. carabea, P. elliottii* at Burrill Lake and Coffs Harbour, NSW;
- Perennial Grasslands in ACT and at Emerald, Qld;
- Annual grasslands at Gunn Point, NT
- Wheat and Oat stubble in ACT and Southern Tablelands, NSW.

While all fires were conducted to collect rate of spread data, many had a dual purpose. Many fires in the ACT were conducted as part of a two-week field exercise for students of the Australian Forestry School as part of their fire control subject. A limited number of experimental fires were also conducted in different forest types in Victoria and NSW to instruct State researchers in experimental fire techniques in order that they could conduct further experiments and develop fire behaviour guides for specific forest types. Pretty much the same method was used in all fuel types.

Site selection and preparation

Most fires in forest types were burnt under mild weather conditions so no special preparation was required. In some areas the site was roughly divided into burning blocks to assist control of individual fires. Mostly fires were directly suppressed after the measurements were completed. Where possible, sites were selected so that slopes were positive in the direction of the prevailing wind.

The location of individual fires was such that the head fire would run up-slope from the ignition point in the direction of the prevailing wind. In some hilly locations fires were driven up-slope by a lee-slope eddy wind.

Fire Spread Measurement

Fires were lit at a point usually in a locally heavy clump of fuel or dry tussock simply for ease of ignition. The origin of the fire was located with a stake and the perimeter of fires in litter fuels was marked at 2-minute intervals; very slow-spreading fires may have been marked at 4-minute intervals, particularly during initial phases of spread so that the perimeter markers would not interfere with the spread.

Perimeter markers were made of galvanized sheet metal approximately 150 x 70 mm; on large grass fires that spread up to 1500 m from the origin the markers were 300 x 150 mm

[8] Cheney, NP. Retired CSIRO Senior Principal Research Scientist

and bent at right-angles to facilitate detection and location in the ash. Each marker was identified with the time interval in minutes since the start of the fire using yellow lumber crayon, which when heated fused with the galvanized coating and remained clearly identifiable. A marker to locate the head of the fire, defined as the fastest spreading section of the perimeter was identified with an "F" in addition to the appropriate time interval. If spotfires occurred a substantial distance ahead of the head fire the tag was identified with the time and an "S". The shape of the fire could be accurately defined using relatively few makers by alternately marking bumps and hollows at successive time intervals.

On small fires the time since ignition was recorded by a "Booker" and called the people allocated to marking to precisely place the markers at two minute intervals. One person was allocated the task of marking the position of the Head fire and was expected to place the marker precisely on the leading edge. On faster spreading high-intensity fires errors greater than ± 0.5 m were estimated and recorded by the booker and personnel were provided with face shields and protective clothing to allow approach to tall flames for marking. Personnel on the flanks used synchronized timers and carried two-way radios to be advised of the completion of the fire.

At some time after the fire the position of the each marker was surveyed using a compass and tape with reference to the origin point and not corrected for slope. The slope of the ground along the major axis of the fire, and the maximum slope of the ground, was measured with a clinometer.

Fire Behaviour Observations

The "Booker" recorded the following observations on a prepared sheet:

- Time of commencement (local time)

At the time of marking, (at 1 or 2 minute intervals) the following observations of the headfire were made:

- Flame height: estimated as the perpendicular height above ground;
- The flame length: estimated as the length of the leading edge of the flame from the ground to the tip
- Flame angle: estimated angle of the leading edge of the fire to ground ahead of the fire (flame angles >90° were flames leaning towards the burnt area.
- Flame depth: the depth of continuously flaming fuel behind the leading edge of the fire.

During the interval some or all of following observations were recorded:

- The estimated maximum height of flashes of flame;
- Colour of smoke ;
- Presence of updraughts or downdraughts and how they affected fire behaviour;
- Average flame depth over the 2-minute period of spread when this differed markedly from the observation at the time integer (such as when a lull in spread occurred);
- Fuel discontinuities (bare patches, logs) and estimates of fuel load were assigned where the fuel differed markedly from the average fuel condition for the area.
- Spot fires – estimated numbers and distance ahead of the fire.

Not all observations were possible or warranted at each interval. The fastest grass fires measured by this technique were spreading at over 6 km/h. This is a fair jogging pace and

when marking at 1-minute intervals, and allowing 15 seconds to call in the marker and record observations, people assigned to the head fire were fairly galloping and more than somewhat relieved to reach the burnt-out area that terminated the experiment.

Wind speed

Most observations of wind speed were made with a sensitive cup anemometer (initially a Cassella and later the Bradley anemometer) located at 1.5 m above the ground and within 20 m upwind of the origin. At 1 or 2-minute intervals from the time of ignition the total wind-run was recorded so that the mean wind speed could be synchronized with the measurements of fire spread. This was converted, first to average counts per minute for the interval, and later to km/hr from individual calibration charts for each anemometer.

The direction of the wind was not recorded but rather inferred from the spread of the fire.

Fuel moisture

Fuel moisture measurements were made of the following parts of the fuel bed:

- *Suspended*: standing grass or stubble; litter suspended above the surface fuel bed on low shrubs or grass; dead outer bark on occasions.
- *Tops*: the uppermost leaves on the surface layer of leaf bark and twigs of a eucalypt litter bed (or needles of a pine litter bed).
- *Full (Profile WA)*: the full depth of the litter bed from the surface layer to the duff and could include all components of the litter bed but excluding coarser twig and stick material.

Generally two grab samples of the litter layer of around 100 g were taken from areas of mottled shade, sealed in pre-numbered glass jars, weighed and oven dried at 103°C for 24 hours. Samples taken from full sunlight or heavy shade were identified as such.

Other meteorological measurements

At the time of fuel sampling aspirated wet and dry bulb readings of ambient temperature were taken with an Assman psychrometer. Temperatures reading were taken at a nominal height of 1.5 m or breast height.

These measurements determined the ambient temperature and relative humidity and were usually associated with an estimate of cloud cover in octals.

Generally a small weather station was set up on an open location near the experimental site with a Stevenson screen containing a wet and dry bulb thermometer, maximum and minimum thermometer, thermo-hygrograph and a run-of-wind anemometer at 10 m. In the ACT the weather station was based in the grounds of the Australian Forestry School at Yarralumla and the 10 m wind speeds were taken from the BoM weather station at Canberra airport. The wind speed readings at Yarralumla were unsuitable because the anemometer was located on the top of the Forestry school building at a non-standard height and the fetch interrupted by buildings and trees.

Fuel load

Prior to each fire fuel was sampled from an area visually assessed to represent the average fuel load of the area and during the course of the experiment additional samples were taken from areas visually assessed to represent high and low fuel loadings of the area. Initially samples were taken from a square wooden sample frame with an inner dimension of 2 x 2 feet. Along the inner edge of the frame the litter was cut with a sharp steel spade and all organic material < 0.25 inch diameter, including duff, was collected and stored in plastic bags to be weighed later in the laboratory. Later circular steel samplers of known area (usually 1.0 m^2) with handles and sharpened edges to cut the litter were used.

The high and low fuel loadings allowed the booker to assign a fuel load other than the average fuel load when the fire moved onto patches of obviously high or low fuel load.

At a later date the fuel samples were weighed in the laboratory and two 100 g grab samples of the contents were taken and dried at 103°C for 24 hours to determine the moisture content. This moisture content was used only to convert the fuel sample to oven-dry-weight and did not represent the moisture content of the litter at the time of the fire.

Experimental procedure

During the day a series of fires would be conducted between 0900 and 1700 hours mostly at low to moderate fire danger. Mostly each fire was terminated after 30 minutes to minimize the degree of diurnal change of moisture content during fire and a new fire commenced. Regular samples of fuel moisture were taken during the day to measure the pattern of the diurnal change of moisture. These were plotted as a running graph and the moisture content at the midpoint time of the fire was estimated for later analysis.

When the experiments were conducted as part of the forestry school field exercise, students were allocated to undertake all tasks including estimation of flame characteristics and fire behaviour under the supervision of more experienced observers (mostly McArthur and Cheney). At the end of each fire a suppression crew suppressed the fire with hand tools and mopped up as the next experimental fire was prepared. Suppression was conducted entirely by the experimental crew with hand tools, knapsacks and a trailer tanker with 400 l of water.

Data reduction

The position of the marking tags were plotted on graph paper and the shape of the fire at each time interval were interpreted by eye. The perimeter between markers at the front was interpolated assuming the head fire was elliptical in shape, while on the flanks in the absence of specific markers, it was assumed that successive perimeters would be parallel to each other.

The perimeter and area of the fire was measured and two measures of forward spread were made:

- *Maximum forward spread*: This was the maximum distance spread in each time interval. This distance was a line taken normal to the previous perimeter to the head of the fire mostly marked as the fire front. This point was not necessarily the point of the perimeter furthest from the origin.
- *Cumulative forward spread*: This was the distance measured to the point of the fire perimeter most distant from the origin. This point was usually, but not always, the part of the perimeter marked as the head of the fire.

Maximum forward spread was plotted against time since ignition. After the initial growth period and when the fire appeared to reach a quasi-steady rate of spread, the maximum forward spread for each interval was correlated with the wind speed for that interval.

Cumulative forward spread was plotted against time since ignition. After the initial growth period and the plot as linear with time the slope of the line was taken as the *cumulative rate of spread* for the fire. This value was correlated with the mean wind speed for the duration of the fire.

5 Vertical fire transition and propagation mechanisms in eucalypt forests

5.1 Introduction

A fire spreading under dry summer burning conditions within a multi-layered fuel complex, such as a dry sclerophyll eucalypt forest with a shrubby understorey, will involve different fuel layers in combustion processes. Changes in fuel structure and environmental conditions (i.e., increase in wind speed or decrease in fuel moisture) will enable the flame front to transition vertically from the surface litter layer into the shrub component and then subsequently into the overstorey fuel strata. As the fire transitions between these fuel layers, its dynamics will change considerably with possibly significant implications for fire management, namely firefighter safety, suppression effectiveness and fire impacts.

The importance of transitions between fuel layers for fire behaviour and consequent impacts cannot be overstated. As a fire transitions into a higher fuel layer there will be a stepwise increase in rate of spread and intensity. The most dramatic changes will be observed when a surface fire transitions into a crown fire. With the onset of crowning, a fire at a minimum typically doubles its spread rate in comparison to its previous state (McArthur 1965, Burrows *et al.* 1988, Taylor *et al.* 2004).

This sudden jump in the fire's rate of spread occurs as a result of (i) increased wind speeds just above the tree canopy (several times faster than understorey winds), (ii) increased efficiency of heat transfer into a taller and more porous fuel layer, and (ii) the enhanced radiant heating owing to a taller and deeper flame front. Fire transitions can also lead to an increase in spotting density and distances (Alexander and Cruz 2011).

The mechanisms of vertical fire transitions in eucalypt forests are not well understood. Although its importance in overall fire behaviour has long been recognized (McArthur 1967, Cheney 1981) no research effort has been made to specifically increase our understanding of fire transitions in eucalypt forests. A contributing factor to our lack of understanding of this key fire dynamics process has been the difficulty of conducting experimental fires under the burning conditions where fire escalates from a surface fire to a fire involving bark and overstorey canopy fuels. Our quantitative knowledge of fire behaviour in eucalypt forests is restricted to the bottom 10% of the potential fire intensity scale (Cheney 1991).

The main objective of the current project is to increase our understanding of the factors and mechanisms involved in vertical fire propagation between (1) surface / near-surface and elevated fuels; (2) surface / near-surface / elevated and bark fuels; and (3) understorey and overstorey fuels. The objective of the this chapter is to introduce a conceptual description of the propagation mechanisms driving fire transitions in eucalypt forests.

5.2 Fire transitions in dry eucalypt forests

Dry sclerophyll eucalypt forests encompass a broad range of vegetation types. Common traits are the presence of a dominant tree layer, seldom exceeding 30 m in height, a canopy cover higher than 30%, and a diverse understorey of small trees, shrubs, sedges or grasses. As a fuel complex, the eucalypt forest presents multiple fuel strata. Gould *et al.* (2011)

presented a stratification of fuels into five layers. From the bottom up these are: (1) surface fuel, (2) near-surface fuel; (3) elevated fuel; (4) intermediate tree and canopy; and (5) overstorey tree and canopy. This stratification is based on the role each layer plays in fire propagation.

5.2.1 FIRE TRANSITIONS BETWEEN UNDERSTOREY FUEL LAYERS

The surface fuel layer is comprised of litter components horizontally layered on the forest floor. Although this layer possesses the highest fuel quantity of all the layers, its compactness (bulk density around 50 – 60 kg m^{-3}; Cheney 1981) restricts its contribution to the fire overall rate of spread (McArthur 1967). The near-surface fuel layer (composed of grasses, sedges, low shrubs and collapsed understorey plants) and the elevated fuel layer (composed mostly of tall shrubs) provide a medium of typically low to moderate fuel quantity but high heat transfer efficiency (Fig 5.1). As a fire is supported by the near-surface and elevated fuels, the flame front extends its three dimensional component. The turbulent flame motion in this fuel layer enables increasing direct flame contact with unburned fuels and faster rates of spread (Cheney 1981, Nelson and Adkins 1988, Burrows 1994).

The surface fuels are still essential to maintaining a deep flame front but the propagation of the ignition interface is largely determined by the processes occurring in the tallest fuel layer involved in flames (Fig. 5.2). This conceptual model of fire spread was introduced in a modelling framework by Bevins (1979) and first suggested for eucalypt forests by Cheney (1990). It considers that distinct fuels have distinct contributions to fire behaviour. Some fuel bed components contribute to the forward movement of the flame front whereas combustion of other fuel components do not contribute to forward heat fluxes but have a strong contribution to upward heat fluxes and ignition of bark and overstorey fuels (Burrows 1999). The fuel structure in Fig. 5.2 is hypothetical and assumes all fuel layers are present and in quantities that provides them with an active role on fire propagation. As an example, in eucalypt forests dominated by gum and ironbark species bark effect on fire propagation will diminish.

Figure 5.1. Medium intensity surface fire spreading in surface, near-surface and sparse elevated fuels in dry sclerophyll jarrah (*E. marginata*) forest. Photo from Project Vesta, Gould *et al.* (2007a).

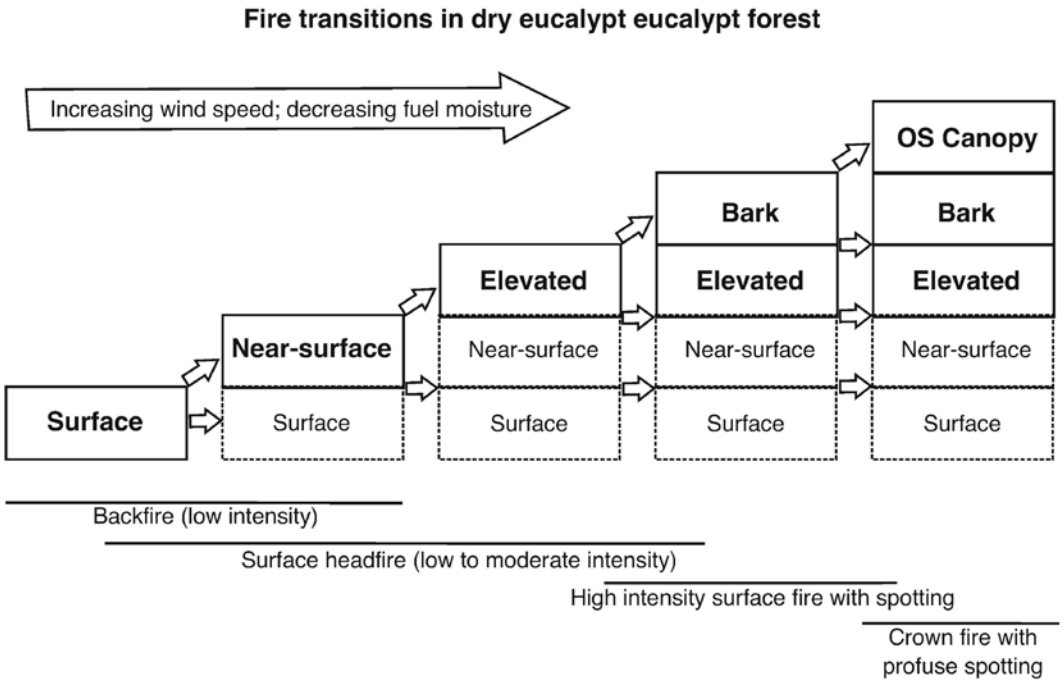

Figure 5.2. Schematic of fuel layers involved in the combustion process as the fire transitions into higher layers with associated fire type. Fuel layers in bold indicate fuels driving fire propagation. Dashed boxes indicate fuel layer with secondary contribution to forward fire propagation. Diagram considers an ideal fuel complex with all fuel layers present in sufficient quantities to affect fire behaviour.

The stepwise increase in rate of spread that occurs when fire transitions from the surface layer to the shrub component is illustrated in Fig. 5.3 (adapted from McArthur 1967). The magnitude of the increase in the fire rate of spread depends on a multitude of factors linked to stand structure, fuel distribution and burning conditions (e.g., fuel moisture content, wind speed). Key determinants are the vertical continuity between separated fuel layers, the height, density and amount of the shrub fuel component and the within-stand wind profile.

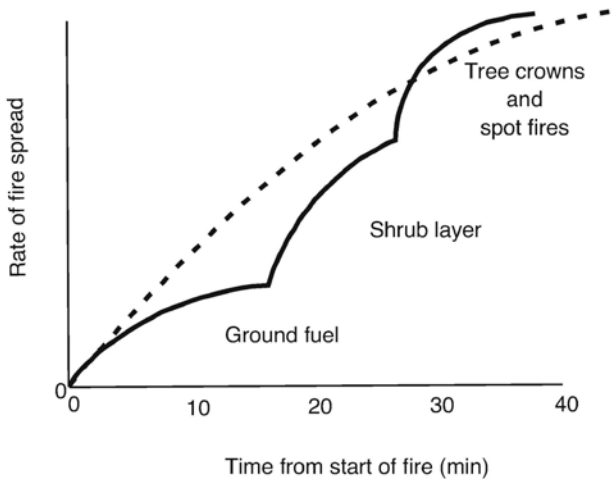

Figure 5.3. Stepwise increase in rate of spread as distinct fuel layers are involved in combustion processes. Conceptual diagram adapted from McArthur (1967).

Table 5.1, derived from qualitative descriptions of fire propagation carried out by fire researchers (McArthur 1967, Cheney 1981, 1990; Burrows 1999), summarises some key aspects of fire spread dynamics in eucalypt forests with emphasis on the fuels and fire

spread mechanisms driving propagation. The information in Table 5.1 is not based on definite measurements or hypothesis testing.

One can expect that the quantitative criteria for crown combustion and sustained propagation described by Van Wagner (1977) will be applicable to understorey fire transitions (see Catchpole 1987, Scott 2008). Van Wagner's (1977) theory considers that vertical transition of the fire between two separate fuel layers will occur when the energy released by combustion of the lower layer reaches a threshold value (largely determined by the vertical distance between the two fuel layers and the combustibility of the upper layer fuels). If the threshold value is exceeded, upper fuel layer ignition will occur and the fire will pulsate into the higher fuel layers.

Sustained fire propagation through the upper fuel layer will occur only if the amount of fuel being volatilised in this layer is enough to maintain a critical forward heat flux that will allow the formation of a contiguous flame front. If this is the case, the rate of spread will then be determined by the upper layer fuels. If the fuel bulk density is below a certain threshold, for example when this layer is made up of scattered shrubs, the fire will involve the layer but the control of the rate of spread is intimately coupled with the lower fuel layer characteristics (e.g., Burrows 1999).

5.2.2 UNDERSTOREY – OVERSTOREY FIRE TRANSITIONS

As with understorey fire transitions, the onset of crowning leads to substantial increases in the rate of fire spread and fireline intensity, albeit larger and more abrupt than between understorey fuel layers. Most dry eucalypt forests have fairly open canopies (McArthur 1967, Gill 1997) that allow the development of an understorey layer of dominated trees, shrubs and/or herbaceous vegetation.

The presence of fibrous bark provides further connectivity between the understorey and overstorey fuel layers (Fig. 5.4). Fibrous bark particles are easily ignited and dislodged allowing simultaneously for vertical fire propagation and profuse spot fire ignitions. Nevertheless, under the conditions that allow the transition from a surface to a crown fire, the spotting process becomes the dominant process in fire propagation in eucalypt forests (McArthur 1967; Luke and McArthur 1978).

In contrast to high intensity fires in conifer forests where propagation is driven by the direct heat output from the flame front in the crowns, high intensity fires in eucalypt forests are typically driven by short to medium range spotting. Nevertheless, ignition and combustion of the upper layers of the fuel complex (e.g., live foliage and upper bark) contributes to the firebrand generation and transport mechanisms that influence spotting distribution, i.e., density and transport distance. As such crowning and spotting are intimately linked in high intensity fire propagation in eucalypt forests.

No specific research into the conditions that lead to crown fire initiation in eucalypt forests has been reported in the literature. High surface fuel load availability, acute fuel dryness, likely below 7% fuel moisture content, and vertical fuel continuity are considered predisposing conditions for the onset of crowning (McArthur 1967, Luke and McArthur 1978; McCaw *et al.* 1988, Catchpole 2002) but little is known.

McArthur (1973) provides a rule of thumb that crown fires occur in dry eucalypt forests when flame heights are greater than 14 m (Fig. 5.5). McArthur's (1967) flame height (h_F; m) model was converted into equation form by Noble *et al.* (1980) as a function of rate of fire spread (*R;* here in m min^{-1}) and fuel load (*w;* here in kg m^{-2}):

$$h_F = 0.78 \cdot R + 2.4 \cdot w - 2.0 \qquad [5.1]$$

Table 5.1. Fire spread dynamics in eucalypt forests

TYPE OF FIRE	SURFACE BACKFIRE	SURFACE HEADFIRE	WHOLE FUEL COMPLEX	HIGH DENSITY SPOTTING / WHOLE FUEL COMPLEX
Definite features	Small flame	Understorey fuels in flames; Ignition of tree trunks	Short range spotting Crown fire behind leading edge of flame front	Concentrated, high density medium range spotting / spot fire coalescence.
Fuels driving propagation	Litter Near-surface	Litter Near-surface Elevated bark	Litter Near-surface Elevated Bark Crown	Litter Near-surface Elevated Bark Crown
Threshold conditions	Moisture content <12%	Moisture content <12%	Moisture content <7%	Moisture content < 5% Average open wind speeds > 50 km h^{-1}
Fire spread mechanisms (by order of importance)	Radiation within fuel bed Flame contact	Advection Flame contact radiation	Short range, high density spotting, Advection Flame contact Radiation	Short range, high density spotting, Advection Flame contact Radiation
Intensity class (kW/m)	10 - 300	300 - 5000	5000 - 40000	>30000

Figure 5.4. Transition between surface and crown fire spread in dry sclerophyll jarrah (*E. marginata*) forest. Image illustrates the importance of understorey shrub vegetation and bark fuels on the onset of crowning. Photo from Project Vesta, Gould *et al.* (2007a).

Figure 5.5A provides a graphical representation of this relationship. For a typical eucalypt forest fuel load between 1 and 2 kg m^{-2}, rates of forward spread between 14 and 18 m min^{-1} are required to sustain crown fire propagation. Assuming that all fuel would be consumed in flaming combustion, this would suggest a critical fireline intensity between 5000 and 8000 kW m^{-1} for crown fire propagation. This rule of thumb does not consider any explicit measure of vertical fuel continuity. Possibly McArthur assumed a general condition of a multilayered understorey with a ladder fuel component providing an "ideally distributed fuel complex for crown fire formation" (Luke and McArthur 1978). Cheney (1981) suggested critical intensities for crowning in low forest types between 3000 and 7000 kW m^{-1}; above 7000 kW m^{-1} crowning is expected to occur in most eucalypt forest types. Fig 5B illustrates the relationship between the onset of sustained crown fire propagation and the Forest Fire Danger Index.

It is important to note that these functions aim to describe crown fire propagation, i.e., there is an element of forward propagation as opposed to vertical propagation as observed in isolated torching. Vertical fire propagation in the form of isolated torching is expected to occur under lower intensities. The model indicates that when flame heights are above 14 m, sustained crown fire propagation is established.

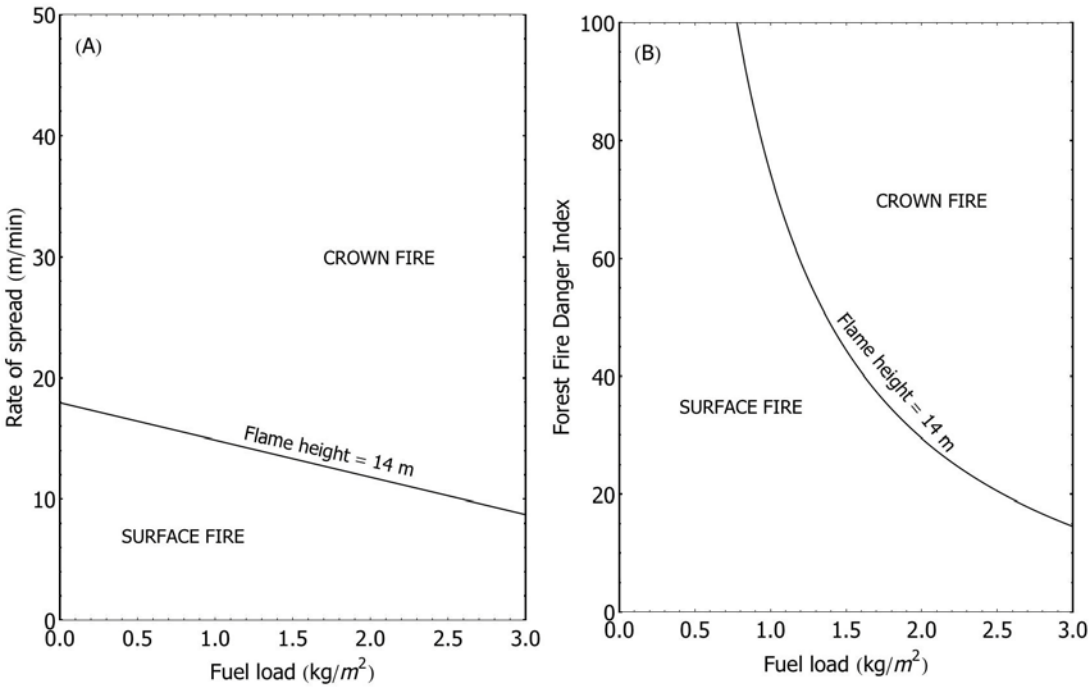

Figure 5.5. Representation of McArthur (1973) rule of thumb for crown fire propagation as a function of (A) rate of spread and fuel load; and (B) Forest Fire Danger Index and fuel load.

5.2.3 FIRE TRANSITIONS IN AUSTRALIAN FIRE SPREAD MODELS

Models developed to predict rate of fire spread in dry eucalypt forests (McArthur 1967, Sneeuwjagt and Peet 1998, Gould *et al.* 2007a, Cheney *et al.* 2012) do not explicitly model the effect of fire transitions into higher fuel layers on overall fire spread. As with other models of surface fire propagation there is an implicit assumption of uniformity of fuel bed characteristics. The treatment of distinct understorey fuel layers is different in the three models used operationally in Australia to predict wildfire behaviour.

The McArthur Mk 5 Forest Fire Danger Meter (McArthur 1967) was developed on the assumption that the quantity of surface (litter and duff) fuels was directly proportional to the rate of fire spread. Although this model does not explicitly consider near-surface, elevated and bark fuels as input, surface fuel load is a surrogate of time of fuel accumulation in its empirical formulation (i.e., time since fire or other disturbance). As fuel quantity within distinct layers is correlated (Gould *et al.* 2011), surface fuel quantity can be a proxy for overall fuel bed structure for fire behaviour estimation purposes.

The Forest Fire Behaviour Tables for Western Australia (Sneeuwjagt and Peet 1998) takes into account the contribution of all understorey fuel layers, excluding bark, as an input. The model considers the contribution of near-surface (trash) and shrub (scrub) fuels by adding their quantity to the surface fuel load in order to calculate the available fuel quantity, which is directly proportional to rate of fire spread (Beck 1995).

The Dry Eucalypt Forest Fire Model (DEFFM, Gould *et al.* 2007a,b, Cheney *et al.* 2012) considers separately the effect of surface and near-surface fuel layer structure as an input. Although not explicitly considering the elevated fuel layer as an input, the effect of this fuel layer in the rate of fire spread is implicit in this empirical model as the structure of the near-surface and elevated layers are significantly correlated (Gould *et al.* 2011).

The assumption of fuel bed uniformity described above is common in operational surface fire spread models developed throughout the world (Cheney *et al.* 1998, Rothermel 1972, Forestry Canada Fire Danger Group 1992). To overcome the limitation of the vertical uniformity assumption, Bevins (1979) and Kessel (1979) suggested a multi-strata fuel bed description. In this approach the distinct fuel layers were described separately with a specific fuel load, compactness, surface area to volume ratio and moisture content. The fire would then be assumed to spread first through the most flammable layer, i.e., the layer with the maximum spread rate, with the overall rate of spread determined by this layer. The fuel layer driving the fire would serve as the ignition source to the other fuel strata.

Figure 5.6 contrasts the behaviour of a conceptual model incorporating the multi-strata approach of Bevins (1979) with a model that considers a single fuel bed with average structure. The simulation for the multi-strata fuel bed assumes that as the mid-flame wind speed increases there is a build-up of intensity that allows the fire to jump into the higher fuel layer. The Bevins and Kessell conceptual approach does not explicitly model when a fire will attain an intensity that would allow it to transition to the upper layer. When their fire modelling approach was developed no models describing the vertical fire propagation between fuel layers existed.

5.3 Approaches to fire modelling

Fire behaviour modelling can be empirical or physical (or theoretical) or combination of both (Catchpole and de Mestre 1986, Pastor *et al.* 2003). Empirical models are based on the relationship between the response variable and explanatory variables without explicitly considering the controlling physical processes (e.g. Cheney *et al.* 1998, Fernandes *et al.* 2000, Cruz *et al.* 2004; Sullivan 2009a). The *reason d'être* for this model is largely to support a decision making process.

Physical models encode the equations that describe the fundamental physical processes as they apply to fire. These models attempt to describe fire phenomenology by numerically solving a set of equations describing the local conservation of mass, momentum, energy and species for the system (Grishin and Perminov 1991, Grishin 1997, Linn 1997, Morvan and Dupuy 2001).

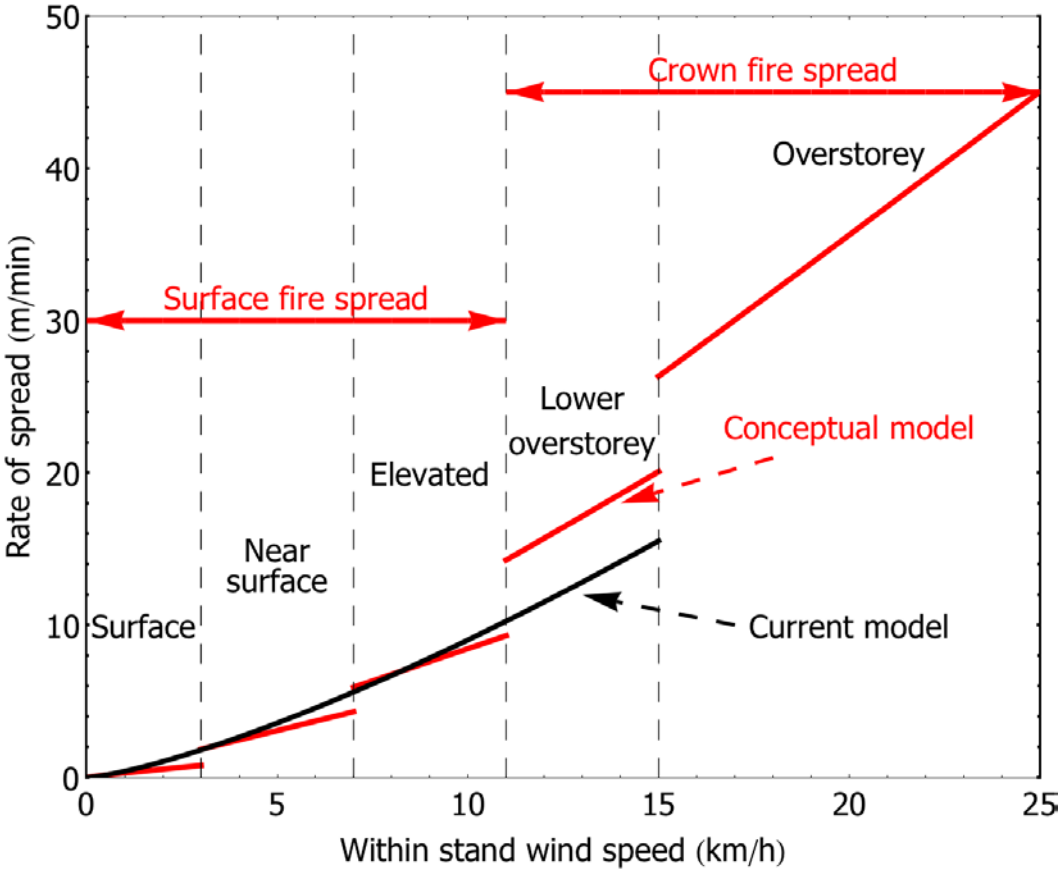

Figure 5.6. Conceptual model of steady state rate of spread in multistorey eucalypt fuel complexes with discontinuities in fire spread as function of fuel determining fire propagation.

The comprehensiveness that physical based models describe the full fire behaviour environment varies widely (see Sullivan 2009b), with their essential differences being in the way they treat combustion and heat transfer processes in the solid and gas phases, and consequently the demands upon empiricism. One of the main constraints for such an approach to be successful is our lack of understanding of the fundamental thermodynamic properties of a combustion zone and its surroundings. Representative measurements of flame radiometric characteristics and fire-derived fluid temperatures and velocities are rare (e.g., Butler *et al.* 2004, Cruz *et al.* 2011, Catchpole *et al.* 2010). This lack of fundamental heat transfer and fuel ignition data has been a hindrance to our improvement of physics-based models and has even limited our understanding of laboratory fires (e.g. de Mestre *et al.* 1989, Catchpole *et al.* 2002, Pagni *et al.* 2005). Physical models are best seen as providing better insight into the processes involved than as models developed for predicting outcomes.

A possible vehicle to improve our understanding of high intensity fire behaviour in eucalypt forests is to construct a solid physical understanding of the processes driving fire propagation. In this chapter we develop a physical formulation for fire spread in eucalypt forests by considering different understorey fuel layers and solving a set of energy balance equations for upward and horizontal energy transfer. The model system is constructed on a modular framework where the key sub-model components used represent a compromise between the best understanding of the processes at hand, the variability of the process and the need for relatively rapid computational speeds. This approach allows (1) for the model to be used in faster than real-time system simulation tools; and (2) to enable implementation of improved formulations of specific processes as our fundamental understanding of fire

behaviour advances. The model framework also allow us to identify critical knowledge gaps where future research should focus to further improve our capability to produce more accurate forecasts of fire propagation and behaviour in eucalypt forests.

5.4 Model framework

The model framework presented here is based on a simplified energy balance of unburned fuels and takes into account as main processes (1) the energy released through combustion processes, (2) flame structure, (3) the structure of the buoyant plume, and (4) radiative and convective (advection and flame contact) energy transfer.

The model framework describes fire propagation based on the following key assumptions:

1. The flame front movement is described by the propagation of a uniform ignition isotherm that spreads at a steady rate of advance;
2. The fuel complex is described by a number of fuel layers of homogeneous characteristics, e.g., compactness, load, surface area to volume ratio, and fuel moisture content.
3. The combustion wave propagates by igniting thermally thin (i.e., temperature is approximately uniform while it is being heated) fuel elements located at the top of the fuel layer (Cheney 1990);
4. Other fuels, such as fuels located within the fuel bed and fuels with higher thermal inertia, are assumed to ignite within the combustion zone; they contribute to the flame development and, to a lesser extent, to fire spread;
5. Ignition temperature is assumed to be 600 K. After the fuel particle passes the ignition isotherm, the exothermic combustion process consumes it.

The spread rate of a fire propagating in a multilayered fuel complex will be largely determined by the combustion processes of the layer exhibiting the most efficient heat transfer, faster reaction velocity and meets a critical mass flow rate to allow flame development. As such, the rate of spread is not directly related to the overall average fuel characteristics but to a large degree dependent on the physical structure of the most flammable fuel layer.

The best example of this rationale is a propagating active crown fire involving the full fuel complex (as per Van Wagner (1977)). The rate of spread of this fire is largely determined by the heat transfer and combustion processes in the canopy fuel layer, although the crown fire phase still depends in part on the combustion of the surface fuels to maintain the overall rate of fire spread.

Our modelling approach considers an iterative process calculating forward and upward energy fluxes to determine which fuel layer (e.g., surface, near-surface, elevated or overstorey) is responsible for sustaining propagation. A first step calculates forward rate of spread through an energy balance of the lowest fuel layer (Fig 5.2). Output from this calculation is used to estimate the ignition of the fuel layer located above it. If this fuel is ignited, the process is repeated until we determine which layer is dominating fire propagation, i.e., the uppermost layer that provides the critical energy flux for the sustained propagation of the combustion wave. The model output is the rate of fire spread determined for this fuel layer with contribution of the combustion of all fuels below.

The horizontal movement of the flame front is calculated from an integrated energy balance based on the conservation of energy principle:

$$-R\,\zeta\,\rho_b\,\frac{dQ}{dx} = q$$

where R is the rate of fire spread, ζ is the proportion of fuel heated to ignition temperature during preheating, ρ_b is fuel bulk density, Q is the fuel enthalpy, and q'' is the net heat flux into the fuel element. Considering that the rate of temperature rise in the fuel element (dT/dt) is related to the rate of heat absorption (dQ/dt) we have:

$$-R\frac{dQ}{dx} = -Rc^*\frac{dT_f}{dx} \qquad [5.3]$$

with x being the direction of fire propagation in the coordinate system, T_f the temperature of the fuel particle and c^* the average specific heat (see Eq. 5.10 below). Equation [5.3] can be integrated as:

$$-R\,\zeta\,\rho_b\,c^*\frac{dT_f}{dx} = \int q$$

ones (e.g., flame height and angle, flame temperature profile, residence time) while others were developed particularly for the needs of this project.

5.5.1 FUEL PARTICLE HEATING

Fuel heating assumes that the net energy gained or lost by a fuel particle equates to its internal energy, hence its temperature. The heat required to bring a unit mass of fuel from ambient (T_a) to ignition temperature (T_{ig}), Q_{ig}, takes into account the specific heat value of the fuel (c_f) and water (c_w), the latent heat of vaporization of water (L) and fuel moisture content (m). A common approach to calculate Q_{ig} considers a three-step heating model (see Albini 1985, de Mestre 1989, Mell *et al.* 2007) treating the heating and boiling off of fuel moisture with:

$$dQ = \begin{cases} (c_f + m\, c_w)dT, & T < 373 \\ -Ldm, & T = 373 \\ c_f dT, & 373 < T < T_{ig} \end{cases} \qquad [5.8]$$

A number of experiments where fuel particle temperature is measured from ambient to ignition temperature does not reveal a step behaviour for dead fuels (Picket *et al.* 2010) but hence a continuous increase in temperature (e.g., de Mestre *et al.* 1989, Picket *et al.* 2010). To capture this continuous evolution of fuel particle temperature Catchpole and Catchpole (2000) proposed a linear relationship between heat input and temperature:

$$dQ = c^*\, dT \qquad T_f < T_{ig} \qquad [5.9]$$

This approach relies on the use of an average specific heat value that incorporates the variables of Eq. [5.8]:

$$Q_{ig} = c^* \left(T_{ig} - T_a\right) = \left(c_f + m\, c_w\right)(373 - T_a) + (m\, L) + c_f \left(T_{ig} - 373\right) \qquad [5.10]$$

This formulation assumes that moisture is continually being evaporated from ambient to ignition temperature and that all moisture must be driven out before ignition takes place. It is worth noting that Picket *et al.* (2010) observed a plateau in fuel surface temperature in laboratory experiments with moist foliage (live fuels) between 500 and 600 K.

The distinction between the three-step and the linear or average c_p approach is relevant when one considers convective heat transfer and radiative cooling. The convective heat flux depends on the difference in temperature between the element surface and the surrounding fluid. Because the three-step model maintains the fuel surface at a lower temperature for a substantial period of time, convective heat transfer is over-predicted. Furthermore, the three-step approach reduces radiative cooling. Overall the three step function will always predict fuel ignition earlier than the linear approach (Fig. 5.7).

The radiative cooling of the particle is described by the net radiative heat transfer between the fuel particle and the surroundings.

$$q_l = F_{23} \cdot A_f \cdot \sigma_{SB} \cdot \varepsilon \cdot \left(T_f^4 - T_a^4\right) \qquad [5.11]$$

The view factor between the fuel particle and the surroundings, F_{23}, is calculated from the application of the reciprocity relation and the summation rule (Incropera and DeWitt 2002):

$$F_{23} = 1 - \frac{A_p}{A_F} F_{12} \qquad [5.12]$$

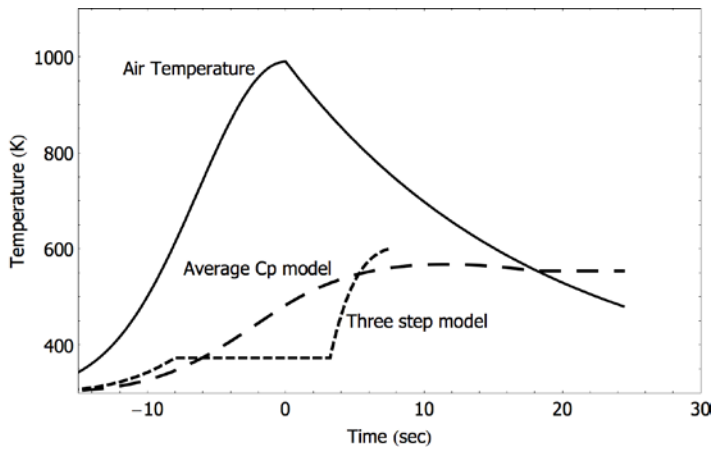

Figure 5.7. Air and calculated fuel particle temperature for the average C_p (Eq. 5.9) and 3-step model (Eq. 5.8). Fixed conditions are air velocity = 2 m s^{-1}; FMC = 130%; σ = 5900 m^{-1}.

5.5.2 HEAT TRANSFER MECHANISMS – FORWARD PROPAGATION

Radiative heating

Radiative heating is modelled by separating the radiation emanating from the free flame from the combustion zone. The free flame is modelled as an opaque surface of finite length and width. The radiant energy flux (E_F) leaving the flame surface is given by integrating the radiative intensity, obtained from the Stefan-Boltzmann equation, over the flame surface:

$$E_F = \int_0^{H_F} \int_0^{W_F} \varepsilon\, \sigma_{SB}\, {T_F}^4\ (x)\, dxdy \qquad [5.13]$$

where ε is the flame emissivity; T_F is the flame temperature and H_F and W_F are respectively the flame height and flame width. To account for the changes in radiosity with flame height (Butler 1994, Butler *et al.* 2004, Wotton *et al.* 1998, Cruz *et al.* 2011) the flame radiometric temperature is assumed to decrease with distance from the flame tip. Assuming a maximum radiosity of 150 kW m^{-2} at the flame base corresponding to an approximate nominal maximum radiometric temperature of 1273 K, the flame vertical radiative profile is given by (Wotton *et al.* 1998):

$$I(z, H_F) = 150\left(1 - e^{-0.75\,(H_F - z)}\right)^{2.89} \qquad [5.14]$$

This radiometric temperature assumption implies a flame depth effect on the radiosity profile. This allows us to assume the flame is a two-dimensional radiating surface instead of requiring the more computationally intensive calculation of the radiating flux from a 3D radiating volume. Radiation from the combustion zone assumes the combustion interface to be a plane with a constant radiometric temperature equal to the temperature at the base of the free flame. i.e., $T_F(z = 0)$.

The view factor represents the fraction of the uniform diffuse radiant energy leaving a surface that is incident upon another surface. The general expression for the view factor (F_{12}) between arbitrarily oriented surfaces is (Modest 1993):

$$F_{12} = \frac{1}{A_1} \int_{A_1} \int_{A_2} \frac{\cos\theta_1\, \cos\theta_2}{\pi\, S^2}\, dA_2 dA_1 \qquad [5.15]$$

where A_1 and A_2 are the surface areas of the emitter and receptor, respectively, S is the distance between the infinitesimal surface elements dA_1 and dA_2, and θ_1 and θ_2 are the angles formed between S and the surface normal.

Radiative heat transfer into the unburned fuel can consider this fuel as an individual particle or as a control volume representative of a fuel agglomerate with fuel particles randomly distributed. For the present study we model heat transfer into the surface of a fuel particle. By considering the simplifying assumption that radiative heat transfer will be most effective to the fuel particle section that is parallel to the flame sheet we consider the view factor between two finite areas with unequal dimensions. For this geometric configuration the radiant heat flux received at the surface of a fuel element is (Wotton *et al.* 1998):

$$I_{12} = \int_{-W_F/2}^{W_F/2} \int_0^{H_F} \frac{150\left(1-e^{-0.75\,(H_F-z)}\right)^{2.89} x\,z}{\pi\,(x^2+(y-y^2)+z^2)^2}\,dz\,dy \qquad [5.16]$$

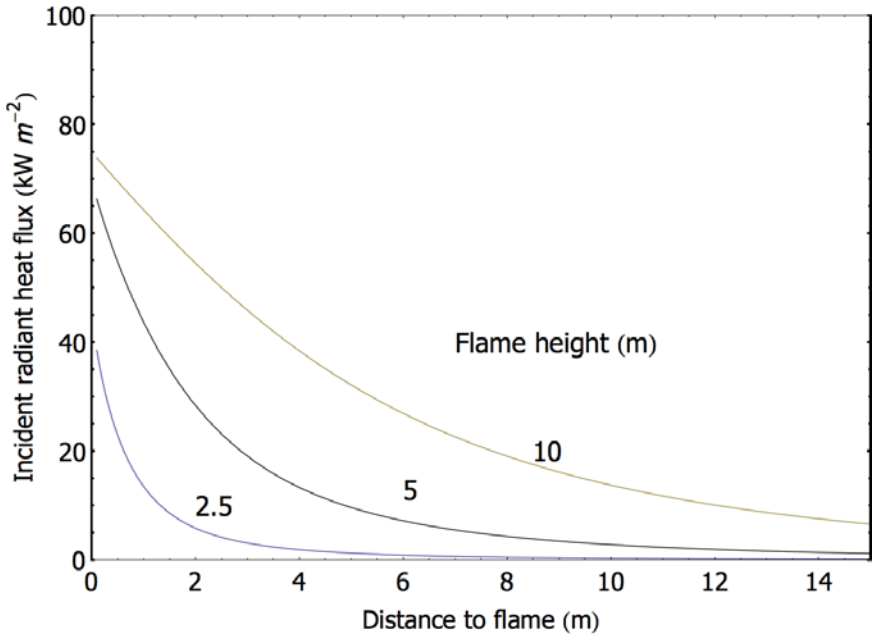

Figure 5.8. Variation in incident radiative heat flux at the top of the fuel bed with flame height and distance from the flame. Calculation from Eq. 5.16 assuming a flame width of 30 m.

The radiation from the combustion zone is reduced due to the attenuation of radiant energy while the radiation travels through the absorbing porous medium consisting of the fuel bed. An exponential decay function incorporating the radiation absorption coefficient is used to account for the contribution of fuel particles in reducing the mean path length. The radiation absorption coefficient is (Committee on Fire Research 1961):

$$\alpha = \frac{\sigma_S\,\beta_S}{4} \qquad [5.17]$$

where σ_S is the representative surface area-to-volume ratio, and β_S is the fraction of the fuel bed filled with matter.

The calculation of the radiative energy absorbed by a fuel particle (q_r) considers only half the area of the fuel particle (i.e. that exposed to flame):

$$q_r = I_{12}\frac{A_f}{2} \qquad [5.18]$$

where A_f is the fuel particle surface area.

Knowledge of flame height (H_F) and flame tilt angle (A_F) are required to solve the preceding equation. Nelson *et al.* (2012) formulates models for flame height and tilt angle based on Albini's (1981) simplified flame height model and physical considerations. The base of the flame coincides with the top of the fuel bed. This assumption is based on the theory that

above the fuel bed mixing of the fuel volatiles with air will approach an optimum (Albini 1981; Dupuy *et al.* 1998). For a combustion regime with a convection number (N_C) less than 10:

$$H_F = \frac{0.0035\, I_B}{U_S} \qquad [5.19]$$

$$\tan A_F = 1.041\, N_C^{-0.334} \qquad [5.20]$$

Alternatively, for a combustion regime with $N_C > 10$

$$H_F = \frac{0.0024\, I_B}{U_S} \qquad [5.21]$$

$$\tan A_F = 4.119\, N_C^{-0.667} \qquad [5.22]$$

where N_C is the convection number (Nelson 1993):

$$N_C = \frac{2\, g\, I_B}{\rho_a\, c_p\, T_a\, u_a^3} \qquad [5.23]$$

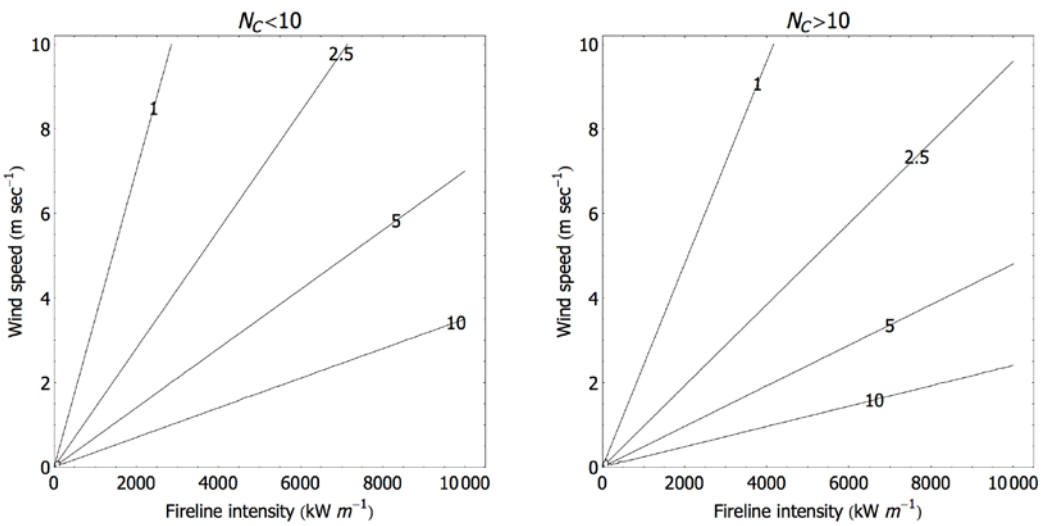

Figure 5.9. Contour plots of flame height as a function of fireline intensity and wind speed (Nelson *et al.* 2012). Left graph is applicable to an environment with a convection number (N_C) lower than 10. Right graph is for N_C larger than 10.

Convective heat transfer

The forced flow of air passing over a fuel particle will cause heat exchanges between the surface of the fuel element and the surrounding fluid. Convective heat transfer is typically divided into (1) advective, heating or cooling, occurring prior to the arrival of the flame front; and (2) flame contact (Pagni and Peterson 1973; Baines 1990). The flickering or transient nature of a free spreading turbulent diffusion flame makes it exceedingly difficult to separate these two processes and for practical purposes they are not formally separated. Convective heat transfer (q_c) to a fuel particle surface is given by:

$$q_c = h_c\, A_f\, (T_g - T_f) \qquad [5.24]$$

where h_c is the average convective heat transfer coefficient, T_g is the gas temperature and T_f is the fuel particle surface temperature. The convective heat transfer coefficient is correlated with the Nusselt (N_u) and Reynolds (R_e) dimensionless numbers as:

$$h_c = \frac{N_u\, k}{d} \qquad [5.25]$$

with k being the gas thermal conductivity (W m^{-1} K^{-1}) and d the characteristic length scale (m), which for our geometry is the fuel particle diameter. The Nusselt number, N_u, the ratio of convective to conductive heat transfer across a boundary, is estimated from empirical correlations for distinct geometries (e.g., Incropera and Dewitt 2002). In the present model we rely on the relationship proposed by Mendes-Lopes *et al.* (2002) for convective heat transfer in litter fuel layers under forced flow with the Reynolds number ranging between 50 and 400:

$$N_u = 0.1417\, R_e^{0.06053} \qquad [5.26]$$

with R_e, the ratio between inertial to viscous force, being:

$$R_e = \frac{V\,L}{v} \qquad [5.27]$$

with V the fluid flow velocity relative to the fuel element (m s^{-1}), L the characteristic dimension (m) and v kinematic viscosity of the fluid (m^2 s^{-1}).

Figure 5.10 depicts the effect of the fluid flow velocity and its temperature on the convective heat transfer coefficient and convective heat flux for the expected range of air velocities and temperatures experienced by unburned fuels ahead of the arrival of a surface fire. These two fire dependent variables are the two key unknowns necessary to determine the convective heat transfer to unburned fuels.

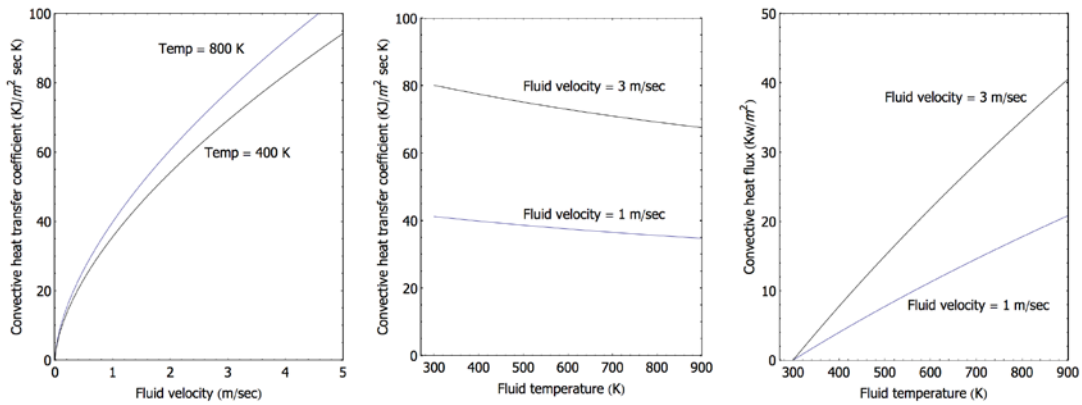

Figure 5.10. Effect of fluid velocity and temperature on the convective heat transfer coefficient using Mendes-Lopes *et al.* (2002) Nusselt number correlation.

Unfortunately, our understanding of how these two quantities change at fuel level ahead of the arrival of a flame front varies from poor, in the case air temperature, to virtually nil in the case of fluid velocity. The discussion on the relative importance of convection versus radiation as drivers of fire propagation goes back to the first attempts to apply physical theory to the modelling of fire spread. While this is still an active topic of debate for fire modellers, it is somewhat clear that where detailed heat transfer and combustion data exists, convection is shown to have a very relevant role (De Mestre *et al.* 1989; Baines 1990; see review by Finney *et al.* 2013). From this precept it becomes clear that successful modelling of fire propagation based on heat transfer principles requires a description of air temperature and velocity ahead of the flame front.

Air flow ahead of the fire

Depending on the location of the fuel particle relative to the flame front, the mean velocity of the air/fluid it experiences will vary. For a fuel particle far from the flame the air velocity and direction can be assumed to equal the ambient wind. As a fire approach the fuel particle an area of stagnant air might be encountered, also called a conversion zone. This area is

characterised by reduced air velocity magnitude and changing, sometimes reversed, air flow direction. The location and width of this region is the result of the interaction of the fire buoyancy and the wind field. Between this area and the flame front the air velocity magnitude will increase and its direction will align with the general wind direction.

Finally, within the flame the buoyant velocity is largely determined by the rate of energy release (Nelson 2013). Although this characterization of the wind field at fuel level is well accepted (e.g., Clements et al 2007; Anderson *et al.* 2010) there is little quantification of how the fire and the wind field interact to define the distances at which each regions are formed. This is partially due to the difficulty of instrumenting free-spreading fires with sensors that will work and survive the thermal environment of a flame front.

Butler (2010) and Anderson *et al.* (2010) report on the use of bidirectional arrays of kiel-static type sensors (McCaffrey and Heskestad 1976) to measure gas flow in experimental fires. Based on the measurement of flow characteristics in wind-driven spreading fires in laboratory experiments, Anderson *et al.* (2010) propose a model for wind speed at the fuel bed surface ahead of the arrival of the flame front. Their model considers three regions of surface flow: (1) far from the flame front a region of constant velocity; (2) a conversion zone of minimum flow characterised by low or reverse flow; and (3) the near flame region where the velocity increases rapidly approaching the free stream velocity. Two important details: this model is for air flow measured on top of a surface fuel layer, a surrogate of a litter layer. At this location the air velocity in the far region was approximately half of the free stream velocity. The second detail is that the measurements were carried out in a closed, i.e., ceilinged, wind tunnel. This precluded the occurrence of natural fire-generated buoyancy and might affect the location and extent of distinct flow regions.

To construct a wind horizontal profile across the x-direction we need to know the boundaries between the far and convergence regions and between the convergence and the near regions, the ambient wind speed, the minimum wind speed in the convergence region and the maximum wind speed as the flame front approaches the fuel element location. Anderson *et al.* (2010) modelled these as:

The x-location for the boundary between the far and convergence region is given by:

$$X_{far} = 0.77 + 0.26\, U_s \qquad [5.28]$$

The x-location for the boundary between the convergence and near region is given by:

$$X_{near} = 0.17 + 0.24\, {U_s}^{0.55} \qquad [5.29]$$

For litter fuels the air velocity at the top of the fuel layer surface is for the far region:

$$U_{far} = -0.07 + 0.48\, U_s \qquad [5.30]$$

The minimum air velocity in the convergence zone is:

$$U_{min} = -0.28 + 0.30\, U_s \qquad [5.31]$$

In the near region, the maximum wind speed is given by:

$$U_{max} = -0.002 + 0.98\, {U_s}^{0.77} \qquad [5.32]$$

As the fuel particle enters the flame region, the vertical air flow is given by the flame characteristic buoyant velocity (w_c), estimated from (Nelson 2003):

$$w_c = \left(\frac{2\, g\, I_B}{\rho_a\, c_p\, T_a}\right)^{1/3} \qquad [5.33]$$

In its current form the model for air flow by the fuel particle follows a piecewise implementation with U_{far} used if x-location > X_{far}, U_{min} used in the convergence zone, and a linear interpolation between the U_{min} and U_{max} used in the near region (Fig. 5.11).

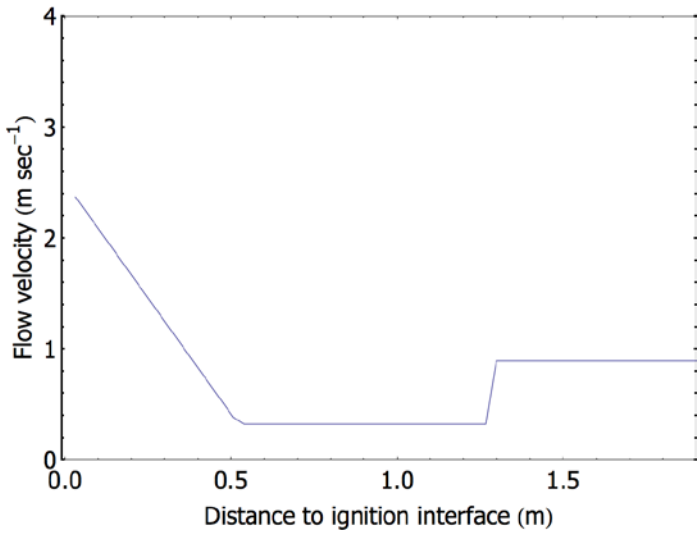

Figure 5.11. Modelled air flow near the surface fuel layer prior to flame front arrival (at x = 0 m) for a free-stream wind speed of 2 m s^{-1}.

Temperature field – Characteristic heating distance

The air temperature ahead of a spreading fire will dictate if at any given moment a fuel element at location *x* will be subject to convective cooling or heating. Anderson et al (2010) found that this temperature can be adequately modelled through a decreasing exponential function of the distance from the flame front, *x*:

$$T_g(x) = T_{amb} + (T_F - T_{amb})Exp\left(-\frac{x}{\lambda_d}\right) \qquad [5.34]$$

with T_{amb} being ambient temperature, T_{max} is the gas temperature at the time of ignition of the fuel element, and λ_d is the characteristic heating number which largely determines the shape of the gas temperature curve. Pagni and Peterson (1973) proposed a similar form for convective heat transfer, albeit suggesting a fixed characteristic heating number. Anderson *et al.* 2008 proposed this parameter to be a function of N_C and fuel bed structure, namely the surface area of fuel per volume of fuel bed (σ β). Anderson *et al.* (2010) modelled λ_d at the top of the surface fuel layer as a direct function of wind speed for wind tunnel experimental fires. Analysis of time – gas temperature profiles in spreading fires (Fig. 5.12) suggest a further dependence of λ_d on the measuring height (Fig. 5.13).

Given the availability of time-temperature profiles for a number of experiment fires in dry sclerophyll eucalypt forest collected during Project Vesta (McCaw *et al.* 2012, Cheney *et al.* 2012) by Wotton *et al.* (2012) we decided to derive λ_d for fires spreading in eucalypt forest instead of using the relationship proposed by Anderson *et al.* (2010) for laboratory fires. For this work Mike Wotton (Canadian Forest Service/University of Toronto) provided us with data from 15 distinct tower measurements where gas temperatures were measured at three heights (0.5. 1.0 and 2.0 m; a few towers also included measurements at 1.5 m) as the fire spread under the tower.

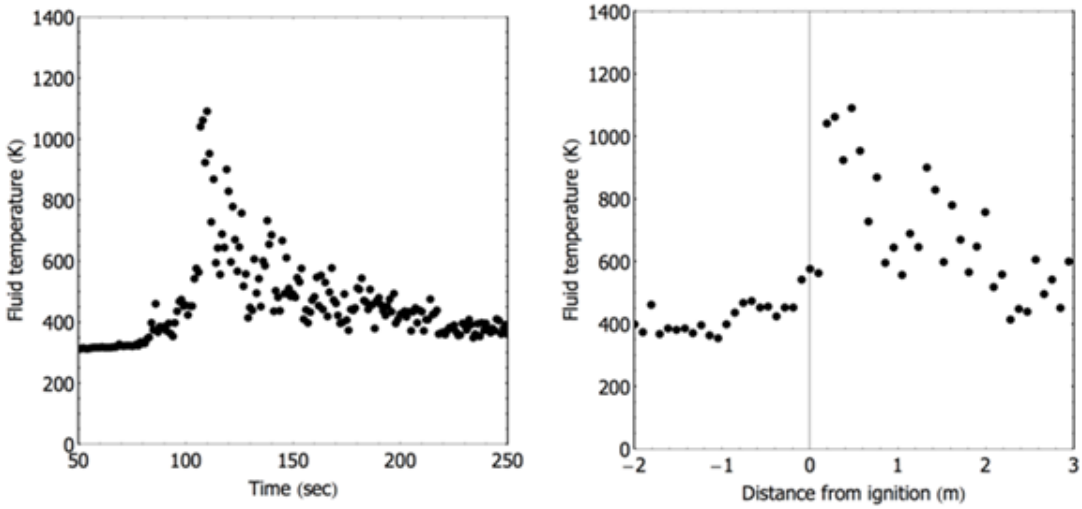

Figure 5.12. Time-temperature profile and distance-temperature evolution assuming constant rate of fire spread (measured to be 0.095 m s^{-1}) for experimental fire K20 (Wotton *et al.* 2012, McCaw *et al.* 2012). Negative distance values indicate fire approaching the sensor; distance = 0 indicates arrival of flame front to sensor.

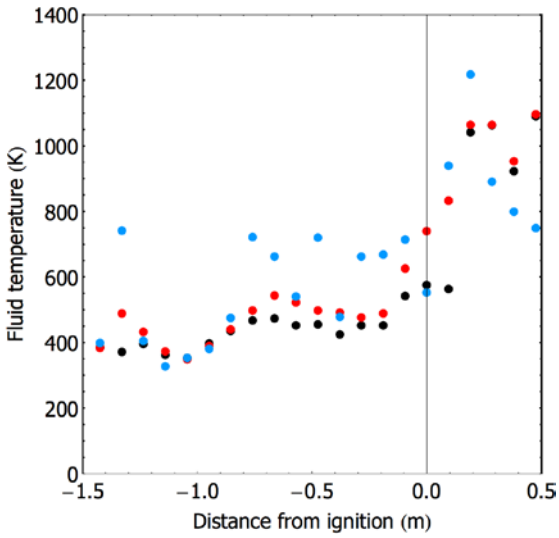

Figure 5.13. Fluid temperature evolution with approaching flame front at three distinct heights (black dots - 0.5 m; red dots - 1.0 m; blue dots - 2.0 m). Data from experimental fire K20 (Wotton *et al.* 2012, McCaw *et al.* 2012).

A step model with three distinct equations was derived to estimate λ_d with height *z* as a function of understorey wind speed (U_s) and the convection number (N_C). Details on model development are given in Appendix 5A.1. Estimation of λ_d follows:

If z is equal to the top of litter fuel layer, i.e., z=0:

$$\lambda_d(z) = 0.002 + 0.08\, U_s \qquad [5.35a]$$

If 0 < z < 0.5 m:

$$\lambda_d(z) = \lambda_d(0)\, \left(0.0427\, {U_s}^{1.157}\, {N_C}^{0.468} - (0.002 + 0.08\, U_s)\right)\left(\frac{0.5-(0.5-z)}{0.5}\right) \qquad [5.35b]$$

If z > 0.5 m:

$$\lambda_d(z) = 0.0427\, {U_s}^{1.157}\, {N_C}^{0.468} + 0.4(z - 0.5) \qquad [5.35c]$$

These functions are illustrated in Figure 5.14 for three values of N_c as a function of U_s and *z*.

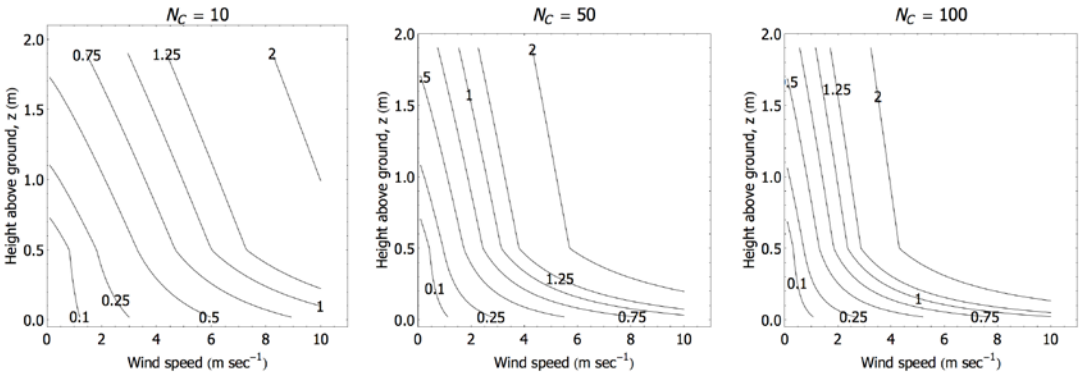

Figure 5.14. Dependence of the estimated λ_d on wind speed and height above ground for three different convection numbers.

Flame temperature with height

The application of Eq. [5.34] requires knowledge of the vertical profile of flame temperature. Following early modelling work by Wotton *et al.* (1998) that considered that the flame radiosity and temperature follow a consistent increasing trend as a function of the downward distance from the flame tip, further corroborated by Cruz *et al.* (2011) for shrubland fires Wotton et al (2012) proposed a model for vertical flame temperature variation in eucalypt forest as:

$$\mathrm{T}_F(z, H_F) = 607 - 258\, ln\left(\frac{z}{H_F}\right) \qquad [5.36]$$

with the intercept of Eq [5.36] being changed so that T_F is in K instead of the original C. Figure 5.15 depicts the change in temperature with height in the flame for three flame heights, 1, 3 and 6 m.

Taking into account the vertical trends in Eqs. [5.35] and [5.36], Eq [5.34] becomes:

$$T_g(z, x) = T_{amb} + (T_F(z) - T_{amb}) Exp\left(-\frac{x}{\lambda_d(z)}\right) \qquad [5.37]$$

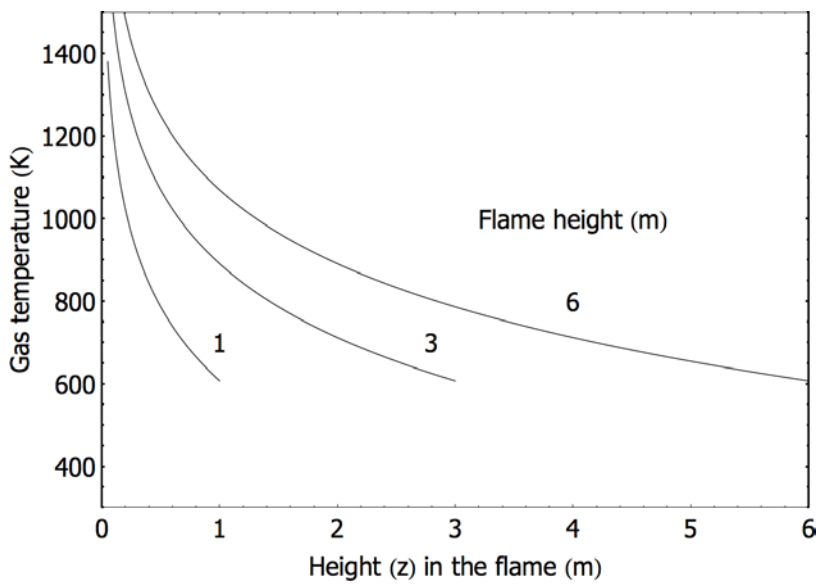

Figure 5.15. Flame temperature with height (z) for three distinct flame heights (1, 3 and 6 m) using Wotton *et al.* (2012) flame temperature vertical profile model.

5.5.3 HEAT TRANSFER MECHANISMS – UPWARD PROPAGATION

The calculation of the energy received by fuels located above a fire follow the model proposed by Cruz *et al.* (2006) to describe the upward radiative and convective heat fluxes of a fire. The fire front is characterized by its: (1) rate of spread, *ROS*; (2) reaction time, τ_r; (3) flame depth, D_F; (4) flame height, H_F; (5) flame temperature-time profile above the fuel bed; and (6) the average gas temperature (T_{pi}) and vertical velocity (U_{pi}) at the tip of the flame. These characteristics define the initial conditions to solve the radiative heat transfer and buoyant plume models.

Radiative heating

The radiative heat transfer process considers the heat transfer between two flat surfaces, the lower fire idealized as a radiating plane, and the base fuel layer above. The radiating plane was defined with dimensions of flame depth by a fixed fireline width.

To take into account the geometric configuration of interest, described by two finite areas with unequal dimensions, non-constant radiosity of the surface fire and the attenuation of radiation in the inter-fuel bed medium space, the impinging radiative transfer to the surface of the fuel elements above the fire is given by:

$$I_{12} = \int_{-\frac{L_p}{2}}^{\frac{L_p}{2}} \int_{D_x}^{D_x+D_F} \int_{-\frac{W_p}{2}}^{\frac{W_p}{2}} \int_{-\frac{W_F}{2}}^{\frac{W_F}{2}} \frac{\varepsilon \cdot \sigma_{SB} \cdot \left(T_F^{\,4}(x_F) - T_f^{\,4}\right) e^{-\alpha S} \cdot \left(\frac{Z}{S}\right)^2}{\pi \cdot S^2} dy_F\, dy_p\, dx_F\, dx_p \qquad [5.38]$$

where T_F is the radiometric temperature of the flame (K), T_f is the fuel particle surface temperature, α is the radiation absorption coefficient and subscripts *F* and *p* refer to the flame surface and particle surface respectively. Eq. [5.38] was numerically integrated through the non-adaptive Halton-Hammersley-Wozniakowski algorithm (Wolfram 1999).

The radiometric temperature of the flame is calculated through a time-temperature model composed of three distinct parts: (1) a model describing the non-dimensional shape of the T-T profile (Weber *et al.* 1995); (2) a model to predict the maximum temperature, T_{Fmax}; and (3) a numerical method to find the shape of the rise and decay components of the temperature curve. The model assumes a fixed rate of increase of gas temperature from the arrival of the ignition interface to attainment of the T_{Fmax} and calculates the cooling rate iteratively through Newton's method so that the decay curve would match the 600 K temperature at $t = \tau_r$, the reaction time. The T-T profile model was then given by the "piece-wise" function:

$$T_F(t) = \begin{cases} T_a + (T_{F\max} - T_a) \cdot \exp\left(\dfrac{-(t+\lambda_F)^2}{\beta_F^2}\right), & T_F \text{ increasing} \\ T_a + (T_{F\max} - T_a) \cdot \exp(-\gamma_F \cdot (t+\lambda_F)), & T_F \text{ decreasing} \end{cases} \qquad [5.39]$$

where *t* is time (sec), β_F is an entrainment constant, and λ_F is a time adjustment variable used to locate the reaction zone interface in the non-dimensional curve at $t = 0$ and γ_F is a proportionality constant determining the cooling rate.

To define both the radiating surface dimensions and the T-T profile an estimate of the surface fire reaction time is required. Reaction time is estimated through Nelson's (2003b) model, which calculates the fuel bed reaction time of a surface fire from the flameout time of a single particle and fuel bed structural properties. Reaction time is defined in the present

study as the time required for the flame front to pass a certain point at the top of the fuel bed. The ignition temperature, 600 K, is used here as the lower threshold value to indicate the presence of flame.

Convective heating

Convective heating to fuels above a heat source considers two distinct methods. If the fuel elements are immersed in the flame, i.e., $z < H_F$, then convective heat transfer (eq. [5.24] considers the fluid temperature to be the flame temperature (eq. [5.36]) and the fluid velocity is the flame characteristic buoyant velocity (eq. [5.33]). If the fuel element is above the flame ($z > H_F$), the fluid temperature and velocity is calculated by the model described by Davidson (1986a, b) and Mercer and Weber (1994). The conservation equations for a control volume in the buoyant plume are given in Table 5.2.

Table 5.2. Conservation equations for the plume model (after Mercer and Weber 1994)

Conservation of mass	$\frac{d(\rho_p \cdot b \cdot U_p)}{ds} = \rho_a \cdot v_e$
Conservation of s-momentum	$\frac{d(\rho_p \cdot b \cdot U_p^2)}{ds} = \rho_a \cdot v_e \cdot U_z \cdot \cos\theta - b(\rho_p - \rho_a) \cdot g \cdot \sin\theta$
Conservation of r-momentum	$\frac{d\theta}{ds} = \frac{\rho_a \cdot v_e \cdot U_z \cdot \sin\theta + b(\rho_p - \rho_a) \cdot g \cdot \cos\theta}{\rho_p \cdot b \cdot U_p^2}$
Conservation of thermal energy	$\frac{d(\rho_p \cdot b \cdot U_p \cdot T_p)}{ds} = \rho_a \cdot v_e \cdot T_a$

The equations for conservation of mass, s-momentum (along the plume centreline), r-momentum (normal to the plume centreline), temperature (by rearranging the mass and thermal energy equations) along the plume centreline and its trajectory in two dimensions form a system of six coupled ordinary differential equations that are solved simultaneously with three other algebraic equations: (1) an equation of state, which for the gaseous plume can be represented by the ideal gas law:

$$\rho_p = \rho_a \cdot \frac{T_a}{T_p} \qquad [5.40]$$

(2) an entrainment assumption, represented by the entrainment velocity. This quantity is implemented considering two entrainment constants α_p and χ_p:

$$v_e = \alpha_p \cdot (U_p - U_s \cdot \cos\theta) + \chi_p \cdot U_s \cdot \sin\theta \qquad [5.41]$$

and (3) an equation describing the vertical ambient wind profile within the stand (Cionco 1965; Amiro 1990):

$$U_s = U_{SH} \cdot \exp\left(\alpha_U \cdot \left(\frac{z}{SH} - 1\right)\right) \qquad [5.42]$$

The steady-state solution does not consider the interaction of the fire-generated buoyancy with the ambient cross flow. The system describing the buoyant plume is solved using a Fehlberg order 4-5 Runge-Kutta method (Wolfram 1999). The required initial conditions are the initial plume half width (b_i), initial vertical velocity in the plume (U_{pi}) and initial plume temperature (T_{pi}). The initial plume temperature is the flame tip temperature, assumed as 800 K (Draper point).

5.5.4 FIRE SPREAD SUSTAINABILITY

For the fuels being volatilised in a fuel layer to contribute to the formation of a self-sustaining solid flame front it is required that the amount of volatile per unit volume is above a critical threshold. Below this threshold the flame is too lean and will fail to form a coherent structure. Van Wagner (1977) aimed at empirically quantifying this parameter for deep fuel beds by taking into account a basic heat balance in a porous fuel bed (Thomas *et al.* 1964):

$$\mathrm{R}\,\rho_b\,\mathrm{Q}_i = E \qquad [5.43]$$

With *E* being the net horizontal heat flux. From this equation, Thomas (1967) considered fire derived property, the mass flow rate of fuel per unit sectional area per unit time, *S* (kg m^{-2} s^{-1}), as a direct function of rate of fire spread and fuel bulk density:

$$\mathrm{R}\,\rho_b = {}^{\mathrm{E}}/_{h} = S \qquad [5.44]$$

For practical purposes there is a threshold S_0 below which the flame front will not be self sustaining (Van Wagner 1977). Albini (1993) called this the lean flammability limit. Experimental values for S_0 have been found to be between 0.06 and 0.08 kg m^{-2} s^{-1} for experimental fuel beds (Thomas 1967) and 0.05 kg m^{-2} s^{-1} for a crown fire experiment (Van Wagner 1977). Assuming for practical purposes an S_0 of 0.06 kg m^{-2} s^{-1}, for any fuel bed of bulk density ρ_b one can find the rate of spread required for sustained propagation:

$$\mathrm{R}_0 = {}^{S_0}/_{\rho_b} \qquad [5.45]$$

5.6 Fuel description

As a fuel complex, a eucalypt forest presents multiple fuel strata (Fig. 5.16), each of which is capable of contributing to the propagation and intensity of a fire. The propagation of the ignition interface of the fire is largely determined by the processes occurring in the highest fuel layer involved in flames.

The surface fuel layer is comprised of litter components horizontally layered on the forest floor. The compactness of this layer (bulk density around 50 – 60 kg/m^3; Cheney 1981) limits heat transfer processes and combustion efficiency and constrains the rate of spread in surface fuel-only fuel beds to relatively slow spread rates (McArthur 1967) but this layer generally contributes to the maintenance of a deep flame front.

The near-surface fuel layer (composed of grasses, sedges, low shrubs and collapsed understorey plants) and the elevated fuel layer (composed mostly of tall shrubs) provide media of typically low to moderate fuel quantity but high heat transfer efficiency. A fire supported by the near-surface and elevated fuels the flame front extends its three-dimensionality component. The turbulent flame motion in this fuel layer allows increasing direct flame contact with unburned fuels and faster rates of spread (Cheney 1981, Nelson and Adkins 1988, Burrows 1994).

A further relevant fuel component of eucalypt forests is the bark fuels. The presence of fibrous bark contributes to the energy released in the understorey and provides further connectivity between the understorey and overstorey fuel layers. Fibrous bark particles are easily ignited and dislodged allowing simultaneously for vertical fire propagation and profuse spotfire ignitions.

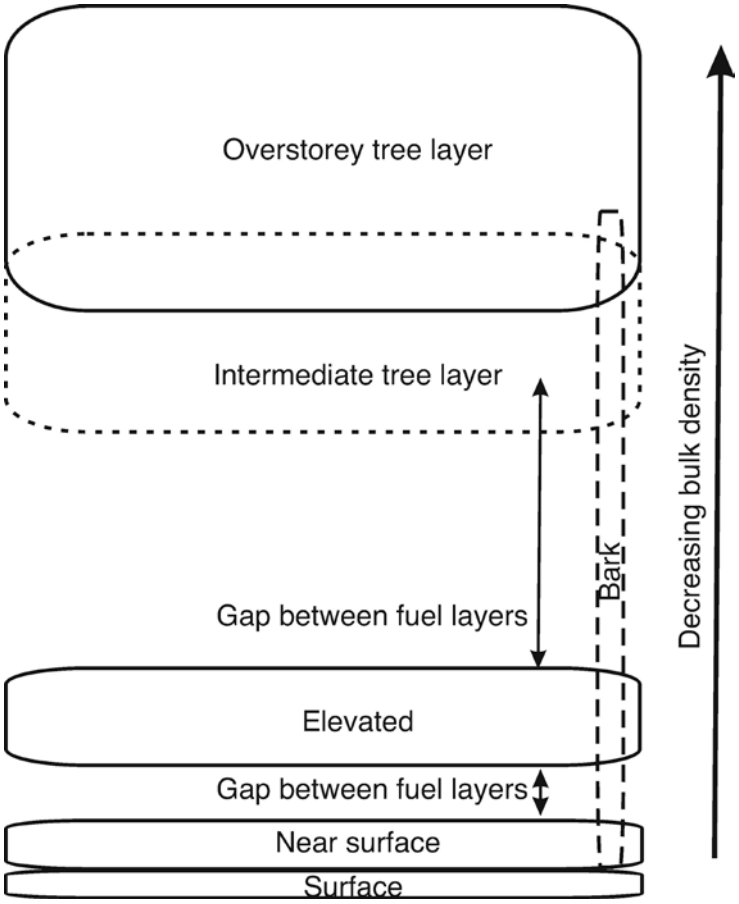

Figure 5.16. Schematic depiction of fuel layers arrangement typical of dry eucalypt fuel complexes. Some fuel types do not have all fuel layers. Gaps between vertical fuel layers might also not exist.

Quantitative fuel descriptions of eucalypt forests fuel complex have mostly been restricted to the determination of surface fuel load (McArthur 1967). As a surrogate of fuel complex structure with time since fire, this metric has been useful as the key input in fire behaviour models for forests in Australia (e.g. McArthur 1962, 1967; Sneeuwjagt and Peet 1998). The quantification of near-surface, elevated and overstorey fuels has received less attention.

The application of a fire behaviour model based on first principles requires a description of the fundamental characteristics of each fuel layer. These characteristics are the distribution of fuel quantity by size classes and state (live and dead), fuel layer height, from which bulk density or compactness can be derived, and a characteristic surface area to volume ratio for each fuel layer. From data from a variety of studies we inferred a set of standardized fuel layers to describe dry eucalypt fuel complexes to test the fire behaviour model (Table 5.3).

Table 5.3. Set of standard fuel characteristics for model testing

FUEL LAYER	W_A (KG M^{-2})	σ (M^{-1})	ρ_B (KG M^{-3})	β	$\sigma\beta$ (M^2 M^{-3})
Surface	1	4000	50	0.125	500
Near-surface	0.8	6000	4.6	0.0115	69
Elevated	0.5	6000	0.33	0.001	6
Overstorey	1	4000	0.1	0.0002	1

Taking into account these standardised fuel layer characteristics, we define three fuel complexes with the objective of studying behaviour of our transition model in different fuels: (1) Eucalypt forest with no understorey vegetation; (2) Eucalypt forest with low / sparse shrub understorey; and (3) Eucalypt forest with dense shrub understorey (Table 5.4). These descriptions do not intend to represent any specific fuel type.

Table 5.4. Fuel complex characteristics of standardised eucalypt fuel complexes for model testing

FUEL LAYER PROPERTY	LITTER ONLY	EUCALYPT FUEL TYPE SPARSE SHRUB UNDERSTOREY	DENSE SHRUB UNDERSTOREY
Surface cover (%)	100	100	100
Surface height (m)	0.02	0.02	0.02
Near-surface cover (%)	0	50	80
Near-surface height (m)	na	0.2	0.3
Elevated cover (%)	0	30	80
Elevated fuel base (m)	na	0.3	0.7
Elevated fuel height (m)	na	0.5	3
Canopy base height	8	10	10
Stand height	15	20	20

5.7 Model implementation

The model is implemented through a multi-step iterative algorithm where three key processes are calculated at different fuel layers to determine which layer is responsible to carry the combustion wave. At each step the three key calculations are (1) the rate of spread (Eqn. 5.5) and energy released (following Byram's equation) for fuel layer *i*; (2) if the mass flow rate associated with fire spread in fuel layer *i* allows for the formation of a self-sustaining flame front, and (3) if the energy released by fuel layer *i* is sufficient to ignite fuel layer *i*+1. If fuel layer *i*+1 is ignited, the process is repeated for this layer. The process stops when the output from a fuel layer does not ignite the fuel layer above or we reach the canopy layer. Then the rate of spread is the one determined by the higher fuel layer where the mass flow indicates self-sustained fire propagation with some contribution of the energy consumed by the combustion of fuel in the layer above (layer *i*+1) (Fig 5.17).

The calculation of rate of spread (Eqn. [5.5]) requires information about the environmental conditions and combustion outputs (e.g., residence time, energy released, flame size and radiometric profile, convection number). As such this calculation is conducted through an inner iterative process that finds the rate of spread that satisfies the equity of the driving equation.

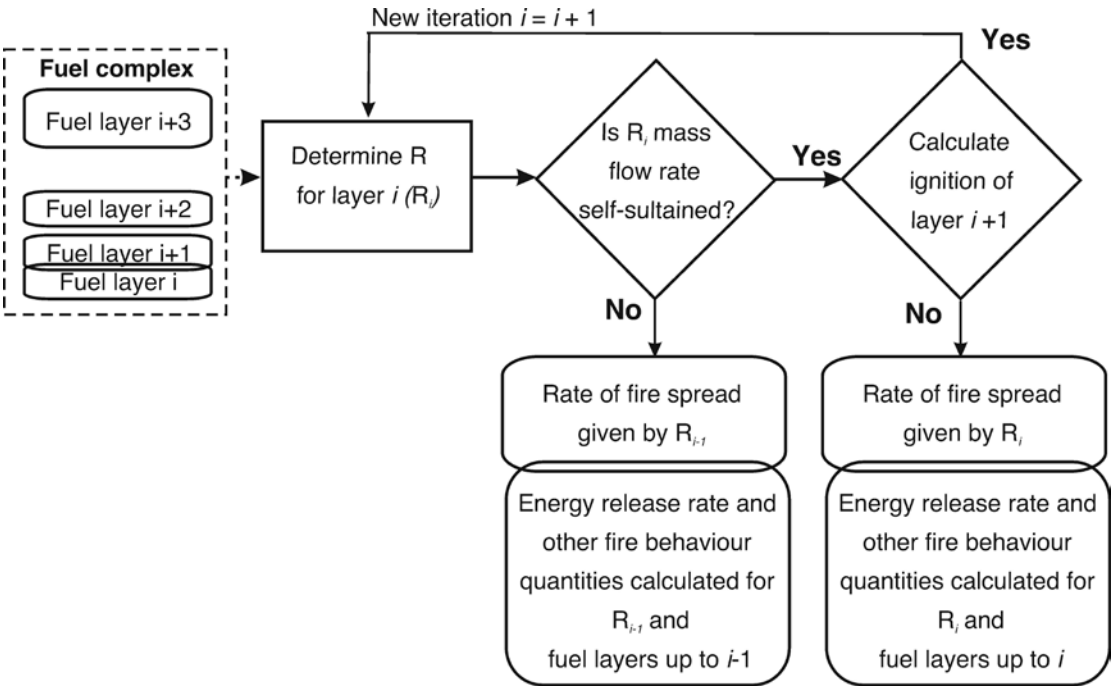

Figure 5.17. Flow chart showing the key fire behaviour calculations and the outer iteration process to determine rate of fire spread and energy released.

5.7.1 TESTING AND MODEL RESULTS

The model system response to changes in environmental and fuel complex variables was investigated by analysing the effect of six variables determining the ignition of crown fuels. They were: 10-m open wind speed (U_{10}), surface fuel available for flaming combustion (w_a), fuel strata gap (*FSG*), moisture content of fine dead surface fuels (*MC*), foliar moisture content (*FMC*) and surface area to volume ratio of crown fuel particles (σ). w_a is assumed to be the fuel consumed in the active combustion zone (Alexander 1982). *FSG* is the vertical distance between the top of the surface fuel strata and the lower limit of the crown fuel layer. Some of these input variables affect intermediate model outputs, such as the surface fire rate of spread (*ROS*) and the depth of the flaming front.

In order to better understand the effect of intermediate model outputs on the final model behaviour, the effect of fire rate of spread, reaction time (τ_r), maximum flame temperature (T_{Fmax}), and wind profile models were also analysed. The influence of the input and intermediate output variables in CFIM were examined through their effect on the final model output – i.e., the canopy fuel particle temperature profile. The effects of the intermediate output variables on the convective and radiative heat sources and transfer processes, namely the surface fire T-T (time – temperature) profile, the convective heat transfer coefficient (h_c), and the incident convective and radiative heat fluxes (q_c and q_r respectively) were also analysed.

Initial testing of the model was carried out by (1) comparing the effect of environmental and fuel variables on the rate of spread of the fire; and (2) analysing the model's predictive capacity against well-documented experimental fires.

The model system response to changes in environmental and fuel complex variables was investigated by analysing the effect of four variables. These were: wind speed at flame level

(U), moisture content of fine dead surface fuels (MC), surface fuel available for flaming combustion (w_a), and fuel bed depth (δ). w_a is assumed to be the fuel consumed in the active combustion zone (Alexander 1982).

The influence of the input variables was examined through their effect on the final model output – i.e. the rate of fire spread. Fig 5.18 illustrates the effect of wind speed at eye level in rate of fire spread for three distinct fuel layers. Considering the relationship $R \propto a\ U^b$, the curves were found to have shapes similar to those found in empirical studies (Sullivan 2009b). The b exponent was found to vary between 1.1 for the elevated fuels and 1.4 for the litter fuels.

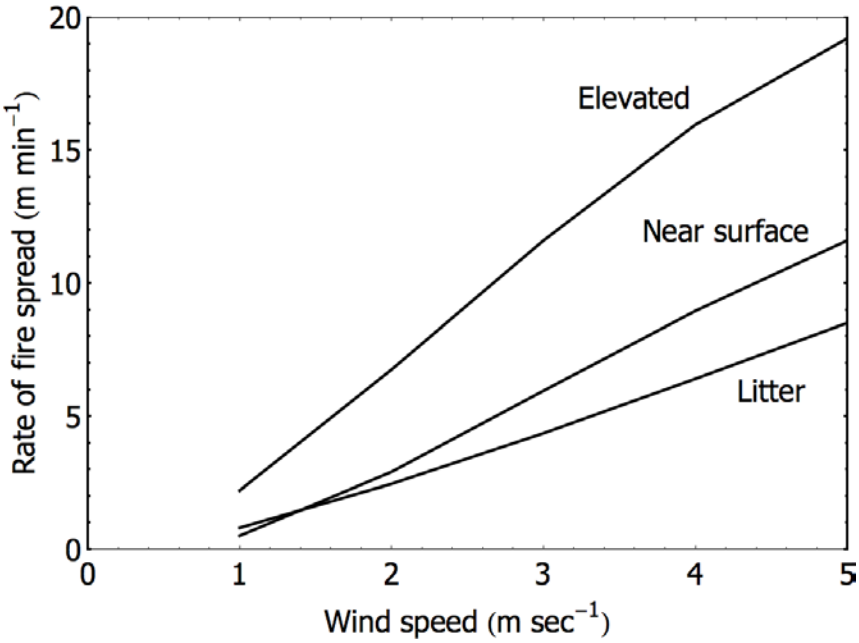

Figure 5.18. Effect of wind speed in the rate of spread of fire propagating in three different fuel layers. Litter depth = 0.05 m; near surface fuel depth = 0.25 m; Elevated fuel depth 1.1 m. Other variables hold constant were: Fine dead fuel moisture content (fraction): 0.1; Fuel available for combustion = 0.65 kg m^{-2}; surface area to volume ratio: 2000 m^{-1}.

Considering the effect of dead fuel moisture content (Fig 5.19), the model results suggest distinct effects depending on the fuel layer being analysed. For the litter and near-surface fuels, the results also follow empirical results (Sullivan 2009b). Considering the well-accepted exponential decay relationship for the effect of fuel moisture, $R \propto a\ \mathrm{Exp}(b\ MC)$ the model results yield curves with b being -0.05 and -0.07 respectively for litter and near-surface fuels. These values are slightly lower than found by Burrows (1994) for eucalypt forests (between -0.12 (lower wind speeds) and -0.34 (higher wind speeds) but similar to other empirical studies such as found by Fernandes *et al.* (2009) – between 0.039 and -0.04. For elevated fuels the model suggests a linear effect of fuel moisture content.

Figure 5.20 shows the effect of fuel available for combustion on rate of fire spread. The model identifies distinct effects depending on the fuel arrangement. In litter fuels, with a more compact fuel bed and a lower heat transfer efficiency, the model predicts that an increase in available fuel load has a lower effect on rate of spread than for near-surface and elevated fuels.

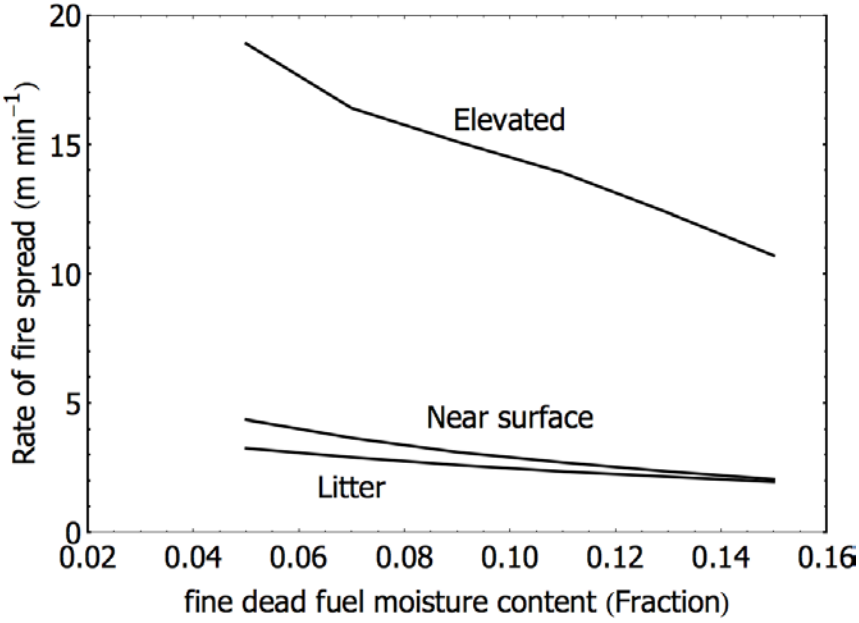

Figure 5.19. Effect of fine dead fuel moisture content on the rate of spread of fire propagating in three different fuel layers. Litter depth = 0.05 m; near surface fuel depth = 0.25 m; Elevated fuel depth 1.1 m. Other variables held constant were: wind speed = 2 m s^{-1}; fuel available for combustion = 0.65 kg m^{-2}; surface area to volume ratio: 2000 m^{-1}.

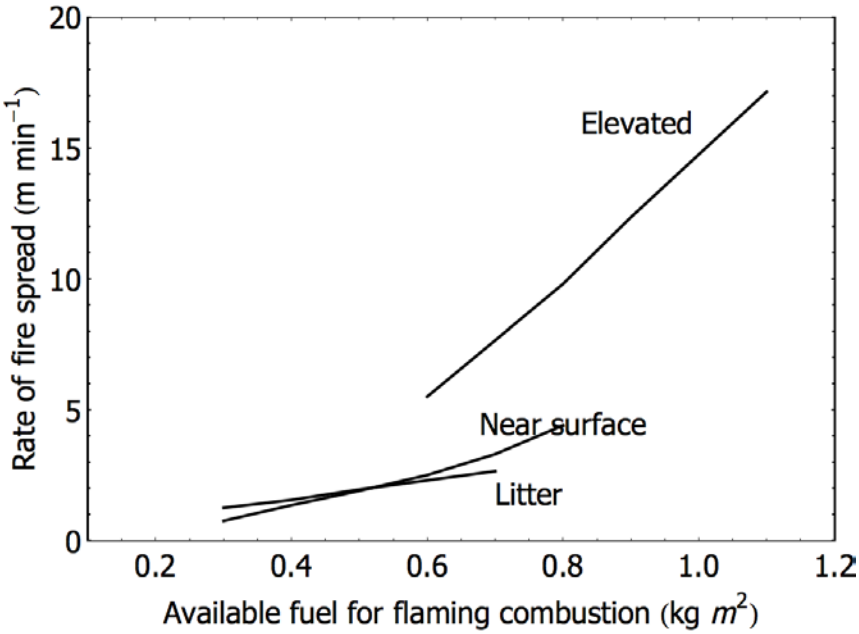

Figure 5.20. Effect of the fuel available for flaming combustion on the rate of spread of a fire propagating in three different fuel layers. Litter depth = 0.05 m; near surface fuel depth = 0.25 m; Elevated fuel depth 1.1 m. Other variables hold constant were: wind speed = 2 m s^{-1}; fine dead fuel moisture content (fraction): 0.1; surface area to volume ratio: 2000 m^{-1}

Fig 5.21 depicts the effect of fuel bed depth on rate of fire spread. The more compacted the fuel bed the higher the effect of this variable. This is expected from an heuristic analysis as fuel compactness is a fuel bed property that limits the availability of fuel for flaming combustion. The model predicts that in the elevated fuel layer the effect is considerably lower than found for litter and near surface fuels.

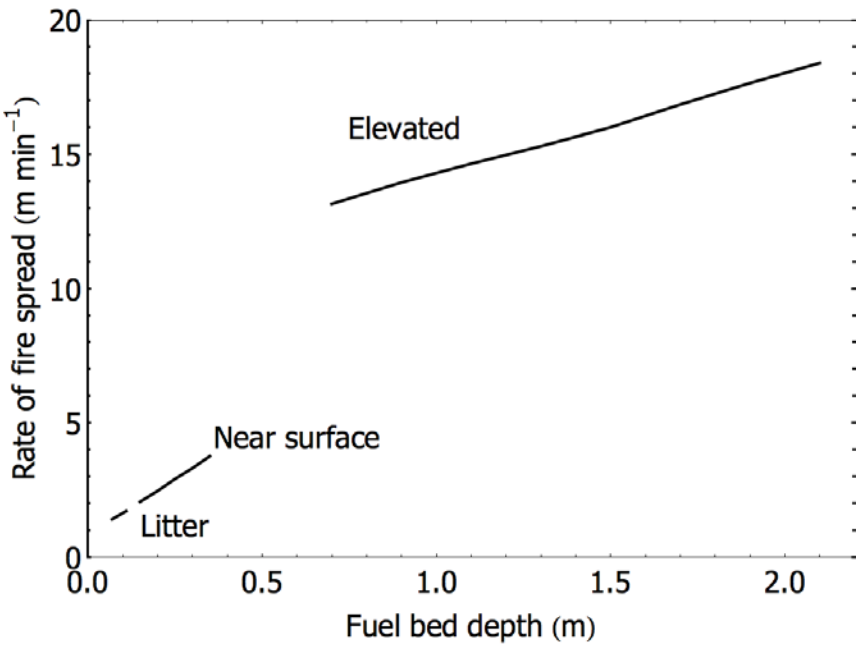

Figure 5.21. Effect of fuel bed depth in the rate of spread of fire propagating in three different fuel layers. Other variables hold constant were: wind speed = 2 m s^{-1}; Fine dead fuel moisture content (fraction): 0.1; Fuel available for combustion = 0.65 kg m^{-2}; surface area to volume ratio: 2000 m^{-1}.

A further model evaluation exercised carried out was to compare the rate of spread predicted by the model with observed fire behaviour from experimental fires. The preliminary work carried out here focussed on three experimental fires carried out in Project Vesta (McCaw *et al.* 2012, Cheney *et al.* 2012). Table 5.5 provides the fire environmental characteristics and the observed and predicted rates of spread. For these illustrative cases the model predicted rate of spread with errors within the range of -12 and 50%. Overall this is well within the bounds considered as good (Alexander and Cruz 2013).

Table 5.5. Fire environment, observed and predicted rate of spread for selected fires

VARIABLE	FIRE		
	DV 6L	DV 22M	MC 11L
Wind speed (km h^{-1})	13	11	14
Fuel moisture content (%)	6.5	6.2	7.8
Fuel age (years)	6	22	11
Surface fuel height (m)/cover (%)	0.02/97%	0.02/95%	0.02/94%
NS fuel height (m)/cover (%)	0.15/17%	0.22/34%	0.26/47%
Elevated fuel height (m)/cover (%)	0.7/26%	0.55/34%	1.6/47%
Observed rate of fire spread (m min^{-1})	3.2	10.8	14.1
Flame height (m)	1.4	4.1	4.2
Predicted rate of fire spread (m min^{-1})	2.1	9.5	21.1
Error (%)	-34%	-12%	50%

5.8 End-user summary

5.8.1 MODEL DESCRIPTION

We developed a semi-physical model that describes understorey fire behaviour in eucalypt forests by quantifying vertical fire propagation transitions between fuel layers and the forward rate of fire spread of the flame front. A key assumption of the model framework is that spread rate of a fire propagating in a multilayered fuel complex will be largely determined by the combustion processes of the layer exhibiting the most efficient heat transfer, fastest reaction velocity and when the pyrolysed fuel mixes with air at a ratio that allows for the formation of a coherent flame.

As such, the rate of spread is not directly related to the overall average fuel characteristics but to a large degree dependent on the physical structure of the most flammable fuel layer.

The model formulation is based on the energy balance equation that takes into account changes in temperature of unburned, thermally-thin fuel elements from the impinging convective and radiative heat fluxes. The model system is closed by using a number of sub-models for flame characteristics.

Radiative energy source is modelled as a solid flat surface with the radiometric temperature varying with height (for forward heat flux computations) and depth (for upward computations). Air temperature and velocity fields necessary for convective heat transfer calculations are determined from a buoyant plume model and knowledge of a characteristic heating distance.

The model is implemented through a multi-step iterative algorithm where three key processes are calculated at different fuel layers to determine which layer is responsible to carry the combustion wave. At each step the three key calculations are

1) the rate of spread and energy released for a fuel layer;
2) if the mass flow rate associated with fire spread in this fuel layer allows for the formation of a self sustaining flame front, and
3) if energy released by this fuel layer allows for the ignition of fuel layer located above. If the fuel layer above is ignited the process is repeated for this layer.

The process stops when the outputs from a fuel layer does not ignite the fuel layer above or the canopy layer is reached. Figure 5.18 presents this iterative process by considering the various fuel layers existent in a fuel complex.

Input variables

The application of the fire propagation model requires knowledge of weather variables commonly used to predict fire behaviour in eucalypt forests (i.e., wind speed and air temperature), moisture content of fuels involved in the combustion processes, and a fuel complex description that quantifies per fuel layer (Fig 5.16): fuel load, fuel layer depth, fuel layer cover, distance between fuel layers and a characteristic surface area to volume ratio of the fuel layer (Table 5.5).

Based on existent fuel inventory work most of these quantities can be inferred from other easy to use methodologies such as the Overall Fuel Hazard Guide or the Vesta Fuel Hazard Scoring System (Gould *et al.* 2007b). The model can also be run with less detail, e.g., a bulk understorey fuel layer and the overstorey fuel layer. Nonetheless, the lower the detail of the fuel description, the higher the uncertainty in the prediction.

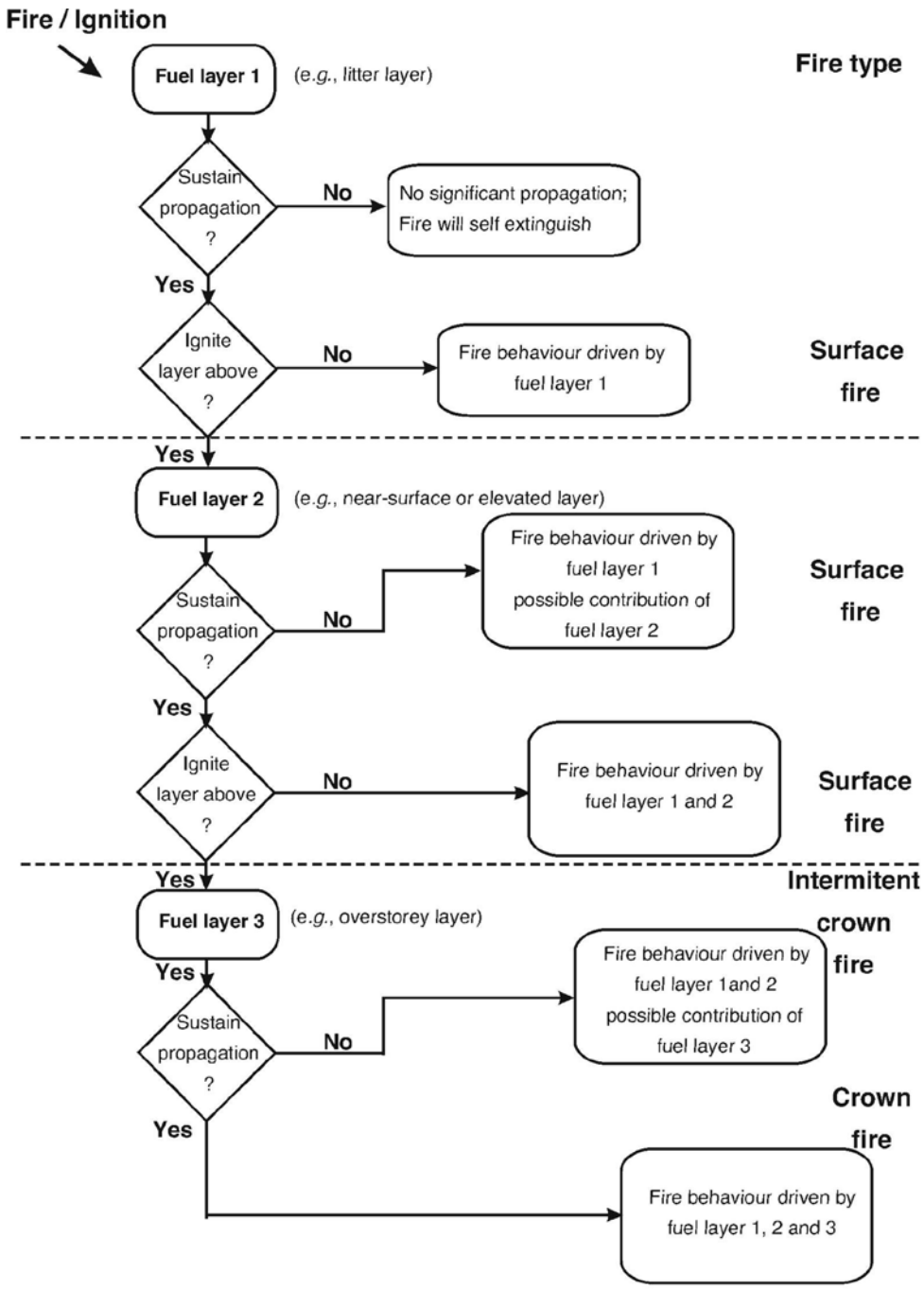

Figure 5.22. Flowchart of iterations used to determine fuel layers involved in combustion and fuel layer contribution to fire propagation and behaviour.

Table 5.6. List of the main fuel and weather input variables required to run the PPPY model system.

VARIABLE	UNITS	PERIOD OF CHANGE[A]
Fuel complex		
Available fuel load per fuel layer[b]	kg/m^2	Medium/Long
Fuel layer depth	m	Medium/Long
Fuel layer cover	%	Medium/Long
Gap between fuel layers	m	Medium/Long
Surface area/volume ratio	m^{-1}	Medium/Long
Stand height	m	Long
Stand cover	%	Long
Fire weather		
Wind velocity	km/h	Very short
Air temperature	°C	Very short
Fine dead fuel moisture content	% oven-dry weight	Very short
Live foliar moisture content	% oven-dry weight	Medium

[a] Very short – minutes or hours; medium – months; and long – years.
[b] Within the present analysis available, available fuel load corresponds to the fuels typically consumed in flaming combustion, namely litter and small twigs < 6 mm in diameter (Luke and McArthur 1978) and live fuels with < 3 mm in diameter.

5.9 Conclusions

We described a novel semi-physical approach to model fire behaviour in eucalypt forests. The model system is based on a simplified energy balance formulation that takes into account changes in temperature of unburned, thermally-thin fuel elements due to impinging convective and radiative heat fluxes.

Radiative energy source is modelled as a solid flat surface with the radiometric temperature varying with height (for forward heat flux computations) and depth (for upward computations). Fluid temperature and velocity fields necessary for convective heat transfer calculations are determined from a buoyant plume model and knowledge of a characteristic heating distance.

Model evaluation tests yield encouraging results. Sensitivity analysis showed the model to respond adequately to changes in input variables. Model evaluation against independent data showed outputs within acceptable margins of error. Nonetheless, a number of weaknesses were identified.

The current model formulation failed to converge under certain conditions, namely under light wind speeds. This weakness arises from our lack of understanding in the fundamental processes driving fire propagation in wildland fuels and the difficulty to adequately parameterize the model under certain conditions. A better fundamental understanding of the thermodynamic environment preceding a flame front is necessary to fine tune the model. Such understanding will require instrumentation of field fires to measure air flow and the radiative and convective heat transfer characteristics under a broad range of burning conditions.

5.10 References

Albini FA (1981) A model for wind-blown flame from a line fire. *Combustion and Flame* **43,** 155-174.

Albini FA (1985) A model for fire spread in wildland fuels by radiation. *Combustion Science and Technology* **42,** 229-258.

Albini FA (1993) Dynamics and modelling of vegetation fires: Observations. Pages 39-52 In Crutzen, P.J., Goldammer, J.G. (eds.) *Fire in the environment: The ecological, atmospheric, and climatic importance of vegetation fires*. John Wiley & Sons, Chichester, England.

Alexander ME, Cruz MG (2011) Crown fire dynamics in conifer forests. Pages 107-142 in Synthesis of Knowledge of Extreme Fire Behavior: Volume 1 for Fire Managers. USDA Forest Service, Pacific Northwest Research Station, Portland, OR. General Technical Report PNW-GTR-854.

Amiro BD (1990) Comparison of turbulence statistics within three boreal forest canopies. *Boundary-Layer Meteorology* **51,** 99-121.

Anderson WR, Catchpole EA, Butler BW (2010) Convective heat transfer in fire spread through fine fuel beds. *International Journal of Wildland Fire* **19**, 284–298.

Baines PG (1990) Physical mechanisms for the propagation of forest fires. *Mathematical and Computer Modelling* **13,** 83-94.

Bevins CD (1979) Fire modeling for natural fuel situations in glacier National Park. Pages 1225-1229 in proceedings of the first Conference on Scientific Research in the National Parks. USDI Natl. Park Serv., Washington D.C. Trans. Proc. Serv. No. 5.

Burrows ND (1994) Experimental development of a fire management model for jarrah (Eucalyptus marginata Donn ex Sm.) forest. Australian National University, Canberra, Australian Capital Territory. Ph.D. Thesis. 293 p.

Burrows ND, Ward B, Robinson A (1988). Aspects of fire behaviour and fire suppression in a Pinus pinaster plantation. Western Australian Department of Conservation and Land Management Landnote 2/99.

Butler B (2010) Characterization of convective heating in full scale wildland fires. In: Viegas DX, ed. Proceedings of the VI international conference on forest fire research. Coimbra, Portugal: University of Coimbra. 9 p.

Butler BW, Cohen J, Latham DJ, Schuette RD, Sopko P, Shannon KS, Jimenez D, Bradshaw LS (2004) Measurements of radiant emissive power and temperatures in crown fires. *Canadian Journal of Forest Research* **34,** 1577-1587.

Butler BW (1994) Experimental measurements of radiant heat fluxes from simulated wildfire flames. Pages 104-111 in Proceedings of 12th Conference on Fire and Forest Meteorology, Jekyll Island, Georgia. Soc. Am. For., Bethesda, Maryland. SAF Publ. 94-02.

Catchpole WR, Catchpole EA (2000) The second generation U.S. fire spread model. US Forest Service – ADFA Joint Research Venture #RMRS-94962-RJVA final report.

Catchpole WR, Catchpole EA, Tate AG, Butler BW, Rothermel RC (2002) A model for the steady spread of fire through a homogeneous fuel bed. In Viegas, D.X. (ed.) Proceedings of 4th International Conference on Forest Fire Research, 2002 Wildland

Fire Safety Summit, Luso - Coimbra, Portugal – 18/23 November 2002. Millpress, Rotherdam. 11 p.

Cheney NP (1981) Fire behaviour. Pages 151-175 in *Fire and the Australian Biota*, edited by Gill, A.M., Groves, R.H., Noble, I.R., Australian Academy of Sciences, Canberra.

Cheney NP (1990) Quantifying bushfires. *Mathematical and Computer Modelling* **13,** 9-15.

Cheney NP (1991) Predicting forest fire behaviour - The Australian experience. In Proceedings of the Workshop Integrating research on hazards in fire-prone environments. The U.S. Man and the Biosphere Program.

Cionco RM (1965) A mathematical model for air flow in a vegetative canopy. *Journal of Applied Meteorology* **4**, 517-522.

Clements CB, Zhong S, Goodrick S, Li J, Bian X, Potter BE, Heilman WE, Charney JJ, Perna R, Jang M, Lee D, Patel M, Street S, Aumann G (2007) Observing the dynamics of wildland grass fires: FireFlux – a field validation experiment. *Bulletin of the American Meteorological Society* **88**, 1369–1382.

Committee on Fire Research (1961). U.S. National Academy of Science Research Council Publication 949.

Cruz MG, Alexander ME (2013) Uncertainty associated with model predictions of surface and crown fire rates of spread. *Environmental Modelling & Software* **47**, 16-28.

Cruz, MG, Butler, BW, Alexander, ME, Forthofer, JM, Wakimoto, RH (2006) Predicting the ignition of crown fuels above a spreading surface fire I: Model idealization. *International Journal of Wildland Fire* **15,** 47-60.

Cruz MG, Butler BM, Viegas DX, Palheiro P (2011). Characterization of flame radiosity in shrubland fires. *Combustion and Flame* **158,** 1970-1976.

Davidson, GA (1986a) A discussion of Schatzmann's integral plume model from a control volume viewpoint. *Journal of Climate and Applied Meteorology* **25,** 858- 867.

Davidson, GA (1986b) Gaussian versus top-hat profile assumptions in integral plume models. *Atmospheric Environment* **20,** 471-478.

de Mestre, N.J., Catchpole, E.A., Anderson, D.H., Rothermel, R.C. 1989. Uniform propagation of a planar fire front without wind. *Combustion Science and Technology* **65,** 231-244.

Finney MA, CohenJD, McAllister SS, Jolly WM (2013) On the need for a theory of wildland fire spread.*International Journal of Wildland Fire* **22**, 25–36.

Gill AM (1997) Eucalypts and fires: interdependent or independent? In Williams J and Woinarski J (Editors) *Ecology – individuals to ecosystems*. Cambridge University Press 430 pp.

Gould JS, McCaw WL, Cheney NP (2011). Quantifying fine fuel dynamics and structure in dry eucalypt forest (Eucalyptus marginata) in Western Australia for fire management. *Forest Ecology and Management* **262,** 531-546.

Gould JS, McCaw WL, Cheney NP, Ellis PE, Knight IK, Sullivan AL (2007a) Project Vesta- Fire in Dry Eucalypt Forest: Fuel structure, fuel dynamics, and fire behaviour, Ensis-CSIRO, Canberra, ACT and Department of Environment and Conservation, Perth, WA.

Gould JS, McCaw WL, Cheney NP, Ellis PF, Matthews S (2007b) Field Guide: Fire in Dry Eucalypt Forest. Ensis-CSIRO, Canberra ACT, and Department of Environment and Conservation, Perth WA, 92 pp.

Incropera FP, DeWitt DP (2002). *Fundamentals of Heat and Mass Transfer.* Fifth Edition, John Wiley and Sons, Inc., 980 pp.

McArthur AG (1962) Control burning in eucalypt forests. Forest and Timber Bureau Leaflet 80, Commonwealth of Australia, Canberra, ACT.

McArthur AG (1965) Fire behaviour characteristics of the Longford fire. Forest and Timber Bureau Leaflet 91, Commonwealth of Australia, Canberra, ACT. 19 pp.

McArthur AG (1967) Fire Behaviour in eucalyptus forests. Forest and Timber Bureau Leaflet 107, Commonwealth of Australia, Canberra, ACT. 36 pp.

McCaffrey BJ, Heskestad G (1976) A robust bi-directional low-velocity probe for flame and fire application. *Combustion and Flame*, **26**, 125.

McCaw WL, Gould JS, Cheney NP, Ellis PFM, Anderson WR, (2012) Changes in behaviour of fire in dry eucalypt forest as fuel increases with age. *Forest Ecology and Management* **271**, 170-181.

Mell W, Jenkins MA, Gould J, Cheney P (2007). A physics based approach to modeling grassland fires. *International Journal of Wildland Fire* **16**, 1-22.

Mendes-Lopes JMC, Ventura JMP, Rogrigues JAM (2002) Determination of heat transfer coefficient through a matrix of Pinus pinaster needles. In Viegas, D.X. (ed.) Proceedings of 4th International Conference on Forest Fire Research, 2002 Wildland Fire Safety Summit, Luso - Coimbra, Portugal – 18/23 November 2002. Millpress, Rotherdam.

Mercer GN, Weber RO (1994) Plumes above line fires in a cross wind. *International Journal of Wildland Fire* **4,** 201-207.

Modest MF (1993) *Radiative heat transfer*. McGraw-Hill, New York.

Nelson Jr. RM (1993) Byram's derivation of the energy criterion for forest and wildland fires. *International Journal of Wildland Fire* **3**, 131–138.

Nelson Jr. RM, Butler BW, Weise DR (2012) Entrainment regimes and flame characteristics of wildland fires. *International Journal of Wildland Fire* **21**, 127–140.

Nelson Jr. RM (2003a) Power of the fire – a thermodynamic analysis. *International Journal of Wildland Fire* **12**:51-63.

Nelson Jr. RM (2003b). Reaction times and burning rates for wind tunnel headfires. *International Journal of Wildland Fire* **12,** 195-211.

Nelson Jr. RM, Adkins CW (1988). A dimensionless correlation for the spread of wind driven fires. *Canadian Journal of Forest Research* **18,** 391-397.

Pagni PJ, Peterson TG (1973). Flame spread through porous fuels. 14th Symposium (international) on Combustion, 1099-1107.

Pickett BM, Isackson C, Wunder R, Fletcher TH, Butler BW, Weise DR. (2010) Experimental measurements during combustion of moist individual foliage samples. *International Journal of Wildland Fire* **19,** 153-162.

Sneeuwjagt RJ, Peet GB. (1998). Forest fire behaviour tables for Western Australia. Department of Conservation and Land Management. 59 p.

Sullivan AL (2009a). Wildland surface fire spread modelling, 1990-2007. 1. Physical and quasi-physical models. *International Journal of Wildland Fire* **18,**349-368.

Sullivan AL (2009b). Wildland surface fire spread modelling, 1990-2007.2. Empirical and quasi-empirical models. *International Journal of Wildland Fire* **18,**369-386.

Thomas PH (1967) Some aspects of the growth and spread of fire in the open. *Forestry* **40,** 139-164.

Thomas PH, Simms DL, Wraight HG (1964) Fire spread in wooden cribs. Joint Fire Research Organisation Fire Research Note 537. Boreham Wood, U.K.

Van Wagner CE (1977). Conditions for the start and spread of crown fire. *Canadian Journal of Forest Research* **7,** 23-34.

Weber RO, Gill AM, Lyons PRA, Mercer GN (1995) Time dependence of temperature above wildland fires. *CALMScience Supplement* **4,** 17-22.

Wolfram S (1999). *The Mathematica book*. Wolfram Media/Cambridge University Press, 4th Ed. 1470 pp.

Wotton BM, Gould JS, McCaw WL, Cheney NP, Taylor SW (2012) Flame temperature and residence time of fires in dry eucalypt forest. *International Journal of Wildland Fire* **21**, 270–281.

Wotton BM, Martin TL, Engel K (1998) Vertical flame intensity profile from a surface fire. Pages 175-182 in Weber, R. (Chair) Proceedings of the 13th Conference on fire and forest meteorology, Oct. 1996, Lorne, Victoria, Australia. International Association of Wildland Fire, Moran WY.

Appendix 5.1 Development of characteristic heating distance (λ_d) equations

Giving the availability of time-temperature profiles for a number of experiment fires in dry sclerophyll eucalypt forest collected during Project Vesta (McCaw *et al.* 2012, Gould *et al.* 2012) by Wotton *et al.* (2012) we decided to derive λ_d for fires spreading in eucalypt forest instead of using the relationship proposed by Anderson *et al.* (2010) for laboratory fires.

For this work Mike Wotton (Canadian Forest Service/University of Toronto) provided us with data from 15 individual tower measurements where air temperature was measured at 0.5. 1.0, 2.0 and 3.0 m (a few towers also included measurements at 1.5 m). Temperatures were measured using Type K bare wire thermocouples (wire diameter ~ 0.13 mm; bead diameter ~ 0.25 mm) with an estimated 0.4 s response time. Thermocouple size insured effects of radiation were minimised. Measurements were recorded at 1 Hz.

Thermocouple data was paired with each location specific fuel structure and fire behaviour (2-min period) from the Vesta experimental burning dataset. For this subset of the Vesta dataset rate of spread and fireline intensity (as per Byram 1959) varied between 1.05 and 29.8 m min^{-1} and 610 and 23 300 kW m^{-1}, respectively. Assuming steady fire spread prior to arrival of the fire front at each thermocouple tower location, each time-temperature pair was transformed into x-location – temperature pair. From each x-temperature traces at 0.5, 1.0 and 2.0 m we calculated the characteristic heating number by nonlinear regression analysis assuming Eqn. (5.33) form with T_{max} being the maximum temperature measured within the first 0.1 m after arrival of the combustion interface. Accessory fire behaviour quantities calculated for this analysis were: power of the fire, power of the wind and Byram's Convection number (Nelson 2003a); flame fluid vertical velocity (as per Nelson 2003b) and a convective Froude number.

Table 5A.1 summarizes the λ_d average and range at each height. There is a clear trend of increasing λ_d with height from the ground. Also notably, average λ_d estimated at 0.5 m was higher than values calculated by Anderson *et al.* (2010) for measurements conducted on top of the surface fuel layer (average λ_d of 0.2 for the highest intensity fires).

Table 5A.1. Statistics of characteristic heating distance determined at three heights (0.5, 1.0 and 2.0 m) in moderate to high intensity experimental fires in dry sclerophyll eucalypt forest

	CHARACTERISTIC HEATING NUMBER (λ_D)			
HEIGHT (M)	MEAN	STANDARD DEV.	MIN	MAX
0.5	0.43	0.30	0.07	1.06
1.0	0.66	0.49	0.14	1.66
2.0	0.94	0.76	0.27	3.12

Correlation analysis showed λ_d at 0.5 and 1.0 m to be the variables with the highest Pearson correlation coefficient with observed rate of spread (eq. 5A.2). The correlation coefficients found for the λ_d values were substantially higher than the ones found for wind speed and fine dead litter fuels, the two variables that in past empirical modelling approaches have shown the highest explanatory power in the variation of fire rate of spread. λ_d at 0.5 m was significantly correlated with N_C (r = 0.66; p<0.05) and U_5 (r = 0.38; p=p<0.05).

TableA 5.2. Correlation between observed rate of spread and fire and environmental variables for the subset of Vesta fires that were instrumented by Wotton *et al.* (2012)

VARIABLE	PEARSON COEFFICIENT
λ_d at 0.5 m	0.83
λ_d at 1.0 m	0.77
U_5	0.66
N_C	0.49
T_{max} at 0.5 m	0.48
Fuel consumed	0.44
Surface fuel moisture	0.40

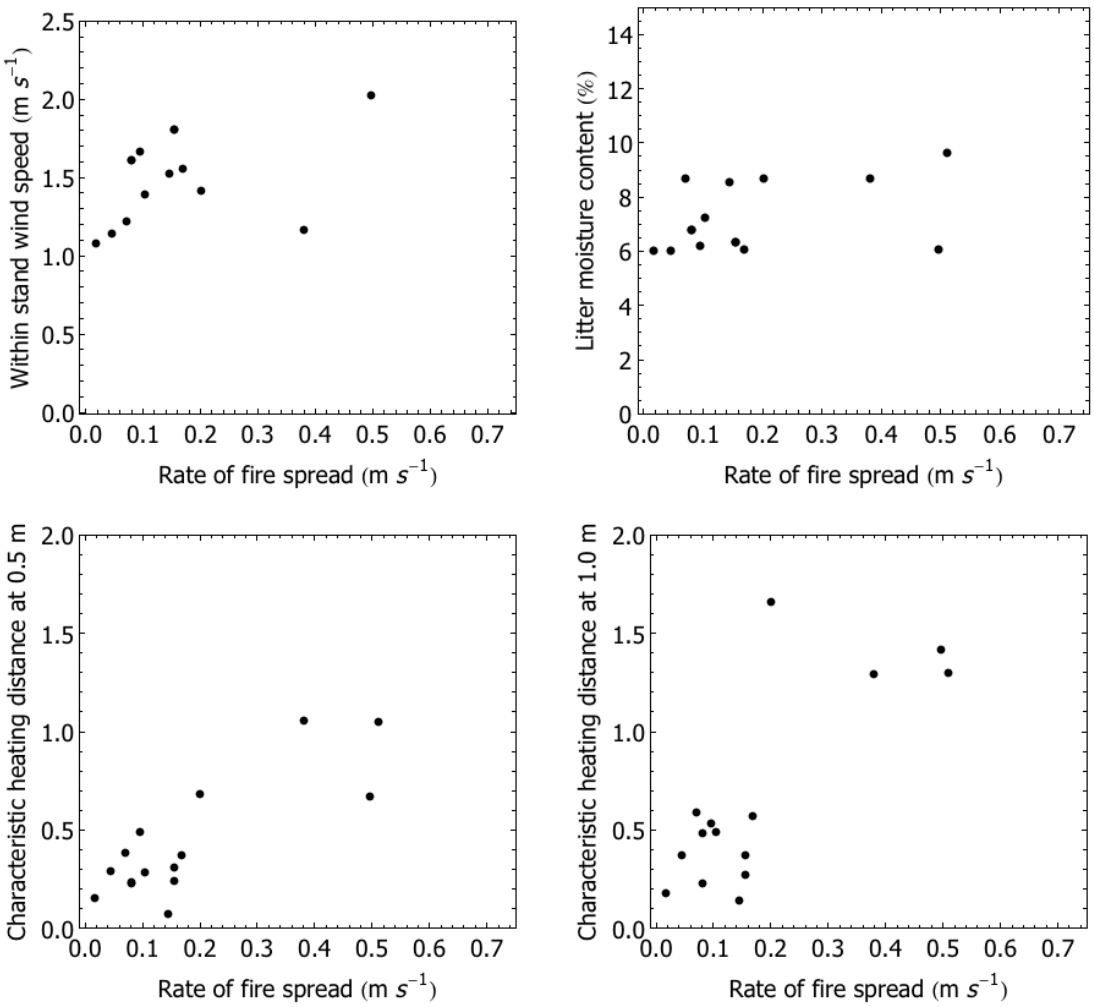

Figure A5.1. Relationship between rate of fire spread and (a) within stand wind speed; (b) litter fuel dead fuel moisture content; (c) characteristic heating distance at 0.5 m; and (d) characteristic heating distance at 1.0 m. Data source is a subset of the Vesta fire database (McCaw *et al.* 2012) for which time-temperature data has been measured (Wotton *et al.* 2012).

Exploratory analysis showed λ_d to be a function of wind speed but also of the interaction between the fire and the wind field. For a fixed wind velocity, the higher the buoyancy forces generated by the fire the more acute the angle of ascent of flame generated gases is and the smaller the λ_d. λ_d at 0.5 m was modelled through nonlinear regression analysis as:

$$\lambda_d(z = 0.5) = \beta_1 \, {U_s}^{\beta_2} {N_C}^{\beta_3} \qquad [5A.1]$$

with the coefficients *β*1,…, *β*3 estimated as follows (with asymptotic standard errors in parentheses): 0.0427 (0.034), 1.157 (0.455) and 0.468 (0.112), respectively. The equation produced an adjusted R^2 of 0.83. Analysis of the variation of λ_d with height suggested an increase of 0.4 per vertical meter.

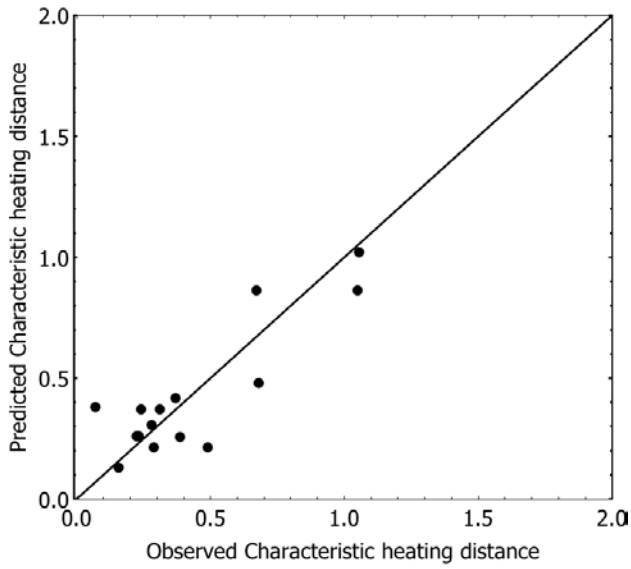

Figure 5A.2. Observed vs. predicted characteristic heating distance (λ_d) at 0.5 m for experimental fires in dry sclerophyll eucalypt forests.

Taking into account this variation and the λ_d estimated by Anderson et al (2010) at the top of a litter layer, a first approach to model this variable with *z* follows:

If z is equal to the top of litter fuel layer, i.e., *z* = 0:

$$\lambda_d(z) = 0.002 + 0.08 \, U_s \qquad [5A.2a]$$

If 0 < z < 0.5 m:

$$\lambda_d(z) = \lambda_d(0) \left(0.0427 \, {U_s}^{1.157} \, {N_C}^{0.468} - (0.002 + 0.08 \, U_s)\right) \left(\frac{0.5-(0.5-z)}{0.5}\right) \qquad [5A.2b]$$

If z > 0.5 m:

$$\lambda_d(z) = 0.0427 \, {U_s}^{1.157} \, {N_C}^{0.468} + 0.4(z - 0.5) \qquad [5A.2c]$$

6 Fire suppression resource allocation framework

6.1 Introduction

Wildfire management agencies have traditionally determined the number and type of suppression resources appropriate for different regions based on the experience and intuition of senior managers (Martell 1982; Martell and Boychuk 1997). However, there is now a greater public expectation of fire management and as a result more scrutiny of performance and need to be accountable for the costs associated with fire suppression and other fire management tasks. Some fire management agencies have sought analytical systems to help them to quantitatively determine the optimal amount and configuration of firefighting resources for a given budget.

6.1.1 SUPPRESSION RESOURCE ALLOCATION MODELS

Wildfire suppression resource allocation models are systems designed to estimate the optimal number and mix of wildfire suppression resources. These modelling systems simulate fire environments and management systems and by doing so can be used to test a range of alternative resourcing and budget scenarios to see their operational effects without consequence (Fried and Gilless 1999), thereby aid long term strategic planning. They can also be used for broader research applications such as estimating the effects of changing climate and ignition frequencies on suppression outcomes (e.g. McAlpine 1999, Fried *et al.* 2004; 2008).

Only a few wildfire suppression resource allocation modelling systems have been developed, probably due to the long term commitment and associated cost required for their development. At present operational wildfire resource allocation modelling systems have only been developed and implemented in two regions, California (USA) and Ontario (Canada). CALFIRE (the agency responsible for fire management on Californian state lands) uses the California Fire Economics Simulator (CFES2) (Fried and Gilless 1999) to anticipate the consequences of organisational changes by measuring the capability of initial attack forces to contain wildfires before they can become large and damaging (CAL FIRE 2007).

The Ontario Ministry of Natural Resources developed the Level of Protection Analysis System (LEOPARDS) (McAlpine and Hirsch 1999) and have been using it to determine the level of protection required to support their strategic planning and policy development. Other previously developed systems exist but are too simple to meet current agency requirements and expectations so are no longer in use. A detailed review of resource allocation modelling systems was presented in Plucinski (2012a).

Resource allocation modelling systems are regionally specific in their inputs and application as they require information about the local environment (e.g. fire regimes, ignition patterns, weather and fuels) and agency policies, procedures and suppression resource availability (including management zones, deployment and dispatch protocols). The existing systems have been developed for regions within North America and cannot be directly transferred to

Australia in their current formats because Australian fire environments and fire management systems are substantially different to those where these systems were developed.

The existing resource allocation modelling systems have common input modules that act to simulate the regional fire environment, resource characteristics and suppression strategies. The characterisation of the regional environment relies on local weather and fire incidence data or simulations. The number and type of available resources are typically specified by the user and their response and productivity capabilities are based on models specific for each resource type. Suppression strategies are based on agency protocols and rules. Existing models only deal with fires during the initial attack phase as computations for the suppression of larger fires is too difficult to generalise because the containment of such fires requires tactics that cater to the specific conditions of each fire.

Resource allocation modelling systems undertake simulations at a daily scale with summarised outputs encompassing multiple fire seasons. Outcome statistics are generated for each day and these are compiled over multiple seasons to determine average outputs at a seasonal scale and the variation in these. Output statistics summarise the number of fires that escape initial containment efforts within a simulation run, as well as estimates of the suppression cost and resource effort.

6.1.2 OBJECTIVE

The objective of the work undertaken in this component of the Fire Development, Transitions and Suppression project was to produce a bushfire suppression resource allocation modelling framework suitable for application in regions of Australia. A model developed from such a framework would be able to simulate wildfire management in a way that would reliably allow management options to be tested and compared for contemporary and altered (e.g. due to climate change) fire environments. This chapter summarises previous work on this topic, including a review of existing resource allocation models (Plucinski 2012a), frameworks for suppression response and productivity and fire history and weather models (Plucinski 2012b, 2013a) and an overall structure for a resource allocation model framework (Plucinski 2013b).

6.2 Proposed model structure

The structure proposed for an Australian bushfire suppression resource allocation model is depicted in Figure 6.1. The raw inputs describing the spatial environment (green boxes: human population, fuels, weather and terrain) and fire history information (orange box) will be used to inform the calculation of fire load (number, extent and behaviour of fires in the landscape) through a modelling process designed to simulate daily fire incident inputs and fire growth and development models. The raw spatial inputs will also inform fireline production rates and resource response times (purple boxes) along with input information describing the available suppression resources and dispatch protocols (blue boxes) to estimate the suppression capability available for each simulation scenario. The fire load and suppression capability will subsequently be used in containment simulations which will run scenarios for individual fires and will be able to deals with multiple fires on a given day and fires that are burning concurrently.

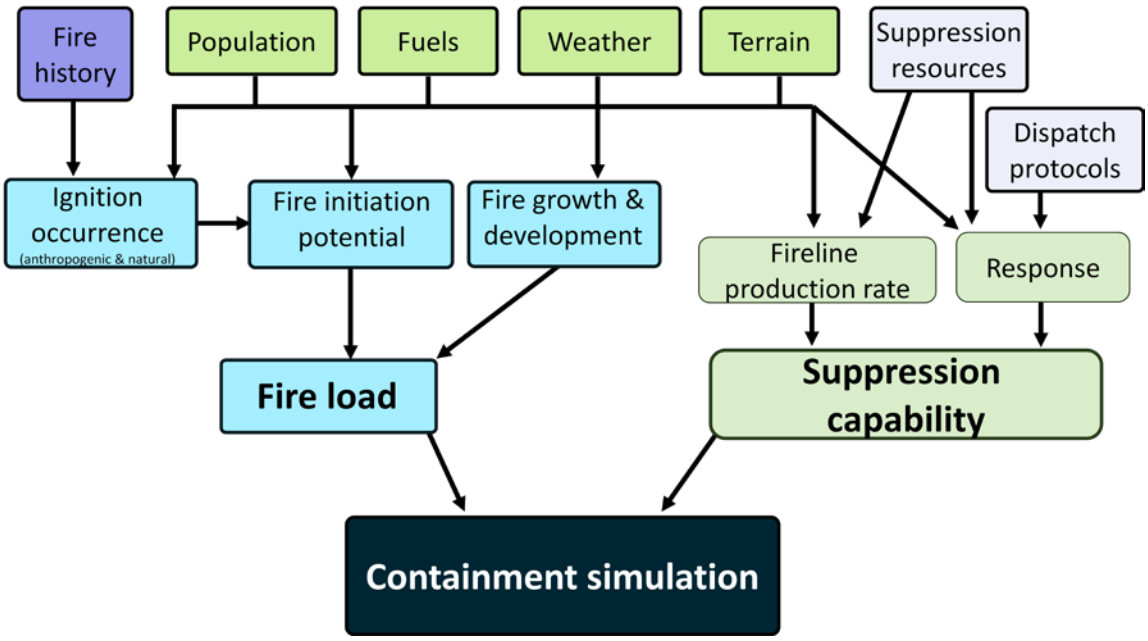

Figure 6.1. Proposed structure of a suppression resource allocation model for Australian bushfire management regions.

The containment simulation estimates the containment of specific fire scenarios based on fire perimeter growth and fire perimeter suppression. Each fire scenario will have a specific ignition time and location, which will have associated weather conditions. Fire growth models (Chapters 4 and 5) will be used for this function and will use this information to estimate the fire size at detection and initial attack and will continue to predict fire growth until a fire is contained (Figure 6.2). Resource response models and dispatch protocols will determine the time taken for resources to arrive at the fire. Productivity models will be used to simulate suppression until the fire is contained. Following containment, information specific to the fire that summarise the suppression effort (e.g. resource use and cost) and the fire outcome (e.g. area burnt), will be compiled with that from other fires. The aggregation of these results over multiple seasons will be summarised at a seasonal level to provide outputs for given input scenarios. Given the stochastic nature of the inputs, a large number of seasonal simulations would need to run to give meaningful results (e.g. Fried *et al.* (2006) considered 100 simulated fire seasons).

6.2.1 FIRE HISTORY AND WEATHER INPUTS

Fire and weather simulation inputs cover a range of variables drawn from historical records that would be used to provide the spatial and temporal probabilities of fire occurrence and the conditions in which they occur. These inputs are critical for defining the simulation parameters for the application of resource allocation models. Without these inputs, simulations may not be able to represent the range and frequency of conditions and events that are experienced in the areas to which resource allocation models are applied. The development of these simulation parameter inputs from historical datasets has been

reported to take a significant proportion of the entire effort required to develop a resource allocation model (Fried *et al.* 2006).

Historical fire and weather data would be used to develop spatial and temporal fire occurrence models (see Chapter 2) that would feed into an Australian resource allocation model. The structure of the databases required for these inputs is illustrated in Figure 6.3. Weather inputs will include standard metrological units such as temperature, humidity, wind speed and rainfall, which will be used to determine relevant fire danger indices and to model fuel moisture.

The raw weather inputs can be sourced from Bureau of Meteorology records. Fire incident database inputs would come from agency fire records that include information identifying each fire and containing information about each fire's timing, cause and location. Geographic data inputs would come from fire and land management agency spatial databases.

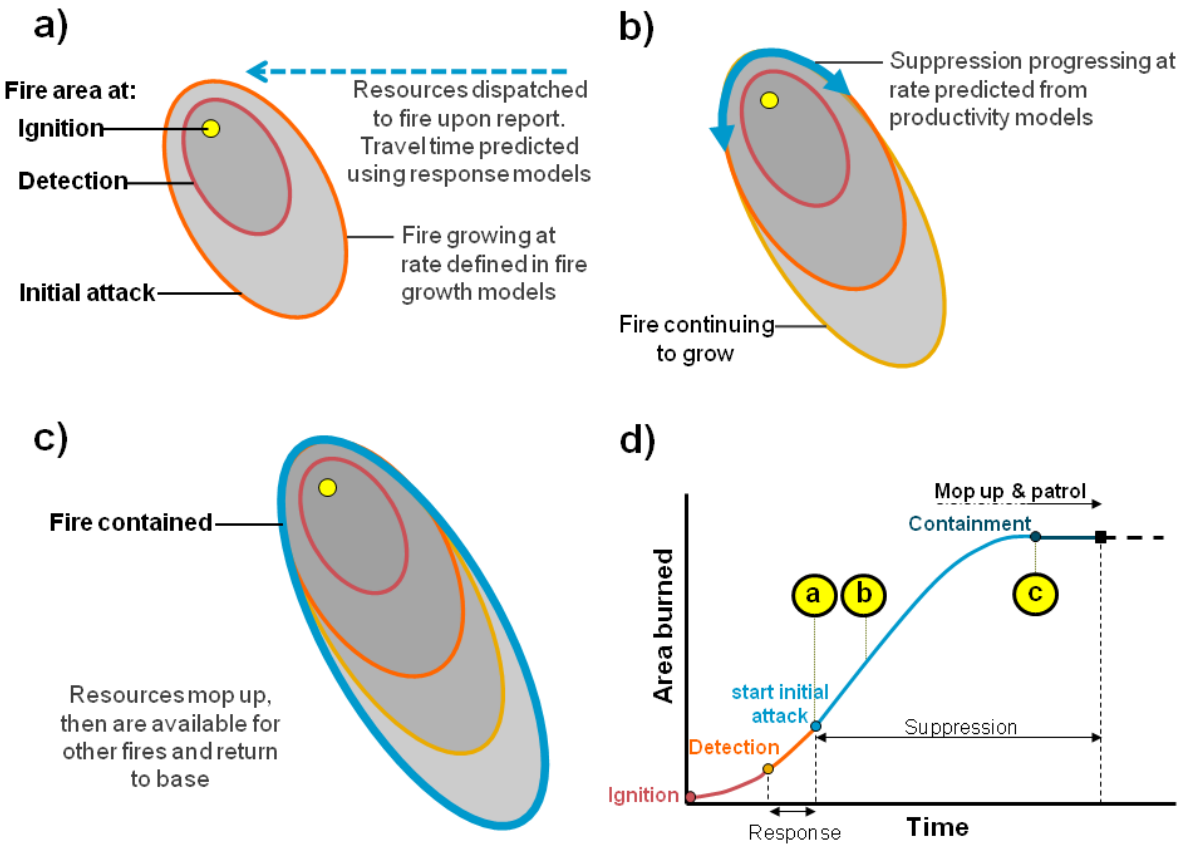

Figure 6.2. Stylised example of a containment simulation for a simple fire. a) unsuppressed fire growth from ignition until initial attack, b) initial attack suppression in progress, c) fire containment and d) plot of fire area with time, showing points associated with a, b and c.

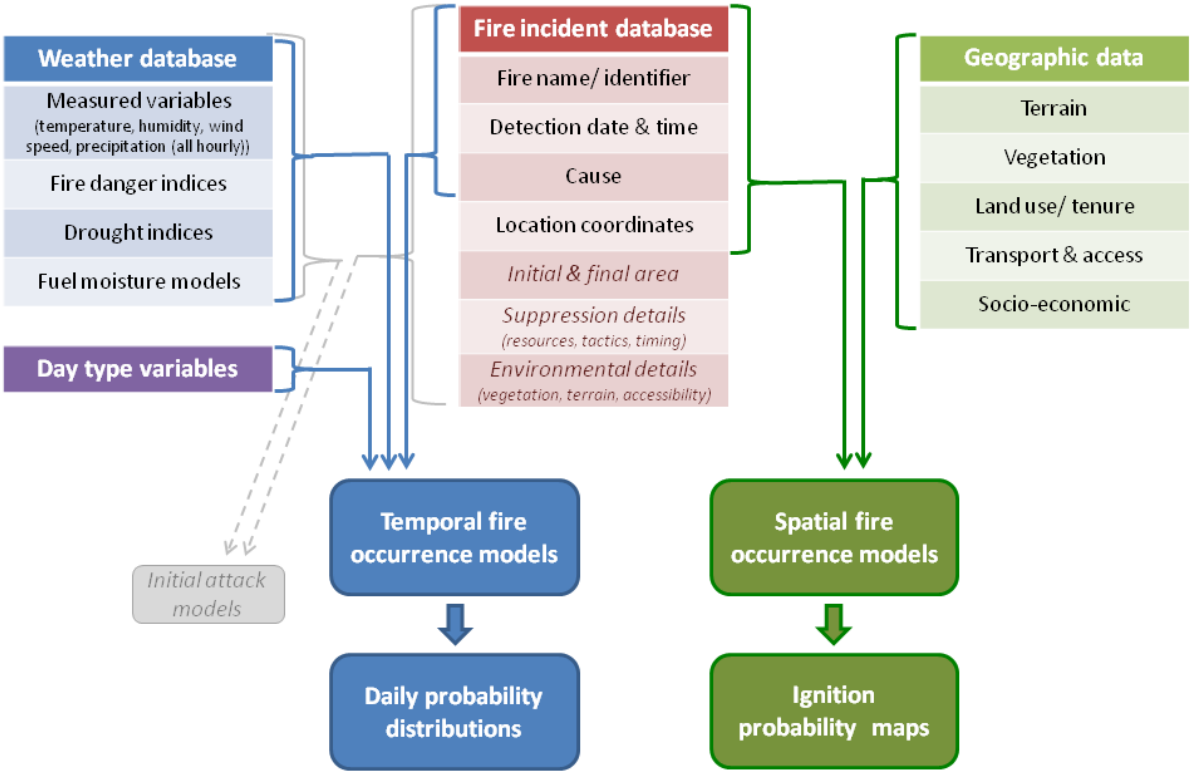

Figure 6.3. Proposed database structure for weather, fire incidents and geographic inputs required for the development of spatial and temporal occurrence models.

Temporal fire occurrence models would be developed to estimate daily distributions for the probability of one or more fires occurring, the number of fires that may occur on that day and the time of the day that these fires might occur (Figure 6.4). These distributions would be based on variables related to fuel availability and causal agents (e.g. Cunningham and Martell 1973, Vega Garcia 1995, Wotton et al 2003, Wotton and Martell 2005, Albertson *et al.* 2009, Wotton *et al.* 2010).

The fire occurrence models will need to treat fires with different causes separately as they have different causal agents (Reineking *et al.* 2010, Vilar *et al.* 2010, Wang and Anderson 2010, Wotton *et al.* 2010). In practice the cause categories that can be used will be limited by those available in the source data. At a minimum, lightning and human-caused fires should be considered separately but ideally human-caused fires would be further split into those that are deliberate (arson) and accidental as these have different temporal patterns (see Chapter 2).

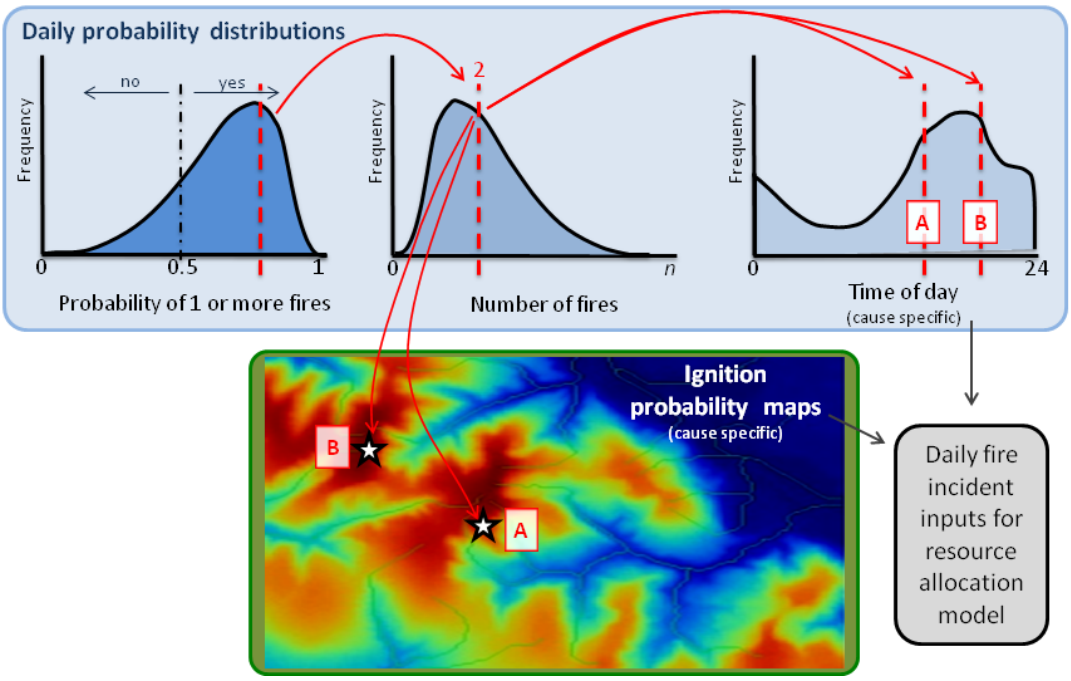

Figure 6.4. Proposed process for obtaining daily fire ignition numbers, times and locations for resource allocation model simulations. The red arrows represent random sampling from the modelled temporal and spatial distributions.

Spatial fire occurrence models would be used to predict the spatial ignition probability in relation to geographic variables, such as terrain and human landscape features (e.g.: Beverly *et al.* 2009, Cardille and Ventura 2001, Díaz-Delgado *et al.* 2004, Syphard *et al.* 2008, Penman *et al.* 2013). Predictor variables may include proximity measures such as distance between an ignition and the nearest road, density measures such as population per square kilometre, or those related to fuels or vegetation condition. Ignition probability maps developed from these models will be used to determine realistic fire locations for the different ignition class categories (e.g. Figure 6.4). These maps can be manipulated for scenario analysis by altering predictor variable layers. Such analyses could be undertaken to investigate issues such as land use changes.

The temporal and spatial fire occurrence models would be used to estimate the daily fire counts and locations using random samples of modelled distributions calculated from the simulated weather for each day, as illustrated in Figure 6.4. In the first step, the probability that a day will have one or more fires will be determined by taking a random sample from a modelled probability distribution. If this probability is greater than a user defined cut-off value then the number of fires for the day will be determined by taking a random sample from the probability distribution for the number of daily fires. Following this, the time of ignition will be determined for each fire by sampling the ignition time distribution for the fire cause type and the location of each ignition will be determined using the ignition probability layer for the fire cause class.

6.2.2 RESOURCE RESPONSE INPUTS

Resource response time is the time taken for a suppression resource to reach a fire once the fire has been reported and the resource has been requested. It incorporates the reaction time (time between dispatch and departure) and travel time (time between departure and arrival) (NWCG 2011). Some previous studies have considered reaction and travel times for tankers and other ground-based resources and have developed spatial models predicting response times from resource bases (e.g. fire stations) that are influenced by road types and distance (e.g.: Hatfield *et al.* 2008, Mees 1978, Wilson and Wiitala 2003, Wilson and Wiitala 2005).

Reaction time is influenced by the timing of the report of fire occurrence, the readiness level, which is usually set by a policy related to a weather index, and the fire load (the number, extent and behaviour of active fires in the landscape) at the time of the report. Travel time calculations are relatively simple for aircraft and can be estimated using cruise speed and distance, assuming a direct route is taken (e.g.: Simard 1978). Travel times for ground-based resources can be predicted by determining the quickest route to the fire and estimating the time taken to travel on different parts of the route based on differences in road quality, gradient and distance from trafficable roads (Wilson and Wiitala 2003). A conceptual structure for a response time database input module for a resource allocation model is given in Figure 6.5.

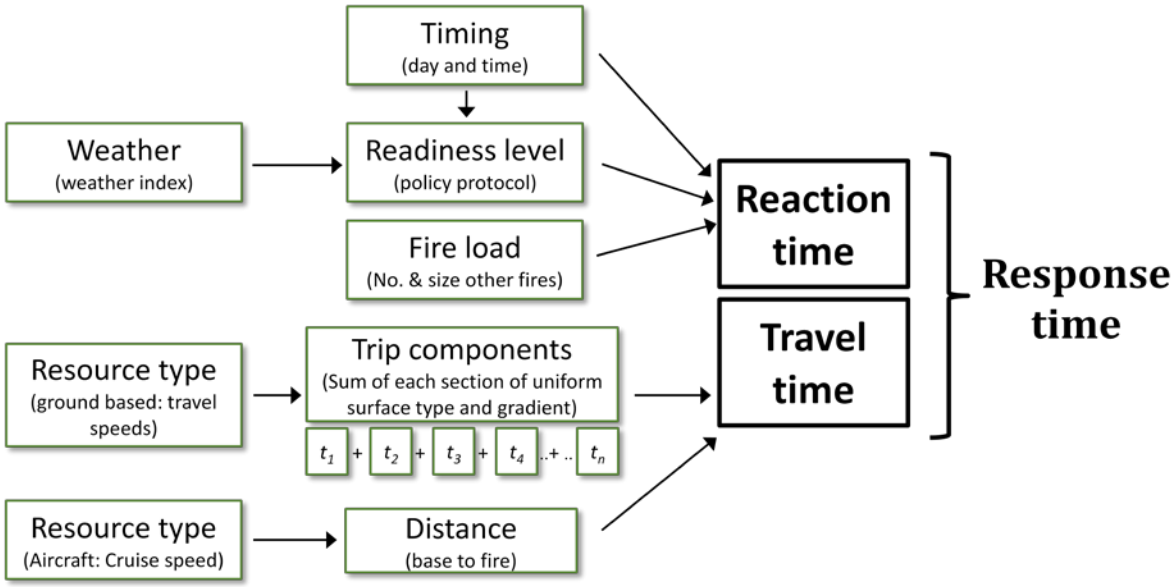

Figure 6.5. Conceptual structure for a response time database input module for a resource allocation model.

6.2.3 RESOURCE PRODUCTIVITY INPUTS

Resource productivity is the rate of fireline construction for a particular type of suppression resource. It is expressed as the length of fireline constructed in a given time and is influenced by fire and environmental conditions. The term fireline is defined as a natural or constructed barrier, or treated fire edge, used to limit the spread of fire (NWCG 2011), which can include sections of fire edge that have been treated either with suppressants or

retardants, or has had adjacent fuels removed through the creation of a mineral earth barrier, to prevent fire progression. The term "fireline construction rate" has been typically been used to describe the rate of establishment of a line that is completely clear of fuels exposing mineral earth. This break in the fuel provides a physical separation between burning and unburnt fuels that aims to stop the fire spread.

All wildfire productivity models and resource allocation models have only considered direct attack or parallel attack tactics as they have focussed on initial attack (e.g.: Fried and Gilless 1999, McAlpine and Hirsch 1999). Studies of large wildfire containment (e.g.: Finney *et al.* 2009, Holmes and Calkin 2012, Mees and Strauss 1992, Wei *et al.* 2011) have also been limited to these tactics. It would be very difficult to include indirect attack in a resource allocation model as decisions regarding when and how to use it can be complex with many contributing factors (e.g. forecast weather, terrain, fuel type and load, strategic premise).

The effort required to produce fireline depends on a number of interacting environmental factors as well as other factors relating to the resource itself, and the longevity and turnaround time for the resource. The interactions between and within these form the conceptual structure for the productivity database input module and are illustrated in Figure 6.6. The interactions and the relative strength of the links would vary with resource type. The variables associated with each input type are listed within the input boxes.

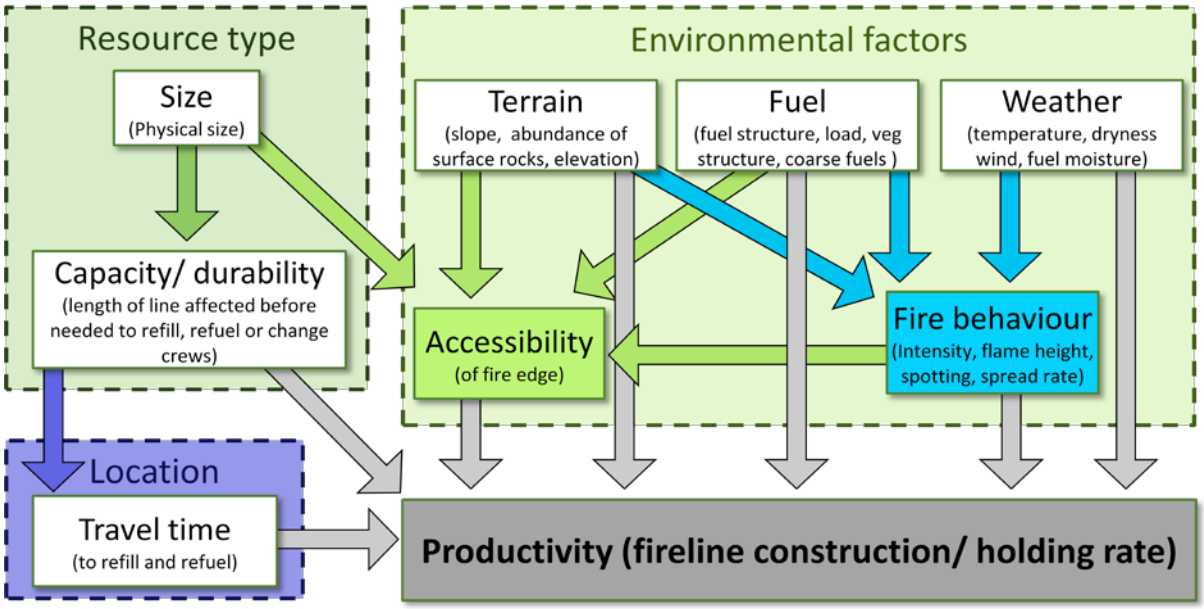

Figure 6.6. Conceptual structure for a productivity database input module for a resource allocation model.

The key environmental input areas influencing productivity are terrain, fuel and weather, which influence on fire behaviour and accessibility. The feasibility of direct attack is strongly dependant on fire behaviour. Some studies have established fire intensity thresholds for the limits of direct attack for some resource types (e.g.: Alexander 2000, Loane and Gould 1986). When fire intensity is above these thresholds suppression actions are limited to roles such as property protection, rather than line construction.

The type of resource also has a strong influence on productivity. Different resources are suited to different conditions. The capacity of some resource types (e.g. tankers and

aircraft) influences the amount of fireline that can be attacked at a time, before the resource needs to be refilled. Refuelling resources is also important in this regard. The distance between a fire and refilling and refuelling points (fixed and mobile) impacts the productivity of different resource types, with aircraft being the most influenced by this.

6.3 Conclusions

Strategic resource allocation modelling systems are complex and require considerable time to develop. They have been developed for few specific regions and fire management agencies around the world. None of the fully developed systems from overseas can be directly transferred to Australia in their current formats. This is because fire environments in regions of Australia are substantially different to those where these systems were developed.

The proposed structure for an Australian Suppression Resource Allocation Modelling system (ASRAMS) presented in Figure 6.1 has some similarities to the structure of CFES2 (Fried and Gilless 1999)and LEOPARDS (McAlpine and Hirsch 1999), mainly due to the organisation of the input modules. The main differences between the proposed model and the existing ones is within the input modules where there is a need to represent regional environments, systems and resources. The majority of work required to develop strategic resource allocation models for Australian regions would be in the development of these input modules and it is likely that core fire suppression processes could be adapted from existing models, as the simulated daily fire management procedures are quiet similar.

Developing the fire occurrence models will rely on data from agency fire history and geographic databases as well as meteorological records from the Bureau of Meteorology. More work will be required to develop resource response and productivity models as there are no existing databases and this work will require the capture of new data. Finally, robust fire initiation and growth models for fires in Australian fuel types and weather conditions (Chapter 3, 4 and 5) are an essential component of the containment simulation.

The first steps in developing Australian strategic resource modelling systems will be to select an initial case study region and to establish input components for this region. This will require significant support from local fire management agencies who will need to provide occurrence and response data. New developments in existing systems should continue to be monitored.

6.4 References

Albertson K, Aylen J, Cavan G, McMorrow J (2009) Forecasting the outbreak of moorland wildfires in the English Peak District. *Journal of Environmental Management* **90**, 2642-2651.

Alexander ME (2000) Fire behaviour as a factor in forest and rural fire suppression. Forest Research, Rotorua, in association with the New Zealand Fire Service Commission and the National Rural Fire Authority, Wellington., Forest Research Bulletin No. 197. Forest and Rural Fire Scientific and Technical Series, Report No. 5., Christchurch, New Zealand.

Beverly JL, Herd EPK, Conner JCR (2009) Modeling fire susceptibility in west central Alberta, Canada. *Forest Ecology and Management* **258**, 1465-1478.

CAL FIRE (2007) The California Fire Economics Simulator (CFES2). http://frap.cdf.ca.gov/tools/CFES. Last accessed 26/11/2013.

Cardille JA, Ventura SJ (2001) Occurrence of wildfire in the northern Great Lakes Region: Effects of land cover and land ownership assessed at multiple scales. *International Journal of Wildland Fire* **10**, 145-154.

Cunningham AA, Martell DL (1973) A stochastic model for the occurrence of man-caused forest fires. *Canadian Journal of Forest Research* **3**, 282-287.

Díaz-Delgado R, Lloret F, Pons X (2004) Spatial patterns of fire occurrence in Catalonia, NE, Spain. *Landscape Ecology* **19**, 731-745.

Finney M, Grenfell IC, McHugh CW (2009) Modeling containment of large wildfires using generalized linear mixed-model analysis. *Forest Science* **55**, 249-255.

Fried JS, Gilless JK (1999) CFES2: The California fire economics simulator version 2 user's guide. University of California, Division of Agriculture and Natural Resources Publication, 21580.

Fried JS, Gilless JK, Riley WJ, Moody TJ, Simon de Blas C, Hayhoe K, Moritz M, Stephens S, Torn M (2008) Predicting the effect of climate change on wildfire behavior and initial attack success *Climatic Change* **87**, 251-264.

Fried JS, Gilless JK, Spero J (2006) Analysing initial attack on wildland fires using stochastic simulation. *International Journal of Wildland Fire* **15**, 137-146.

Fried JS, Torn MS, Mills E (2004) The impact of climate change on wildfire severity: a regional forecast for northern California. *Climatic Change* **64**, 169-191.

Hatfield DC, Wiitala MR, Wilson AE, Levy EJ (2008) A fast method for calculating emergency response times using travel resistance surfaces. *General Technical Report - Pacific Southwest Research Station, USDA Forest Service*, 591-596.

Holmes TP, Calkin DE (2012) Econometric analysis of fire suppression production functions for large wildland fires. *International Journal of Wildland Fire* **22**, 246-255.

Loane IT, Gould JS (1986) *Aerial suppression of bushfires: cost-benefit study for Victoria*. CSIRO Division of Forest Research: Canberra.

Martell DL (1982) A review of operational research studies in forest fire management. *Canadian Journal of Forest Research* **12**, 119-140.

Martell DL, Boychuk D (1997) Levels of fire protection for sustainable forestry in Ontario: a discussion paper. In *NODA/NFP Technical Report*, Natural Resources Canada, Canadian Forest Service, Ontario Region: Sault Ste. Marie Canada. 34 pp.

McAlpine RS (1999) Searching for a climate change effect in fire management expenditures. *International Journal of Wildland Fire* **9**, 203-206.

McAlpine RS, Hirsch KG (1999) An overview of Leopards: the level of protection analysis system. *The Forestry Chronicle* **75**, 615-621.

Mees RM (1978) Computing arrival times of firefighting resources for initial attack. USDA Forest Service, PSW-27, Pacific Southwest Forest and Range Experiment Station, Berkeley California, USA.

Mees RM, Strauss D (1992) Allocating resources to large wildland fires: a model with stochastic production rates. *Forest Science* **38**, 842-853.

NWCG (2011) Glossary of Wildland Fire Terminology. National Wildfire Coordinating Group, Boise, ID. http://www.nwcg.gov/pms/pubs/glossary. Last accessed 26/11/2013.

Penman TD, Bradstock RA, Price O (2013) Modelling the determinants of ignition in the Sydney Basin, Australia: implications for future management. *International Journal of Wildland Fire* **22**, 469-478.

Plucinski MP (2012a) Review of strategic wildfire resource allocation modelling systems. CSIRO Ecosystem Sciences and CSIRO Climate Adaptation Flagship Client Report EP12149, Canberra ACT.

Plucinski MP (2012b) Database structure for resource response time and production input modules for a resource allocation model. CSIRO Ecosystem Sciences and CSIRO Climate Adaptation Flagship Client Report EP127657, Canberra ACT.

Plucinski MP (2013a) Database structure for historical fire and weather input module for a resource allocation model. CSIRO Ecosystem Sciences and CSIRO Climate Adaptation Flagship Client Report EP1312291, Canberra ACT.

Plucinski MP (2013b) Proposed structure for an Australian resource allocation framework. CSIRO Ecosystem Sciences and CSIRO Climate Adaptation Flagship Client Report EP1312289, Canberra ACT.

Reineking B, Weibel P, Conedera M, Bugmann H (2010) Environmental determinants of lightning- v. human-induced forest fire ignitions differ in a temperate mountain region of Switzerland. *International Journal of Wildland Fire* **19**, 541-557.

Simard A (1978) AIRPRO - an air tanker productivity computer simulation model: the equations (summary). Canadian Department of Fisheries and the Enviroment, Canadian Forestry Service, Forest Fire Research Institute, FF-X-66 part1, Ottawa, Ontario.

Syphard AD, Radeloff VC, Keuler NS, Taylor RS, Hawbaker TJ, Stewart SI, Clayton MK (2008) Predicting spatial patterns of fire on a southern California landscape. *International Journal of Wildland Fire* **17**, 602-613.

Vega-Garcia C, Woodard PM, Titus SJ, Adamowic V, Lee BS (1995) A logit model for predicting the daily occurence of human caused forest fires. *International Journal of Wildland Fire* **5**, 101-111.

Vilar L, Nieto H, Martin MP (2010) Integration of lightning- and human-caused wildfire occurrence models. *Human and Ecological Risk Assessment* **16**, 340-364.

Wang YH, Anderson KR (2010) An evaluation of spatial and temporal patterns of lightning- and human-caused forest fires in Alberta, Canada, 1980-2007. *International Journal of Wildland Fire* **19**, 1059-1072.

Wei Y, Rideout DB, Hall TB (2011) Toward efficient management of large fires: A mixed integer programming model and two iterative approaches. *Forest Science* **57**, 435-447.

Wilson AE, Wiitala MR (2003) Estimating travel times to forest-fires using resistance surfaces. In *Twenty-Third Annual ESRI International User Conference*. unpaginated CD-ROM, Environmental Systems Research Institute, Inc., Redlands, California: San Diego, California.

Wilson AE, Wiitala MR (2005) An empirically based model for estimating wildfire suppression resource response times. In *System analysis in forest resources: proceedings of the 2003 symposium.* (Eds M Bevers and TM Barrett) U.S. Department of Agriculture, Forest Service, Stevenson, WA. pp. 189-194.

Wotton BM, Martell DL (2005) A lightning fire occurrence model for Ontario. *Canadian Journal of Forest Research* **35**, 1389-1401.

Wotton BM, Martell DL, Logan KA (2003) Climate change and people-caused forest fire occurrence in Ontario. *Climatic Change* **60**, 275-295.

Wotton BM, Nock CA, Flannigan MD (2010) Forest fire occurrence and climate change in Canada. *International Journal of Wildland Fire* **19**, 253-271.

7 Discussion and conclusions

This work represents the first comprehensive effort to investigate the behaviour of a bushfire from its inception and initiation, its growth and transitions through fuel strata, to its development to steady-state rate of spread, and also provides a framework within which to combine this knowledge. While previous research efforts have considered aspects of the bushfire lifecycle (ignition, growth, suppression), these have not done so for a consistent vegetation type nor in the context of providing critical fire behaviour information necessary to enable fire authorities to make improved decisions regarding firefighting resource requirements.

Such critical fire behaviour information includes determination of:

- the potential for fires to break out (determined from analysis of recent historical fire occurrences)
- how long fire authorities will have before a fire completes its acceleration phase and achieves a steady-state rate of spread for the conditions (and thus may be beyond the direct suppression efforts of initial attack)
- the conditions necessary for that fire to develop sufficiently to involve more than just the surface litter fuels (and thus the potential for it to escalate into a high intensity crown fire), changing the expected rate of spread of the fire, and
- the probability that firebrands generated by the fire will successfully initiate sustained fire spread in the form of spotfires ahead of the main fire, which restarts the bushfire lifecycle.

This information (obtained here for the most prevalent forest type in the country (dry sclerophyll forest), combined within the framework for construction of an Australian Suppression Resource Allocation Modelling System (ASRAMS), provides the vehicle for allowing fire authorities to predict and manage the expected demand for fire fighting resources for a given region over a given period. This expected demand will depend on a number of factors related to suppression capability and capacity but also on the current fire load (the number and extent of fire already burning in the landscape) and the expectation of new fire outbreaks and the rate at which these fires will develop and spread (future fire load).

Our existing knowledge of bushfire behaviour and the current operational tools developed for prediction of their spread assume that fires have completed development from ignition and have reached steady-state behaviour for the environmental conditions. That is, fires have finished any post-ignition acceleration and are moving at a speed commensurate to the prevailing conditions.

We have long known that initiating fires, particularly those starting from a point ignition (such as a dropped match, lightning strike or firebrand), spread relatively slowly for the prevailing conditions and accelerate up to the steady-state rate of spread. This fire growth

period has been observed to be as short as a couple of minutes in grassy fuels under blustery conditions, up to days for a slow moving forest fire under mild conditions. Attempts to identify the factors that influence this acceleration period have floundered due to the complexity of the phenomena which is influenced by a combination of biological, topographic and meteorological variations compounded by the highly complex and often chaotic (and seemingly capricious) nature of open biomass combustion.

This project has attempted to develop foundational knowledge of the potential for fire outbreaks to develop to the point where they are burning at the steady-state rate of spread for the prevailing conditions and are thus beyond the potential for successful initial suppression using direct attack strategies (i.e. ascertaining the window of opportunity for successful initial attack). This foundational knowledge has been developed for a particular set of circumstances (south-west Western Australia, dry eucalypt forest, limited fine fuel moisture contents, limited wind speed regimes, etc.) but the research results (methodologies, data analysis techniques, numerical model forms) are applicable more generally and may be used to develop either generic models for broad application or other specific models for particular application.

7.1 Fire occurrence (Chapter 2)

Determining the potential for fires to break out on a given day and the number of fires that might be expected is an essential step in determining the future fire load for a given region. The research carried out in the development of a fire occurrence model for Australian conditions utilised the case study area of Perth and surrounding regions. As a result, the analyses of the historical fire occurrence data for these locations are specific to those regions. However, the methodologies developed for the analysis and many of the results of the analyses themselves are pertinent to other locations in the country.

Fire occurrence was investigated via two components: the expected number of human caused fires per day and the timing of fire outbreaks for a range of fire cause categories. Each considered a number of potential independent variables that might be used as predictor variables including environmental (e.g. fuel and weather), day type (e.g. weekend and school holiday) and recent fire activity.

It was found that fires caused by cutting and welding sources, small open fires, incendiary arson, lightning and vehicles had higher rates of occurrence on days of very high fire danger than days of extreme fire danger when total fire bans are likely to have been declared. Fires attributed to electrical failures, fireworks and explosives, rekindled previous fires, cigarettes and smoking materials and lightning had daily occurrence rates on days of elevated fire danger that were four or more times greater than for all days.

While the magnitude of the occurrence results for the range of potential fire sources is likely to vary across the country, the nature of the results are likely to be similar due to the nature of the fire sources and their potential to initiate successful ignitions. Those ignition sources that have relatively low heat flux potential (e.g. sparks, embers, etc), are more likely to result in a successful ignition when the moisture content of the fuel is suitably low and thus ignitability of the fuel is high.

Those ignition sources that are likely to be reduced by the introduction of a total fire ban are more likely to have lower occurrence when a total fire ban has been called but will have a higher occurrence when fire conditions are just below that of a total fire ban.

7.2 Spotfire initiation (Chapter 3)

The phenomenon of spotting is not unique to the Australian environment, occurring in nearly all vegetation types around the world to various extents. In dry eucalypt forests, however, spotting and in particular mass spotting, is a hallmark of extreme fire behaviour. Understanding the potential for, and the development and behaviour of, spotfires is essential to developing a full and complete understanding of bushfire behaviour under all fire weather conditions but most importantly under extreme conditions.

The research work undertaken here concentrated on the ignition potential of flaming and glowing firebrand material (pieces of combustion biomass) in dry sclerophyll litter fuel beds; however the results on ignition probability are just as relevant to other ignition sources. Those low heat flux sources identified in the previous fire occurrence study as being important when fuel moisture contents are low (e.g. sparks, embers, etc), will have the same or similar phenomenology as that of firebrands.

In all cases studied, the presence of wind played a critical role in ignition success. In the absence of wind a critical threshold fuel bed moisture content of 14% was found for flaming firebrands to successfully ignite the fuel bed. Ignitions at fuel bed moisture contents greater than 14% will be unstainable. Ignitions occurring at a moisture content of 9% will have a 50% ignition probability. That is, at a fuel bed moisture content of 9%, approximately half of the firebrands that land in the fuel bed will successfully ignite the fuel bed.

When wind was present, the critical threshold fuel bed moisture content for successful ignition from a flaming firebrand was found to increase to 21%, with a 50% probability of ignition occurring at a moisture content of 13%. At a moisture content of less than 7% in the presence of wind, ignition from a flaming firebrand was found to be consistently successful.

For glowing firebrands, the magnitude of the wind was found to be important. In a wind speed of 2 m s^{-1} at fuel level (equivalent to about 30 km h^{-1} in the open), a critical threshold fuel moisture content of 10% was found for ignition to occur.

These results, taken with those of the fire occurrence study, suggest that the presence and strength of wind is essential for ignitions from low heat flux sources such as firebrands and embers to be successful. However, strength alone is not sufficient for ignition to be success, particular for ignition sources at the lower limit of heat output—the turbulence in the air flow is also likely to be a primary agent of ignition success.

The more turbulent the air flow, the larger the difference between the gust component and the lull component, the greater the potential for an ignition source to result in a successful ignition. Higher, more consistent air flow is likely to result in much of the heat output from a source being advected away from the fuel bed, cooling the source and reducing the potential for ignition to occur.

Glowing firebrands in particular are likely to be influenced by the gust-lull structure of the air flow in their potential to ignite fuels. Air movement is necessary to provide oxygen at the surface of the solid-phase combustion process. Too little and the reaction interface is

starved of oxygen and fails. Too much and the temperature of the reacting substrate drops below the activation energy of the oxidation reaction. While an optimum speed may be possible, a mix of air speeds may provide greater potential for the reaction pathways to result in maximum heat generation and thus heat flux to unburnt fuel.

While turbulence was identified in the study as being a key difference between the controlled laboratory experiments conducted here and the open field conditions associated with bushfires, it was not possible to study the effects of turbulence and would be key to the next step in developing this work in the future.

7.3 Fire growth and acceleration (Chapter 4)

All current fire spread prediction models designed to predict the spread of fire in the field assume that the fire has developed to a stage where it is spreading at a steady-state. That is, the mean rate of forward spread of the fire is determined by the mean values of the environmental and fuel variables. The time it takes for a fire starting from a point to reach this condition has not been well defined. While there have been a number of rules of thumb regarding the time it may take a fire to reach a given size or the size a fire may reach after a given period, these have been too general to provide much information for the purposes of planning and enacting suppression strategies.

This study provides the first in-depth investigation of the growth of point ignition fires under repeatable conditions. The results of this study suggest that, as with the ignition study above, fuel moisture content and wind are the critical factors determining the rate of progression of ignitions to the steady state. The study, however, was necessarily highly restricted in the range and types of variations that could be investigated during the project. Again, the role of turbulence (particularly in regard to changes in wind direction) was identified as being the key difference between the laboratory-based experiments conducted here and fires in the open.

The results provide an indication of the likely quantum of time required for a successful ignition to reach a steady-state condition. Investigation of a larger range of fuel bed moisture content values and wind conditions are necessary to develop a robust predictive tool suitable for operational use. The conditions studied here would be of immediate use for prescribed burn planning.

Controlled investigation of the effect of varying wind direction would also be essential in any next phase of research. It has been shown that the increases in headfire width as a result of changes in wind direction have a direction impact on the rate of spread and thus the time of development of a fire. Generating variable wind environments in a consistent and repeatable manner is essential.

Additionally, investigation of the effect of turbulence on fire develop is also essential. The periodic gust-lull structure of the wind has been observed to have an effect on flame propagation and thus may influence fire development. The laminar air flow in this study showed that consistent air flow interacts with the buoyant structure of the fire to produce turbulent flow downwind of the fire front. Quantifying this effect and the effect of periodic

structures in the air flow are critical to building a more complete understanding of wind/fire interactions.

The work carried out here, provides not only an insight into the rate of development and propagation of fire outbreaks but, in conjunction with the spotfire initiation work of the preceding chapter, the potential growth rate of spotfires to steady-state. Determination of when these spotfires themselves become a source of firebrands producing new spotfires completes the lifecycle circle and was part of the subsequent study.

7.4 Vertical fire transitions (Chapter 5)

The mechanisms of vertical fire transitions in eucalypt forests are not well understood. Although its importance in overall fire behaviour has long been recognized, no research effort has been made to specifically increase our understanding of fire transitions in eucalypt forests. A contributing factor to our lack of understanding of this key fire dynamics process has been the difficulty of conducting experimental fires under the burning conditions where fire escalates from a surface fire to a fire involving bark and overstorey canopy fuels. Our quantitative knowledge of fire behaviour in eucalypt forests is essentially restricted to the bottom 10% of the potential fire intensity scale. While the potential to use numerical models of fire propagation to study this phenomenon exists, these models are not yet sophisticated enough to replicate these behaviours.

This study undertook a quasi-physical approach to increase our understanding of the factors and mechanisms involved in vertical fire propagation between (1) surface / near-surface and elevated fuels; (2) surface / near-surface / elevated and bark fuels; and (3) understorey and overstorey fuels. A conceptual description of the propagation mechanisms driving fire transitions in eucalypt forests was introduced and used to construct a conditional numeric flowchart (algorithm) model. This model utilised a conceptual model of forest structure to determine critical thresholds of heat output and ignition requirements to determine if and when a fire burning in a given layer would ignite the next vertical layer and whether this layer would have sufficient heat output to sustain fire spread.

This model enables the prediction of vertical transition of fire spread through multi-layered fuels and would provide an able vehicle for the determination of when bark fuels would become involved in fire spread and thus provide the potential fuel for firebrand generation.

7.5 Suppression resource allocation framework (ASRAMS) (Chapter 6)

A framework for a fire suppression resource allocation model was developed in this component of the project, called ASRAMS. This framework provides a model for combining information about current and expected fire load (based on fire occurrence, fire ignition probability, fire growth and vertical fuel transitions) with information about suppression resource capability and capacity.

Although a post-graduate research project was initiated in order to provide information about suppression capability in regards to suppression resource response (despatch, travel time, etc) and productivity (length of fireline construction per unit time, per unit volume, etc), no results from this work were available for discussion here. However, this component forms the biggest gap in the knowledge necessary to actually build a suppression resource

allocation tool. Future work will need to concentrate on filling this gap for all suppression resource types currently used in Australia, including tankers and aircraft.

The first steps in developing ASRAMS will be to select an initial case study region and to establish input components. This will require significant support from local fire management agencies who will need to provide occurrence and response data. New developments in existing operational systems should continue to be monitored.

7.6 Conclusions

Bushfire is a dynamic natural phenomenon that responds to changes in the fuel, weather, topographic and atmospheric environments occurring over a broad range of spatial and temporal scales. As the fire response to these changes depends not only on the magnitude and extent of the change but also on the state of development of the fire itself, it is non-linear. Dynamic feedback mechanisms result in the fire modifying itself, its local environment and the way the fire reacts to this environment.

Current operational fire spread models do not explicitly describe the full spectrum of fire behaviour transitions and its non-linear dynamics but only a subset of steady-state behaviour. This project has endeavoured to investigate key components of the non-linear dynamics of the behaviour of bushfires, namely the probability of fire outbreaks and their propagation and development to the steady-state.

The knowledge gathered in this project is particularly relevant for situation awareness for fire authorities as well as the general public, firefighter safety, suppression resourcing and action success, and the issuing of timely and useful public warnings. It is also relevant to improving house design and survival rates. Understanding of the capacity of suppression resources and the rapidly changing demands for suppression will provide end users with greater confidence in pre-season planning and incident management, particularly where multiple fire events coincide.

The knowledge gathered, however, is only the tip of the iceberg in regard to the extent of knowledge needed to develop adequate operational models of fire load and suppression allocations. Extension to other fuel types and broader burning conditions is vital to achieving tools applicable to all regions in which effective fire management is essential.

The research undertaken in this project has identified important aspects that should be investigated in future work, particularly the influence of wind direction variation and turbulence on the initiation and growth of fires, and productivity rates for suppression resources used in Australia.

Appendices

Appendix 1: Fire Notes

TITLE	AUTHORS	DELIVERED	PUBLISHED	FIRE NOTE NO.
Fire Development, Transitions and Suppression, an overview	Sullivan, A; Gould, J; Cruz, M; Ellis, P; Plucinski, M.	6/2011	8/2012	94
Firebrand Behaviour and the Probability of Fuel Bed Ignition	Ellis, P	3/2012	10/2012	99
First Hour: How Fast, How Big.	Gould, J	6/2012	TBD	TBD
Predicting Daily Human-caused Bushfire Ignitions	Plucinski, M	3/2012	TBD	TBD
Fire Development, Transitions and Suppression, Final Report Overview	Sullivan, A; Gould, J; Cruz, M; Ellis, P; Plucinski, M.	2/2014	TBD	TBD

Appendix 2: Research posters

TITLE	AUTHORS	PRESENTED
Studying Firebrands Using a Vertical Wind Tunnel.	Ellis, P	8/2011
The When and Where of Future Fire: Towards an Australian Fire Occurrence Model.	Plucinski, M; McCaw, L; Wotton, M; Gould, J and Sullivan, A	8/2011
From the Archives: A New Insight into Fire Growth	Gould, J; Koul, V	9/2012
Predicting the probability of human caused bushfire days in south west management regions	Plucinski, M; Gould, J; McCaw, L; Wotton, M and Sullivan, A	9/2012
Spotfire Initiation by Firebrands	Ellis, P	9/2013
Vertical Fire Transitions and Propagation Mechanisms in Eucalypt Forests	Cruz, M	9/2013

Appendix 3: 2013 CSIRO Bushfire Science Symposium Program

Day 1		
9:00	Registration	
10:30	***Morning tea***	
Opening session		Chair: Andrew Sullivan
11:00	Welcome: Acknowledgement of country CSIRO Opening Address	 Andrew Sullivan Dr Robyn Russell, CSIRO Ecosystem Sciences Assistant Chief
11:20	Opening Keynote: Fire behaviour- McArthur beginnings to the present	Phil Cheney (CSIRO retired)
12:00	Keynote: Fire science in the control room	Joe Buffone (CFA)
12:30	***Lunch***	
Fire weather and forecasting		Chair: Miguel Cruz
13:30	New tools for fire weather forecasting	Jeff Kepert (BoM)
14:00	Weather information for prescribed burning	Sarah Chadwick (BoM)
14:30	Linking weather to fuel availability	Stuart Matthews (CSIRO)
15:00	What are practitioners needs	Andrew Stark (ACT RFS)
15:15	***Afternoon tea***	
Fuels		Chair: Michael Doherty
15:45	Remote sensing fuel moisture: from leaves to landscapes and beyond	Ross Bradstock (UoW)
16:15	Application of visual fuel hazard assessments to fire behaviour prediction	Lachie McCaw (DEC, WA)
16:45	Australian fuel classification- update	Jim Gould (CSIRO)
17:15	Role of fuel- practitioner	Simon Heemstra (NSW RFS)
17:30	***Closing***	
17:30	**Welcome drinks**	**Discovery Foyer**

Day 2		
International perspective fuel and fire behaviour science		Chair: Jim Gould
8:30	Keynote: LANDFIRE and beyond: the challenges of describing, classifying, and mapping fuels for fire management in the US	Bob Keane (USFS)
9:15	Keynote: Fire behaviour in the next generation of the Canadian Forest Fire Danger Rating System	Mike Wotton (CFS)
	Morning Tea	

Ignition and spotting		Chair: Mike Wotton
10:30	Fire occurrence	Matt Plucinski (CSIRO)
11:00	Prediction of lightning ignition based on atmospheric and fuel moisture conditions	Andrew Dowdy (BoM)
11:30	Plume dynamics and spotting	Robert Fawcett for Will Thurston (BoM)
12:00	Fire brands and spot ignition	Andrew Sullivan for Peter Ellis (CSIRO)
	Lunch	
Fire behaviour		Chair: Stuart Matthews
13:30	Grassland fire behaviour	Andrew Sullivan (CSIRO)
14:00	Shrubland and mallee-heath fires	Wendy Anderson (UNSW)
14:30	Predicting fire behaviour in dry eucalypt forest	Jim Gould (CSIRO)
	Afternoon tea	
15:30	Plantations- pine/hardwoods	Paul deMar (GHD)
16:00	Prescribe burning- review of knowledge Tasmania and South Australia	Jon Marsden-Smedley (UTas)
16:30	Role of fire behaviour for preparedness and planning- practitioner perspective	Andy Ackland (DSE)
	Symposium Close- Day 2	
18:30	Symposium Dinner	University House

Day 3		
New initiatives in fire behaviour science		Chair: Stuart Matthews
8:30	Keynote: Research perspective on fire behaviour prediction in the US	Mark Finney (USFS)
9:15	Fire acceleration and development in eucalypt litter fuel	Jim Gould (CSIRO)
9:45	A model for fire propagation and vertical transitions in eucalypt forests	Miguel Cruz (CSIRO)
	Morning Tea	
Fire spread simulation		Chair: Matt Plucinski
10:45	PHOENIX RapidFire	Kevin Tolhurst (UMelb)
11:15	AURORA	Adrian Allen (Landgate)

11:45	Landscape fire regime modelling with FIRESCAPE	Geoff Cary (ANU)
	Lunch	
Fire behaviour science outlook		Chair: Andrew Sullivan
13:15	Error uncertainty in fire spread predictions	Miguel Cruz (CSIRO)
13:45	The role of the FBAN	Kevin Tolhurst (UMelb)
14:15	Amicus: Fire behaviour software bringing together the best information for the best decisions	Jim Gould (CSIRO)
14:45	Closing Keynote: One Fire Manager's Perspective: The operational reality and the future fire research need	Brian Simpson (BC)
	Closing the symposium	*Neil Cooper (ACT PCS)*
	Afternoon tea available	

FOR FURTHER INFORMATION

Ecosystem Sciences
Dr Andrew Sullivan
t +61 2 6246 4051
e Andrew.sullivan@csiro.au
w www.csiro.au

CONTACT CSIRO
t 1300 363 400
+61 3 9545 2176
e enquiries@csiro.au
w www.csiro.au